


12-2012

Capillary and Microchip Electrophoresis for the Monitoring of Disease Causing Amyloid Proteins

Elizabeth Nancy Pryor
University of Arkansas, Fayetteville

Follow this and additional works at: <http://scholarworks.uark.edu/etd>

 Part of the [Biochemical and Biomolecular Engineering Commons](#), and the [Biochemistry Commons](#)

Recommended Citation

Pryor, Elizabeth Nancy, "Capillary and Microchip Electrophoresis for the Monitoring of Disease Causing Amyloid Proteins" (2012). *Theses and Dissertations*. 579.
<http://scholarworks.uark.edu/etd/579>

This Dissertation is brought to you for free and open access by ScholarWorks@UARK. It has been accepted for inclusion in Theses and Dissertations by an authorized administrator of ScholarWorks@UARK. For more information, please contact scholar@uark.edu, ccmiddle@uark.edu.

CAPILLARY AND MICROCHIP ELECTROPHORESIS FOR THE MONITORING OF
DISEASE CAUSING AMYLOID PROTEINS

CAPILLARY AND MICROCHIP ELECTROPHORESIS FOR THE MONITORING OF
DISEASE CAUSING AMYLOID PROTEINS

A dissertation submitted in partial fulfillment
of the requirements for the degree of
Doctor of Philosophy in Chemical Engineering

By

Elizabeth Nancy Pryor
Texas A&M University
Bachelor of Science in Biochemistry, 2006

December 2012
University of Arkansas

ABSTRACT

The detection of oligomers and aggregates formed by two amyloid proteins, insulin and amyloid- β ($A\beta$), is of particular importance due to the role which these species play in Diabetes and Alzheimer's disease, respectively. However, existing techniques are limited in the ability to detect insulin and $A\beta$ oligomers due to the fact that these early aggregates are transient, present at low concentrations, and difficult to isolate. Improvements must be made to existing techniques or alternative techniques must be explored in order to identify and quantify the size of these oligomeric and aggregate species without disrupting their structure.

Capillary and microchip electrophoresis (CE and ME) are two promising electrophoretic methods for amyloid oligomer and aggregate detection. The present work demonstrated the potential for CE and ME to detect native aggregation of insulin and $A\beta$ proteins, in particular the formation of oligomers and aggregates. Furthermore, the effect of hydrodynamic size on separation was increased through the use of a highly entangled polymer matrix introduced into the capillary, thus offering the potential to resolve populations of amyloid species. Using this novel separation, we investigated variables such as sample salt concentration, sample preparation method, and fluorescent dye structure. We demonstrated the ability of CE with ultraviolet detection (UV-CE) to detect native insulin aggregates estimated to range in size from 30 – 100 kDa and native $A\beta_{1-40}$ aggregates estimated to range in size from 10 – 30 kDa, 10 – 300 kDa and > 300 kDa. These studies demonstrated the successful detection of physiological concentrations (pM) of monomeric fluorescein isothiocyanate labeled insulin (FITC-insulin) and carboxy-fluorescein labeled $A\beta$ (FAM- $A\beta$) using CE with laser induced fluorescence detection (LIF-CE). However, the detection of oligomeric and aggregate species was altered from unlabeled samples, indicating the need for future work in the study of fluorescent dye attachment.

This dissertation is approved for recommendation to the Graduate Council.

Dissertation Director:

Dr. Christa N. Hestekin

Dissertation Committee:

Dr. Robert R. Beitle, Jr

Dr. Roger E. Koeppe II

Dr. Donald K. Roper

Dr. Shannon L. Servoss

DISSERTATION DUPLICATION RELEASE

I hereby authorize the University of Arkansas Libraries to duplicate this dissertation when needed for research and/or scholarship.

Agreed

Elizabeth Nancy Pryor

Refused

Elizabeth Nancy Pryor

ACKNOWLEDGEMENTS

First and foremost, I would like to thank my research advisor, Dr. Christa Hestekin. I would not be where I am today without her knowledge, support, and passion for this project. She has taught me to stay positive during the ups and downs of research and serves as an excellent role model for me as an engineer, scientist, and teacher. My thanks also extend to the members of my committee, Dr. Bob Beitle, Dr. Roger Koeppe, Dr. Keith Roper, and Dr. Shannon Servoss, and professors in the Chemical Engineering department for their continued guidance and support throughout this project.

Thank you to my longtime friends as well as the friends I have made during graduate school whose support system has made my graduate school experience a positive one. I especially want to thank McKinzie Fruchtl, Melissa Hebert, and Alice Jernigan for being there for me not only as friends but as colleagues who I could ask for advice and opinions on lab related issues.

Finally, I would not have made it through graduate school without the love and care of my family. To my Mom, words cannot express how much your belief in my abilities and encouragement to strive for the best has helped me during my doctoral research. To my Step-Dad and Kristy, thank you for your constant interest in my research and encouragement along the way.

DEDICATION

To the memory of my Dad

Neil Birnie Pryor

August 22, 1936 – November 16, 2009

TABLE OF CONTENTS

INTRODUCTION	1
CHAPTER 1: UNRAVELING THE EARLY EVENTS OF AB AGGREGATION: TECHNIQUES FOR THE DETERMINATION OF AB AGGREGATE SIZE	2
ABSTRACT	2
KEYWORDS	2
1. INTRODUCTION	3
2. ELECTROPHORETIC TECHNIQUES FOR THE QUANTIFICATION OF AB OLIGOMER SIZES	7
2.1. SDS- and Native-PAGE	7
2.2 SDS-PAGE in Combination with Western Blotting.....	11
2.3 SDS-PAGE in Combination with Other Techniques	18
2.4. Summary of SDS-Based Methods.....	21
2.5. Capillary and Microfluidic Capillary Electrophoresis.....	22
3. SPECTROSCOPIC TECHNIQUES FOR THE QUANTIFICATION OF AB OLIGOMER SIZES	26
3.1 Mass Spectrometry	26
3.2 Matrix-Assisted Laser-Desorption Ionization (MALDI)-MS	27
3.3 Electrospray Ionization (ESI)-MS	28
3.4 Ion Mobility (IM)-MS	30
3.5 Fluorescence Correlation Spectroscopy	33
3.6 Summary of Spectroscopic Methods.....	36
4. ADDITIONAL TECHNIQUES UTILIZED FOR AB AGGREGATE SIZE DETERMINATIONS	36
4.1 Light Scattering Techniques.....	36
4.2 Light Scattering in Combination with Other Techniques.....	40
4.3 Centrifugation.....	42
4.4 Size Exclusion Chromatography	43
4.5 Summary of Additional A β Aggregate Size Determination Techniques	46
5. TECHNIQUES UTILIZED FOR AB OLIGOMER IDENTIFICATION.....	46
5.1 Dot Blot	47
5.2 Enzyme-Linked Immunosorbent Assay	50
5.3 Summary of A β Oligomer Identification Techniques.....	51

6. CONCLUSIONS.....	51
REFERENCES	56
APPENDIX.....	68
CHAPTER 2: TECHNIQUES FOR THE DETERMINATION OF INSULIN AGGREGATE SIZE	70
1. INSULIN PROTEIN	70
2. ELECTROPHORETIC TECHNIQUES FOR THE QUANTIFICATION OF INSULIN OLIGOMER SIZE	75
2.1 Sodium dodecyl sulfate- and native-polyacrylamide gel electrophoresis (SDS- and native-PAGE)	75
2.2 Capillary electrophoresis (CE)	75
3. SPECTROSCOPIC TECHNIQUES FOR THE QUANTIFICATION OF INSULIN OLIGOMER SIZE	76
3.1 Electrospray ionization mass spectrometry (ESI)-MS	76
3.2 Ion mobility mass spectrometry (IM)-MS.....	77
4. ADDITIONAL TECHNIQUES UTILIZED FOR INSULIN AGGREGATE SIZE DETERMINATION	77
4.1 Light scattering techniques.....	77
4.2 Light scattering in combination with other techniques	78
4.3 Centrifugation.....	78
4.4 Size exclusion chromatography.....	78
4.5 Transmission electron microscopy	79
5. TECHNIQUES UTILIZED FOR AMYLOID OLIGOMER IDENTIFICATION	79
5.1 Dot blot	79
6. SUMMARY OF ELECTROPHORETIC AND NON-ELECTROPHORETIC BASED INSULIN AND A β SIZE DETECTION METHODS	79
REFERENCES	81
CHAPTER 3: MONITORING INSULIN AGGREGATION VIA CAPILLARY ELECTROPHORESIS.....	85
ABSTRACT.....	85
KEYWORDS	86
1. INTRODUCTION.....	86
2. RESULTS AND DISCUSSION	88
2.1. Detection of Insulin Oligomers Using CE with UV Detection	88

2.2. Effect of Salt Concentration on the Time Course for Insulin Oligomer Formation.....	92
2.3. Determination of Insulin Limit of Detection.....	101
2.4. Analysis of FITC Tracer Incorporation into Unlabeled Insulin.....	104
3. MATERIALS AND METHODS.....	108
3.1. Materials.....	108
3.2. Insulin Preparation.....	108
3.3. Electrophoresis Conditions for UV and LIF Studies.....	108
3.4. Limit of Detection Studies.....	109
3.5. Oligomer Formation Assay.....	110
3.6. Statistical Analysis.....	111
ACKNOWLEDGEMENTS.....	113
REFERENCES.....	114
APPENDIX.....	122

CHAPTER 4: MONITORING A β AGGREGATION VIA CAPILLARY

ELECTROPHORESIS.....	126
1. INTRODUCTION.....	126
2. MATERIALS AND METHODS.....	129
2.1. A β preparation.....	129
2.2. Poly(ethylene oxide) coating and separation matrix synthesis.....	130
2.3. Poly-N-hydroxyethyl acrylamide coating and separation matrix synthesis and characterization.....	131
2.4. Electrophoresis conditions for UV and LIF studies.....	131
2.5. A β oligomer formation assay.....	132
2.6. Dot blot analyses of A β aggregation.....	134
2.7. Limit of detection studies.....	135
2.8. Statistical analysis.....	135
3. RESULTS AND DISCUSSION.....	136
3.1. Detection of A β_{1-40} oligomers using CE with UV detection.....	136
3.2. Effect of sample preparation on A β_{1-40} aggregate sizes formed.....	142
3.3 Validation of CE detection with traditional measures of A β aggregation states.....	150
3.4 Determination of A β_{1-40} limit of detection.....	155

3.5 Analysis of FAM tracer incorporation into unlabeled A β	156
4. CONCLUSIONS	165
REFERENCES	168
APPENDIX.....	175
 CHAPTER 5: MICROCHIP ELECTROPHORESIS FOR DETECTION OF B-SHEET FORMATION BY AB AGGREGATES	
1. INTRODUCTION.....	178
2. MATERIALS AND METHODS.....	180
2.1. A β preparation	180
2.2. Poly-N-hydroxyethyl acrylamide coating and separation matrix synthesis and characterization.....	181
2.3. A β ₁₋₄₀ aggregation assay with BTA-1 and ThT.....	181
2.4. Microfluidic chips and polymer matrix loading into microfluidic chips.....	182
2.5. Microchip Electrophoresis.....	183
3. RESULTS AND DISCUSSION	183
3.1. Detection of FAM-A β ₁₋₄₀ using LIF-ME.....	183
3.2. Detection of β -sheet formation by A β ₁₋₄₀ using LIF-ME and comparison to ThT binding	185
4. CONCLUSIONS	192
REFERENCES	193
 CHAPTER 6: CONCLUSIONS AND FUTURE DIRECTIONS	
1. IMPACT OF THE PRESENTED WORK.....	196
2. FUTURE DIRECTIONS.....	200
2.1. Testing of alternative dyes with LIF-CE	200
3. CONCLUSIONS	209
REFERENCES	210
APPENDIX.....	212
CONCLUSION.....	260

LIST OF ABBREVIATIONS

AD	alzheimer's disease
ADDLs	amyloid-derived diffusible ligands
AFFF	asymmetric field flow fractionation
AMCA	aminomethylcoumarin acetate
ASPDs	amylospheroids
A β	amyloid- β
BCIP	bromo-4-chloro-3-indolyl phosphate
BODIPY	4,4-difluoro-5,7-dimethyl-4-bora-3a,4a-diaza- <i>s</i> -indacene-3-propionic acid
BTA-1	2-(4'-methylaminophenyl)benzothiazole
CCD	charge-coupled device
CE	capillary electrophoresis
CSF	cerebrospinal fluid
DLS	dynamic light scattering
DMSO	dimethyl sulfoxide
ELISA	enzyme-linked immunosorbent assay
EOF	electroosmotic flow
ESI	electrospray ionization
FAM	carboxy-fluorescein
FCS	fluorescence correlation spectroscopy
FITC	fluorescein isothiocyanate
HFIP	1,1,1,3,3,3-hexafluoro-2-propanol
IAPP	islet amyloid polypeptide
IM-MS	ion mobility mass spectrometry
LDI	laser desorption ionization
LIF	laser induced fluorescence
MALDI	matrix assisted laser desorption ionization
MALS	multi-angle light scattering
ME	microchip electrophoresis
μ M	micromolar
MS	mass spectrometry
nM	nanomolar
Native-PAGE	native-polyacrylamide gel electrophoresis
NBT	nitroblue tetrazolium chloride
PBS	phosphate buffered saline
PEO	polyethylene oxide
PHEA	poly- <i>N</i> -hydroxyethyl acrylamide
pM	picomolar
PICUP	photoinduced cross-linking of unmodified proteins
QELS	quasi-elastic light scattering
R _H	hydrodynamic radius
R _{ms}	root mean square
S/N	signal-to-noise
SDS	sodium dodecyl sulfate
SDS-PAGE	sodium dodecyl sulfate-polyacrylamide gel electrophoresis

SEC	size exclusion chromatography
s-value	sedimentation coefficient value
TBS-T	tris buffered saline containing 0.01% Tween 20
TEM	transmission electron microscopy
ThT	thioflavin T
UV	ultraviolet

LIST OF FIGURES

Figure 1 The A β aggregation process.....	5
Figure 2 Tricine-SDS-PAGE analysis of the aggregation states of A β peptides freshly dissolved or incubated for 7 days.....	9
Figure 3 SDS-PAGE with Western Blotting Analysis of A β ₁₋₄₂ oligomers obtained upon incubation at 4°C for 24 hours.....	17
Figure 4 SDS-PAGE analysis of non-cross-linked and cross-linked A β ₁₋₄₀ and A β ₁₋₄₂	20
Figure 5 CE Electropherograms for A β ₁₋₄₂ species formed in room temperature PBS (pH 7.4) at different elapsed aggregation times from t ₀	24
Figure 6 ESI-Mass spectra of 4.0 μ M freshly dissolved A β ₁₋₄₀ , freshly dissolved A β ₁₋₄₀ Met35(O), A β ₁₋₄₀ and A β ₁₋₄₀ Met35(O) incubated for 41 minutes, and A β ₁₋₄₀ and A β ₁₋₄₀ Met35(O) incubated for >95 minutes.....	29
Figure 7 IM-MS arrival time distributions for (a) 30 μ M A β ₁₋₄₂ in 49.5% H ₂ O, 49.5% acetonitrile, and 1% NH ₄ OH and (b) 30 μ M A β ₁₋₄₀ in ammonium acetate (pH 7.4). D = dimer, Te = tetramer, H = hexamer, Do = dodecamer with a z/n = -5/2.....	32
Figure 8 Size distributions obtained via FCS for A β ₁₋₄₀ dissolved in 2.8 mM NaOH, diluted to 10 μ M in HEPES (pH 7.4), and incubated at room temperature.....	35
Figure 9 Time evolution of R _H for a 185 μ M A β ₁₋₄₀ sample incubated at pH 3.1 and 37°C.....	39
Figure 10 HPLC-SEC chromatograms of A β aggregates produced using sample preparations of 50 μ M synthetic A β designed to optimize (a) low molecular weight A β ₁₋₄₀ oligomers and (c) A β ₁₋₄₂ protofibrils.....	45
Figure 11 A β aggregation monitored via dot blot.....	49
Figure 12 Detection of insulin monomer, oligomer, and higher molecular weight aggregation states using UV-CE.....	90
Figure 13 Effect of solution ionic strength on the formation of insulin oligomers detected by ...	94
Figure 14 Effect of solution ionic strength on the formation of insulin aggregates detected by ThT binding.	97
Figure 15 Comparison of lag times observed by UV-CE (■) and ThT binding.....	100
Figure 16 Limit of detection for monomeric insulin.	103
Figure 17 Effect of aggregation time on the normalized migration time for the coaggregation of FITC-labeled insulin and unlabeled insulin.....	106

Figure 18 Detection of smaller, intermediate, and larger molecular weight A β_{1-40} aggregation states using UV-CE.....	138
Figure 19 Comparison of A β_{1-40} peak pattern obtained with and without the presence of inhibitory compounds	139
Figure 20 Effect of aggregation time on the peak areas obtained for 10 – 30 kDa (◆, n = 3) and > 300 kDa (■, n = 3) A β_{1-40} species	140
Figure 21 Detection of smaller, intermediate, and larger SEC-purified A β_{1-40} molecular weight aggregation states using UV-CE.....	144
Figure 22 Comparison of peak pattern obtained at the onset of aggregation for SEC-purified A β_{1-40} and non-purified A β_{1-40} using UV-CE	145
Figure 23 Effect of aggregation time on the peak areas obtained for A) 10 – 30 kDa (◆, n = 3) and > 300 kDa (■, n = 3) non-purified A β_{1-40} species and B) 10 – 30 kDa (●, n = 3) and > 300 kDa (▲, n = 3) SEC-purified A β_{1-40} species.....	146
Figure 24 Effect of aggregation time on the 10 – 30 kDa peak areas obtained for non-purified (◆, n = 3) and SEC-purified(●, n = 3) A β_{1-40} species	147
Figure 25 Effect of aggregation time on the > 300 kDa peak area obtained for non-purified (■, n = 3) and SEC-purified (▲, n = 3) A β_{1-40} species.....	149
Figure 26 Monitoring A β_{1-40} aggregation by dot blotting.....	152
Figure 27 Representation of distinct types of A β_{1-42} oligomers and their relationship to A β_{1-42} fibrils.....	154
Figure 28 Coaggregation of FAM-labeled A β_{1-42} and unlabeled A β_{1-42}	159
Figure 29 Change in peak areas and normalized migration times for the coaggregation of FAM-labeled A β_{1-42} and unlabeled A β_{1-42}	160
Figure 30 Effect of peptide lot on the coaggregation of FAM-labeled A β_{1-42} and unlabeled A β_{1-42}	162
Figure 31 Change in early peak area for the coaggregation of FAM-labeled A β_{1-42} and unlabeled A β_{1-42} using two different lots.....	164
Figure 32 Detection of FAM-labeled A β_{1-42} using LIF-ME and LIF-CE.....	184
Figure 33 Effect of increased LIF-ME separation voltage on the detection of FAM-labeled A β_{1-42}	186
Figure 34 Detection of BTA-1 binding to A β_{1-40} using LIF-ME.....	189

Figure 35 Detection of ThT binding to A β ₁₋₄₀ using fluorometry.	190
Figure 36 Coaggregation of BODIPY-labeled A β ₁₋₄₀ and unlabeled A β ₁₋₄₀ with analysis via LIF-CE.	204
Figure 37 Effect of aggregation time on the area for peaks 1 - 8 (◆, n = 1 - 2) and peak 9 (■, n = 1 - 2) obtained for BODIPY-A β ₁₋₄₀	205
Figure 38 Effect of aggregation time on the peak areas obtained for A) 10 – 30 kDa (◆, n = 3) and > 300 kDa (■, n = 3) A β ₁₋₄₀ species analyzed via UV-CE and B) peak 1 - 8 (◆, n = 1 - 2) and peak 9 (■, n = 1 - 2) BODIPY-A β ₁₋₄₀ species analyzed via LIF-CE.	206
Figure 39 Effect of aggregation time on the peak areas obtained for > 300 kDa (◆, n = 3) A β ₁₋₄₀ species detected via UV-CE and peak 9 (■, n = 1 - 2) BODIPY-A β ₁₋₄₀ species detected via LIF-CE.	208

LIST OF TABLES

Table 1 Antibodies used for A β detection in Western blot analysis and their respective A β recognition motifs	13
Table 2 Summary of techniques for the quantitative detection and/or identification of A β aggregate sizes formed throughout the aggregation process	53
Table 3 Summary of techniques for the quantitative detection and/or identification of A β and insulin aggregate sizes formed throughout the aggregation process.	72
Table 4 Lag times observed at 100, 150, and 250 mM NaCl by CE versus ThT binding	93
Table 5 Structure and spectral properties of FAM and FITC.	157
Table 6 Structure and spectral properties of ThT and BTA-1.	187
Table 7 Structure and spectral properties of FITC, FAM, BODIPY, CE503, Adrazide	202

LIST OF PAPERS

Chapter 1 Pryor, E.; Moss, M. A.; Hestekin, C. N. <i>Int. J. Mol. Sci.</i> Unraveling the Early Events of A β Aggregation: Techniques for the Determination of A β Aggregate Size 2012, <i>13</i> , 3038-3072.....	2
Chapter 3 Pryor, E.; Kotarek, J. A.; Moss, M. A.; Hestekin, C. N. <i>Int. J. Mol. Sci.</i> Monitoring Insulin Oligomer Formation Via Capillary Electrophoresis, 2011, <i>12</i> , 9369-9388.....	85

INTRODUCTION

The detection of oligomers and aggregates formed by two amyloid proteins, insulin and amyloid- β ($A\beta$), is of particular importance due to the role which these species play in Diabetes and Alzheimer's disease, respectively. However, existing techniques are limited in the ability to detect insulin and $A\beta$ oligomers due to the fact that these early aggregates are transient, present at low concentrations, and difficult to isolate. Improvements must be made to existing techniques or alternative techniques must be explored in order to identify and quantify the size of these oligomeric and aggregate species without disrupting their structure. Capillary and microchip electrophoresis (CE and ME) are two promising electrophoretic methods for amyloid oligomer and aggregate detection. The present work demonstrated the potential for CE and ME to detect native aggregation of insulin and $A\beta$ proteins, in particular the formation of oligomers and aggregates.

During the earliest portion of this doctoral research (Fall 2009), a literature review was conducted by the author in order to determine alternative techniques suitable for the detection of amyloid oligomers and aggregates, in particular $A\beta$. Furthermore, this literature review was published in Spring 2012 in the *International Journal of Molecular Sciences* as a review paper. Since this publication gave a good outline for the techniques utilized to detect $A\beta$ oligomeric size, this publication was reproduced in Chapter 1 as a part of the literature review for this dissertation. The author of this dissertation contributed to writing over 50% of this literature review. Furthermore, Chapter 3 outlines studies conducted using CE to detect insulin oligomers and aggregates. This information was published in Fall 2011 in the *International Journal of Molecular Sciences*. Again, since this author contributed to writing over 50% of this publication, this publication was reproduced in Chapter 3 as a part of this dissertation.

Chapter 1: Unraveling the Early Events of A β Aggregation: Techniques for the Determination of A β Aggregate Size

Pryor, E.; Moss, M. A.; Hestekin, C. N. *Int. J. Mol. Sci.* Unraveling the Early Events of A β Aggregation: Techniques for the Determination of A β Aggregate Size 2012, *13*, 3038-3072

Abstract

The aggregation of proteins into insoluble amyloid fibrils coincides with the onset of numerous diseases. An array of techniques is available to study the different stages of the amyloid aggregation process. Recently, emphasis has been placed upon the analysis of oligomeric amyloid species, which have been hypothesized to play a key role in disease progression. This paper reviews techniques utilized to study aggregation of the amyloid- β protein (A β) associated with Alzheimer's disease. In particular, the review focuses on techniques that provide information about the size or quantity of oligomeric A β species formed during the early stages of aggregation, including native-PAGE, SDS-PAGE, Western blotting, capillary electrophoresis, mass spectrometry, fluorescence correlation spectroscopy, light scattering, size exclusion chromatography, centrifugation, enzyme-linked immunosorbent assay, and dot blotting.

Keywords

amyloid, capillary electrophoresis, centrifugation, dot blotting, enzyme-linked immunosorbent assay, fluorescence correlation spectroscopy, light scattering, mass spectrometry, native-polyacrylamide gel electrophoresis, oligomer, size exclusion chromatography, sodium dodecyl sulfate polyacrylamide gel electrophoresis, photoinduced cross-linking of unmodified proteins, Western blotting

1. Introduction

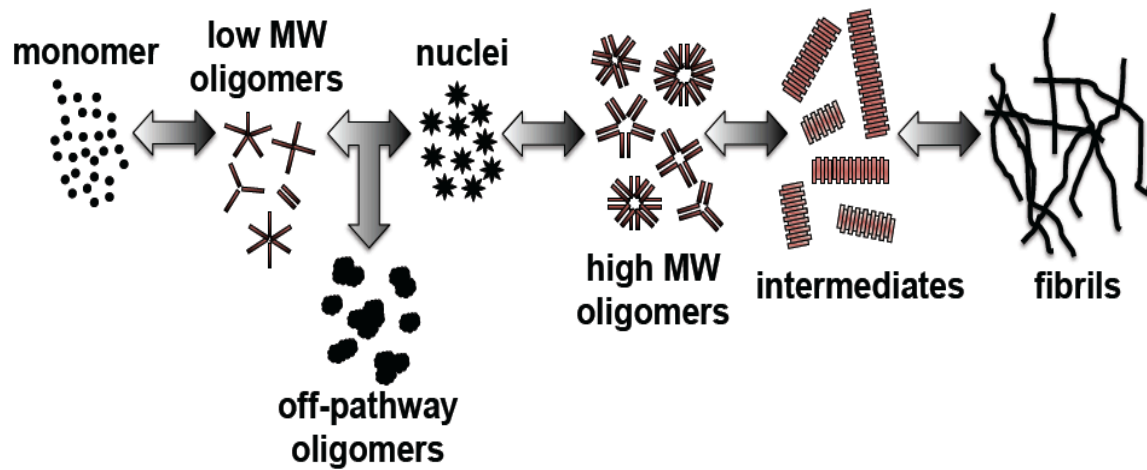
Protein aggregation leads to the formation of insoluble fibrous aggregates, termed amyloids, which are commonly associated with disease. However, understanding of the mechanism by which proteins aggregate has remained elusive. Although larger aggregates, including fibrils, remain important for clinical determination [1,2], small oligomeric aggregates are of interest due to their potentially toxic nature and hypothesized role in disease progression. However, the study of oligomers is complex due to the fact that these early aggregates are highly unstable, present at low concentrations, and difficult to isolate.

Among the diseases to which amyloids contribute are Alzheimer's disease (AD), Parkinson's disease, prion diseases, Type II diabetes mellitus, Huntington's disease, as well as many others [3]. The clinical presentation of each amyloid disease is very different, yet the presence of amyloid fibrils is a common characteristic of each disease. These amyloid fibrils exhibit a cross β -sheet structure in which the β -strands are oriented perpendicular to and hydrogen bonding is oriented parallel to the long axis of the fibril [4-9]. In addition, it has been shown that the amyloidogenic proteins amyloid- β ($A\beta$), α -synuclein, huntingtin, prion, and islet amyloid polypeptide (IAPP) form structurally similar soluble oligomeric species, which share an epitope recognized by oligomer-specific antibodies [10,11]. The commonalities shared by each amyloid disease protein suggest that studying the aggregation of one amyloid protein could provide insight into the general aggregation mechanism of other amyloid proteins.

AD is the most common cause of dementia and the most prevalent neurodegenerative disorder [12,13]. The neurodegenerative effects of AD are hypothesized to arise from $A\beta$, a partially folded protein that aggregates during the disease process. $A\beta$ was first identified by Masters *et al.* as the aggregated protein [14] deposited within plaque cores found in AD brain. In

its monomeric form, this protein may be harmless [15]. However, A β monomer can self-assemble via a nucleation-dependent pathway into A β oligomers, larger A β aggregation intermediates, and eventually the fibrillar aggregates that deposit in the brain (Figure 1) [5,16-18]. Steps within the A β aggregation pathway are reversible, such that deposited fibrils could give rise to soluble oligomers and intermediates. Soluble aggregate species that appear between monomer and insoluble fibrils have been termed within the literature as oligomers [19], micelles [20], amyloid-derived diffusible ligands (ADDLs) [21,22], β amy balls [23], amylospheroids (ASPDs) [24], and protofibrils [25,26], and the aggregate sizes associated with these definitions overlap in range. Smaller species are most commonly referred to as oligomers, including both low molecular weight and high molecular weight species, while larger intermediates are often referred to as protofibrils. Controversy exists concerning the exact size of the nucleus formed within the rate-limiting step of the aggregation pathway; however, most reports speculate that the nucleus is oligomeric in nature [27-29]. In addition to oligomers formed along the aggregation pathway, off pathway oligomers and higher order assemblies, which fail to give rise to an organized fibril structure, have also been identified [29,30].

Figure 1: The A β aggregation process. A β monomer self-assembles into low molecular weight oligomeric species that can give rise to either off-pathway oligomers or nuclei of an undetermined size. Nuclei, which arise within the rate-limiting step of the A β aggregation pathway, will increase in size to form high molecular weight oligomers, soluble aggregation intermediates, and finally the fibrillar aggregates that deposit in AD brain to yield amyloid plaques.



A β proteins comprised of either 40 or 42 amino acids, termed A β_{1-40} and A β_{1-42} , are the major components found in amyloid plaques [31]. A β_{1-42} has implications for the formation of initial aggregates, while A β_{1-40} is more soluble and is the main circulating form in normal plasma and cerebrospinal fluid (CSF) [32]. Controversy currently exists over the direct effect A β has on neurodegeneration, but it is theorized that soluble aggregates of A β , rather than monomers or insoluble fibrils, may be responsible for the cellular pathology associated with AD [33-35]. This hypothesis is supported by experimental observations *in vitro* which show that soluble aggregates formed by synthetic A β_{1-40} and A β_{1-42} can induce cellular dysfunction and toxicity in cultured cells [21,36,37] and *in vivo* where A β dodecamers (A β *56) have been isolated from the brains of transgenic mice and shown to induce memory deficits [38]. In addition, soluble A β aggregates generated in cell culture drastically inhibit hippocampal long-term potentiation in rats [39]. Furthermore, data from mouse models show a poor correlation between the levels of insoluble A β fibrils and disease severity [40]. It is now more widely accepted that soluble A β oligomers impair cognitive function and, in addition to synapse loss, correlate most accurately with the stage of neurological impairment [11,41-43]. However, the progression from monomer to oligomer to insoluble A β aggregates is not well understood. Therefore, it is important to develop an analytical tool that is suitable for analysis of the A β aggregation process.

A range of techniques are available to study the different stages of the A β aggregation process. These techniques fall into three main categories: 1) Methods for the quantitative detection of monomeric and oligomeric A β sizes; 2) Methods for the qualitative detection and characterization of oligomeric A β species; 3) Methods for the qualitative detection of A β fibrils. As a result of the imminent need to understand oligomerization events, the focus of this review is on techniques from the first and second categories, which give information about A β oligomeric

species formed during aggregation. Accumulating evidence suggests that these A β oligomeric species play a role in AD progression and severity. Therefore, it is important to gain a better understanding of the formation of smaller A β species in order to halt the progression of AD. The ability to identify and quantify the size of these A β oligomeric species without disrupting their structure is of utmost importance in order to effectively study the aggregation process and develop treatments that target these pivotal oligomerization events. Accordingly, this review focuses primarily upon techniques that have been employed in the study of *in vitro* aggregation of A β . Currently, a commonly used technique for the quantification of A β oligomer sizes within *in vitro* studies is polyacrylamide gel electrophoresis (PAGE). Other techniques that have been applied for determining the size of A β oligomers include Western blotting, capillary electrophoresis, mass spectrometry, fluorescence correlation spectroscopy, light scattering, centrifugation, and size exclusion chromatography (SEC). Furthermore, techniques including enzyme-linked immunosorbent assay (ELISA) and dot blot have been applied to identify A β oligomers, but give no size estimates. In the subsequent sections, we will discuss the application of each of these techniques to study A β oligomers.

2. Electrophoretic Techniques for the Quantification of A β Oligomer Sizes

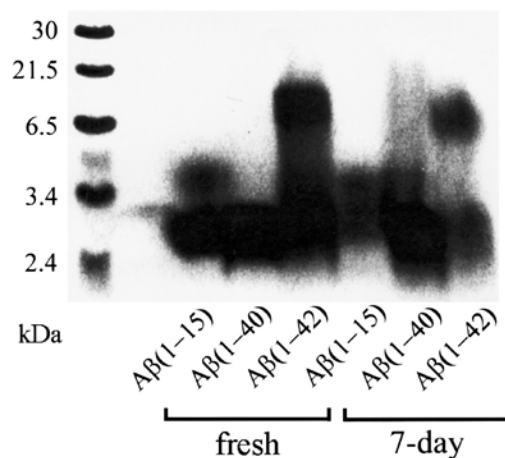
2.1. SDS- and Native-PAGE

SDS-PAGE is the most common electrophoretic technique used for A β oligomer size determination in protein aggregation studies. Furthermore, a review by Bitan *et al.* cited SDS-PAGE as the most common method used to characterize toxic protein oligomers [44]. SDS-PAGE relies on the ability of SDS, a negatively charged detergent, to bind to the protein of interest. This binding typically results in the removal of secondary, tertiary, and quaternary structures from the protein. The SDS groups attach to the protein in a nearly uniform manner that

gives the protein a charge approximately proportional to its length, thereby allowing for size based separations. Following the gel electrophoretic separation of proteins, the gel may be stained with a dye such as Coomassie Brilliant Blue or silver stain.

Many research groups have utilized SDS-PAGE, as a standalone technique, to study the evolution of A β species over time. A study by Ying *et al.* used SDS-PAGE to separate oligomers formed by 100 μ M A β ₁₋₄₂ incubated at 4°C for 1 day [45]. SDS-PAGE revealed bands for monomer (4.5 kDa), trimer/tetramer (16.5 kDa), and higher molecular weight intermediates (>83 kDa) that appeared as a smear. The oligomer pattern of freshly dissolved A β peptides and A β peptides after a 7 day incubation have been observed by Satoh *et al.* [46]. Both A β ₁₋₄₀ and A β ₁₋₄₂ peptides incubated for 7 days as well as the freshly dissolved A β ₁₋₄₂ peptide exhibited a range of species from 5 - 20 kDa (Figure 2). However, the resolution of these species was low due to gel smearing. Smearing in these gels may be due to the resolution limitations of the gel or could be due to continuous associations and disassociations of the aggregating species occurring during the electrophoresis analysis. Whatever the cause, gel smearing interferes with the ability to identify a particular species and is often overcome by combining SDS-PAGE with another technique (see Sections 2.2 and 2.3).

Figure 2: Tricine-SDS-PAGE analysis of the aggregation states of A β peptides freshly dissolved or incubated for 7 days. A β ₁₋₄₂ exhibits bands at 5 - 20 kDa in both freshly prepared samples and samples incubated for 7 days. A β ₁₋₄₀ incubated for 7 days also exhibits a smear at higher molecular weights, which is absent in freshly prepared samples. Reprinted from [46], with permission from Elsevier.



Although the anionic micelles formed by SDS enhance separation, they can also induce non-native behavior. SDS has been reported to accelerate the generation of A β fibrils. Sureshbabu *et al.* have shown that A β_{1-42} freshly prepared in phosphate buffered saline exhibits monomer, trimer (~13.5 kDa), and tetramer (~18 kDa) bands when analyzed via Western blotting [47]. The addition of 1.5 mM SDS to the sample produced bands at 20 and 50 kDa. They proposed that the addition of 1.5 mM SDS causes A β_{1-42} to develop a partial helical structure whose hydrophobicity induces aggregation. One way to counter this phenomenon is to add urea to the sample to further denature the peptide and prevent aggregation. However, the migration behavior of A β peptides in urea SDS-PAGE is inconsistent. A study by Kawooya *et al.* showed that the A β peptide exhibits an unusual electrophoretic mobility in urea SDS-PAGE that is proportional to the sum of the hydrophobicity consensus of the peptide rather than the number of amino acids in the peptide [31]. Therefore, under these conditions SDS-PAGE may provide information about the hydrophobicity of the peptide and not the size. The drawbacks of SDS-PAGE may be overcome by using native-PAGE to separate various A β sizes under conditions that allow the protein to remain in a native state.

Native or “non-denaturing” gel electrophoresis is similar to SDS gel electrophoresis, except this technique is run in the absence of SDS. With native-PAGE, protein mobility depends on both charge and hydrodynamic size. This differs from SDS-PAGE, where protein mobility depends primarily on molecular mass. Since A β aggregation is a process that involves changes in protein conformation, native-PAGE is often a suitable technique to detect various sizes of A β species. A study by Iurascu *et al.* used both SDS-PAGE and Tris-tricine PAGE to analyze the species formed by a solution of A β_{1-40} solubilized in fibril growth buffer at pH 7.5 for 5 days at 37°C [48]. They found that SDS-PAGE was able to detect A β_{1-40} monomeric species, A β_{1-40}

oligomeric species of 20 kDa, and high molecular weight aggregates >98 kDa. In contrast, Tris-tricine PAGE was able to separate these A β oligomers into monomer, dimer, trimer, and high molecular weight A β sizes. Klug *et al.* have also compared native and SDS-PAGE analyses of A β aggregation [49]. They observed the presence of oligomers and high molecular weight species using native-PAGE with the majority of A β species observed in the high molecular mass region of the gel. In contrast, SDS-PAGE showed lower molecular weight species (<14 kDa) with only trace amounts of high molecular weight species (>50 kDa), suggesting that the removal of higher order protein structures by SDS may destabilize aggregates. The differences between native-PAGE and SDS-PAGE highlight the importance of examining more than one method for studies of the various A β aggregate sizes formed throughout the aggregation process.

2.2 SDS-PAGE in Combination with Western Blotting

Western blotting is a popular technique used to further process samples after electrophoretic separation. This technique provides a more sensitive detection of separated proteins. This detection is achieved by transferring separated proteins to a membrane where they are detected using antibodies specific to the protein of interest. Antibodies may be either monoclonal or polyclonal and are typically specific for a particular part of the A β sequence or a particular amyloid conformation. Some common antibodies and their recognition motifs are listed in Table 1. Selecting the proper antibody is an important consideration in order to achieve detection of the desired A β species or aggregation state.

Numerous research groups have utilized Western blot analyses of SDS-PAGE separations to characterize SDS-stable A β assemblies [21,39,45,50-54]. Ryan *et al.* analyzed A β ₁₋₄₂ oligomer preps via silver staining and immunoblot with the 6E10 antibody [53]. The band intensity for monomer, trimer, and tetramer bands was similar for both methods. However, 46 and 56 kDa

intermediate sized oligomers were more apparent in the immunoblot analysis. Moore *et al.* have also found that immunoblot stains of A β ₁₋₄₂ oligomers yield better results than silver stains [55].

Table 1: Antibodies used for A β detection in Western blot analysis and their respective A β recognition motifs.

Antibody	Recognition Motif	Monoclonal/Polyclonal	References
6E10	A β ₁₋₁₇	Monoclonal	[50,52-54]
Ab9	A β ₁₋₁₆	Monoclonal	[55]
6C6	A β ₁₋₁₆	Monoclonal	[50]
4G8	A β ₁₇₋₂₄	Monoclonal	[50]
2G3	A β ₃₁₋₄₀	Monoclonal	[51]
BA-27	A β ₁₋₄₀ , C-terminal	Monoclonal	[56]
BC-05	A β ₁₋₄₂ , C-terminal	Monoclonal	[56]
A8	amyloid oligomers	Monoclonal	[45]
A11	amyloid oligomers	Monoclonal	[10,57,58]
NU-4	amyloid oligomers	Monoclonal	[59]
OC	amyloid fibrils	Polyclonal	[60]

SDS-PAGE with Western blotting has also been used to monitor the formation of A β oligomers in cell culture. A study by Walsh *et al.* employed SDS-PAGE followed by Western blotting to probe the formation of A β oligomers in APP-expressing Chinese hamster ovary (CHO) cells [50]. Bands corresponding to ~4, 6, 8, and 12 kDa were obtained using the monoclonal antibody 6E10. However, it was necessary to concentrate the A β protein via immunoprecipitation with an A β -specific antibody prior to performing electrophoretic separation.

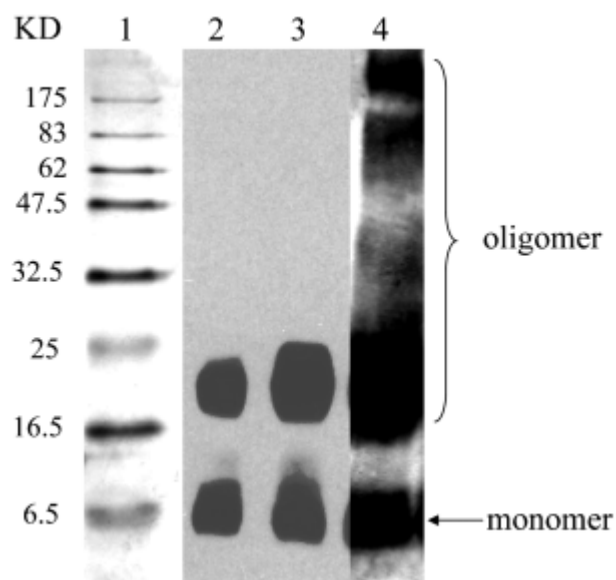
Within *in vitro* studies of A β aggregation, A β is typically solubilized in 1,1,1,3,3,3-hexafluoro-2-propanol (HFIP) to break up any residual aggregates that may be present in solution [61]. The HFIP is allowed to evaporate, and the peptide film is either resuspended in an organic solvent such as dimethyl sulfoxide (DMSO) and diluted into culture media or resuspended in a buffer solution such as phosphate buffered saline (PBS). Following incubation, samples are analyzed to detect the presence of oligomeric species. Dahlgren *et al.* utilized such an A β_{1-40} oligomer preparation employing DMSO and F12 culture media with incubation at 4°C for 24 hours [52]. Western blot analysis using the 6E10 antibody showed bands corresponding to monomer and tetramer. Similar results were obtained by Stine *et al.* using the same sample preparation [54]. Walsh *et al.* utilized an A β_{1-40} oligomer preparation in PBS (pH 7.4) at 37°C [51]. After 5 days, Western blot analysis using the antibody 2G3 showed bands corresponding to monomer, dimer, and tetramer. However, intermediate sizes of oligomeric species >20 kDa were not obtained.

In addition to A β_{1-40} , oligomeric A β_{1-42} species formed *in vitro* have been well characterized using Western blot analyses. Stine *et al.* studied the formation of A β_{1-42} oligomers using two different antibodies, 6E10 and 4G8 [54]. At 0 hours, bands for monomer, trimer, and a

faint tetramer band were obtained. After 24 hours, these bands were more intense and a smear corresponding to oligomeric species ranging from 30 to 70 kDa was present. Furthermore, no differences in the band patterns obtained using the 6E10 and 4G8 antibodies were observed. Dahlgren *et al.* obtained comparable 24 hour incubation results using the same oligomer preparation as Stine *et al.* [52]. In addition, similar 0 and 24 hour results were obtained by Ryan *et al.* using a monomer preparation with dilution into PBS and an oligomer preparation with dilution into cold PBS+0.05% SDS [53]. Stine *et al.* also examined the effect of temperature and ionic strength on the oligomeric band pattern obtained after incubation of 100 μ M A β ₁₋₄₂ for 24 hours. An increase in temperature from 4 to 37°C resulted in a decreased intensity of monomer and trimer bands and an increased intensity of the tetramer band. In addition, a smear for oligomeric species ranging from 30 to 70 kDa appeared at 25°C with increased intensity at 37°C. The effect of ionic strength was probed using the oligomer preparation at 37°C with incubation for 24 hours in either 10 mM Tris (pH 7.4) or 10 mM Tris supplemented with 150 mM NaCl. Both preparations yielded bands for monomer, trimer, and tetramer. However, the oligomer preparation in 10 mM Tris gave an intense oligomer smear from 30 to 97 kDa while the preparation in 10 mM Tris supplemented with 150 mM NaCl showed a less intense oligomer smear from 40 to 50 kDa. Ying *et al.* have also utilized the same A β ₁₋₄₂ oligomer preparation as Stine *et al.* but employed for detection the monoclonal antibody A8, which is specific for oligomers [45]. A smear for oligomeric species ranging from 16.5 to 25 kDa was observed with antibody A8 (Figure 3, lanes 2 and 3). A poorer resolution of oligomers and larger species were obtained using the 6E10 antibody (Figure 3, lane 4). These results show that 6E10 may be reacting more strongly with higher molecular weight oligomers or that these antibodies bind preferentially to different sizes of A β ₁₋₄₂ oligomers. While Western blotting does facilitate

detection of intermediate A β oligomers, the presence of a gel smear in many of the studies outlined above indicates that this technique does not allow quantification of individual sizes of oligomers in this range.

Figure 3: A β_{1-42} oligomers obtained upon incubation at 4°C for 24 hours. A 5 mM A β_{1-42} sample was prepared in DMSO and diluted to 100 μ M in Ham's F12 medium without phenol red. Oligomer mixture was separated by 15% SDS-PAGE, transferred to nitrocellulose membranes, and probed with monoclonal antibody A8 (Lanes 2 and 3) or 6E10 (Lane 4). Sample in Lane 2 was heat denatured prior to analysis, while sample in Lane 3 was untreated. Reprinted from [45] with permission. The publisher for this copyrighted material is Mary Ann Liebert, Inc. publishers.



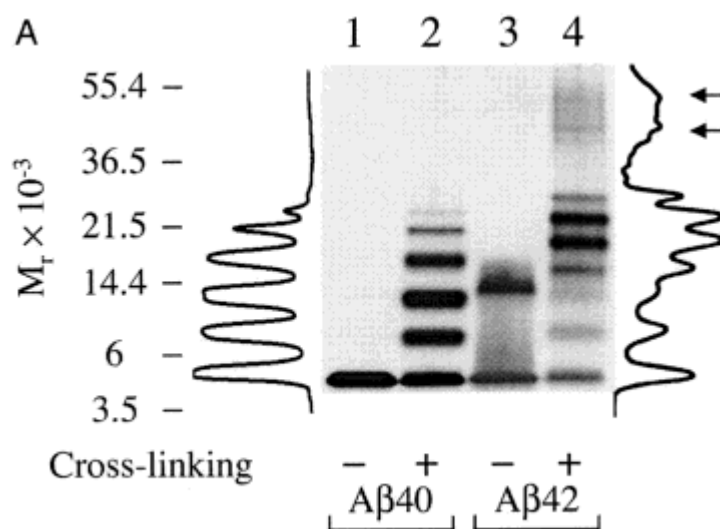
2.3 SDS-PAGE in Combination with Other Techniques

SDS-PAGE has been used in combination with oligomer stabilization techniques. One such technique that has been applied by Bitan *et al.* is Photoinduced Cross-Linking of Unmodified Proteins (PICUP) [62]. PICUP was developed in the Kodadek laboratory in 1999 to study proteins that naturally form stable homo- or heterooligomers [63]. This technique provides a snapshot of different oligomer species present in solution at different times. Protein cross-linking is achieved via the visible light excitation of a tris(2,2'-bipyridyl)dichlororuthenium(II) complex which, through a series of steps, leads to the generation of a free protein radical [62,64]. This radical can attack an unmodified neighboring protein and form a covalent bond. Therefore, PICUP can be used to covalently freeze components of the sample, and these components may be separated and analyzed via techniques such as SDS-PAGE [62].

Bitan *et al.* have applied PICUP to compare low molecular weight fractions of $A\beta_{1-40}$ and $A\beta_{1-42}$, where these fractions were isolated by SEC and analyzed via SDS-PAGE [65]. $A\beta_{1-40}$ exhibited bands for monomer, dimer, trimer, and tetramer with more faint bands for pentamer and heptamer (Figure 4, lane 2). A distinctly different low molecular weight $A\beta_{1-42}$ oligomer size distribution, consisting of three groups of oligomers of varying band intensity, was obtained (Figure 4, lane 4). This pattern led to the conclusion that the initial phase of $A\beta_{1-42}$ oligomerization involves the formation of pentamer/hexamer subunits which then associate to form larger oligomers and intermediates, or protofibrils [65]. Furthermore, they found that for $A\beta_{1-40}$, monomer through tetramer were preexisting species in solution, while pentamer through heptamer were formed via a diffusion-dependent reaction of these preexisting species with free monomer. Their results verified that PICUP was capable of “freezing” preexisting oligomers but was also capturing oligomeric species which were not formed under typical aggregation

conditions, thereby misrepresenting the true $A\beta_{1-40}$ oligomerization pattern. In addition, this study examined samples that were not cross-linked via PICUP before separation by SDS-PAGE. A single monomer band was obtained for $A\beta_{1-40}$ (Figure 4, lane 1), while $A\beta_{1-42}$ exhibited only bands for monomer and trimer (Figure 4, lane 3). These results indicate that oligomers not stabilized via PICUP were underestimated by SDS-PAGE results.

Figure 4: SDS-PAGE analysis of non-cross-linked (lanes 1 and 3) and cross-linked (lanes 2 and 4) $A\beta_{1-40}$ and $A\beta_{1-42}$. Densitometric intensity profiles of lanes 2 and 4 are shown on the right and left sides of the gel, respectively. Molecular weight standards are shown on the left in kDa. Reprinted with permission from [62].



SDS-PAGE has also been combined with SEC to investigate A β aggregation [25,66,67]. A study by Podlisny *et al.* used SDS-PAGE and SEC to observe the aggregation process of A β ₁₋₄₀ secreted from CHO cells [66]. Soluble, SDS-stable aggregates of 6 - 25 kDa, were detected during the first 4.5 hours of incubation at 37°C via added radioiodinated synthetic A β ₁₋₄₀ at low nanomolar concentrations. These 6 – 25 kDa A β oligomers represented ~18% of the total A β signal via SDS-PAGE and ~31% of the total A β signal via SEC. This low conservation of the A β gel signal over time to oligomeric species again indicates that SDS-PAGE underestimates the amount of aggregation. A study by Walsh *et al.* compared size estimations via SEC to those obtained by analyzing these SEC fractions by SDS-PAGE [25]. A β ₁₋₄₀ and A β ₁₋₄₂ were dissolved in Tris-HCl (pH 7.4) and incubated for 48 and 6 hours, respectively, at room temperature. SEC fractions corresponding to A β ₁₋₄₀ dimers, protofibrils, and fibrils produced a single band at ~4 kDa on SDS-PAGE. The SEC fraction for A β ₁₋₄₂ dimers produced a single SDS-PAGE band at ~4 kDa, while the SEC fraction for A β ₁₋₄₂ protofibrils and fibrils produced a ladder of sizes ranging only from monomer to pentamer. These results suggest that SDS-PAGE may not accurately detect A β aggregate sizes produced throughout aggregation.

2.4. Summary of SDS-Based Methods

As a standalone technique, SDS-PAGE is able to detect A β ₁₋₄₂ species ranging from monomer to tetramer. Native-PAGE has been used to separate A β ₁₋₄₀ species ranging from monomer to pentamer. However, for higher order oligomers, these techniques only give a range of sizes that appear as a smear on the gel. SDS-PAGE is often coupled with other techniques such as Western blotting and PICUP to enhance the resolution of A β sizes. By coupling SDS-PAGE to these techniques, a better resolution of A β ₁₋₄₀ species which appear as individual gel bands corresponding to monomer, dimer, trimer, and tetramer and A β ₁₋₄₂ species which appear as

individual gel bands corresponding to monomer, trimer, tetramer, and hexamer has been obtained. However, the resolution of intermediate sized A β oligomers ranging from 30 - 70 kDa by PAGE remains a significant challenge. The addition of SDS may also lead to complications including the acceleration of aggregation and the increased instability of oligomers, thereby misrepresenting the distribution of A β oligomeric species.

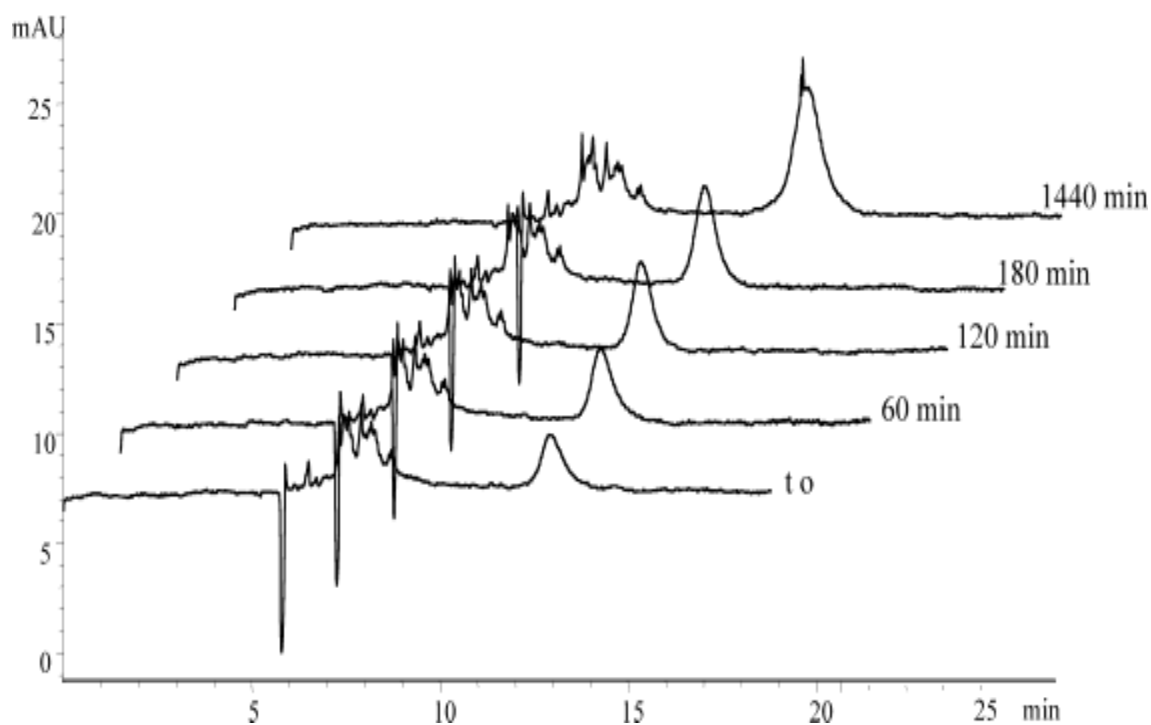
2.5. Capillary and Microfluidic Capillary Electrophoresis

Capillary electrophoresis (CE) is another electrophoretic technique employed for size based separations of A β . CE offers a fast and highly efficient separation of molecules with a broad range of properties thereby making it well suited for the separation of different sizes of protein aggregates [68]. CE separates molecules based on electrophoretic mobility, which results from differences in charge, shape, and/or size, and may be used either with or without SDS. Thus, CE allows a highly efficient separation and resolution of native forms of A β species, thereby overcoming the problem of gel smearing in many SDS and native-PAGE gel separations. CE detection typically uses either ultraviolet (UV) absorbance or laser induced fluorescence (LIF) to detect proteins. UV can detect proteins without any additional labeling, but typically has a lower sensitivity than LIF. LIF usually requires labeling of the molecules, but is highly sensitive, with previous reports of CE-LIF detection of double-stranded DNA down to the pg/ μ L range [69,70]. The ability to detect biomolecules at these low concentrations is necessary for the analysis of physiologically relevant protein concentrations.

CE with UV detection has been utilized by various researchers to detect A β species from monomers to large aggregates. Verpillot *et al.* used CE-UV to separate monomeric A β ranging in size from 37 - 42 residues and differing in length by a single residue, however they did not examine A β aggregation [71]. A study by Sabella *et al.* applied CE-UV with an SDS rinse for the

detection of $A\beta_{1-40}$ and $A\beta_{1-42}$ oligomers formed in PBS (pH 7.4) at room temperature [72]. At 0 hours, peaks for $A\beta_{1-42}$ oligomers in a size range from monomers to undecamers (~50 kDa)/dodecamers (~54 kDa) and larger aggregates were obtained (Figure 5, t_0). A similar peak pattern was obtained over an incubation time period of 24 hours with an increase in intensity of the higher molecular mass (>50 kDa) oligomer peak (Figure 5, $t = 1440$ minutes). However, resolution of individual species, especially in the larger aggregate peak, was not achieved. Compared to $A\beta_{1-42}$, the peaks for $A\beta_{1-40}$ were better resolved, but a drastically different peak pattern was observed. At 0 hours, three peaks ranging in size from 3 to 30 kDa were obtained. A decrease in the intensity of the 10 to 30 kDa peak was observed over an incubation period of 24 hours with the disappearance of all peaks after 48 hours. This result shows that CE-UV is capable of detecting small $A\beta_{1-40}$ species and intermediate oligomeric $A\beta_{1-42}$ species. In addition, the CE electrophoretic profiles of $A\beta_{1-40}$ and $A\beta_{1-42}$ differ significantly, supporting observations by PAGE that these two proteins differ in their early stages of aggregation.

Figure 5: Electropherograms for A β_{1-42} species formed in room temperature PBS (pH 7.4) at different elapsed aggregation times from t_0 . CE was performed with 50 mbar pressure injection for 8 s with separation at 16 kV. Molecular weights corresponding to each peak were determined using Microcon centrifugal filter units with molecular weight cutoffs of 3, 10, 30, and 50 kDa. Peaks with migration times of 5 – 10 min represent monomers to undecamers/dodecamers (3 – 50 kDa) and peaks with migration times of 10 – 15 min represent larger aggregates (>50 kDa). Reprinted from [72] published by John Wiley and Sons, © 2004 WILEY-VCH Verlag GmbH & Co. KGaA.



A study by Picou *et al.* also observed substantial differences in the CE-UV electrophoretic profiles of A β ₁₋₄₀ and A β ₁₋₄₂ [73]. Two different preparations typically employed to form A β monomer or fibril were used. The A β ₁₋₄₀ monomer preparation yielded a single monomer peak with a molecular weight of 4.3 kDa. In contrast to A β ₁₋₄₀, the A β ₁₋₄₂ monomer preparation gave peaks for both monomer and fibrillar species. A peak pattern similar to the A β ₁₋₄₂ monomer preparation was also obtained for the A β ₁₋₄₀ fibril preparation. The A β ₁₋₄₂ fibril preparation produced multiple aggregate peaks and no monomer peak. Although this study was able to separate A β monomer from mature fibrils, the detection of oligomeric A β species was not achieved.

LIF detection has also been utilized as a more sensitive means of identifying lower concentrations of A β aggregate species separated using CE. A study of the aggregation patterns of A β ₁₋₄₂ using CE-LIF was conducted by Kato *et al.* [74]. The fluorescent dye thioflavin T (ThT) was used to detect two different A β ₁₋₄₂ aggregate sizes with a 5 minute analysis time [74]. In addition, this study examined the effect of seeding a freshly prepared A β ₁₋₄₂ sample with a fibrillar A β ₁₋₄₂ seed. For samples without a seed, a broad peak was observed with CE-LIF as opposed to seeded samples that contained both a sharp and broad peak, although no specific sizes were determined.

In addition to CE-LIF, microfluidic capillary electrophoresis (MCE) has been used to study A β . MCE is similar to CE except operates on a much smaller scale. The advantages of MCE over conventional electrophoresis methods include low sample consumption and a strong potential for automation and integration [75,76]. MCE has been utilized to study A β monomeric species. A study by Mohamadi *et al.* utilized MCE-LIF for the separation of five A β isoforms

(A β ₁₋₃₇, A β ₁₋₃₈, A β ₁₋₃₉, A β ₁₋₄₀, and A β ₁₋₄₂) [77]. However, MCE has yet to be applied for the study of A β oligomers.

CE as a technique for the detection of A β species formed throughout aggregation is still in its early stages. CE-UV has been utilized to detect small A β ₁₋₄₀ species ranging from 3 - 30 kDa as well as to separate A β ₁₋₄₀ monomer from fibrillar species. A β ₁₋₄₂ species ranging from 3 - 50 kDa and >50 kDa have been detected using CE-UV. In addition, the separation of A β ₁₋₄₂ monomer from fibrillar species has been achieved using CE-UV, and the separation of two different A β ₁₋₄₂ fibrils has been accomplished with CE-LIF. The development of MCE has prompted researchers to apply this technique to the study of A β , with initial investigations demonstrating the separation of five A β isoforms differing in length by a single residue. The ability of CE to detect sizes from monomers to fibrils offers the potential to monitor the amyloid aggregation process over time, and the use of LIF provides the potential for examining physiologically relevant concentrations. However, further improvements to this technique must be made in order to enhance the resolution of intermediate sized A β species.

3. Spectroscopic Techniques for the Quantification of A β Oligomer Sizes

3.1 Mass Spectrometry

Mass spectrometry (MS) is a widely used technique for the detection of monomeric and oligomeric A β . In MS, the sample undergoes vaporization, and components are ionized by impacting them with an electron beam. Ions are separated by their mass-to-charge ratio using electromagnetic fields, and the ion signal is processed into a mass spectrum characteristic of the analyte. MS uses a variety of ionization sources depending on the sample state. For vapor samples, the most common source used to generate gas-phase ions is a radioactive ionization (RI) source [78,79]. However, other ion sources such as corona discharge ionization (CDI)

[80,81], photoionization (PI) [80,82], and secondary electrospray ionization (SESI) [83-86] have been used as well. The most commonly used ionization source for liquid samples is electrospray ionization (ESI) [83-86], and for solid samples matrix assisted laser desorption ionization (MALDI) [87-90] and laser desorption ionization (LDI) [91-93] are widely used ionization sources. In addition, there are various types of mass analyzers that process the ion signal into a mass spectrum. These include time-of-flight, quadrupole, ion trap, Fourier transform ion cyclotron, magnetic sector, and tandem instruments as recently reviewed by Kanu *et al.* [94]. The most common MS techniques used for protein analyses are MALDI-MS and ESI-MS.

3.2 Matrix-Assisted Laser-Desorption Ionization (MALDI)-MS

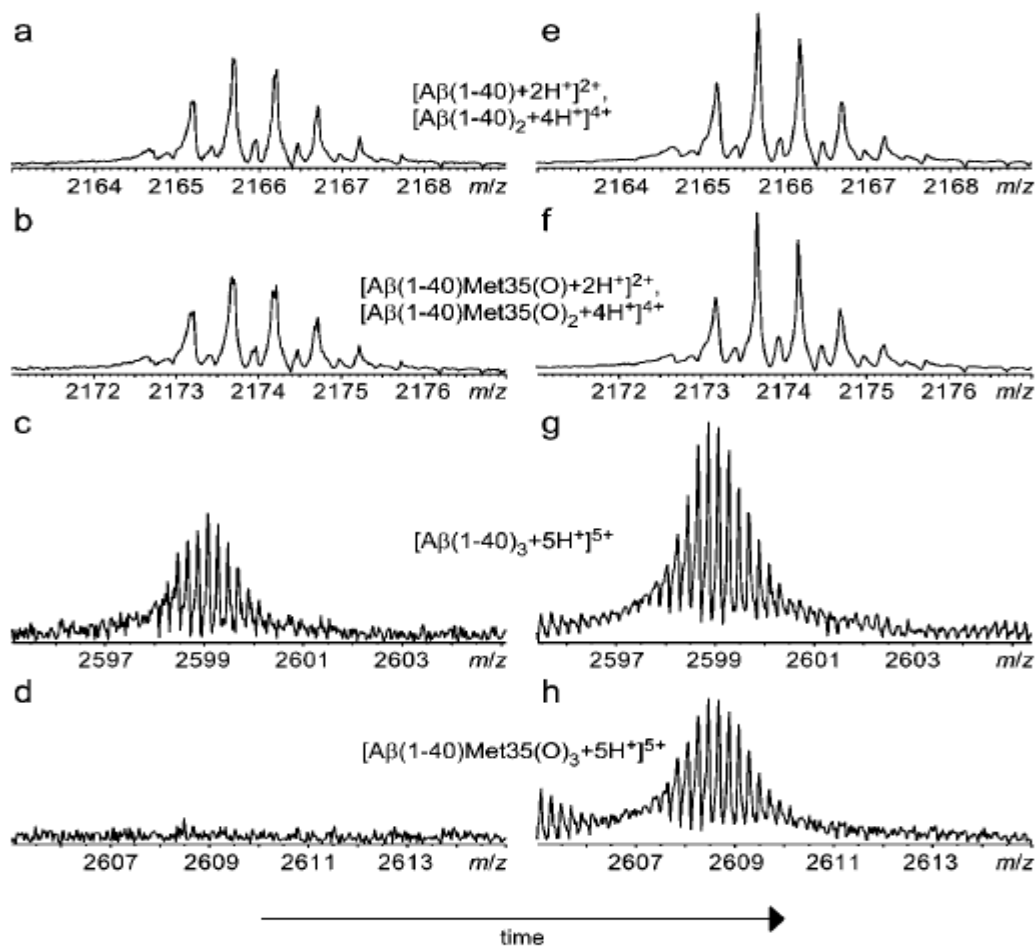
MALDI-MS may be combined with other separation techniques such as SDS-PAGE to provide more quantitative size estimates. Iurascu *et al.* utilized SDS-PAGE in combination with MALDI-MS to analyze a solution of A β ₁₋₄₀ solubilized in fibril growth buffer at pH 7.5 for 5 days at 37°C [48]. MALDI-MS indicated that the soluble fraction contained two different ion mobilities, indicative of oligomerization. Parallel analysis using SDS-PAGE and Tris-tricine PAGE revealed the presence of oligomeric A β ₁₋₄₀ of ~20 kDa (pentamer). A study by Maji *et al.* subjected wild-type and tyrosine substituted A β ₁₋₄₀ and A β ₁₋₄₂ to PICUP and quantified the resulting aggregate sizes via MALDI-MS and SDS-PAGE [95]. SDS-PAGE yielded wild-type A β ₁₋₄₀ bands for monomer through hexamer. However, MALDI-MS was only able to attain masses for the monomer through tetramer bands, while masses for the pentamer and hexamer bands could not be measured. This inconsistency could be attributed to the presence of very small quantities of pentamer and hexamer. Alternatively, these species may not be desorbed from the MALDI matrix as readily as smaller oligomers. In addition, MALDI-MS spectra of tyrosine substituted A β ₁₋₄₂ oligomers were not obtained, suggesting that either these oligomers could not

be incorporated into the MALDI matrix due to their exceptional hydrophobicity or their covalent or weak noncovalent interactions were disrupted by the desorption/ionization process. These results show that although MALDI-MS may be used to quantify A β oligomers, this technique does have drawbacks including limited matrix interactions as well as the inability to distinguish molecules with overlapping charge-to-mass ratios, expense, and labor intensive analyses [96,97]. In addition, since MALDI is typically coupled with a pre-separation step such as SDS-PAGE, its detection capabilities may vary depending on the pre-separation technique used.

3.3 Electrospray Ionization (ESI)-MS

ESI-MS has been used to analyze liquid A β samples. Palmblad *et al.* have utilized ESI-MS to study the effect of Met-35 oxidation on the formation of A β ₁₋₄₀ oligomers [98]. They found that freshly dissolved A β ₁₋₄₀ and A β ₁₋₄₀Met35(O) both exhibited monomers and dimers (Figure 6, panels a and b). In addition, A β ₁₋₄₀ and A β ₁₋₄₀Met35(O) incubated for 41 minutes exhibited similar monomer and dimer signals (Figure 6, panels e and f). In contrast, trimers and tetramers were detected for freshly dissolved A β ₁₋₄₀ (Figure 6, panel c) whereas these species were not detectable for freshly dissolved A β ₁₋₄₀Met35(O) (Figure 6, panel d). However, after >95 minutes of incubation, A β ₁₋₄₀ and A β ₁₋₄₀Met35(O) exhibited similar trimer and tetramer signals (Figure 6, panels g and h). These results suggest that Met-35 oxidation slows a conformational change that may be necessary for early formation of A β ₁₋₄₀ trimers. Although ESI-MS can be used as a way to freeze protein oligomers in time, complications arise when a protein could simultaneously populate a number of states with the same mass-to-charge ratio [97]. This complication makes it difficult to quantify different size oligomers that have the same mass-to-charge ratio.

Figure 6: ESI-Mass spectra of 4.0 μM freshly dissolved $\text{A}\beta_{1-40}$ (panels a and c), freshly dissolved $\text{A}\beta_{1-40}\text{Met35(O)}$ (panels b and d), $\text{A}\beta_{1-40}$ and $\text{A}\beta_{1-40}\text{Met35(O)}$ incubated for 41 minutes (panels e and f), and $\text{A}\beta_{1-40}$ and $\text{A}\beta_{1-40}\text{Met35(O)}$ incubated for >95 minutes (panels g and h). $\text{A}\beta_{1-40}$ samples were dissolved in H_2O and $\text{A}\beta_{1-40}\text{Met35(O)}$ samples were dissolved in H_2O and 2.7% H_2O_2 . Reprinted with permission from [98]. Copyright (2002) The American Society for Biochemistry and Molecular Biology.



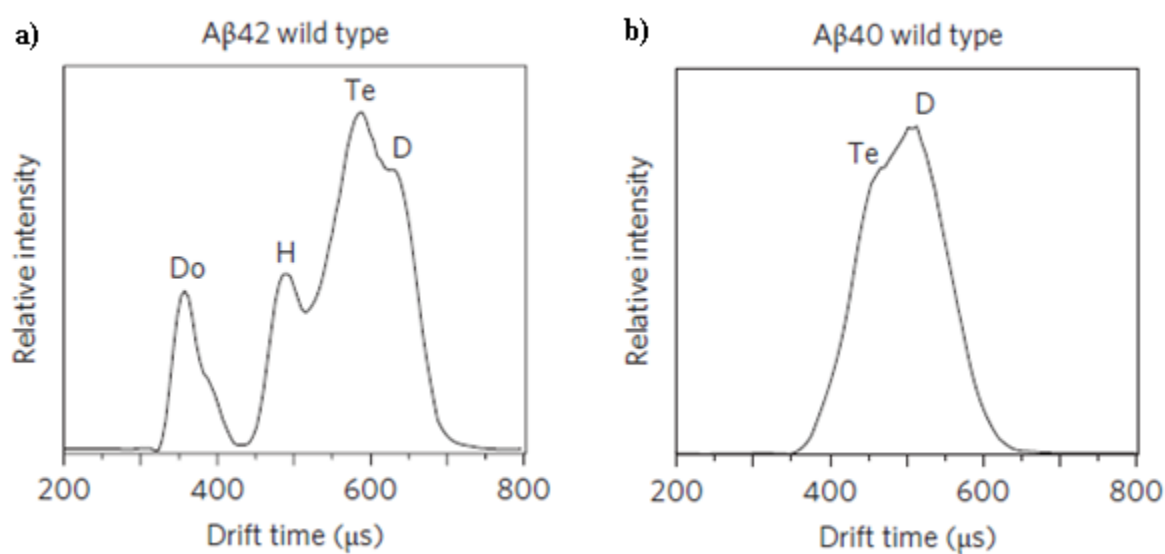
3.4 Ion Mobility (IM)-MS

IM-MS is capable of separating ions by both their shape and charge, which has rendered it a successful technique for the separation of conformers of various shapes arising from a single protein [94,99-101]. Ions are separated in time according to their cross sections by passing them through a drift cell containing helium gas under the influence of a weak electric field [102]. The flight times are combined with the drift times to yield the mass-to-charge IM distributions for all ions in the sample. The ability of IM-MS to separate species that differ in shape or size but have the same mass-to-charge ratio has made this technique a powerful tool for analyses of the early stages of A β oligomerization.

Various research groups have utilized IM-MS to gain a better understanding of the early events of A β aggregation. A β_{1-40} conformational states in freshly dissolved and aggregated solutions have been studied by Iurascu *et al.* [48]. Two different conformational states were obtained for freshly dissolved A β_{1-40} and the soluble fraction obtained by A β_{1-40} incubation for 5 days at 37°C and pH 7.5. Bernstein *et al.* used IM-MS to study the aggregation of A β_{1-42} versus A β_{1-42} with a Phe19→Pro19 substitution [103]. Monomers and large oligomers were produced by unfiltered A β_{1-42} , while protein passed through a 10,000 amu filter yielded monomer, dimer, tetramer, hexamer, and an aggregate of two hexamers. In contrast, the Pro19 alloform produced monomer, dimer, trimer, and tetramer but no large oligomers. In a more recent study by Bernstein *et al.*, a mechanism for A β_{1-40} and A β_{1-42} oligomerization and eventually fibril formation was postulated [104]. Using IM-MS, this group was able to determine the shape and size of A β_{1-40} and A β_{1-42} oligomers. A β_{1-40} oligomerization proceeded via the formation of dimer and tetramer followed by the very slow formation of fibrils containing a β -sheet structure. In contrast, A β_{1-42} proceeded via the formation of dimer, tetramer, and a hexameric paranucleus

followed either by the formation of dodecameric species or the slow conversion into fibrils containing a β -sheet structure. Representative IM-MS data obtained by Berstein *et al.* for $A\beta_{1-42}$ and $A\beta_{1-40}$ are shown in Figure 7. Similar findings about the early oligomerization behavior of $A\beta_{1-40}$ and $A\beta_{1-42}$ were obtained by Murray *et al.* using IM-MS [102]. In addition, these researchers found that in an equimolar mixture of $A\beta_{1-40}$ and $A\beta_{1-42}$, $A\beta_{1-40}$ inhibited the formation of higher molecular weight oligomers by $A\beta_{1-42}$. This result suggests that $A\beta_{1-40}$ could sequester $A\beta_{1-42}$ into stable tetramers and prevent the further oligomerization of $A\beta_{1-42}$ into dodecameric species.

Figure 7: IM-MS arrival time distributions for (a) 30 μM $\text{A}\beta_{1-42}$ in 49.5% H_2O , 49.5% acetonitrile, and 1% NH_4OH and (b) 30 μM $\text{A}\beta_{1-40}$ in ammonium acetate (pH 7.4). D = dimer, Te = tetramer, H = hexamer, Do = dodecamer with a $z/n = -5/2$. Figure 7a adapted with permission from [103]. Copyright (2005) American Chemical Society. Figure 7b adapted by permission from Macmillan Publishers Ltd.: Nature Chemistry [104], copyright (2009).



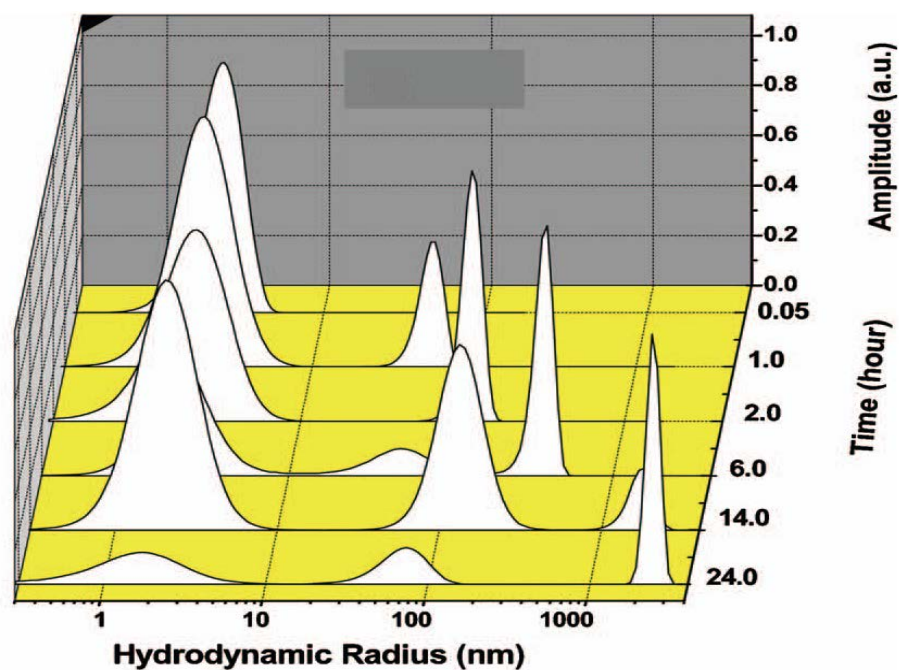
3.5 Fluorescence Correlation Spectroscopy

Fluorescence correlation spectroscopy (FCS) has also been utilized to gain information about the size of A β species formed throughout aggregation [24,105-107]. FCS was originally developed by Eigen and Rigler in the early 1990s [108]. In FCS, unlabeled protein is combined with fluorescently labeled protein and, at various times throughout aggregation, the fluorescent dye is excited by a sharply focused laser beam. The emitted fluorescence of a small number of molecules in solution is observed. The fluorescence intensity fluctuates due to Brownian motion of the particles, and an intensity correlation function can be used to determine the average number and average diffusion time (ie. molecular size) of molecules. Advantages of FCS include high sensitivity (nM range and below), ability to examine a wide range of molecular sizes (ie. monomer, oligomer, fibrils) [109], fast analysis times [109], and small sample volumes (femtoliter) [110]. In addition, no pre-separation step is required for the determination of particle radius via FCS. However, assumptions must be made about the kinetics of the aggregation process as well as molecular shape in order to determine molecular weight.

Various researchers have employed FCS to monitor A β aggregation. A study by Matsumura *et al.* utilized FCS to monitor the aggregation of A β ₁₋₄₀ and A β ₁₋₄₂ and observed distinct aggregation pathways, dependent upon incubation conditions, that resulted in the formation of either oligomeric species or fibrils [24]. Two different site-specific labels at either the N-terminus or Lys¹⁶ were used to monitor aggregation. One pathway involved the formation of 10 - 15 nm spherical A β ₁₋₄₂ assemblies of ~330 kDa, termed amylospheroids (ASPDs), appearing after 5 hours of gentle agitation of a 50 μ M A β ₁₋₄₂ solution in F12 buffer at 4°C. These ASPDs were formed from A β species of ~12.7 kDa initially present in solution. In addition, the aggregation pathways were similar for the N-terminus and Lys¹⁶ site-specific labels. An

alternative pathway involved fibril formation from 100 μ M A β_{1-40} solutions in Dulbecco's PBS (pH 3.5) with gentle agitation at 4°C. This pathway began with dimer formation at 0 hours, followed by the formation of intermediate sized species of 15 - 40 nm after 2 - 9 hours. Eventually, larger molecular weight fibrils (14,000 kDa) were formed after 24 hours using A β labeled site-specifically at Lys¹⁶. However, much larger aggregates (120,000 and 3,900,000,000 kDa) were formed after 24 hours using A β labeled site-specifically at the N-terminus. It was thus postulated that the Lys¹⁶ fluorescent probe interfered with aggregation into larger fibrils. By employing oligomer formation conditions, Cizas *et al.* used FCS to observe much smaller A β_{1-42} oligomers [105]. They dissolved A β_{1-42} in HFIP with subsequent dilution into de-ionized water and incubation at 20°C with or without agitation (500 rpm) for 24 hours. The average radius observed for unagitated samples was ~3.4 nm while the radius for agitated samples was ~8 nm. Garai *et al.* have applied FCS to monitor the A β_{1-40} aggregation process when monomer is initially the predominant species present in solution (Figure 8, time = 0.05 hours) [107]. After 1 hour, intermediate aggregates of 20 - 100 nm formed and grew to sizes >1000 nm after 24 hours (Figure 8, time = 2 - 24 hours). These A β_{1-40} intermediate sizes are larger than those observed by Mastmura *et al.* and could be due to different sample preparations or the presence of different A β species at 0 hours. These studies again show that although A β_{1-40} and A β_{1-42} differ by only two amino acid residues, the aggregates formed are considerably different.

Figure 8: Size distributions obtained via FCS for A β_{1-40} dissolved in 2.8 mM NaOH, diluted to 10 μ M in HEPES (pH 7.4), and incubated at room temperature. Sample taken at \sim 3 minutes shows predominantly monomeric species with the formation of intermediate aggregates of 20 – 100 nm after 1 hour and further growth into larger aggregates $>$ 1000 nm after 24 hours. Reprinted with permission from [107]. Copyright (2008), American Institute of Physics.



3.6 Summary of Spectroscopic Methods

MS is capable of detecting low oligomer concentrations but is expensive and has difficulty separating species with identical mass-to-charge ratios such as A β aggregates [96,97]. To address this problem, MS is often coupled with an upstream separation technique such as SDS-PAGE [48,95]. In addition, IM-MS has been utilized for the separation of different sizes and conformations of A β ₁₋₄₀ and A β ₁₋₄₂ with promising results for small oligomers. However, the addition of a step such as IM also increases the time needed for analysis and therefore decreases the chances of detecting transient species. Consistent results for A β ₁₋₄₀ and A β ₁₋₄₂ oligomer sizes formed during the earliest events of aggregation have been obtained using MS techniques. However, the detection of larger A β ₁₋₄₀ and A β ₁₋₄₂ oligomeric species ranging from ~32 - ~100 kDa has not been achieved using MS. FCS does not require a pre-separation step to determine the particle radius of species in a sample. This technique has been successfully applied for the detection of small and intermediate sized A β oligomers as well as large A β fibrils. However, FCS yields average values of particle radius for a population of aggregates and not individual particle sizes or their distributions.

4. Additional Techniques Utilized for A β Aggregate Size Determinations

4.1 Light Scattering Techniques

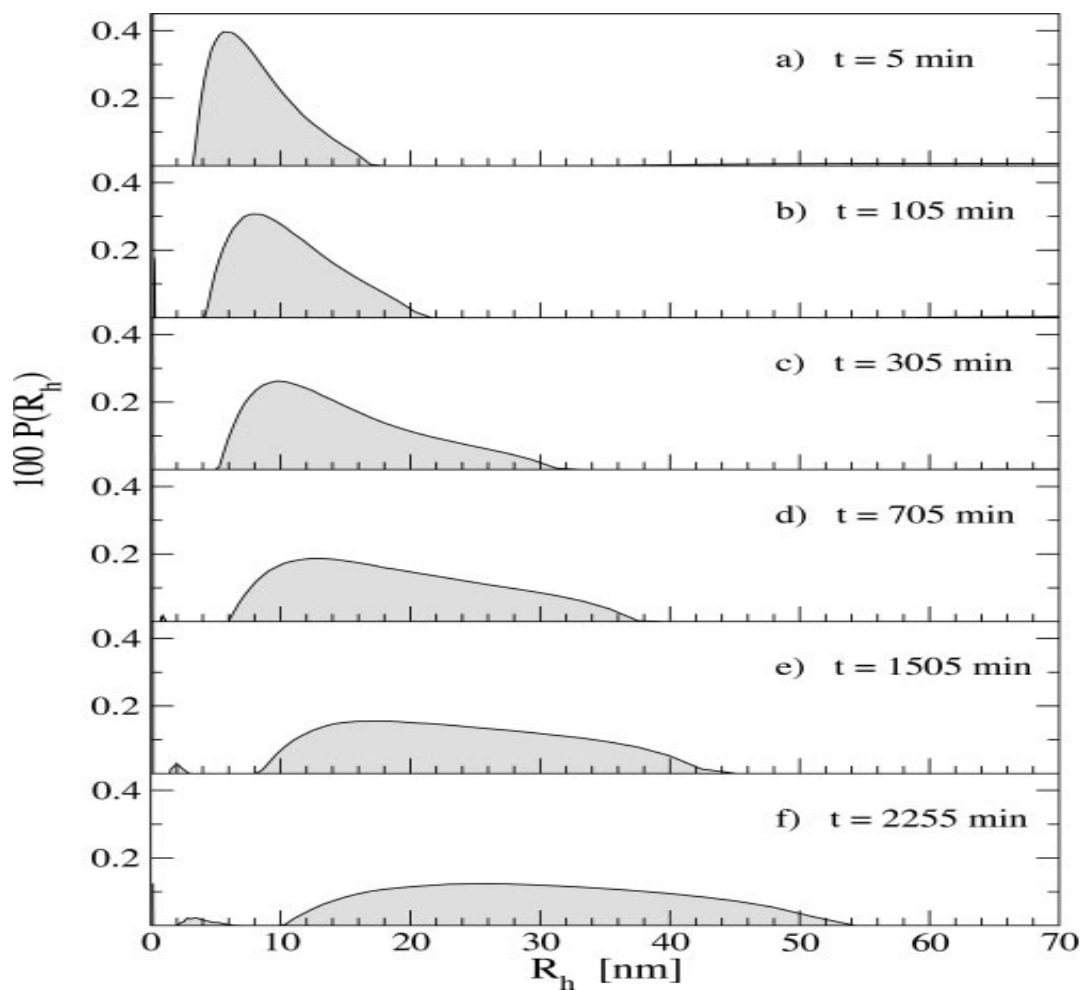
Light scattering techniques have been used to measure A β aggregate sizes. Classical, or multi-angle, light scattering (MALS) employs a well collimated, single frequency light beam to illuminate a sample of macromolecules [111]. When incident light interacts with the macromolecules in solution, an oscillating dipole is induced and the light is re-radiated, or scattered [112]. Aggregated structures induce coherent scattering, and as a result the intensity of scattered light is dependent upon molar mass. Furthermore, destructive and constructive

scattering that result from the independent scattering of individual molecular elements can give rise to an angular dependence of the scattered light, which is a function of the size of the molecule. Thus, the intensity of the scattered light is measured as a function of scattering angle, often referred to as Rayleigh scattering, to yield the molar mass and root mean square (rms) radius of the macromolecules [112]. MALS is ideal for characterizing larger assemblies (>10 nm). In contrast, for analyses in which smaller molecules are present in solution, dynamic light scattering (DLS), also known as quasi-elastic light scattering (QELS), is used. DLS employs a fast photon counter to measure time dependent fluctuations in scattered light at a single angle (usually 90°), which are related to the rate of diffusion of the macromolecules [112,113]. Measurement of diffusion rates allows calculation of the hydrodynamic radius (R_H) of macromolecules using the Stokes-Einstein equation [113]. When used as standalone techniques, MALS yields the weight-averaged molar mass for all molecules in solution. While DLS can distinguish populations that differ in size by a factor of five or more, individual peaks exhibit a high degree of polydispersity. Therefore, it is often necessary to utilize a pre-separation step in conjunction with light scattering to obtain an accurate estimate of the relative amounts of individual aggregates present in solution. In addition, the exponential dependence of scattering on aggregate size prohibits the detection of low quantities of small aggregates in the presence of larger species.

Various researchers have utilized MALS and/or DLS to characterize A β assemblies formed throughout aggregation [114-117]. Carrotta *et al.* utilized both MALS and DLS to monitor the aggregation of a 185 μ M A β_{1-40} sample at pH 3.1 and 37°C [117]. DLS was used to characterize aggregate sizes formed during the early stages of aggregation up to ~38 hours, as shown in Figure 9. After 5 minutes (Figure 9a), an average R_H of 7 nm was obtained. The size

distribution became more polydisperse over time and ranged from 10 - 52 nm after 37 hours (Figure 9f). However, only average size distributions could be obtained and no information was reported about the concentrations of each aggregate species (ie. monomer, dimer, etc.). Larger aggregates (hundreds of microns) were formed after 2 weeks as detected by MALS.

Figure 9: Time evolution of R_H for a 185 μM $\text{A}\beta_{1-40}$ sample incubated at pH 3.1 and 37°C. Distributions were determined using a constrained regularization method. Reprinted with permission from [117]. Copyright (2005) The American Society for Biochemistry and Molecular Biology.



Similar to these findings, Lomakin *et al.* observed using DLS the initial formation of a spherocylindrical micelle with average R_H of 7 nm immediately following dissolution of $A\beta_{1-40}$ at pH 2 [115]. In addition, they reported two different kinetic patterns for aggregation of $A\beta_{1-40}$ prepared at a concentration either above or below the critical micelle concentration (CMC) of 100 μ M [114]. Complimentary DLS and MALS studies by Murphy and Pallitto also demonstrated an effect of $A\beta$ concentration upon aggregate formation [118]. They demonstrated that dilution of $A\beta_{1-40}$ from urea into PBS yielded larger aggregates at lower protein concentrations, while the increase in R_H for aggregates was proportional to the protein concentration. In addition, MALS data indicated that the linear density of aggregates increased with protein concentration. Thunecke *et al.* have utilized MALS and DLS to study the aggregation of $A\beta_{1-40}$ and $A\beta_{1-42}$ in acetonitrile-water mixtures [116]. At the onset of aggregation, $A\beta_{1-42}$ was present as a 2 nm oligomer and rapidly formed fibrils with a length <50 nm within 4.5 hours. In contrast, $A\beta_{1-40}$ initially exhibited large aggregates that grew 70 times slower than aggregates of $A\beta_{1-42}$. However, the presence of these large aggregates may preclude observation of a separate population of oligomers. These findings highlight differences in the dissolution and aggregation of $A\beta_{1-40}$ and $A\beta_{1-42}$.

4.2 Light Scattering in Combination with Other Techniques

Because light scattering techniques provide information about the weight-average molar mass and radius for all molecules in solution, they are often coupled with a pre-separation technique such as asymmetric field flow fractionation (AFFF) [119] or SEC [25,120,121] to better characterize individual $A\beta$ oligomeric species. A study by Nichols *et al.* utilized MALS with SEC as well as DLS to characterize $A\beta_{1-40}$ protofibrils following growth by monomer elongation or lateral association [120]. They found that protofibrils isolated by SEC exhibited an

average R_H of 51 nm and molecular weight, determined via MALS of 30,000 kDa. Protofibrils that had grown by monomer deposition had an average R_H of 143 nm and molecular weight of 57,000 kDa, while protofibrils that had grown by lateral association had an average R_H of 104 nm and molecular weight of 86,000 kDa. Furthermore, SEC-MALS revealed that the mass per unit length of protofibrils was unchanged during elongation, but was increased following association. The temporal change in size of $A\beta_{1-40}$ protofibrils isolated by SEC has also been monitored via DLS by Walsh *et al.* [121]. The initial average R_H for protofibrils isolated by SEC was ~27.8 nm, and protofibril size grew to 80.6 nm over a period of 9 days when 17 μ M $A\beta_{1-40}$ in Tris-HCl (pH 7.4) containing 0.04% w/v sodium azide was incubated at room temperature.

AFFF is another technique that has been coupled with light scattering to estimate the molecular weight of individual $A\beta$ aggregates. AFFF exploits the parabolic flow profile created by the laminar flow of a sample through a thin, parallel plate flow channel, where the lower surface is solvent permeable [122]. A perpendicular force applied to the laminar flow stream drives molecules towards the permeable boundary layer of the channel [123]. Because Brownian motion of the particles creates a counteracting force, smaller particles localize higher in the channel leading to separation of different molecular sizes, with smaller molecules eluting first [122]. Rambaldi *et al.* utilized AFFF-MALS to monitor the aggregation of $A\beta_{1-42}$ in PBS (pH 7.4) at room temperature over 24 hours [119]. At 0 hours, two major peaks were obtained corresponding to molecular weights of ~60 kDa and ~1,000 - 100,000 kDa. In addition, the retention time of the ~60 kDa species decreased between 0 and 4 hours, corresponding to an increase in aggregate size of 6.5 - 4.7 nm. The intensity of the two peaks also decreased over 24 hours, possibly due to irreversible adsorption of the sample to the permeable surface. Although AFFF-MALS has several advantages, including gentle, rapid, and non-destructive separation,

improvements to the ultrafiltration membrane are critical to enhance analysis capabilities. In addition, the smallest molecular weight cutoff for membranes is 5 kDa, making detection of A β monomeric species difficult.

4.3 Centrifugation

Centrifugation has also been explored as a method for determining A β size. Here, sedimentation coefficient (s) values can be correlated with molecular weight. Mok and Howlett provide a nice overview of sedimentation velocity centrifugation in the context of A β analysis [124]. Ward *et al.* used density gradient centrifugation to fractionate A β_{1-40} samples incubated at pH 7.4, 35°C for 30 minutes, 18 hours, or 18 days [26]. Using SDS-PAGE with Western blotting to analyze sedimented samples, they found that A β_{1-40} incubated for 18 hours contained only small molecular weight oligomers (4 – 17 kDa), while A β_{1-40} incubated for 18 days showed the presence of a >250 kDa band as well as significant streaking, indicating other unresolved sizes. Huang *et al.* used analytical ultracentrifugation to compare A β_{1-40} samples prepared at pH 3, 5, and 7 [125]. They determined that at pH 5 there were no soluble aggregate species. At pH 7, they identified small oligomers with an average molar mass of 12.1 kDa, and at pH 3 they identified a range of aggregate sizes with an average molecular weight of 1 MDa. Nagel-Stefer *et al.* also used sedimentation velocity centrifugation for the analysis of A β_{1-42} samples after 5 days of agitation at room temperature and were able to detect “globular species” ranging in size from ~270 kDa - 3.8 MDa as well as even larger aggregates [126]. Interestingly, they also compared three different simulation methods for determining molecular weight from sedimentation values and obtained molar masses that differed by approximately one order of magnitude.

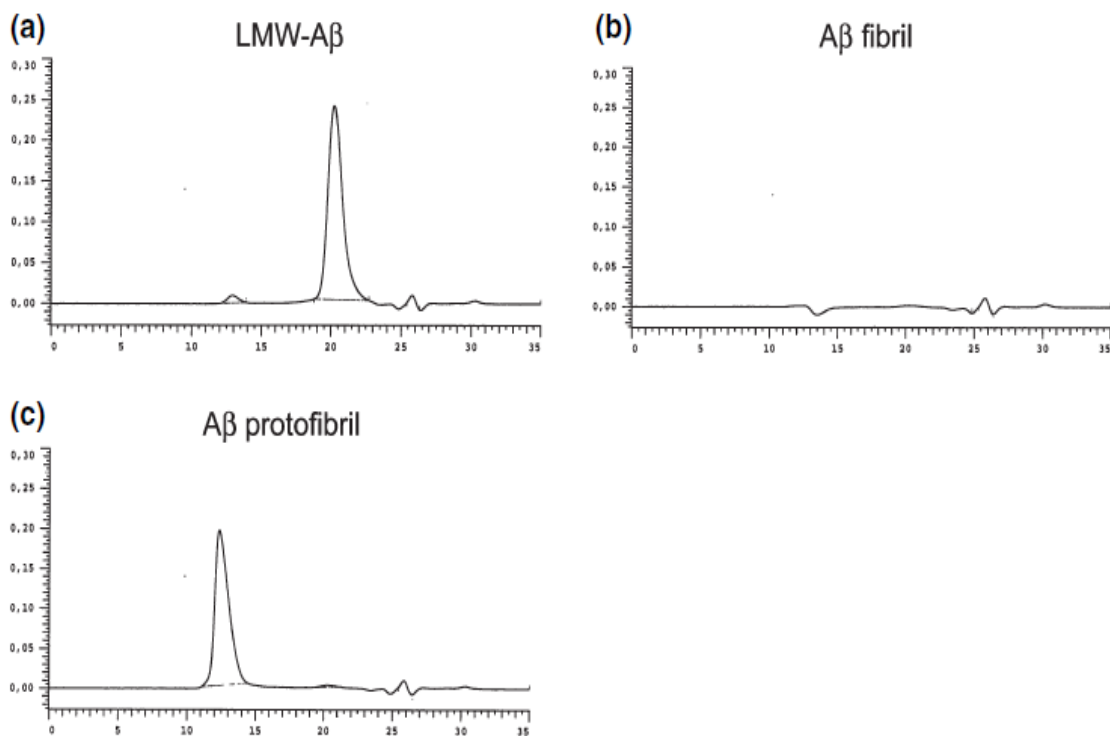
4.4 Size Exclusion Chromatography

SEC, a chromatographic technique, separates molecules based on molecular hydrodynamic volume or size. Molecules too large to penetrate the pores of the column packing material elute in the void volume, while smaller molecules travel through the pores and elute at later times. Globular proteins are often used as standards to estimate the size of A β oligomers. However, since A β is a linear, hydrophobic peptide, comparisons between the elution behavior of A β oligomers and size standards are difficult [127]. In addition, the sample is subjected to a several-fold dilution, which facilitates the dissociation of small unstable oligomers [128], thereby precluding the detection and size estimation of these species.

Although SEC is typically utilized in conjunction with another technique, SEC as a standalone technique has been employed for the study of A β aggregates [129-131]. Englund *et al.* used SEC to detect low molecular weight A β aggregates, A β protofibrils, and A β fibrils formed using different A β sample preparations [130]. The size of low molecular weight A β aggregates ranged from 4 - 20 kDa (Figure 10, panel a), while A β protofibrils were >100 kDa (Figure 10, panel c). A more narrow size distribution of A β_{1-42} oligomers of 24 ± 3 kDa (pentamer - hexamer) has been obtained by Ahmed *et al.* with SEC [129]. This resolution was achieved by stabilizing A β_{1-42} oligomers at a low temperature (4°C) and low salt concentration (10 mM NaCl). Zheng *et al.* have analyzed via SEC freshly prepared 1 mg/mL A β_{1-40} in PBS (pH 7.4), diluted from DMSO, and achieved resolution of an A β_{1-40} trimer with molecular weight of 11.6 - 15.7 kDa [131]. The difference in sizes obtained by Ahmed *et al.* and Zheng *et al.* most likely result from differences in sample preparation. While these studies show promising results for resolution of a single low molecular weight A β oligomer, the resolution of individual

intermediate A β oligomeric sizes formed during aggregation has not been achieved using SEC as a standalone technique.

Figure 10: HPLC-SEC chromatograms of A β aggregates produced using sample preparations of 50 μ M synthetic A β designed to optimize (a) low molecular weight A β_{1-40} oligomers and (c) A β_{1-42} protofibrils. To ensure that insoluble fibrils were not present in solution, these species were removed via centrifugation prior to analysis, and this was confirmed by an absence of SEC signal in (b), a fibrillar A β_{1-42} preparation. Absorbance at 214 nm is given on the y-axis and retention time is given on the x-axis. Reprinted from [130] published by John Wiley and Sons, © 2007 The Authors Journal Compilation © 2007 International Society for Neurochemistry.



4.5 Summary of Additional A β Aggregate Size Determination Techniques

Light scattering techniques, such as MALS and DLS, have been used to detect both small and large A β aggregates. DLS is more suitable for the detection of smaller aggregates and gives information about aggregate size, or R_H , while MALS has been utilized for the detection of larger A β species, including fibrils, and can provide information about molar mass. MALS and DLS, however, give a weight-average molar mass or R_H for all molecules in solution and must be coupled to another technique in order to increase the resolution of individual sizes. SEC as a standalone technique has been utilized to detect low molecular weight A β oligomers and protofibrils, and SEC-MALS has been used to characterize protofibrils formed via different growth mechanisms. However, due to the dilutions required by SEC, small unstable oligomers are often dissociated, thereby precluding their analysis. AFFF-MALS does not require a pre-fractionation step and has been used to separate A β oligomers of ~60 kDa from larger species. This technique yields a gentle, non-destructive separation of molecules. However, further improvements to the ultrafiltration membranes must be made in order to reduce adsorption of the sample to the membrane. Centrifugation has also been explored for the separation of small oligomers (4 – 17 kDa) and larger species (>250 kDa) but requires an uncertain correlation of sedimentation coefficients with molar mass. Each of these techniques are suitable for the detection of a wide range of A β aggregates present throughout aggregation but present difficulties with respect to the resolution and quantification of individual A β aggregate sizes.

5. Techniques Utilized for A β Oligomer Identification

While this review focuses primarily on techniques capable of qualitatively determining the size of A β oligomers, techniques that can identify the presence of oligomers, without providing information about oligomer size, are also available. Although qualitative in nature, we

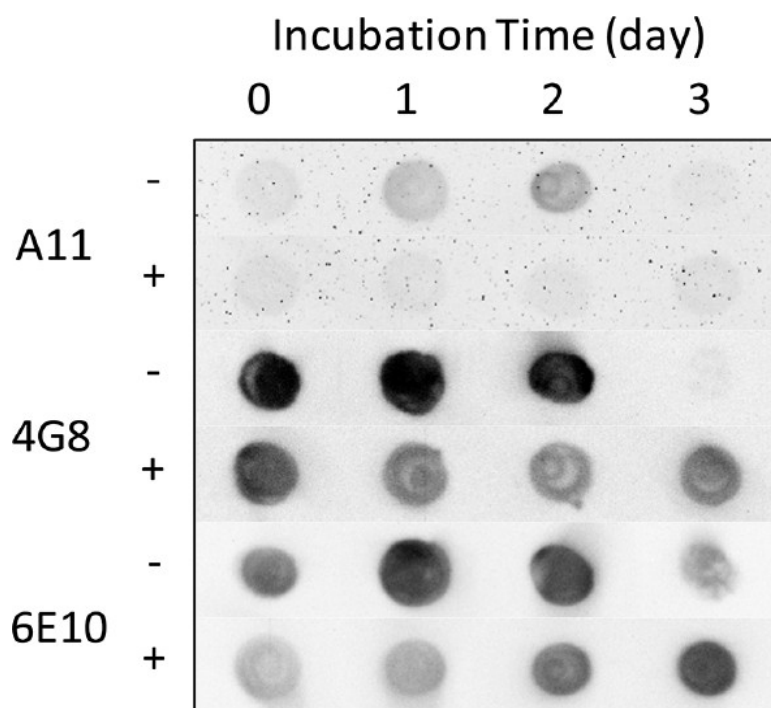
have chosen to briefly discuss two of these techniques, dot blot and ELISA, as a result of their frequent use and emerging interest.

5.1 Dot Blot

Dot blots employ a protein captured upon a membrane as a spot, or dot. A primary antibody binds to the protein epitope of interest followed by the binding of a secondary antibody to facilitate detection. When dot blots are probed with antibodies that specifically recognize oligomeric A β , they can confirm the presence of oligomers but give no information about aggregate size. Three different A β antibodies, oligomer-specific A11 or sequence specific 4G8 and 6E10 (see Table 1 for A β binding epitopes), were employed in conjunction with a dot blot assay for detection of aggregating A β by Wong *et al.* [57]. A β_{1-40} was diluted to 50 μ M in PBS (pH 7.4) and incubated at 37°C. At times ranging from 0 - 3 days, a sample was analyzed via dot blot, as shown in Figure 11. A11 binding revealed the transient appearance of oligomers in uninhibited samples, while detection via 4G8 and 6E10 remained constant until later times when signals decreased, presumably due to masking of binding sites following aggregation. Changes in these patterns in the presence of inhibitor demonstrated the ability of the inhibitor to prevent oligomer formation and slow the evolution of larger aggregates. Necula *et al.* used a dot blot assay to monitor the oligomerization of A β_{1-42} dissolved in 100 mM NaOH, diluted to 45 μ M in PBS (pH 7.4), and incubated at room temperature for 10 days [132]. Similar to Wong *et al.*, they probed the specificity of three different antibodies, oligomer-specific A11 and sequence specific 6E10 and 4G8. At 0 days, 6E10 and 4G8 strongly reacted with A β_{1-42} aliquots, while A11 reacted weakly, indicating that only monomeric species were present. A strong immunoreactivity for A11 was observed after 4 days and continued to increase in intensity over 10 days, similar to

results obtained by Wong *et al.* Again, this was accompanied by a decrease in immunoreactivity of 6E10 and 4G8.

Figure 11: A β aggregation monitored via dot blot. A 50 μ M A β_{1-40} sample was incubated in PBS (pH 7.4) at 37°C in the presence (+) or absence (-) 3 x Brilliant Blue G (BBG) inhibitor. Samples were taken on the indicated days and spotted on a nitrocellulose membrane. Oligomer-specific A11 antibody and A β -sequence specific antibodies 4G8 and 6E10 were used to detect aggregates. Reprinted with permission from [57]. Copyright (2011) American Chemical Society.



5.2 Enzyme-Linked Immunosorbent Assay

ELISA is a commonly used technique for the identification of A β oligomers. ELISA may be used in a traditional or sandwich assay format. In the traditional format, protein adsorbed at a surface can be detected using a primary antibody that is specific for A β oligomers (see Table 1). This primary antibody can be directly linked to an enzyme that converts added substrate to a detectable signal (direct ELISA) or can be coupled with a secondary antibody containing the enzyme moiety (indirect ELISA). The latter format serves to enhance the assay signal. Alternatively, in the sandwich ELISA format, a sequence-specific capture antibody (see Table 1) adsorbed onto the surface is used to capture A β protein, which is subsequently detected using the same sequence-specific antibody, such that only A β species containing multiple monomeric units, and therefore multiple epitopes, are detected [130,133]. Consequently, this sandwich ELISA will recognize only aggregated A β , but not A β monomer. Although ELISA can identify the presence of A β oligomers in a sample, this technique is not capable of determining sizes of these oligomeric species. Therefore, ELISA is most advantageous for the detection of oligomeric A β within a sample containing many different proteins.

Various researchers have utilized ELISA for the detection of A β oligomers [128,130,133-135]. A study by Englund *et al.* employed a sandwich ELISA with monoclonal antibody 158 for the detection of low molecular weight oligomeric A β_{1-40} produced by dissolving A β_{1-40} in 10 mM NaOH with dilution to 50 μ M in 2 X PBS and A β_{1-42} protofibrils produced by dissolving A β_{1-42} in 10 mM NaOH with dilution to 443 μ M in 2 X PBS and incubation overnight at 37°C [130]. Gonzales *et al.* utilized a similar ELISA assay to detect low molecular weight A β_{1-42} formed by dissolving A β_{1-42} in HFIP with dilution to 200 nM in PBS (pH 7.2) and incubation at 37°C for 24 hours [133]. The size of these species was confirmed with PAGE to be tetramer and pentamer;

however, the bands were very faint, indicating the superior sensitivity of the ELISA assay for these oligomeric species. A detection limit for A β ₁₋₄₀ oligomers of 80 nM was obtained in these studies.

5.3 Summary of A β Oligomer Identification Techniques

Dot blots and ELISAs have been employed to detect oligomeric A β assemblies. Dot blots have been used to observe the transient evolution of oligomers during aggregation, but provided no information about A β aggregate size. Low molecular weight A β oligomers and A β protofibrils have been detected via ELISA at nanomolar concentrations. However, PAGE was required to estimate the size of these species. Thus, these techniques can sensitively confirm the presence of oligomers but yield no size information.

6. Conclusions

This review describes a variety of techniques, summarized in Table 2, that are currently utilized to determine the size or presence of A β aggregates, with a focus upon oligomeric species. These techniques have been explored for the quantitative detection of different aggregate sizes with various limitations to their resolution, dependence on pre-analysis procedures, sensitivity, cost, etc. Electrophoretic techniques, such as SDS-PAGE, Western blotting, and CE, are widely used for size-based separations of A β aggregates. In particular, SDS-PAGE and Western blotting are suitable for the detection of monomeric and small oligomeric A β species. The separation of larger oligomers via SDS-PAGE is more difficult due to the sensitivity of these sizes to denaturing conditions, which can result in aggregate decomposition during analysis. The recent development of antibodies specific for A β oligomers has led to an increase in the application of Western blotting, dot blotting, and ELISA to study A β aggregation. However, the detection limits of Western and dot blotting prohibit study of

physiologically relevant A β concentrations. While more sensitive, ELISA is better suited for the identification of specific analytes, such as A β oligomers, present within a mixed population but cannot distinguish individual oligomer sizes. CE with LIF detection offers a highly sensitive detection of physiologically relevant concentrations, but the application of CE to amyloid aggregation analyses is still in the early stages. MS is another commonly used technique for A β aggregate size-based separations. MS has been successfully used to detect small oligomeric species (especially IM-MS) but quantitative analyses of aggregate size may be limited by the pre-separation step, the ability to differentiate species with highly similar charge-to-mass ratios, and high equipment costs. FCS, MALS, and DLS may be utilized for determination of A β aggregate size, but yield a weight-averaged molecular weight of species, thereby limiting the resolution of individual A β aggregate species. Centrifugation has been used to examine small oligomeric species up to large fibrils; however, selection of the method for determination of molar mass from sedimentation coefficients can play an important role in size estimation. SEC may be coupled with these approaches or used as a standalone technique; however, SEC is complicated by dilution of the analyte during separation, inadequate resolution of intermediate oligomeric species, and limited utility of size standards.

Although each of the methods discussed in this review has the capability to determine A β aggregate size, the pathogenic events that initiate the misfolding of A β and formation of aggregate species remain elusive. Hence, there is a continued need for improvement of these techniques in order to realize the effective detection of small size differences in A β oligomers. In order to leverage the advantages of each A β detection method, a combination of approaches must be utilized, allowing validation of findings from different techniques and a better understanding of the early events of the A β aggregation process.

Table 2: Summary of techniques for the quantitative detection and/or identification of A β aggregate sizes formed throughout the aggregation process.

Technique	Advantages	Disadvantages	Aggregate Sizes Detected	References
SDS-PAGE	<ul style="list-style-type: none"> • SDS offers strong size-based separation 	<ul style="list-style-type: none"> • SDS may induce non-native behavior and destabilize oligomers • Gel smearing 	4.5 - 20 kDa, >83 kDa	[45,46]
Native PAGE	<ul style="list-style-type: none"> • Ability to separate based on charge and hydrodynamic size 	<ul style="list-style-type: none"> • Gel smearing 	8 - 20 kDa, high molecular weight	[48,49]
Western Blotting	<ul style="list-style-type: none"> • High sensitivity and specificity, 	<ul style="list-style-type: none"> • Requires specific and expensive antibodies • Incomplete transfer of proteins onto membrane • Technically demanding 	4 - 16 kDa, 16.5 - 25 kDa, 30 - 97 kDa (with SDS-PAGE)	[45,50-54]
Capillary and Microfluidic Capillary Electrophoresis	<ul style="list-style-type: none"> • Fast, highly sensitive separation of proteins based on charge and hydrodynamic size • Low sample volume 	<ul style="list-style-type: none"> • Low resolution of intermediate sized Aβ oligomers • Irreproducibility 	4 - 50 kDa, >50 kDa, fibrils	[72-74]
Mass Spectrometry	<ul style="list-style-type: none"> • Fast data acquisition • Can identify multiple species with different mass-to-charge ratios 	<ul style="list-style-type: none"> • Inability to distinguish molecules with overlapping mass-to-charge ratios (MALDI, ESI) • Expensive • Labor intensive 	4 - 24 kDa, ~48 kDa, fibrils,	[48,95,98, 102-104]

Fluorescence Correlation Spectroscopy	<ul style="list-style-type: none"> • High sensitivity, ability to look at wide range of sizes within a sample • Fast analysis time • Low sample volume 	<ul style="list-style-type: none"> • Relies on assumptions about shape and kinetics of protein to determine molecular weight • Yields average molecular weight values 	~10 nm – 1 μ m (small oligomers – aggregates)	[24,105,107]
Light Scattering	<ul style="list-style-type: none"> • Direct measurement of molar mass and radius (MALS) • Simultaneous detection of multiple populations within a sample (DLS) 	<ul style="list-style-type: none"> • Yields weight-average molar mass and not size of individual species or their distribution • Exponential dependence of scattering on aggregate size 	>10 kDa (MALS) 1 nm – 1 μ m (DLS)	[112,116,117]
Centrifugation	<ul style="list-style-type: none"> • Ability to detect a wide range of sizes (oligomers – fibrils) • Fast analysis time 	<ul style="list-style-type: none"> • Theoretical size estimate depends on appropriate assumptions in the model 	4 - 17 kDa, >250 kDa, ~270 kDa - 3.8 MDa	[26,126]
Size Exclusion Chromatography	<ul style="list-style-type: none"> • Well established technique 	<ul style="list-style-type: none"> • Leads to sample dilution which can dissociate unstable oligomers • Comparisons between elution behavior of oligomers and globular protein standards make molecular weight estimations difficult 	4 - 20 kDa, 24 kDa, >100 kDa	[129-131]

Enzyme-Linked Immunosorbent Assay	<ul style="list-style-type: none"> • Highly sensitive and specific • Ability to measure specific analytes within a crude preparation • Versatile 	<ul style="list-style-type: none"> • Gives information about presence of oligomers and not size • Requires expensive and specific antibodies 	No size determination	[130,133]
Dot Blot	<ul style="list-style-type: none"> • Straight-forward, rapid technique 	<ul style="list-style-type: none"> • Gives information about presence of oligomers and not size • Requires expensive and specific antibodies 	No size determination	[57,132]

References

1. Robinson, J.L.; Geser, F.; Corrada, M.M.; Berlau, D.J.; Arnold, S.E.; Lee, V.M.; Kawas, C.H.; Trojanowski, J.Q. Neocortical and Hippocampal Amyloid- β and Tau Measures Associate with Dementia in the Oldest-Old. *Brain* **2011**, *134*, 3708-3715.
2. Montine, T.J.; Phelps, C.H.; Beach, T.G.; Bigio, E.H.; Cairns, N.J.; Dickson, D.W.; Duyckaerts, C.; Frosch, M.P.; Masliah, E.; Mirra, S.S. *et al.* National Institute on Aging-Alzheimer's Association Guidelines for the Neuropathologic Assessment of Alzheimer's Disease: A Practical Approach. *Acta Neuropathol.* **2012**, *123*, 1-11.
3. Kagan, B.L.; Jang, H.; Capone, R.; Arce, F.T.; Ramachandran, S.; Lal, R.; Nussinov, R. Antimicrobial Properties of Amyloid Peptides. *Mol. Pharmaceutics*, Ahead of Print.
4. Miranker, A.D. Unzipping the Mysteries of Amyloid Fiber Formation. *Proc. Natl. Acad. Sci. USA* **2004**, *101*, 4335-4336.
5. Murphy, R.M. Peptide Aggregation in Neurodegenerative Disease. *Annu. Rev. Biomed. Eng.* **2002**, *4*, 155-174.
6. Selkoe, D.J. Folding Proteins in Fatal Ways. *Nature* **2003**, *426*, 900-904.
7. Gazit, E. Mechanisms of Amyloid Fibril Self-Assembly and Inhibition. Model Short Peptides as a Key Research Tool. *Febs J* **2005**, *272*, 5971-5978.
8. Xing, Y.; Higuchi, K. Amyloid Fibril Proteins. *Mech. Ageing Dev.* **2002**, *123*, 1625-1636.
9. Kisilevsky, R. Review: Amyloidogenesis-Unquestioned Answers and Unanswered Questions. *J. Struct. Biol.* **2000**, *130*, 99-108.
10. Kaye, R.; Head, E.; Sarsoza, F.; Saing, T.; Cotman, C.W.; Necula, M.; Margol, L.; Wu, J.; Breydo, L.; Thompson, J.L. *et al.* Fibril Specific, Conformation Dependent Antibodies Recognize a Generic Epitope Common to Amyloid Fibrils and Fibrillar Oligomers that is Absent in Prefibrillar Oligomers. *Mol Neurodegener* **2007**, *2*, 18.
11. Kaye, R.; Head, E.; Thompson, J.L.; McIntire, T.M.; Milton, S.C.; Cotman, C.W.; Glabe, C.G. Common Structure of Soluble Amyloid Oligomers Implies Common Mechanism of Pathogenesis. *Science* **2003**, *300*, 486-489.
12. Alzheimer's Association. 2011 Alzheimer's Disease Facts and Figures. *Alzheimer's and Dementia* **2011**, *7*, 1-63.
13. Wang, X.; Ding, H. Alzheimer's Disease: Epidemiology, Genetics, and Beyond. *Neurosci. Bull.* **2008**, *24*, 105-109.

14. Masters, C.L.; Simms, G.; Weinman, N.A.; Multhaup, G.; McDonald, B.L.; Beyreuther, K. Amyloid Plaque Core Protein in Alzheimer Disease and Down Syndrome. *Proc. Natl. Acad. Sci. U. S. A.* **1985**, *82*, 4245-4249.
15. Giuffrida, M.L.; Caraci, F.; de, B., P.; Pappalardo, G.; Nicoletti, F.; Rizzarelli, E.; Copani, A. The Monomer State of β -Amyloid: Where the Alzheimer's Disease Protein Meets Physiology. *Rev. Neurosci. (London, U. K.)* **2010**, *21*, 83-93.
16. Teplow, D.B. Structural and Kinetic Features of Amyloid β -Protein Fibrillogenesis. *Int J Exp Clin Invest* **1998**, *5*, 121-142.
17. Morris, A.M.; Watzky, M.A.; Finke, R.G. Protein Aggregation Kinetics, Mechanism, and Curve-Fitting: A Review of the Literature. *Biochim. Biophys. Acta, Proteins Proteomics* **2009**, *1794*, 375-397.
18. Kodali, R.; Wetzel, R. Polymorphism in the Intermediates and Products of Amyloid Assembly. *Curr. Opin. Struct. Biol.* **2007**, *17*, 48-57.
19. Walsh, D.M.; Selkoe, D.J. A β Oligomers - A Decade of Discovery. *J. Neurochem.* **2007**, *101*, 1172-1184.
20. Sabate, R.; Estelrich, J. Evidence of the Existence of Micelles in the Fibrillogenesis of β -Amyloid Peptide. *J Phys Chem B* **2005**, *109*, 11027-11032.
21. Lambert, M.P.; Barlow, A.K.; Chromy, B.A.; Edwards, C.; Freed, R.; Liosatos, M.; Morgan, T.E.; Rozovsky, I.; Trommer, B.; Viola, K.L. *et al.* Diffusible, Nonfibrillar Ligands Derived from A β 1-42 are Potent Central Nervous System Neurotoxins. *Proc. Natl. Acad. Sci. USA* **1998**, *95*, 6448-6453.
22. Catalano, S.M.; Dodson, E.C.; Henze, D.A.; Joyce, J.G.; Krafft, G.A.; Kinney, G.G. The Role of Amyloid- β Derived Diffusible Ligands (ADDLs) in Alzheimer's Disease. *Curr. Top. Med. Chem. (Sharjah, United Arab Emirates)* **2006**, *6*, 597-608.
23. Westlind-Danielsson, A.; Arnerup, G. Spontaneous in Vitro Formation of Supramolecular β -Amyloid Structures, "Bamy Balls", by β -Amyloid 1-40 Peptide. *Biochemistry* **2001**, *40*, 14736-14743.
24. Matsumura, S.; Shinoda, K.; Yamada, M.; Yokojima, S.; Inoue, M.; Ohnishi, T.; Shimada, T.; Kikuchi, K.; Masui, D.; Hashimoto, S. *et al.* Two Distinct Amyloid β -Protein (A β) Assembly Pathways Leading to Oligomers and Fibrils Identified by Combined Fluorescence Correlation Spectroscopy, Morphology, and Toxicity Analyses. *Journal of Biological Chemistry* **2011**, *286*, 11555-11562.
25. Walsh, D.; Lomakin, A.; Benedek, G.; Condron, M.; Teplow, D. Amyloid β -Protein Fibrillogenesis: Detection of a Protofibrillar Intermediate. *The Journal of Biological Chemistry* **1997**, *272*, 22364-22372.

26. Ward, R.; Jennings, K.; Howlett, D. Fractionation and Characterization of Oligomeric, Protofibrillar and Fibrillar Forms of β -Amyloid Peptide. *Biochem. J.* **2000**, *348*, 137-138-144.
27. Thirumalai, D.; Klimov, D.; Dima, R. Emerging Ideas on the Molecular Basis of Protein and Peptide Aggregation. *Curr. Opin. Struct. Biol.* **2003**, *13*, 146-159.
28. Roher, A.E.; Baudry, J.; Chaney, M.O.; Kuo, Y.-.; Stine, W.B.; Emmerling, M.R. Oligomerization and Fibril Assembly of the Amyloid- β Protein. *Biochim. Biophys. Acta, Mol. Basis Dis.* **2000**, *1502*, 31-43.
29. Morgan, C.; Colombres, M.; Nunez, M.T.; Inestrosa, N.C. Structure and Function of Amyloid in Alzheimer's Disease. *Prog. Neurobiol. (Amsterdam, Neth.)* **2004**, *74*, 323-349.
30. Barghorn, S.; Nimmrich, V.; Striebinger, A.; Krantz, C.; Keller, P.; Janson, B.; Bahr, M.; Schmidt, M.; Bitner, R.S.; Harlan, J. *et al.* Globular Amyloid β -peptide1-42 Oligomer - a Homogeneous and Stable Neuropathological Protein in Alzheimer's Disease. *J. Neurochem.* **2005**, *95*, 834-847.
31. Kawooya, J.; Emmons, T.; Gonzalez-DeWhitt, P.; Camp, M.; D'Andrea, S. Electrophoretic Mobility of Alzheimer's Amyloid- β Peptides in Urea-Sodium Dodecyl Sulfate-Polyacrylamide Gel Electrophoresis. *Anal. Biochem.* **2003**, *323*, 103-113.
32. Gursky, O.; Aleshkov, S. Temperature-Dependent β -Sheet Formation in β -Amyloid A β ₁₋₄₀ Peptide in Water: Uncoupling β -Structure Folding from Aggregation. **2000**, 93-102.
33. Caughey, B.; Lansbury, P.T. Protofibrils, Pores, Fibrils, and Neurodegeneration: Separating the Responsible Protein Aggregates from the Innocent Bystanders. *Annu. Rev. Neurosci.* **2003**, *26*, 267-298.
34. Glabe, C.G. Common Mechanisms of Amyloid Oligomer Pathogenesis in Degenerative Disease. *Neurobiol. Aging* **2006**, *27*, 570-575.
35. Roychaudhuri, R.; Yang, M.; Hoshi, M.M.; Teplow, D.B. Amyloid β -Protein Assembly and Alzheimer's Disease. *J. Biol. Chem.* **2009**, *284*, 4749-4753.
36. Gonzalez-Velasquez, F.J.; Kotarek, J.A.; Moss, M.A. Soluble Aggregates of the Amyloid- β Protein Selectively Stimulate Permeability in Human Brain Microvascular Endothelial Monolayers. *J. Neurochem.* **2008**, *107*, 466-477.
37. Hartley, D.M.; Walsh, D.M.; Ye, C.P.; Diehl, T.; Vasquez, S.; Vassilev, P.M.; Teplow, D.B.; Selkoe, D.J. Protofibrillar Intermediates of Amyloid β -Protein Induce Acute Electrophysiological Changes and Progressive Neurotoxicity in Cortical Neurons. *J. Neurosci.* **1999**, *19*, 8876-8884.

38. Lesne, S.; Koh, M.T.; Kotilinek, L.; Kaye, R.; Glabe, C.G.; Yang, A.; Gallagher, M.; Ashe, K.H. A Specific Amyloid- β Protein Assembly in the Brain Impairs Memory. *Nature* **2006**, *440*, 352-357.
39. Walsh, D.M.; Klyubin, I.; Fadeeva, J.V.; Rowan, M.J.; Selkoe, D.J. Amyloid- β Oligomers: Their Production, Toxicity and Therapeutic Inhibition. *Biochem. Soc. Trans.* **2002**, *30*, 552-557.
40. Westerman, M.; Cooper-Blacketer, D.; Mariash, A.; Kotilinek, L.; Kawarabayashi, T.; Younkin, L.; Carlson, G.; Younkin, S.; Ashe, K. The Relationship between A β and Memory in the Tg2576 Mouse Model of Alzheimer's Disease. *J. Neurosci.* **2002**, *22*, 1858-1867.
41. Lue, L.F.; Kuo, Y.M.; Roher, A.E.; Brachova, L.; Shen, Y.; Sue, L.; Beach, T.; Kurth, J.H.; Rydel, R.E.; Rogers, J. Soluble Amyloid β Peptide Concentration as a Predictor of Synaptic Change in Alzheimer's Disease. *Am. J. Pathol.* **1999**, *155*, 853-862.
42. Scheff, S.; Price, D.; Schmitt, F.; Mufson, E. Hippocampal Synaptic Loss in Early Alzheimer's Disease and Mild Cognitive Impairment. *Neurobiology of Aging* **2006**, *27*, 1372-1384.
43. Yang, T.; Hsu, C.; Kuo, Y. Cell-Derived Soluble Oligomers of Human Amyloid- β Peptides Disturb Cellular Homeostasis and Induce Apoptosis in Primary Hippocampal Neurons. *J. Neural Transm.* **2009**, *116*, 1561-1569.
44. Bitan, G.; Fradinger, E.A.; Spring, S.M.; Teplow, D.B. Neurotoxic Protein Oligomers--what You See is Not always what You Get. *Amyloid* **2005**, *12*, 88-95.
45. Ying, Z.; Xin, W.; Jin-Sheng, H.; Fu-Xiang, B.; Wei-Min, S.; Xin-Xian, D.; Xiao-Bo, W.; Yi-Qin, L.; Xian-Xian, Z.; Hong-Gang, H. *et al.* Preparation and Characterization of a Monoclonal Antibody with High Affinity for Soluble A β Oligomers. *Hybridoma* **2009**, *28*, 349-354.
46. Satoh, Y.; Hirakura, Y.; Kirino, Y. β -Amyloid Peptides Inhibit Acetylcholine Release from Cholinergic Presynaptic Nerve Endings Isolated from an Electric Ray. *Neuroscience Letters* **2001**, *302*, 97-100.
47. Sureshbabu, N.; Kirubakaran, R.; Jayakumar, R. Surfactant-Induced Conformational Transition of Amyloid β -Peptide. *EBJ* **2009**, *38*, 355-367.
48. Iurascu, M.; Cozma, C.; Tomczyk, N.; Rontree, J.; Desor, M.; Drescher, M.; Przybylski, M. Structural Characterization of β -Amyloid Oligomer-Aggregates by Ion Mobility Mass Spectrometry and Electron Spin Resonance Spectroscopy. *Anal Bioanal Chem* **2009**, *395*, 2509-2519.

49. Klug, G.; Losic, D.; Small, D. B-Amyloid Protein Oligomers Induced by Metal Ions and Acid pH are Distinct from those Generated by Slow Spontaneous Ageing at Neutral pH. *Eur. J. Biochem.* **2003**, *270*, 4282-4293.
50. Walsh, D.; Tseng, B.; Rydel, R.; Podlisny, M.; Selkoe, D. The Oligomerization of Amyloid β -Protein Begins Intracellularly in Cells Derived from Human Brain. *Biochemistry* **2000**, *39*, 10831-10839.
51. Walsh, D.; Hartley, D.; Condron, M.; Selkoe, D.; Teplow, D. *in Vitro* studies of Amyloid β -Protein Fibril Assembly and Toxicity Provide Clues to the Aetiology of Flemish Variant (Ala⁶⁹² \rightarrow Gly) Alzheimer's Disease. *Biochem. J.* **2001**, *355*, 869-877.
52. Dahlgren, K.N.; Manelli, A.M.; Stine, W.B., Jr.; Baker, L.K.; Krafft, G.A.; LaDu, M.J. Oligomeric and Fibrillar Species of Amyloid- β Peptides Differentially Affect Neuronal Viability. *J. Biol. Chem.* **2002**, *277*, 32046-32053.
53. Ryan, D.; Narrow, W.; Federoff, H.; Bowers, W. An Improved Method for Generating Consistent Soluble Amyloid- β Oligomer Preparations for *in Vitro* Neurotoxicity Studies. *Journal of Neuroscience Methods* **2010**, *190*, 171-179.
54. Stine, W.B., Jr.; Dahlgren, K.N.; Krafft, G.A.; LaDu, M.J. In Vitro Characterization of Conditions for Amyloid- β Peptide Oligomerization and Fibrillogenesis. *J. Biol. Chem.* **2003**, *278*, 11612-11622.
55. Moore, B.; Rangachari, V.; Tay, W.; Milkovic, N.; Rosenberry, T. Biophysical Analyses of Synthetic Amyloid- β (1-42) Aggregates before and After Covalent Cross-Linking. Implications for Deducing the Structure of Endogenous Amyloid- β Oligomers. *Biochemistry* **2009**, *48*, 11796-11806.
56. Gravina, S.A.; Ho, L.; Eckman, C.B.; Long, K.E.; Otvos, L., Jr.; Younkin, L.H.; Suzuki, N.; Younkin, S.G. Amyloid β Protein (A β) in Alzheimer's Disease Brain. Biochemical and Immunocytochemical Analysis with Antibodies Specific for Forms Ending at A β 40 Or A β 42(43). *J. Biol. Chem.* **1995**, *270*, 7013-7016.
57. Wong, H.E.; Qi, W.; Choi, H.; Fernandez, E.J.; Kwon, I. A Safe, Blood-Brain Barrier Permeable Triphenylmethane Dye Inhibits Amyloid- β Neurotoxicity by Generating Nontoxic Aggregates. *ACS Chem. Neurosci.* **2011**, *2*, 645-657.
58. Hu, Y.; Su, B.H.; Kim, C.S.; Hernandez, M.; Rostagno, A.; Ghiso, J.; Kim, J.R. A Strategy for Designing a Peptide Probe for Detection of β -Amyloid Oligomers. *ChemBioChem* **2010**, *11*, 2409-2418.
59. Lambert, M.P.; Velasco, P.T.; Chang, L.; Viola, K.L.; Fernandez, S.; Lacor, P.N.; Khuon, D.; Gong, Y.; Bigio, E.; Shaw, P. *et al.* Monoclonal Antibodies that Target Pathological Assemblies of A β . *J. Neurochem.* **2007**, *100*, 23-25.

60. Wu, J.W.; Breydo, L.; Isas, J.M.; Lee, J.; Kuznetsov, Y.G.; Langen, R.; Glabe, C. Fibrillar Oligomers Nucleate the Oligomerization of Monomeric Amyloid β but do Not Seed Fibril Formation. *J. Biol. Chem.* **2010**, *285*, 6071-6079.
61. Zagorski, M.G.; Barrow, C.J. NMR Studies of Amyloid β -Peptides: Proton Assignments, Secondary Structure, and Mechanism of an Alpha-Helix--Beta-Sheet Conversion for a Homologous, 28-Residue, N-Terminal Fragment. *Biochemistry* **1992**, *31*, 5621-5631.
62. Bitan, G.; Teplow, D. Rapid Photochemical Cross-Linking--A New Tool for Studies of Metastable, Amyloidogenic Protein Assemblies. *Acc. Chem. Res.* **2004**, *37*, 357-364.
63. Fancy, D.S.; Kodadek, T. Chemistry for the Analysis of Protein-Protein Interactions: Rapid and Efficient Cross-Linking Triggered by Long Wavelength Light. *Proc. Natl. Acad. Sci. U. S. A.* **1999**, *96*, 6020-6024.
64. Gerardi, R.D.; Barnett, N.W.; Lewis, S.W. Analytical Applications of Tris(2,2'-Bipyridyl)Ruthenium(III) as a Chemiluminescent Reagent. *Anal. Chim. Acta* **1999**, *378*, 1-43.
65. Bitan, G.; Kirkitadze, M.; Lomakin, A.; Vollers, S.; Benedek, G.; Teplow, D. Amyloid β -Protein (A β) Assembly: A β 40 and A β 42 Oligomerize through Distinct Pathways. *PNAS* **2003**, *100*, 330-335.
66. Podlisny, M.; Walsh, D.; Selkoe, D. Oligomerization of Endogeneous and Synthetic Amyloid β -Protein at Nanomolar Levels in Cell Culture and Stabilization of Monomer by Congo Red. *Biochemistry* **1998**, *37*, 3602-3611.
67. Townsend, M.; Shankar, G.M.; Mehta, T.; Walsh, D.M.; Selkoe, D.J. Effects of Secreted Oligomers of Amyloid β -Protein on Hippocampal Synaptic Plasticity: A Potent Role for Trimers. *J. Physiol. (Lond.)* **2006**, *572*, 477-492.
68. Zuberovic, A.; Hanrieder, J.; Wetterhall, M. Proteome Profiling of Human Cerebrospinal Fluid: Exploring the Potential of Capillary Electrophoresis with Surface Modified Capillaries for Analysis of Complex Biological Samples. *Eur. J. Mass Spectrom.* **2008**, *14*, 249-260.
69. Lee, Y.-I.; Maus, R.; Smith, B.; Winefordner, J. Laser-Induced Fluorescence Detection of a Single Molecule in a Capillary. *Anal. Chem.* **1994**, *66*, 4142-4149.
70. Skeidsvoll, J.; Ueland, P. Analysis of Double-Stranded DNA by Capillary Electrophoresis with Laser-Induced Fluorescence Detection using the Monomeric Dye SYBR Green I. *Anal. Biochem.* **1995**, *231*, 359-365.
71. Verpillot, R.; Otto, M.; Taverna, M. Simultaneous Analysis by Capillary Electrophoresis of Five Amyloid Peptides as Potential Biomarkers of Alzheimer's Disease. *Journal of Chromatography A* **2008**, *1214*, 157-164.

72. Sabella, S.; Quaglia, M.; Lanni, C.; Racchi, M.; Govoni, S.; Caccialanza, G.; Calligaro, A.; Bellotti, V.; Lorenzi, E. Capillary Electrophoresis Studies on the Aggregation Process of β -Amyloid 1-42 and 1-40 Peptides. *Electrophoresis* **2004**, *25*, 3186-3194.
73. Picou, R.; Kheterpal, I.; Wellman, A.; Minnamreddy, M.; Ku, G.; Gilman, S.D. Analysis of $A\beta(1-40)$ and $A\beta(1-42)$ Monomer and Fibrils by Capillary Electrophoresis. *J. Chromatogr. B* **2011**, *879*, 627-632.
74. Kato, M.; Kinoshita, H.; Toyooka, T. Analytical Method for β -Amyloid Fibrils using CE-Laser Induced Fluorescence and its Application to Screening for Inhibitors of β -Amyloid Protein Aggregation. *Anal. Chem.* **2007**, *79*, 4887-4891.
75. Jakeway, S.C.; de Mello, A.J.; Russell, E.L.; Fresenius, J. Miniaturized Total Analysis Systems for Biological Analysis. *Anal. Chem.* **2000**, *366*, 525-539.
76. Chovan, T.; Guttman, A. Microfabricated Devices in Biotechnology and Biochemical Processing. *Trends Biotechnol.* **2002**, *20*, 116-122.
77. Mohamadi, M.R.; Svobodova, Z.; Verpillot, R.; Esselmann, H.; Wiltfang, J.; Otto, M.; Taverna, M.; Bilkova, Z.; Viovy, J. Microchip Electrophoresis Profiling of $A\beta$ Peptides in the Cerebrospinal Fluid of Patients with Alzheimer's Disease. *Anal. Chem.* **2010**, *82*, 7611-7617.
78. Steiner, W.E.; Klopsch, S.J.; English, W.A.; Clowers, B.H.; Hill, H.H. Detection of a Chemical Warfare Agent Simulant in various Aerosol Matrixes by Ion Mobility Time-of-Flight Mass Spectrometry. *Anal. Chem.* **2005**, *77*, 4792-4799.
79. Huertas, M.L.; Marty, A.M.; Fontan, J.; Alet, I.; Duffa, G. Measurement of Mobility and Mass of Atmospheric Ions. *Journal of Aerosol Science* **1971**, *2*, 145-150.
80. Borsdorf, H.; Rudolph, M. Gas-Phase Ion Mobility Studies of Constitutional Isomeric Hydrocarbons using Different Ionization Techniques. *International Journal of Mass Spectrometry* **2001**, *208*, 67-72.
81. Hill, C.A.; Thomas, C.L.P. Programmable Gate Delayed Ion Mobility Spectrometry-Mass Spectrometry: A Study with Low Concentrations of Dipropylene-Glycol-Monomethyl-Ether in Air. *The Analyst* **2005**, *130*, 1155-1161.
82. Sielemann, S.; Baumbach, J.I.; Schmidt, H.; Pilzecker, P. Quantitative Analysis of Benzene, Toluene, and m-Xylene with the use of a UV-Ion Mobility Spectrometer. *Field Analytical Chemistry and Technology* **2000**, *4*, 157-169.
83. Valentine, S.J.; Anderson, J.G.; Ellington, A.D.; Clemmer, D.E. Disulfide-Intact and -Reduced Lysozyme in the Gas Phase: Conformations and Pathways of Folding and Unfolding. *Journal of Physical Chemistry* **1997**, *101*, 3891-3900.

84. Ells, B.; Barnett, D.A.; Froese, K.; Purves, R.W.; Hrudey, S.; Guevremont, R. Detection of Chlorinated and Brominated Byproducts of Drinking Water Disinfection using Electrospray Ionization-High-Field Asymmetric Waveform Ion Mobility Spectrometry-Mass Spectrometry. *Anal. Chem.* **1999**, *71*, 4747-4752.
85. Matz, L.M.; Hill, H.H.J. Evaluation of Opiate Separation by High-Resolution Electrospray Ionization-Ion Mobility spectrometry/mass Spectrometry. *Anal. Chem.* **2001**, *73*, 1664-1669.
86. Smith, D.P.; Giles, K.; Bateman, R.H.; Radford, S.E.; Ashcroft, A.E. Monitoring Copopulated Conformational States Fduring Protein Folding Events using Electrospray Ionization-Ion Mobility Spectrometry-Mass Spectrometry. *Journal of the American Society for Mass Spectrometry* **2007**, *18*, 2180-2190.
87. Gillig, K.J.; Ruotolo, B.; Stone, E.G.; Russell, D.H.; Fuhrer, K.; Gonin, M.; Schultz, A.J. Coupling High-Pressure MALDI with Ion mobility/orthogonal Time-of-Flight Mass Spectrometry. *Anal. Chem.* **2000**, *72*, 3965-3971.
88. Woods, A.S.; Koomen, J.M.; Ruotolo, B.T.; Gillig, K.J.; Russel, D.H.; Fuhrer, K.; Gonin, M.; Egan, T.F.; Schultz, J.A. A Study of Peptide-Peptide Interactions using MALDI Ion Mobility o-TOF and ESI Mass Spectrometry. *Journal of the American Society for Mass Spectrometry* **2002**, *13*, 166-169.
89. Steiner, W.E.; Clowers, B.H.; English, W.A.; Hill, H.H.J. Atmospheric Pressure Matrix-Assisted Laser desorption/ionization with Analysis by Ion Mobility Time-of-Flight Mass Spectrometry. *Rapid Communications in Mass Spectrometry* **2004**, *18*, 882-888.
90. McLean, J.A.; Ruotolo, B.T.; Gillig, K.J.; Russell, D.H. Ion Mobility-Mass Spectrometry: A New Paradigm for Proteomics. *International Journal of Mass Spectrometry* **2005**, *240*, 301-315.
91. Von Helden, G.; Gotts, N.G.; Bowers, M.T. Experimental Evidence for the Formation of Fullerenes by Collisional Heating of Carbon Rings in the Gas Phase. *Nature (London, United Kingdom)* **1993**, *363*, 60-63.
92. Von Helden, G.; Kemper, P.R.; Gotts, N.G.; Bowers, M.T. Isomers of Small Carbon Cluster Anions: Linear Chains with Up to 20 Atoms. *Science (Washington, DC, United States)* **1993**, *259*, 1300-1302.
93. Jarrold, M.F.; Constant, V.A. Silicon Cluster Ions: Evidence for a Structural Transition. *Physical Review Letters* **1991**, *67*, 2994-2997.
94. Kanu, A.B.; Dwivedi, P.; Tam, M.; Matz, L.; Hill, H.H. Ion Mobility-Mass Spectrometry. *J. Mass Spectrom.* **2008**, *43*, 1-22.

95. Maji, S.; Ogorzalek Loo, R.; Inayathullah, M.; Spring, S.; Vollers, S.; Condrón, M.; Bitan, G.; Loo, J.; Teplow, D. Amino Acid Position-Specific Contributions to Amyloid β -Protein Oligomerization. *J. Biol. Chem.* **2009**, *284*, 23580-23591.
96. Oe, T.; Ackermann, B.L.; Inoue, K.; Berna, M.J.; Garner, C.O.; Gelfanova, V.; Dean, R.A.; Siemers, E.R.; Holtzman, D.M.; Farlow, M.R. *et al.* Quantitative Analysis of Amyloid β Peptides in Cerebrospinal Fluid of Alzheimer's Disease Patients by Immunoaffinity Purification and Stable Isotope Dilution Liquid chromatography/negative Electrospray Ionization Tandem Mass Spectrometry. *Rapid Communications in Mass Spectrometry* **2006**, *20*, 3723-3735.
97. Ashcroft, A. Mass Spectrometry and the Amyloid Problem-how Far can we Go in the Gas Phase? *J. Am. Soc. Mass Spectrom.* **2010**, *21*, 1087-1096.
98. Palmblad, M.; Westlind-Danielsson, A.; Bergquist, J. Oxidation of Methionine 35 Attenuates Formation of Amyloid β -Peptide 1-40 Oligomers. *J. Biol. Chem.* **2002**, *277*, 19506-19510.
99. Clemmer, D.E.; Hudgins, R.R.; Jarrold, M.F. Naked Protein Conformations: Cytochrome *c* in the Gas Phase. *J. Am. Chem. Soc.* **1995**, *117*, 10141-10142.
100. Clemmer, D.E.; Jarrold, M.F. Ion Mobility Measurements and their Applications to Clusters and Biomolecules. *J. Mass Spectrom.* **1997**, *32*, 577-592.
101. Henderson, S.C.; Valentine, S.J.; Counterman, A.E.; Clemmer, D.E. ESI/Ion Trap/Ion Mobility/Time-of-Flight Mass Spectrometry for Rapid and Sensitive Analysis of Biomolecular Mixtures. *Anal. Chem.* **1999**, *71*, 291-301.
102. Murray, M.; Bernstein, S.; Nyugen, V.; Condrón, M.; Teplow, D.; Bowers, M. Amyloid β Protein: A β 40 Inhibits A β 42 Oligomerization. *JACS* **2009**, *131*, 6316-6317.
103. Bernstein, S.; Wyttenbach, T.; Baumketner, A.; Shea, J.; Bitan, G.; Teplow, D.; Bowers, M. Amyloid β -Protein: Monomer Structure and Early Aggregation States of A β 42 and its Pro19 Alloform. *J. Am. Chem. Soc.* **2005**, *127*, 2075-2084.
104. Bernstein, S.; Dupuis, N.; Lazo, N.; Wyttenbach, T.; Condrón, M.; Bitan, G.; Teplow, D.; Shea, J.; Ruotolo, B.; Robinson, C. *et al.* Amyloid- β Protein Oligomerization and the Importance of Tetramers and Dodecamers in the Aetiology of Alzheimer's Disease. *Nature Chemistry* **2009**, *1*, 326-331.
105. Cizas, P.; Budvytyte, R.; Morkuniene, R.; Moldovan, R.; Broccio, M.; Loesche, M.; Niaura, G.; Valincius, G.; Borutaite, V. Size-Dependent Neurotoxicity of β -Amyloid Oligomers. *Arch. Biochem. Biophys.* **2010**, *496*, 84-92.

106. Tjernberg, L.O.; Pramanik, A.; Bjorling, S.; Thyberg, P.; Thyberg, J.; Nordstedt, C.; Berndt, K.D.; Terenius, L.; Rigler, R. Amyloid β -Peptide Polymerization Studied using Fluorescence Correlation Spectroscopy. *Chem. Biol.* **1999**, *6*, 53-62.
107. Garai, K.; Sahoo, B.; Sengupta, P.; Maiti, S. Quasihomogeneous Nucleation of Amyloid β Yields Numerical Bounds for the Critical Radius, the Surface Tension, and the Free Energy Barrier for Nucleus Formation. *J. Chem. Phys.* **2008**, *128*, 045102/1-045102/7.
108. Eigen, M.; Rigler, R. Sorting Single Molecules: Application to Diagnostics and Evolutionary Biotechnology. *Proc. Natl. Acad. Sci. U. S. A.* **1994**, *91*, 5740-5747.
109. Garai, K.; Sengupta, P.; Sahoo, B.; Maiti, S. Selective Destabilization of Soluble Amyloid β Oligomers by Divalent Metal Ions. *Biochem. Biophys. Res. Commun.* **2006**, *345*, 210-215.
110. Funke, S.A.; Birkmann, E.; Henke, F.; Goertz, P.; Lange-Asschenfeldt, C.; Riesner, D.; Willbold, D. Single Particle Detection of A β Aggregates Associated with Alzheimer's Disease. *Biochem. Biophys. Res. Commun.* **2007**, *364*, 902-907.
111. Godderz, L.J.; Peak, M.M.; Rodgers, K.K. Analysis of Biological Macromolecular Assemblies using Static Light Scattering Methods. *Curr. Org. Chem.* **2005**, *9*, 899-908.
112. Villari, V.; Micali, N. Light Scattering as Spectroscopic Tool for the Study of Disperse Systems Useful in Pharmaceutical Sciences. *J. Pharm. Sci.* **2008**, *97*, 1703-1730.
113. Alexander, M.; Dalgleish, D. Dynamic Light Scattering Techniques and their Applications in Food Science. *FOBI* **2006**, *1*, 2-13.
114. Lomakin, A.; Teplow, D.B.; Kirschner, D.A.; Benedek, G.B. Kinetic Theory of Fibrillogenesis of Amyloid β -Protein. *Proc. Natl. Acad. Sci. U. S. A.* **1997**, *94*, 7942-7947.
115. Lomakin, A.; Chung, D.S.; Benedek, G.B.; Kirschner, D.A.; Teplow, D.B. On the Nucleation and Growth of Amyloid β -Protein Fibrils: Detection of Nuclei and Quantitation of Rate Constants. *Proc. Natl. Acad. Sci. U. S. A.* **1996**, *93*, 1125-1129.
116. Thuncke, M.; Lobbia, A.; Kosciessa, U.; Dyrks, T.; Oakley, A.E.; Turner, J.; Saenger, W.; Georgalis, Y. Aggregation of A β Alzheimer's Disease-Related Peptide Studied by Dynamic Light Scattering. *J. Pept. Res.* **1998**, *52*, 509-517.
117. Carrotta, R.; Manno, M.; Bulone, D.; Martorana, V.; San, B., Pier Luigi. Protofibril Formation of Amyloid β -Protein at Low pH Via a Non-Cooperative Elongation Mechanism. *J. Biol. Chem.* **2005**, *280*, 30001-30008.
118. Murphy, R.M.; Pallitto, M.M. Probing the Kinetics of β -Amyloid Self-Association. *J. Struct. Biol.* **2000**, *130*, 109-122.

119. Rambaldi, D.C.; Zattoni, A.; Reschiglian, P.; Colombo, R.; De, L.E. In Vitro Amyloid A $\beta_{(1-42)}$ Peptide Aggregation Monitoring by Asymmetrical Flow Field-Flow Fractionation with Multi-Angle Light Scattering Detection. *Anal Bioanal Chem* **2009**, *394*, 2145-2149.
120. Nichols, M.; Moss, M.; Rosenberry, T. Growth of β -Amyloid(1-40) Protofibrils by Monomer Elongation and Lateral Association. Characterization of Distinct Products by Light Scattering and Atomic Force Microscopy. *Biochemistry* **2002**, 6115-6127.
121. Walsh, D.; Hartley, D.; Kusumoto, Y.; Fezoui, Y.; Condron, M.; Lomakin, A.; Benedek, G.; Selkoe, D.; Teplow, D. Amyloid β -Protein Fibrillogenesis: Structure and Biological Activity of Protofibrillar Intermediates. *J. Biol. Chem.* **1999**, *274*, 25945-25952.
122. Yohannes, G.; Jussila, M.; Hartonen, K.; Riekkola, M. Asymmetrical Flow Field-Flow Fractionation Technique for Separation and Characterization of Biopolymers and Bioparticles. *J. Chromatogr. , A* **2011**, *1218*, 4104-4116.
123. Roda, B.; Zattoni, A.; Reschiglian, P.; Moon, M.H.; Mirasoli, M.; Michelini, E.; Roda, A. Field-Flow Fractionation in Bioanalysis: A Review of Recent Trends. *Anal. Chim. Acta* **2009**, *635*, 132-143.
124. Mok, Y.; Howlett, G.J. Sedimentation Velocity Analysis of Amyloid Oligomers and Fibrils. *Methods Enzymol.* **2006**, *413*, 199-217.
125. Huang, T.H.J.; Yang, D.; Plaskos, N.P.; Go, S.; Yip, C.M.; Fraser, P.E.; Chakrabartty, A. Structural Studies of Soluble Oligomers of the Alzheimer β -Amyloid Peptide. *J. Mol. Biol.* **2000**, *297*, 73-87.
126. Nagel-Steger, L.; Demeler, B.; Meyer-Zaika, W.; Hochdoerffer, K.; Schrader, T.; Willbold, D. Modulation of Aggregate Size- and Shape-Distributions of the Amyloid- β Peptide by a Designed β -Sheet Breaker. *Eur. Biophys. J.* **2010**, *39*, 415-422.
127. Paivio, A.; Jarvet, J.; Graslund, A.; Lannfelt, L.; Westlind-Danielsson, A. Unique Physicochemical Profile of β -Amyloid Peptide Variant A $\beta_{1-40E22G}$ Protofibrils: Conceivable Neuropathogen in Arctic Mutant Carriers. *J. Mol. Biol.* **2004**, *339*, 145-159.
128. Wiberg, H.; Ek, P. Separation and Characterization of Aggregated Species of Amyloid- β Peptides. *Anal Bioanal Chem* **2010**, *397*, 2357-2366.
129. Ahmed, M.; Davis, J.; Aucoin, D.; Sato, T.; Ahuja, S.; Aimoto, S.; Elliott, J.I.; Van, N., William E.; Smith, S.O. Structural Conversion of Neurotoxic Amyloid- β_{1-42} Oligomers to Fibrils. *Nat. Struct. Mol. Biol.* **2010**, *17*, 561-567.
130. Englund, H.; Sehlin, D.; Johansson, A.; Nilsson, L.N.G.; Gellerfors, P.; Paulie, S.; Lannfelt, L.; Pettersson, F.E. Sensitive ELISA Detection of Amyloid- β Protofibrils in Biological Samples. *J. Neurochem.* **2007**, *103*, 334-345.

131. Zheng, X.; Wang, L.; Zhang, L.; Hong, Y.; Huang, L.; Sha, Y. Separation and Analysis of the Soluble Trimer of A β 1-40 and its Effects on the Rise in Intracellular Calcium. *Chin. Sci. Bull.* **2006**, *51*, 830-838.
132. Necula, M.; Kaye, R.; Milton, S.; Glabe, C.G. Small Molecule Inhibitors of Aggregation Indicate that Amyloid β Oligomerization and Fibrillization Pathways are Independent and Distinct. *J. Biol. Chem.* **2007**, *282*, 10311-10324.
133. Gonzales, A.M.; Orlando, R.A. A Sensitive A β Oligomerization Assay for Identification of Small Molecule Inhibitors. *Open Biotechnol. J.* **2009**, *3*, 108-116.
134. Kamali-Moghaddam, M.; Pettersson, F.E.; Wu, D.; Englund, H.; Darmanis, S.; Lord, A.; Tavoosidana, G.; Sehlin, D.; Gustafsdottir, S.; Nilsson, L.N.G. *et al.* Sensitive Detection of A β Protofibrils by Proximity Ligation--Relevance for Alzheimer's Disease. *BMC Neurosci.* **2010**, *11*, 124.
135. Stenh, C.; Englund, H.; Lord, A.; Johansson, A.; Almeida, C.G.; Gellerfors, P.; Greengard, P.; Gouras, G.K.; Lannfelt, L.; Nilsson, L.N.G. Amyloid- β Oligomers are Inefficiently Measured by Enzyme-Linked Immunosorbent Assay. *Ann. Neurol.* **2005**, *58*, 147-150.

©2011 by the authors; licensee MDPI, Basel, Switzerland. This article is an open access article distributed under the terms and conditions of the Creative Commons Attribution license (<http://creativecommons.org/licenses/by/3.0/>).

Appendix

I (Christa Hestekin) give permission to Elizabeth Pryor to reproduce the following copyrighted publications in her dissertation:

Publication 1) Pryor, E.; Moss, M. A.; Hestekin, C. N. Int. J. Mol. Sci. Unraveling the Early Events of A β Aggregation: Techniques for the Determination of A β Aggregate Size 2012, 13, 3038-3072

Publication 2) Pryor, E.; Kotarek, J. A.; Moss, M. A.; Hestekin, C. N. Int. J. Mol. Sci. Monitoring Insulin Oligomer Formation Via Capillary Electrophoresis, 2011, 12, 9369-9388

As one of the copyright holders for both of these publications, I verify that more than 50% of the work was conducted by Elizabeth Pryor and thus grant her permission to reproduce these two publications in her dissertation.

I, Melissa A Moss, give permission to Elizabeth Pryor to reproduce the following copyrighted publications in her dissertation:

Publication 1) Pryor, E.; Moss, M. A.; Hestekin, C. N. Int. J. Mol. Sci. Unraveling the Early Events of A β Aggregation: Techniques for the Determination of A β Aggregate Size 2012, 13, 3038-3072
Publication 2) Pryor, E.; Kotarek, J. A.; Moss, M. A.; Hestekin, C. N. Int. J. Mol. Sci. Monitoring Insulin Oligomer Formation Via Capillary Electrophoresis, 2011, 12, 9369-9388

As one of the copyright holders for both of these publications, I verify that more than 50% of the work was conducted by Elizabeth Pryor and thus grant her permission to reproduce these two publications in her dissertation.

CHAPTER 2: TECHNIQUES FOR THE DETERMINATION OF INSULIN

AGGREGATE SIZE

1. Insulin protein

Human insulin is a 51-residue protein hormone which stimulates the transport of glucose from blood into cells [1]. *In vivo*, insulin exists as a Zn^{2+} containing hexamer and is stored in the pancreas [2]. Upon dilution in the bloodstream, insulin dissociates rapidly through dimers to biologically active monomers [2]. *In vitro*, insulin exists as a mixture of monomer and oligomers, including dimers and hexamers [3]. Insulin is prone to form amyloid fibrils under various conditions *in vitro* [4,5]. It has been postulated that insulin aggregation *in vitro* occurs due to the presence of a destabilized monomer that undergoes non-native self-assembly by overcoming the free energy barrier [6-8]. This self-assembly proceeds through the formation of high-order oligomeric species and culminates with the appearance of insoluble fibrillar aggregates. Insulin fibrillization poses a problem for the treatment of Type II diabetes where insulin amyloid deposits have been observed at sites of repeated insulin injection [9-11]. These amyloid deposits are associated with the clinical syndrome, injection-localized amyloidosis [9,10]. It has been proposed that insulin is destabilized in the presence of hydrophobic interfaces such as the solid-aqueous interface of insulin pumps [5,12], leading to its aggregation. The deposition of insulin aggregates can lead to injection site problems for Type II diabetes patients, such as infection, bleeding, bruising, irritation, and inflammation [13]. In addition, insulin fibrillization *in vitro* presents a problem for the quality control of pharmaceutical insulin production [5]. Therefore, it is important to elucidate the molecular mechanisms underlying insulin amyloid fibrillization to improve the treatment of diabetes.

Similar to $A\beta$, a range of techniques are available to detect the insulin aggregate sizes formed throughout aggregation. Table 1 summarizes the advantages and disadvantages of these techniques as well as the insulin aggregate sizes which have been detected. In the subsequent sections, we will describe these literature studies in more detail.

Table 1: Summary of techniques for the quantitative detection and/or identification of insulin aggregate sizes formed throughout the aggregation process.

Technique	Advantages	Disadvantages	Insulin Aggregate Sizes Detected
SDS-PAGE	<ul style="list-style-type: none"> • SDS offers strong size-based separation 	<ul style="list-style-type: none"> • SDS may induce non-native behavior and destabilize oligomers • Gel smearing 	6, 12 kDa [14]
Native PAGE	<ul style="list-style-type: none"> • Ability to separate based on charge and hydrodynamic size 	<ul style="list-style-type: none"> • Gel smearing 	6 – 30 kDa [15]
Western Blotting	<ul style="list-style-type: none"> • High sensitivity and specificity, 	<ul style="list-style-type: none"> • Requires specific and expensive antibodies • Incomplete transfer of proteins onto membrane • Technically demanding 	6 – 30 kDa 30 – 185 kDa smear (with native-PAGE) [16]
Capillary and Microchip Electrophoresis	<ul style="list-style-type: none"> • Fast, highly sensitive separation of proteins based on charge and hydrodynamic size • Low sample volume 	<ul style="list-style-type: none"> • Low resolution of intermediate sized Aβ oligomers • Irreproducibility 	< 30 – 50 kDa 50 – 100 kDa [17]
Mass Spectrometry	<ul style="list-style-type: none"> • Fast data acquisition • Can identify multiple species with different mass-to-charge ratios 	<ul style="list-style-type: none"> • Inability to distinguish molecules with overlapping mass-to-charge ratios (MALDI, ESI) • Expensive • Labor intensive 	6 – 68 kDa [18-20]

Fluorescence Correlation Spectroscopy	<ul style="list-style-type: none"> • High sensitivity, ability to look at wide range of sizes within a sample • Fast analysis time • Low sample volume 	<ul style="list-style-type: none"> • Relies on assumptions about shape and kinetics of protein to determine molecular weight • Yields average molecular weight values 	No size determination [21,22]
Light Scattering	<ul style="list-style-type: none"> • Direct measurement of molar mass and radius (MALS) • Simultaneous detection of multiple populations within a sample (DLS) 	<ul style="list-style-type: none"> • Yields weight-average molar mass and not size of individual species or their distribution • Exponential dependence of scattering on aggregate size 	6, 12 kDa (SEC-MALS) [23] 2.3 – 6.5 nm 150 – 190 nm > 700 nm (DLS) [7,23-26]
Centrifugation	<ul style="list-style-type: none"> • Ability to detect a wide range of sizes (oligomers – fibrils) • Fast analysis time 	<ul style="list-style-type: none"> • Theoretical size estimate depends on appropriate assumptions in the model 	6 – 28 kDa[27,28] 28-60 kDa [28]
Size Exclusion Chromatography	<ul style="list-style-type: none"> • Well established technique 	<ul style="list-style-type: none"> • Leads to sample dilution which can dissociate unstable oligomers • Comparisons between elution behavior of oligomers and globular protein standards make molecular weight estimations difficult 	6, 12, 30, 36 kDa [23,28-30]

Transmission Electron Microscopy	<ul style="list-style-type: none"> • Good information on surface features, structure, and shape 	<ul style="list-style-type: none"> • Results skewed toward species which adhere to the support • Inability to distinguish between similarly sized oligomers (ie. dimer and trimer) • Laborious sample preparation • Expensive 	<p>5 – 15 nm (diameter) [27,31] 50 nm (diameter) [32] 100s nm -5 μm (length) [32]</p>
Enzyme-Linked Immunosorbent Assay	<ul style="list-style-type: none"> • Highly sensitive and specific • Ability to measure specific analytes within a crude preparation • Versatile 	<ul style="list-style-type: none"> • Gives information about presence of oligomers and not size • Requires expensive and specific antibodies 	<p>No size determination [15]</p>
Dot Blot	<ul style="list-style-type: none"> • Straight-forward, rapid technique 	<ul style="list-style-type: none"> • Gives information about presence of oligomers and not size • Requires expensive and specific antibodies 	<p>No size determination [33,34]</p>

2. Electrophoretic techniques for the quantification of insulin oligomer size

2.1 Sodium dodecyl sulfate- and native-polyacrylamide gel electrophoresis (SDS- and native-PAGE)

Compared to A β , fewer studies have been conducted which utilize SDS-PAGE to detect insulin aggregates. Low concentrations of SDS (0.1, 0.3, and 1 μ M) have been reported to accelerate insulin aggregation while higher SDS concentrations (10 to 360 μ M) led to a reduction in insulin aggregation [35]. One way to counter this phenomenon is to add urea to the sample to further denature the peptide and prevent aggregation. However, it has been shown that urea increases the rate of insulin fibrillation [5]. The drawbacks of SDS-PAGE may be overcome by using native-PAGE to separate various insulin sizes under conditions that allow the protein to remain in a native state.

Native-PAGE followed by Western Blotting has been applied to monitor the sizes of insulin oligomers formed at pH 2 and 60°C [16]. At 0 hours, insulin monomer (6 kDa) was present. After incubation for 24 hours, the appearance of ~12 and 18 kDa oligomers was observed. The formation of insulin species of ~24 kDa with a smear for sizes ranging from 30 to 185 kDa was observed after 48 hours. The differences between native-PAGE and SDS-PAGE highlight the importance of examining more than one method for studies of the various insulin aggregate sizes formed throughout the aggregation process.

2.2 Capillary electrophoresis (CE)

The utility of CE for the detection of insulin has been demonstrated by various researchers. Kunkel *et al.* have used CE with UV detection to analyze the degradation products formed by a 0.6 mg/mL human insulin solution in 0.9% NaCl (pH 7.8) which was incubated at 8°C for 2 weeks [36]. Separation of insulin from two degradation products was achieved. A

study by Gao *et al.* determined the dimerization constant of bovine insulin at pH 8.4 using CE with UV detection [37]. However, the determination of changes in insulin size with incubation time was not accomplished in either of the above mentioned studies. A study by Iwasa *et al.* used UV-CE to monitor the aggregation of insulin dissolved in HCl and incubated at 60°C for 1 – 4 days [38]. At 0 hours, a peak for native insulin was present. After 24 and 48 hours of incubation, this native insulin peak decreased in area and a new peak appeared with a faster migration time than the native insulin. After 96 hours, all peaks had essentially disappeared, indicating that insulin was fully aggregated into larger structures. Although this study looked at changes in the insulin peak pattern over time, no estimates of the sizes of these species were obtained. CE as a technique for the detection of insulin species formed throughout aggregation is still in its early stages. However, further improvements to this technique must be made in order to enhance the resolution of intermediate sized insulin species.

3. Spectroscopic techniques for the quantification of insulin oligomer size

3.1 Electrospray ionization mass spectrometry (ESI)-MS

ESI-MS has been used to analyze liquid insulin samples. Nettleton *et al.* studied the time course of insulin oligomer appearance using nano-ESI-MS. Oligomers exhibiting sizes up to 12 monomeric units were detected when insulin was aggregated at very high, millimolar concentrations [18]; however, large aggregates could not be studied using this technique. In addition, identification of insulin oligomers was complicated by the presence of overlapping charge states among the aggregates present. A study by Devlin *et al.* analyzed lower concentrations (0.44 mM) of insulin incubated at pH 2.0 and 60°C [19]. They found that insulin existed as a mixture of monomeric and dimeric species. These results are consistent with the observation that low pH helps solubilize proteins, thereby producing monomeric species.

3.2 Ion mobility mass spectrometry (IM)-MS

Various research groups have utilized IM-MS to gain a better understanding of the early events of insulin aggregation. Insulin monomer, dimer, and hexamer species formed at pH 7.4 have been detected using IM-MS, but changes in insulin size with aggregation time were not conducted in this study [20].

3.3 Fluorescence correlation spectroscopy

While FCS has been widely used in the literature as a way to estimate sizes of A β species, less work has been done using FCS to determine insulin sizes. The interaction between insulin and an inhibitory molecule p-FTAA has been characterized via FCS [22]. Furthermore, the association constant (K_{ass}) between insulin and its membrane-bound receptor has been determined via FCS by Zhong *et al* [21]. These studies illustrate that while FCS is a useful technique for size estimates, this technique has not been used specifically to determine the sizes of insulin species formed throughout aggregation.

4. Additional techniques utilized for insulin aggregate size determination

4.1 Light scattering techniques

Light scattering techniques are the more widely used technique to characterize insulin aggregate sizes. A study by Sluzky *et al.* utilized DLS to determine the particle diameter of insulin species generated upon agitation at 37 °C and 80 rpm in PBS (pH 7.4) [7]. A range of insulin species with diameters from 2.5 to 10 nm were observed initially in solution. Upon agitation for 1 h in the presence of Teflon spheres, a second peak appeared corresponding to insulin particles ~150 nm in diameter. After aggregation for 21 h, three species of insulin were present: native molecules with sizes ranging from 2.5 to 10 nm, stable intermediates with sizes ranging from 150 to 190 nm, and fully aggregated particles > 800 nm. Similar to the findings by

Sluzky *et al.* for the initial insulin sizes in solution, Kadima *et al.* observed species with a weight average molecular mass close to that of a hexamer (~5.6 nm) for a 12 mg/mL insulin solution at pH 7.5 with 100 mM NaCl [24]. Furthermore, they found that a 1.9 mg/mL insulin solution at pH 10.5 and 10 mM NaCl existed as primarily monomer (~3 nm).

4.2 Light scattering in combination with other techniques

Oliva *et al.* utilized SEC in conjunction with MALS and DLS to determine the molecular weight and size of insulin solutions [23]. SEC-MALS detected the presence of monomeric and dimeric species with r.m.s. radius values of 20 and 40 nm, respectively. In contrast, SEC-DLS yielded R_H values of 2.7, 3.8, and 5.5 nm which correspond to monomer, dimer, and hexamer, respectively.

4.3 Centrifugation

Ultracentrifugation has been utilized by Whittingham *et al.* to determine the molecular mass of insulin species formed under different solution conditions [27]. Insulin dissolved in sulfuric acid, citric acid, and a pH 2.0 solution existed as a mixture of monomer and dimer. In a 20% acetic acid solution insulin existed as monomer whereas in 0.1 M Tris-HCl at pH 8, insulin sizes ranging from dimer to tetramer were observed.

4.4 Size exclusion chromatography

A study by Ahmed *et al.* utilized SEC to monitor the effect of Gdn-HCl on insulin sizes formed at pH 7.4 [30]. Native insulin eluted at a volume of 6.1 mL, corresponding to hexamer. In the presence of 0.5 – 3 M Gdn-HCl, insulin existed as a mixture of monomer and dimer while at Gdn-HCl concentrations > 3.5 M, insulin was primarily monomeric. Similar to Ahmed *et al.*, Oliva *et al.* achieved separation of insulin dimer and monomer formed after incubation for 5 days at 60°C [23].

4.5 Transmission electron microscopy

Insulin protofibrils with a diameter of 5 nm and length of 4 – 5 μm have been observed by Whittingham *et al* [27]. Furthermore, the protofibrils sizes were found to be highly dependent on the type of acid used to dissolve insulin. Fibrillar insulin species with a diameter of ~14 – 15 nm formed by twisting at least two protofibrils into a flat ribbon-like fibril have been detected using TEM by Bouchard *et al* [31]. Contrary to these findings, Liu *et al.* observed insulin fibrils with a width of 50 nm and length of 100s of nm [32]. These fibrils were formed in the presence of 100 mM NaCl and this most likely explains the differences in diameter obtained.

5. Techniques utilized for amyloid oligomer identification

5.1 Dot blot

Studies utilizing dot blots for the detection of insulin monomer or fibrillar species have also been conducted, while studies on the detection of insulin oligomeric species are limited. The binding of aprotinin, an antiprotease which is known to be present in amyloid deposits, to insulin fibrils has been characterized via dot blots by Cardoso *et al* [34]. Dots were obtained for 100, 50, 25, and 10 μg of insulin fibrils in the presence of iodinated-aprotinin. Stains used to image protein gels such as SYPRO Ruby have been used to detect insulin monomer via dot blots [33]. These studies illustrate that dot blots have not been extensively used in the literature for the detection of insulin oligomers.

6. Summary of electrophoretic and non-electrophoretic based insulin and A β size detection methods

Chapters 1 and 2 describe a variety of techniques that are currently utilized to determine the size or presence of amyloid aggregates, with a focus upon oligomeric species. These techniques have been explored for the quantitative detection of different aggregate sizes with

various limitations to their resolution, dependence on pre-analysis procedures, sensitivity, cost, etc. Electrophoretic techniques, such as SDS-PAGE, Western blotting, and CE, are widely used for size-based separations of A β aggregates. These techniques have been less widely used to detect insulin aggregates. In particular, SDS-PAGE and Western blotting are suitable for the detection of monomeric and small oligomeric insulin A β species. The separation of larger oligomers via SDS-PAGE is more difficult due to the sensitivity of these sizes to denaturing conditions, which can result in aggregate decomposition during analysis. The recent development of antibodies specific for A β oligomers has led to an increase in the application of Western blotting, dot blotting, and ELISA to study A β aggregation. However, the detection limits of Western and dot blotting prohibit study of physiologically relevant A β concentrations. While more sensitive, ELISA is better suited for the identification of specific analytes, such as A β oligomers, present within a mixed population but cannot distinguish individual oligomer sizes. CE with LIF detection offers a highly sensitive detection of physiologically relevant concentrations, but the application of CE to amyloid aggregation analyses is still in the early stages. MS is another commonly used technique for A β aggregate size-based separations and is a more widely used technique for the detection of insulin aggregates. MS has been successfully used to detect small oligomeric species (especially IM-MS) but quantitative analyses of aggregate size may be limited by the pre-separation step, the ability to differentiate species with highly similar charge-to-mass ratios, and high equipment costs. FCS, MALS, and DLS may be utilized for determination of insulin A β aggregate size, but yield a weight-averaged molecular weight of species, thereby limiting the resolution of individual A β aggregate species. Centrifugation has been used to examine small oligomeric species up to large fibrils; but, selection of the method for determination of molar mass from sedimentation coefficients can

play an important role in size estimation. SEC may be coupled with these approaches or used as a standalone technique. SEC is complicated by dilution of the analyte during separation, inadequate resolution of intermediate oligomeric species, and limited utility of size standards. TEM is widely used to estimate the size of insulin and A β aggregates. TEM is a technique which is more suited for the detection of protofibrils and fibrils and does not possess the ability to distinguish between small oligomeric species which differ in size by a single monomer unit.

References

1. Hales, C.N. The Role of Insulin in the Regulation of Glucose Metabolism. Symposium Proceedings **1971**, *30*, 282-288.
2. Blundell, T.; Dodson, G. Adv. Protein Chem. **1972**, *26*, 279-402.
3. Grudzielanek, S.; Smirnovas, V. Solvation-Assisted Pressure Tuning of Insulin Fibrillation: From Novel Aggregation Pathways to Biotechnological Applications. J. Mol. Biol. **2006**, *356*, 497-509.
4. Waugh, D.F.; Wilhelmson, D.F. Studies of the Nucleation and Growth Reactions of Selected Types of Insulin Fibrils. J. Am. Chem. Soc. **1953**, *75*, 2592-2600.
5. Nielsen, L.; Khurana, R.; Fink, A. Effect of Environmental Factors on the Kinetics of Insulin Fibril Formation: Elucidation of the Molecular Mechanism. Biochemistry **2001**, *40*, 627-632.
6. Dobson, C.M. Protein Misfolding, Evolution and Disease. Trends Biochem. Sci. **1999**, *24*, 329-332.
7. Sluzky, V.; Tamada, J.; Klibanov, A.; Langer, R. Kinetics of Insulin Aggregation in Aqueous Solutions upon Agitation in the Presence of Hydrophobic Surfaces. Proc. Natl. Acad. Sci. USA **1991**, *88*, 9377-9381.
8. Jeffrey, P.; Milthorpe, B.; Nichol, L. Polymerization Pattern of Insulin at pH 7.0. Biochemistry **1976**, *15*, 4660-4665.
9. Dische, F.E.; Wernstedt, C. Insulin as an Amyloid-Fibril Protein at Sites of Repeated Insulin Injections in a Diabetic Patient. Diabetologia **1988**, *31*, 158-161.
10. Brange, J.; Andersen, L. Toward Understanding Insulin Fibrillation. J. Pharm. Sci. **1997**, *86*, 517-525.

11. Shikama, Y.; Kitazawa, J.; Yagihashi, N.; Uehara, O.; Murata, Y.; Yajima, N.; Wada, R.; Yagihashi, S. Localized Amyloidosis at the Site of Repeated Insulin Injection in a Diabetic Patient. *Intern Med.* **2010**, *49*, 397-401.
12. Mauro, M.; Craparo, E. Kinetics of Different Processes in Human Insulin Amyloid Formation. *J. Mol. Biol.* **2007**, *366*, 258-274.
13. Herman, W.; Ilag, L. A Clinical Trial of Continuous Subcutaneous Insulin Infusion Versus Multiple Daily Injections in Older Adults with Type 2 Diabetes. *Diabetes Care* **2005**, *28*, 1568-1573.
14. Chi, Q.; Huang, K. Polyacrylamide Gel Electrophoresis of Insulin. *Anal. Lett.* **2007**, *40*, 95-102.
15. Marcus, W.D.; Wang, H.; Lindsay, S.M.; Sierks, M.R. Characterization of an Antibody scFv that Recognizes Fibrillar Insulin and Beta-Amyloid using Atomic Force Microscopy. *Nanomedicine* **2008**, *4*, 1-7.
16. Velkova, A.; Tatarek-Nossol, M.; Andreetto, E.; Kapurniotu, A. Exploiting Cross-Amyloid Interactions to Inhibit Protein Aggregation but Not Function: Nanomolar Affinity Inhibition of Insulin Aggregation by an IAPP Mimic. *Angew. Chem., Int. Ed.* **2008**, *47*, 7114-7118.
17. Pryor, E.; Kotarek, J.A.; Moss, M.A.; Hestekin, C.N. Monitoring Insulin Oligomer Formation Via Capillary Electrophoresis. *Int. J. Mol. Sci.* **2011**, *12*, 9369-9388.
18. Nettleton, E.; Tito, P. Characterization of the Oligomeric States of Insulin in Self-Assembly and Amyloid Fibril Formation by Mass Spectrometry. *Biophysical Journal* **2000**, *79*, 1053-1065.
19. Devlin, G.L.; Knowles, T.P.J.; Squires, A.; McCammon, M.G.; Gras, S.L.; Nilsson, M.R.; Robinson, C.V.; Dobson, C.M.; MacPhee, C.E. The Component Polypeptide Chains of Bovine Insulin Nucleate Or Inhibit Aggregation of the Parent Protein in a Conformation-Dependent Manner. *J. Mol. Biol.* **2006**, *360*, 497-509.
20. Salbo, R.; Bush, M.F.; Naver, H.; Campuzano, I.; Robinson, C.V.; Pettersson, I.; Jorgensen, T.J.D.; Haselmann, K.F. Traveling-Wave Ion Mobility Mass Spectrometry of Protein Complexes: Accurate Calibrated Collision Cross-Sections of Human Insulin Oligomers. *Rapid Commun. Mass Spectrom.* **2012**, *26*, 1181-1193.
21. Zhong, Z.; Pramanik, A.; Ekberg, K.; Jansson, O.T.; Joernvall, H.; Wahren, J.; Rigler, R. Insulin Binding Monitored by Fluorescence Correlation Spectroscopy. *Diabetologia* **2001**, *44*, 1184-1188.

22. Wigenius, J.; Persson, G.; Widengren, J.; Inganaes, O. Interactions between a Luminescent Conjugated Oligoelectrolyte and Insulin during Early Phases of Amyloid Formation. *Macromol. Biosci.* **2011**, *11*, 1120-1127.
23. Oliva, A.; Farina, J.; Llabres, M. Development of Two High-Performance Liquid Chromatographic Methods for the Analysis and Characterization of Insulin and its Degradation Products in Pharmaceutical Preparations. *J. Chromatogr. , B: Biomed. Sci. Appl.* **2000**, *749*, 25-34.
24. Kadima, W.; Oegendal, L.; Bauer, R.; Kaarsholm, N.; Brodersen, K.; Hansen, J.F.; Porting, P. The Influence of Ionic Strength and pH on the Aggregation Properties of Zinc-Free Insulin Studied by Static and Dynamic Laser Light Scattering. *Biopolymers* **1993**, *33*, 1643-1657.
25. Bohidar, H.B. Dynamic Light Scattering Study of Heat Aggregation of Insulin. *Colloid Polym. Sci.* **1989**, *267*, 159-66.
26. Malik, R.; Roy, I. Probing the Mechanism of Insulin Aggregation during Agitation. *Int. J. Pharm.* **2011**, *413*, 73-80.
27. Whittingham, J.L.; Scott, D.J.; Chance, K.; Wilson, A.; Finch, J.; Brange, J.; Dodson, G.G. Insulin at pH 2: Structural Analysis of the Conditions Promoting Insulin Fibre Formation. *J. Mol. Biol.* **2002**, *318*, 479-490.
28. Jeffrey, P.D. Polymerization Behavior of Bovine Zinc-Insulin at Neutral pH. Molecular Weight of the Subunit and the Effect of Glucose. *Biochemistry* **1974**, *13*, 4441-4447.
29. Yu, C.; Chin, C. In Situ Probing of Insulin Aggregation in Chromatography Effluents with Spectroturbidimetry. *Journal of Colloid and Interface Science* **2006**, *299*, 733-739.
30. Ahmad, A.; Millett, I. Partially Folded Intermediates in Insulin Fibrillation. *Biochemistry* **2003**, *42*, 11404-11416.
31. Bouchard, M.; Zurdo, J.; Nettleton, E.J.; Dobson, C.M.; Robinson, C.V. Formation of Insulin Amyloid Fibrils Followed by FTIR Simultaneously with CD and Electron Microscopy. *Protein Sci.* **2000**, *9*, 1960-1967.
32. Liu, R.; Su, R.; Qi, W.; He, Z. Photo-Induced Inhibition of Insulin Amyloid Fibrillation on Online Laser Measurement. *Biochem. Biophys. Res. Commun.* **2011**, *409*, 229-234.
33. Yamada, N.; Ozawa, S.; Kageyama, N.; Miyano, H. Detection and Quantification of Protein Residues in Food Grade Amino Acids and Nucleic Acids using a Dot-Blot Fluorescent Staining Method. *J. Agric. Food Chem.* **2004**, *52*, 5329-5333.
34. Cardoso, I.; Pereira, P.J.B.; Damas, A.M.; Saraiva, M.J.M. Aprotinin Binding to Amyloid Fibrils. *Eur. J. Biochem.* **2000**, *267*, 2307-2311.

35. Badraghi, J.; Yousefi, R.; Saboury, A.A.; Sharifzadeh, A.; Haertle, T.; Ahmad, F.; Moosavi-Movahedi, A.A. Effect of Salts and Sodium Dodecyl Sulfate on Chaperone Activity of Camel αS_1 -CN: Insulin as the Target Protein. *Colloids Surf. , B* **2009**, *71*, 300-305.
36. Kunkel, A.; Gunter, S.; Watzig, H. Quantitation of Insulin by Capillary Electrophoresis and High-Performance Liquid Chromatography. Method Comparison and Validation. *Journal of Chromatography* **1997**, *781*, 445-455.
37. Gao, J.; Mrksich, M.; Gomez, F.A.; Whitesides, G.M. Using Capillary Electrophoresis to Follow the Acetylation of the Amino Groups of Insulin and to Estimate their Basicities. *Anal. Chem.* **1995**, *67*, 3093-100.
38. Iwasa, S.; Enomoto, A.; Onoue, S.; Nakai, M.; Yajima, T.; Fukushima, T. Chromatographic Analysis of Conformationally Changed Insulin and its Cytotoxic Effect on PC12 Cells. *J. Health Sci.* **2009**, *55*, 825-831.

CHAPTER 3: MONITORING INSULIN AGGREGATION VIA CAPILLARY ELECTROPHORESIS

Pryor, E.; Kotarek, J. A.; Moss, M. A.; Hestekin, C. N. *Int. J. Mol. Sci.* Monitoring Insulin Oligomer Formation Via Capillary Electrophoresis, 2011, *12*, 9369-9388.

Abstract

Early stages of insulin aggregation, which involve the transient formation of oligomeric aggregates, are an important aspect in the progression of Type II diabetes and in the quality control of pharmaceutical insulin production. This study is the first to utilize capillary electrophoresis (CE) with ultraviolet (UV) detection to monitor insulin oligomer formation at pH 8.0 and physiological ionic strength. The lag time to formation of the first detected species in the aggregation process was evaluated by UV-CE and thioflavin T (ThT) binding for salt concentrations from 100 mM to 250 mM. UV-CE had a significantly shorter (5–8 h) lag time than ThT binding (15–19 h). In addition, the lag time to detection of the first aggregated species via UV-CE was unaffected by salt concentration, while a trend toward an increased lag time with increased salt concentration was observed with ThT binding. This result indicates that solution ionic strength impacts early stages of aggregation and β -sheet aggregate formation differently. To observe whether CE may be applied for the analysis of biological samples containing low insulin concentrations, the limit of detection using UV and laser induced fluorescence (LIF) detection modes was determined. The limit of detection using LIF-CE, 48.4 pM, was lower than the physiological insulin concentration, verifying the utility of this technique for monitoring biological samples. LIF-CE was subsequently used to analyze the time course for fluorescein isothiocyanate (FITC)-labeled insulin oligomer formation. This study is the first to report that the

FITC label prevented incorporation of insulin into oligomers, cautioning against the use of this fluorescent label as a tag for following early stages of insulin aggregation.

Keywords

capillary electrophoresis; ultraviolet absorbance; laser induced fluorescence; thioflavin T; insulin; oligomer; amyloid

1. Introduction

Human insulin is a 51-residue protein hormone which stimulates the transport of glucose from blood into cells [1]. *In vivo*, insulin exists as a Zn^{2+} containing hexamer and is stored in the pancreas [2]. Upon dilution in the bloodstream, insulin dissociates rapidly through dimers to biologically active monomers [2]. *In vitro*, insulin exists as a mixture of monomer and oligomers, including dimers and hexamers [3]. Insulin is prone to form amyloid fibrils under various conditions both *in vitro* and *in vivo* [4,5]. It has been postulated that insulin aggregation both *in vitro* and *in vivo* occurs due to the presence of a destabilized monomer that undergoes non-native self-assembly by overcoming the free energy barrier [6–8]. This self-assembly proceeds through the formation of high-order oligomeric species and culminates with the appearance of insoluble fibrillar aggregates. Insulin fibrillization poses a problem for the treatment of Type II diabetes where insulin amyloid deposits have been observed at sites of repeated insulin injection [9–11]. These amyloid deposits are associated with the clinical syndrome, injection-localized amyloidosis [9,10]. It has been proposed that insulin is destabilized in the presence of hydrophobic interfaces such as the solid-aqueous interface of insulin pumps [5,12], leading to its aggregation. The *in vivo* deposition of insulin aggregates can lead to injection site problems for Type II diabetes patients, such as infection, bleeding, bruising, irritation, and inflammation [13]. In addition, insulin fibrillization *in vitro* presents a problem for

the quality control of pharmaceutical insulin production [5]. Therefore, it is important to elucidate the molecular mechanisms underlying insulin amyloid fibrillization to improve the treatment of diabetes.

The visualization of oligomers, which appear in the early stages of aggregation, is one key to understanding the molecular mechanisms underlying amyloid formation. Various techniques have been utilized to detect soluble and low-molecular weight oligomeric species formed by amyloid proteins such as atomic force microscopy (AFM) [12,14], light scattering [12,14], hydrogen-deuterium exchange mass spectrometry [15,16], matrix assisted laser desorption ionization mass spectrometry (MALDI-MS) [17,18], electrospray ionization mass spectrometry (ESI-MS) [19], ion mobility mass spectrometry (IM-MS) [20–23], and oligomer specific antibodies [24–26]. A major analytical challenge is developing a technique which is capable of identification, quantification, and characterization of a wide range of amyloid species. Electrophoretic techniques can be used to detect soluble and low-molecular weight oligomeric species and provide a compliment for other traditional techniques. These electrophoretic techniques include sodium dodecyl sulfate polyacrylamide gel electrophoresis (SDS-PAGE) [27–30], Western immunoblotting [27,29,31–37], and capillary electrophoresis (CE) [38–43]. SDS-PAGE is a commonly used technique, but SDS has been reported to accelerate β sheet formation during amyloid aggregation [44,45], to induce and possibly stabilize aggregation [36], and to misrepresent the native species and their assembly [46]. Western blotting necessitates the use of expensive and specific antibodies and can also require a pre-concentration step such as immunoprecipitation [47,48]. In addition, these gel-based methods can produce smears making specific oligomer size determination impossible [29,30]. In contrast, CE provides the ability to inexpensively monitor the aggregation of insulin under native conditions.

Capillary electrophoresis (CE) offers fast and highly efficient separation of molecules with a broad range of properties thereby making it well suited for the analyses of biological samples, which contain different types and sizes of proteins [49]. CE separates proteins based on electrophoretic mobility, which is related to charge, shape, and/or size. Previous studies have demonstrated the utility of CE to detect low concentrations of insulin [50–52] and identify differences in insulin analogs [42]. In this work, we have extended CE to monitor the appearance of insulin oligomers over time when aggregation is carried out under varying solution conditions. In addition, we have probed the ability of CE to detect insulin at physiological concentrations. This study is the first report of the use of UV-CE to monitor insulin oligomer formation at pH 8.0 and physiological ionic strength. Our results demonstrate the utility of CE as a complimentary technique for studying the early stages of insulin aggregation and define the hurdles that must be overcome before the aggregation of biological insulin concentrations can be explored.

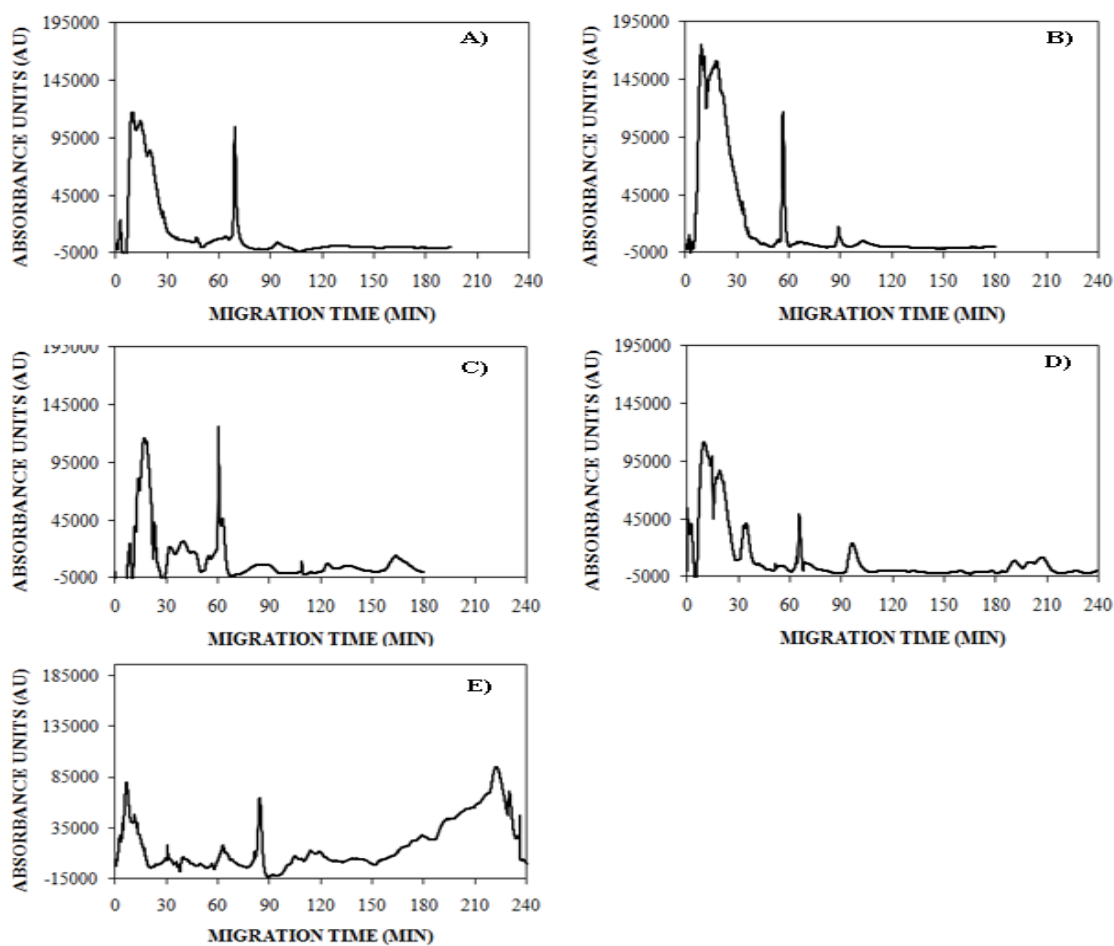
2. Results and Discussion

2.1. Detection of Insulin Oligomers Using CE with UV Detection

To explore the use of CE for the detection of insulin oligomers that appear during early stages of insulin aggregation, lyophilized insulin was solubilized in 5 mM NaOH, diluted into 40 mM Tris (pH 8.0), subjected to 150 mM NaCl, and agitated at 185 rpm to promote amyloid assembly. The reaction was analyzed using UV-CE at early and late time points to assess the appearance of oligomers and progression into larger aggregate species. At 0 h, UV-CE demonstrated the presence of an early, broad peak in addition to a sharper peak migrating at ~70 min (Figure 1A). The size of these species was probed using a filtration analysis similar to that performed by Sabella *et al.* who used molecular weight cutoff membranes to size early amyloid-

β aggregation species detected via UV-CE. For our experiments, we used membranes with molecular weight cutoffs of 30, 50, and 100 kDa to determine that the species present at 0 h correspond to molecular weights <30–50 kDa, or oligomers of <5–8 monomer units. A similar peak pattern was obtained after 4 h with the appearance of another peak migrating at ~90 min (Figure 1B). At 8 and 12 h, broad peaks migrating at times >90 min appeared (Figure 1C,D). The size of these species was estimated by filtration analysis to be >50 kDa, or larger than 8 monomer units, thus indicating the detection by UV-CE of the first species in the aggregation process. By 24 h, aggregate peaks of greater intensity appeared at migration times >150 min, indicating the formation of larger and more concentrated aggregate species, estimated via filtration analysis to be <100 kDa, or less than 17 monomer units (Figure 1E). Due to experimental time constraints, UV-CE runs for the 0, 4, and 8 h time points were terminated at 180 min. Separate experiments with run times of 240 min were conducted for the 0, 4, and 8 h time points and confirm that no significant species (signal to noise or S/N >3) were present at migration times >180 min (see supplementary materials).

Figure 1. Detection of insulin monomer, oligomer, and higher molecular weight aggregation states using UV-CE. Insulin was aggregated under agitation (185 rpm) at 0.2 mg/mL in 40 mM Tris (pH 8.0) containing 150 mM NaCl and at 25 °C. At 0 h (panel **A**), 4 h (panel **B**), 8 h (panel **C**), 12 h (panel **D**), and 24 h (panel **E**), CE was performed in conjunction with UV detection with a 0.5 psi pressure injection for 8 s with separation at 15 kV using 0.5% PHEA separation matrix in a PHEA coated capillary. Results are representative of three independent experiments. Supplementary data confirms the absence of significant peaks at a migration time of >180 min for 0, 4, and 8 h time points.



Other measurement techniques have been employed previously to characterize insulin oligomers. Quasi elastic light scattering (QELS) [7], high performance liquid chromatography (HPLC) [53], small angle neutron scattering (SANS) [54], and nanoflow electrospray (nano-ES) mass spectrometry [55] have been successfully used to detect oligomeric insulin species. A study by Sluzky *et al.* utilized QELS to determine the particle diameter of insulin species generated upon agitation at 37 °C and 80 rpm in PBS (pH 7.4) [7]. Similar to the UV-CE results at 0 hr, a range of insulin species with diameters from 2.5 to 10 nm were observed initially in solution. Upon agitation for 1 h in the presence of Teflon spheres, a second peak appeared corresponding to insulin particles ~150 nm in diameter. After aggregation for 21 h, three species of insulin were present: native molecules with sizes ranging from 2.5 to 10 nm, stable intermediates with sizes ranging from 150 to 190 nm, and fully aggregated particles >800 nm. Nayak *et al.* and Vestergaard *et al.* utilized SANS and SAXS to monitor the formation of insulin oligomers and proposed a model for nucleus formation and growth [54,56]. However, insulin oligomers were generated under extreme conditions (45–65 °C, pH = 1.6–2.0, 5–10 mg/mL) which may not accurately reflect insulin aggregation *in vivo*. Nettleton *et al.* studied the time course of insulin oligomer appearance using nano-ES. Oligomers exhibiting sizes up to 12 monomeric units were detected when insulin was aggregated at very high, millimolar concentrations [55]; however, large aggregates could not be studied using this technique. In addition, identification of insulin oligomers was complicated by the presence of overlapping charge states among the aggregates present. The drawbacks of each technique listed above show that other complementary methods may be needed to verify the results obtained. The UV-CE method in the current study was able to detect insulin oligomers that appeared transiently during amyloid formation at a pH of 8.0 and at micromolar insulin concentrations. This

highlights the potential for CE to be used as a complementary technique to follow the evolution of insulin oligomer appearance.

2.2. Effect of Salt Concentration on the Time Course for Insulin Oligomer Formation

Solution conditions such as protein concentration [5,57], pH [5], and ionic strength [5,58,59] have been reported to have a pronounced impact upon the rate at which insulin aggregates, and understanding these effects can provide insight into the mechanism of insulin aggregation. Here, CE was employed to study the effect of solution ionic strength on the early events of insulin aggregation by examining the time to appearance of oligomers formed when insulin is aggregated at 25 °C and pH 8.0 (40 mM Tris) in the presence of three different concentrations of NaCl: 100 mM, 150 mM, and 250 mM. Figure 2 illustrates the change in normalized migration time of the largest species present throughout the early stages of aggregation. During the first 5 h of aggregation, there was little change in the migration time at all three salt concentrations. After 5 h, oligomeric species began to form. While the time to oligomer appearance was unaffected by NaCl concentration (Table 1), the size of oligomers formed increased with salt concentration. At 10 h, oligomers formed in the presence of 150 and 250 mM NaCl exhibiting significantly longer migration times than those formed in the presence of 100 mM NaCl (Figure 2). To our knowledge, no other studies have used methods focused on oligomer detection to examine the effect of ionic strength on insulin aggregation.

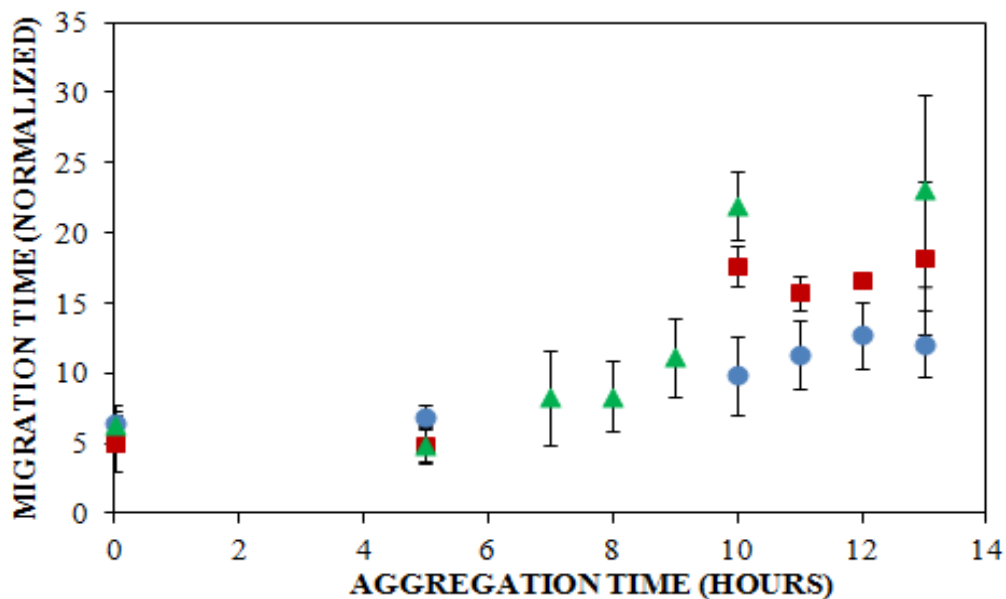
Table 1. Lag times observed at 100, 150, and 250 mM NaCl by CE *versus* ThT binding.

NaCl concentration	Lag time for CE	Lag time for ThT Binding
(mM)	(h) ¹	(h) ²
100	6.7 ± 1.7	16 ± 1.0 ***
150	5.0 ± 0.0	15 ± 1.4 ***
250	7.6 ± 1.3	19 ± 2.4 ***

¹ Results are reported as the mean ± SE, $n = 3$. ² Results are reported as the mean ± SE, $n = 4$.

*** $p < 0.001$ for comparison between detection via UV-CE and ThT binding.

Figure 2. Effect of solution ionic strength on the formation of insulin oligomers detected by UV-CE. Insulin was diluted to 0.2 mg/mL in 40 mM Tris (pH 8.0) containing 100 mM (●), 150 mM (■), or 250 mM (▲) NaCl. Aggregation was induced at 25 °C by continuous agitation (185 rpm) and monitored using UV-CE. CE was performed with sample injection at 0.5 psi for 8 s with 15 kV separation using 1% PHEA separation matrix in a PHEA coated capillary. Migration times were normalized to those observed prior to the onset of aggregation using the peak corresponding to monomer to facilitate comparison between individual runs. Error bars represent SE, $n = 3$. For the 10 h time point, the migration times of the 150 mM and 250 mM NaCl were both determined to be statistically different from the 100 mM NaCl migration time with a $p < 0.1$.

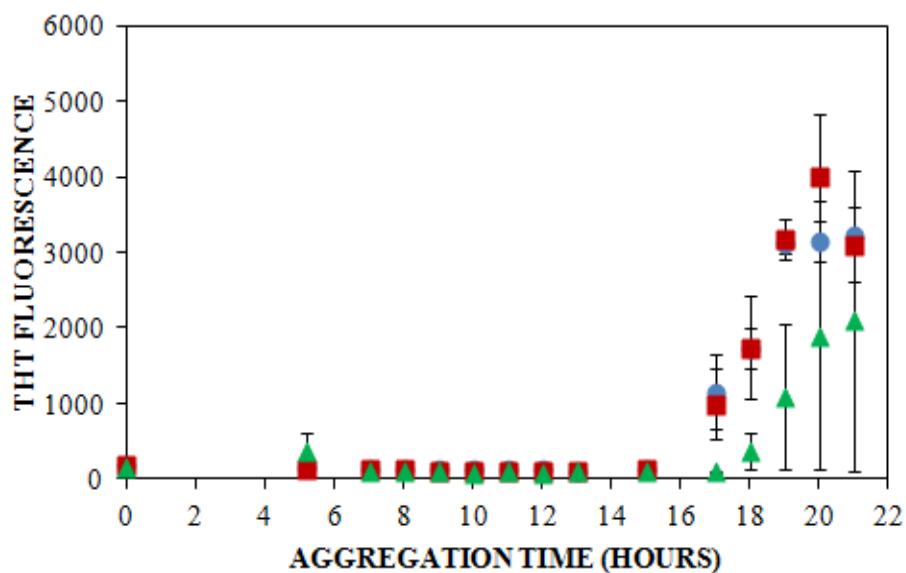


A traditional method of detecting amyloid aggregates containing a cross β -sheet structure is through the examination of thioflavin T (ThT) binding, which has been used to study insulin aggregation under a variety of solution conditions. ThT is an intercalating fluorescent dye that binds to the β -sheet structure within amyloid fibrils, giving rise to a shifted excitation maximum at 450 nm and a shifted and enhanced emission at 482 nm [5,60]. For our study, ThT was also used to follow insulin aggregation in order to compare the lag times obtained using ThT fluorescence with those observed using CE. When insulin was aggregated at pH 8.0 (40 mM Tris) and 25 °C with agitation (185 rpm) in the presence of 100 mM NaCl, 150 mM NaCl, or 250 mM NaCl, the lag time, or initial increase in ThT fluorescence, was observed at 16 ± 1.0 h, at 15 ± 1.4 h, and at 19 ± 2.4 h, respectively (Figure 3, Table 1). These results demonstrate a trend toward a longer lag time at the highest salt concentration.

Other researchers have examined the effect of ionic strength on insulin structure [58,59] and aggregation lag time, but under slightly different conditions. At a similar solution pH of 7.0–8.0, lag times of 6–9 h have been reported in studies that have employed higher insulin concentrations [61] or higher temperatures with more vigorous agitation [62], which have both been reported to enhance amyloid protein aggregation [5,57,63–65]. Furthermore, changes in the lag time to ThT fluorescence have been observed to depend upon the change in solution ionic strength when insulin is aggregated under continuous agitation. Nielsen *et al.* observed that an increase in the NaCl concentration from 50 to 500 mM led to an initial decrease in the lag time from 1.6 to 1.3 h, whereas at the highest salt concentration of 500 mM, the lag time increased to 1.5 h [5]. Although much shorter lag times were observed in this study, likely due to the higher incubation temperature (37 °C) and acidic solution pH (1.6), the latter result parallels the effect of NaCl concentration on ThT detection of insulin aggregates observed in the current study,

where an increase in the NaCl concentration to 250 mM resulted in an increase in the lag time (Figure 3).

Figure 3. Effect of solution ionic strength on the formation of insulin aggregates detected by ThT binding. Insulin was diluted to 0.2 mg/mL in 40 mM Tris (pH 8.0) containing 100 mM (●), 150 mM (■), or 250 mM (▲) NaCl. Aggregation was induced at 25 °C by continuous agitation (185 rpm) and monitored via ThT fluorescence by periodic dilution into 10 μM ThT. Error bars represent SE. Results are representative of two independent experiments.

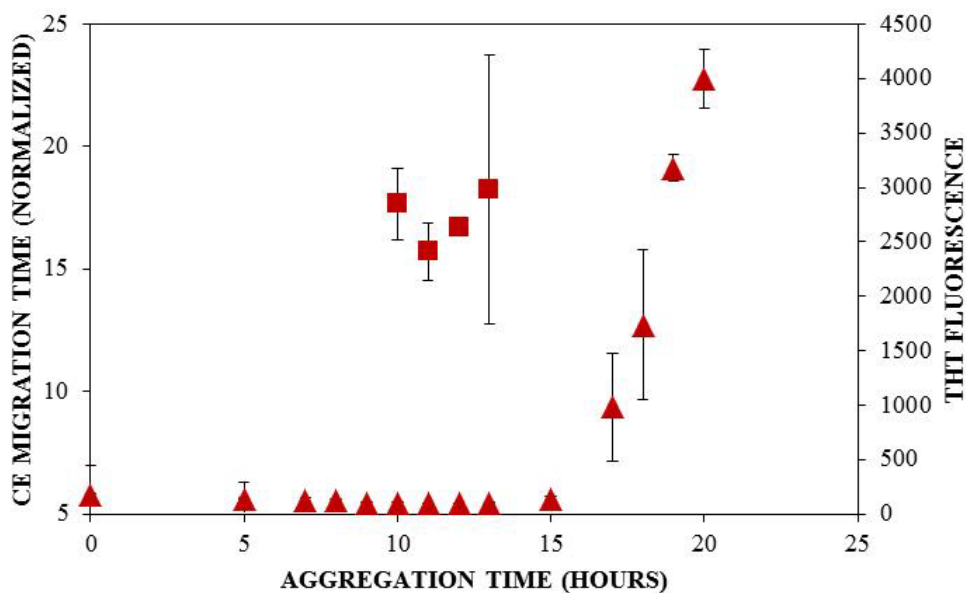


When results from UV-CE (Figure 2) and ThT binding detection (Figure 3) of the initial aggregation state are compared (Figure 4, Table 1), it is clear that UV-CE is able to detect the aggregation process significantly earlier than ThT binding. In the presence of 100 and 150 mM NaCl, oligomers were detected using UV-CE 10 h prior to the observed increase in ThT fluorescence, and in the presence of 250 mM NaCl, UV-CE was able to resolve oligomers more than 11 h prior to the detection of aggregates using ThT. These differences most likely result from the inability of ThT to recognize early oligomeric species due to their lack of β -sheet structure. In contrast, UV-CE does not rely on the binding of a dye to this specific conformation but can instead detect oligomers regardless of their conformation. These results show that CE is capable of detecting early insulin oligomeric species while ThT binding can be used to verify the appearance of larger aggregates present in higher quantities. Therefore, CE and ThT binding can be used in a complimentary manner to detect species formed during all stages of aggregation.

Differences in detection capabilities of UV-CE and ThT binding lead to a more comprehensive understanding of the effect of NaCl on insulin aggregation. Results from UV-CE suggest that NaCl has little effect on the appearance of early aggregated states, shown by filtration studies to be oligomeric in nature. In contrast, results from ThT binding conversely suggest that increasing the NaCl concentration extends the lag time to formation of aggregated states with β -sheet conformations (Table 1). This comparison underscores the differences in amyloid protein aggregation that can be observed between oligomer and β -sheet aggregate behavior and emphasizes the need for a complimentary detection method, like CE, that can follow early stages in the aggregation process. A higher solution ionic strength could alter the structure of oligomers, leading to a slower conversion to the β -sheet structure detectable by ThT binding. Alternatively, concentrations of oligomers may remain low under conditions of higher

solution ionic strength, thus precluding their detection by ThT binding, which exhibits high nanomolar to low micromolar limit of detection, for longer periods of time. An increase in the lag time detected by ThT binding at higher NaCl concentrations has also been observed in studies of other proteins that form amyloid aggregates [66]. The conclusion drawn by Lin *et al.* in these studies was that short and thick fibrils are formed at higher NaCl concentrations, and these fibrils are characterized by low intensity ThT binding signals. Thus, the ability of CE to detect insulin species independent of their conformation and at very low concentrations provides additional insight into the early events of insulin aggregation.

Figure 4. Comparison of lag times observed by UV-CE (■) and ThT binding (▲). Insulin was diluted to 0.2 mg/mL in 40 mM Tris (pH 8.0) containing 150 mM NaCl. Aggregation was induced at 25 °C by continuous agitation (185 rpm) and monitored via UV-CE or ThT fluorescence as described in Figure 2 and Figure 3, respectively.



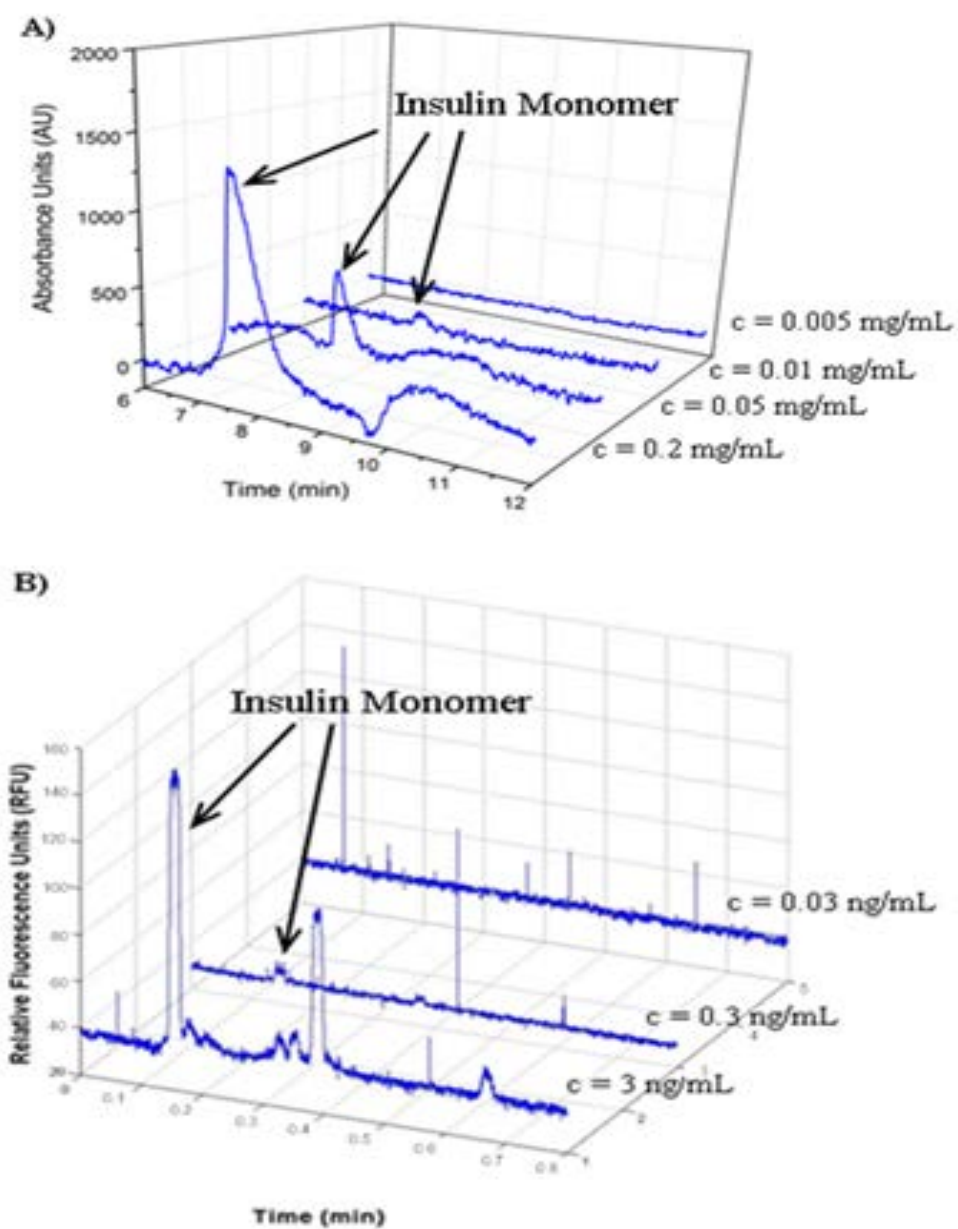
2.3. Determination of Insulin Limit of Detection

The ability to detect proteins at low concentrations will be necessary for the study of insulin aggregation at biological concentrations (300 pM) [67]. CE typically uses either UV absorbance or LIF to detect proteins. UV can detect proteins without any additional labeling, but typically has a lower sensitivity than LIF. LIF usually requires fluorescent labeling of the molecule to be detected, but is highly sensitive with previous reports of LIF-CE detection of double-stranded DNA down to the pg/ μ L range [68,69]. To determine the insulin detection limit using UV-CE, insulin monomer prepared at concentrations ranging from 0.005 mg/mL to 0.2 mg/mL was analyzed. The S/N ratio of the insulin peak was >3 at concentrations of 0.01 mg/mL and higher, defining 0.01 mg/mL (1.72 μ M) as the limit of detection for insulin using UV-CE (Figure 5A). The definition of the detection limit as the analyte concentration with a S/N ratio >3 has been used previously in studies utilizing CE detection [70,71]. In addition, a similar limit of detection for insulin of 0.02 mg/mL (3.44 μ M) has been obtained by Kunkel *et al.* using UV-CE [52].

A parallel limit of detection study was performed for fluorescein isothiocyanate (FITC)-labeled insulin monomer using LIF-CE. First, injection conditions were optimized by studying a range of sample injection voltages and injection times. As both the injection voltage and injection time were increased, observed insulin peaks increased in intensity. However, when the injection voltage and injection time were increased beyond 12 kV and 12 s, respectively, significant carryover of insulin between runs was observed due to the large amount of insulin injected into the capillary. Therefore, an injection voltage of 12 kV and an injection time of 12 s were selected as optimal. To determine the insulin detection limit using LIF-CE, FITC-labeled insulin monomer prepared at concentrations ranging from 0.03 to 3 ng/mL was analyzed. The

S/N ratio of the insulin peak was >3 at concentrations of 0.3 ng/mL and higher, thus establishing 0.3 ng/mL (48.4 pM) as the limit of detection for FITC-labeled using LIF-CE (Figure 5B) and illustrating the superior limit of insulin detection for LIF-CE compared with UV-CE. In fact, the LIF detection limit of 48.4 pM is lower than the physiological insulin concentration of 300 pM [67] and to the authors' knowledge, is the lowest LIF detection limit of insulin for an electrophoresis based method. Thus, LIF-CE is a promising technique for the detection of physiologically relevant insulin concentrations. Figure 5B also demonstrates the detection of four peaks in addition to the peak corresponding to monomeric protein. These additional peaks are most likely the presence of dimers and hexamers that have been reported to exist *in vitro* in freshly dissolved insulin solutions [72,73]. These species may be present at concentrations below the limit of insulin detection by UV-CE. The lower limit of detection offered by LIF-CE should facilitate the detection of these species.

Figure 5. Limit of detection for monomeric insulin. **(A)** UV-CE detection of insulin with a 0.5 psi pressure injection for 8 s at 15 kV separation voltage using 0.1% PHEA separation matrix in a PHEA coated capillary; **(B)** LIF-CE detection of insulin with a 12 kV electrokinetic injection for 12 s at 15 kV separation voltage using 0.1% PHEA separation matrix in a PHEA coated capillary.



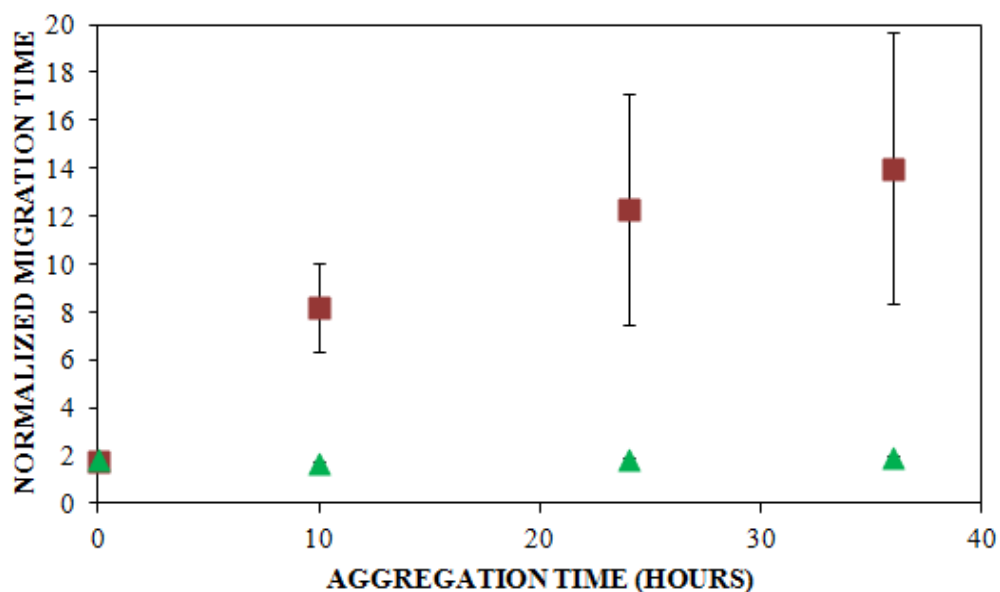
2.4. Analysis of FITC Tracer Incorporation into Unlabeled Insulin

The ability of LIF-CE to detect insulin at sub-physiological concentrations suggests that this technique holds promise for the study of insulin aggregation at physiological insulin concentrations. Such studies will require the presence of a fluorescent label within insulin oligomers that appear during early stages of aggregation. Therefore, the ability of FITC-labeled insulin and unlabeled insulin to co-aggregate was explored. FITC-labeled insulin was selected because it has been previously shown to be an effective insulin label for LIF-CE applications [74,75]. FITC is covalently bound to the ϵ -amino groups of internal lysine residues and the α -amino group of the *N*-terminal residue. Unlike fluorescent amyloid-binding dyes, the covalent incorporation of this FITC label ensures its presence within both monomeric protein and aggregates that incorporate the labeled protein, including those that precede the appearance of β -sheet structure.

A sample consisting of 75% unlabeled insulin and 25% FITC-labeled insulin was prepared in 40 mM Tris (pH 8.0) containing 150 mM NaCl and agitated at 185 rpm to promote amyloid assembly. The reaction was analyzed using LIF-CE to assess the appearance of insulin oligomers. As shown in Figure 6, no change in the normalized migration time was observed over a 36 h period. Because oligomers of unlabeled insulin were observed using UV-CE beginning after 5 h following the onset of aggregation (Figure 2), this result suggested that the presence of the FITC label was preventing the aggregation of FITC-labeled insulin. To explore this possibility, LIF-CE was used to monitor the aggregation of 100% FITC-labeled insulin solubilized in Tris (pH 8.0), subjected to 150 mM NaCl, and agitated at 185 rpm (data not shown). Again, the normalized migration time was unchanged during the first 24 h following the

initiation of agitation, confirming that the presence of the FITC label prevents aggregation within this timeframe.

Figure 6. Coaggregation of FITC-labeled insulin and unlabeled insulin. Insulin solutions consisting of 25% FITC-labeled insulin and 75% unlabeled insulin with LIF detection (\blacktriangle , $n = 6$) and UV detection (\blacksquare , $n = 3$) were prepared at a concentration of 0.2 mg/mL in 40 mM Tris (pH 8.0) containing 150 mM NaCl. Solutions were subjected to agitation (185 rpm), and the formation of aggregates was monitored. LIF-CE was performed with a sample injection at 12 kV for 12 s with 15 kV separation and UV-CE was performed with a sample injection at 10 kV for 12 s with 15 kV separation. Both separations were performed using 1% PHEA separation matrix in PHEA coated capillary. Migration times were normalized as described in Figure 2. Error bars represent SE, $n = 3$ –6. Some error bars lie within symbols. For all time points >0 h, UV data was statistically different from the LIF data with a $p < 0.015$.



To further determine whether the FITC-labeled insulin was inhibiting the formation of unlabeled insulin aggregates or failing to incorporate into aggregates formed from the unlabeled protein, UV-CE was performed in parallel with LIF-CE to monitor the aggregation of 75% unlabeled insulin and 25% FITC-labeled insulin solubilized in 40 mM Tris (pH 8.0) containing 150 mM NaCl and subjected to agitation at 185 rpm. As shown in Figure 6, the normalized migration time for UV-CE increased significantly over a period of 36 h, beginning by 10 h following the onset of agitation, while the normalized migration time for LIF-CE remained unchanged. These results indicate that insulin oligomers and larger aggregates were formed from the unlabeled protein and that the FITC-labeled insulin did not incorporate into these aggregates. Since some small compounds have been previously reported as inhibitors of β -sheet formation, it is possible that the FITC label is acting as an inhibitor to insulin aggregation. Another possibility is that the FITC attachment site is critical for proper β -sheet folding. A similar extension of the lag time to aggregation has been observed following the methylation of amino groups within the amyloid- β protein [76] and the introduction of a mutant that mimics phosphorylation of serine residues within Huntington protein [77]. In addition, the quantity of amyloid aggregates formed is reduced following the citraconylation of lysine residues within lysozyme [78] or stilbine modification of ϵ -amino groups within transthyretin [79]. Therefore, dyes with alternative properties or attachment sites need to be explored. In particular, less bulky fluorescent probes, such as BODIPY, or attachment of dyes exclusively at the *N*- or *C*- terminus would be less likely to impact aggregate formation.

3. Materials and Methods

3.1. Materials

Previous studies have shown no differences between the three-dimensional structures of bovine and synthetic human insulin [80] and the binding affinity of bovine and synthetic insulin to insulin receptors at three major sites of insulin action are similar [81]. Similar to human insulin, bovine insulin contains 51 amino acids but differs from human insulin in residues A8 (Thr→Ala), A10 (Iso→Val), and B30 (Thr→Ala) [82]. Therefore, bovine insulin was used for all studies. Insulin and fluorescein isothiocyanate (FITC)-labeled insulin from bovine pancreas, poly-*N*-hydroxyethyl acrylamide (PHEA) and thioflavin T (ThT) were obtained from Sigma-Aldrich (St. Louis, MO). Polymerization initiation compound 2,2'-azobis(2-amidinopropane) dihydrochloride (V-50) was purchased from Wako Chemical (Richmond, CA). Amicon centrifugal filter units were purchased from Millipore (Billerica, MA).

3.2. Insulin Preparation

Lyophilized insulin and FITC-labeled insulin were stored at $-20\text{ }^{\circ}\text{C}$. Unlabeled insulin was reconstituted to a final concentration of 0.005–0.2 mg/mL in 40 mM Tris (pH 8.0) containing 0–250 mM NaCl. FITC-labeled insulin was reconstituted to a final concentration of 0.03 ng/mL–0.2 mg/mL in 40 mM Tris (pH 8.0) containing 0–150 mM NaCl. Samples consisting of 75% unlabeled insulin and 25% FITC-labeled insulin were prepared by mixing the necessary proportions of insulin and FITC-labeled insulin from individual stock concentrations of 0.3 and 0.2 mg/mL, respectively.

3.3. Electrophoresis Conditions for UV and LIF Studies

All studies were carried out in 0.1% w/v PHEA coated capillaries with a 0.1–1% PHEA separation matrix and a capillary temperature of $25\text{ }^{\circ}\text{C}$. Capillary dimensions for UV-CE studies

were $L_t = 31$ cm, $L_d = 10$ cm and for LIF-CE studies were $L_t = 36$ cm, $L_d = 10$ cm. The first UV-CE study was conducted using a 0.5% PHEA separation matrix. For the study on the effect of salt concentration on insulin oligomer formation, the capillary was filled with 1% PHEA and rinsed with 40 mM Tris (pH 8.0) for 5 min prior to each run. This rinse was utilized to dilute the PHEA on-column and overcome the long run times associated with the 0.5% PHEA separation matrix. Polymers of HEA were synthesized as described previously [83] with the following changes: 4% w/w initial monomer concentration and polymerization for 5 h. CE separations using UV detection were carried out using a P/ACE MDQ Glycoprotein System from Beckman Coulter, Inc. (Fullerton, CA) (214 nm filter) interfaced with an IBM computer utilizing 32 Karat software (V. 5.0, Beckman Coulter, Inc.) for data collection. Samples were pressure injected at 0.5 psi for 8 s and separated at 15 kV. Between each run, the capillary was rinsed with deionized water for 10 min to ensure that the insulin was not retained on the capillary wall. CE separations using LIF detection were carried out using an Applied Biosystems (Foster City, CA) 3130 Genetic Analyzer (excitation = 494 nm, emission = 522 nm) interfaced with a Dell computer utilizing Foundation Data Collection V 3.0 software. Samples were electrokinetically injected at 10 or 12 kV for 12 s and separated at 15 kV.

3.4. Limit of Detection Studies

Unlabeled insulin was prepared at concentrations of 0.05–0.2 mg/mL in 40 mM Tris (pH 8.0), and FITC-labeled insulin was prepared at concentrations of 0.03–3 ng/mL. Immediately following preparation, 100 μ L samples of unlabeled insulin and 10 μ L samples of FITC-labeled insulin were analyzed by UV-CE or LIF-CE, respectively, to determine the intensity of the first peak. Between runs for determining the limit of detection, the capillary was rinsed with

deionized water for 20–120 min, and elution of 40 mM Tris (pH 8.0) was analyzed to ensure that insulin was not retained on the capillary wall.

3.5. *Oligomer Formation Assay*

To observe the time course for insulin oligomer formation, insulin was solubilized in 5 mM NaOH for 30 min and diluted into 40 mM Tris (pH 8.0) to make a 1 mg/mL stock. The stock was then diluted to 0.2 mg/mL in 40 mM Tris (pH 8.0) containing 150 mM NaCl and incubated at 25 °C under continuous agitation (185 rpm). At times of 0, 4, 8, 12, and 24 h, a 50 μ L sample was removed and analyzed by UV-CE, with 0.5% PHEA separation matrix, to determine the migration time and intensity of all peaks. Separate experiments were conducted using the same sample preparation and CE conditions in order to determine the size range of insulin oligomers observed. At 0, 4, 8, and 12 h, a 50 μ L sample was taken and ultrafiltrated (20 min, 14,000 \times g) through Amicon filters with cut-off values of 30 kDa, 50 kDa and 100 kDa. The filtrate was removed and analyzed via UV-CE to determine the relative size of oligomers.

To examine the effect of solution ionic strength on insulin oligomer formation, insulin was prepared at a concentration of 0.2 mg/mL in 40 mM Tris (pH 8.0) containing 100, 150, or 250 mM NaCl. Samples were incubated at 25 °C under continuous agitation (185 rpm). Both prior to the onset of agitation and at times between 5 and 24 h following the onset of agitation, a 50 μ L sample was removed and analyzed by UV-CE to determine the migration time of the first and last peaks. In parallel experiments, aggregation was monitored using ThT binding as described previously [84] by diluting an aliquot into ThT (10 μ M) and evaluating fluorescence using a Perkin-Elmer LS-45 luminescence spectrometer (Waltham, MA) (excitation = 450 nm, emission = 470–500 nm) with baseline (ThT) subtraction. Lag times to aggregate formation were determined for individual runs as the last time point prior to a marked increase in signal. For UV-

CE, this increase was an extension of the migration time for the last peak greater than 2-fold that of the monomer migration time. For ThT binding, this increase was 5% of the fluorescence observed at equilibrium.

The co-incorporation of unlabeled insulin and FITC-labeled insulin into oligomers was examined using LIF-CE and UV-CE in parallel. FITC-labeled insulin was prepared alone at a concentration of 0.2 mg/mL or combined with unlabeled insulin for final concentrations of 0.2 mg/mL unlabeled insulin and 0.067 mg/mL FITC-labeled insulin (75% unlabeled, 25% FITC-labeled). Both samples were prepared in 40 mM Tris (pH 8.0) containing 150 mM NaCl and incubated at 25 °C under continuous agitation (185 rpm). Both prior to the onset of agitation and at times between 5 and 24 h following the onset of agitation, the migration times of the first and last peak were determined by both UV-CE and LIF-CE. Here, a 50 μ L sample was removed for analysis by UV-CE and a 20 μ L sample was removed and diluted to 0.013 mg/mL for analysis by LIF-CE.

3.6. Statistical Analysis

The migration time and intensity of peaks were analyzed using Chromagna (VO 9.8) software (provided by Mark Miller, NIH) and Origin (V. 8.0) software from OriginLab Corporation (Northampton, MA). Chromagna software was used to convert the fsa file format of the ABI 3130 Genetic Analyzer to excel files, which are compatible with Origin. A Gaussian fit was used to calculate the peak area and migration time in Origin. The migration times of peaks observed in the insulin oligomer time course and salt concentration studies were normalized in order to draw qualitative conclusions about the sizes of insulin species present at various times throughout aggregation. Peak migration times were determined by normalizing the migration time for the last peak observed relative to the migration time of the first peak observed prior to

the onset of aggregation. In addition, the peak height for the monomeric peaks detected in the UV and LIF limit of detection studies was determined and the S/N ratio was calculated. Peaks with a S/N ratio >3 were considered significant. Statistical analysis for comparison of lag times was performed using Prism 5 software (GraphPad Software Inc., San Diego, CA). The effect of detection method upon lag time was assessed using a one-way ANOVA with Bonferroni post-test. Unpaired *t*-tests were performed using GraphPad QuickCalcs (GraphPad Software Inc., San Diego, CA) to compare CE normalized migration times.

4. Conclusion

Insulin aggregation poses problems both *in vivo* and *in vitro*. These problems include injection site bleeding and bruising which can occur during the treatment of Type II diabetes in addition to problems with the pharmaceutical quality control of insulin. Elucidating the molecular mechanism by which insulin aggregation occurs, in particular the early stages of aggregation during which oligomeric species are formed, will facilitate the prevention of these problems. However, most techniques utilized for studies of insulin aggregation are not sensitive enough to detect physiologically relevant concentrations or oligomeric species present transiently throughout aggregation under physiologically relevant solution conditions. These limitations highlight the importance of employing a complementary technique to explore the evolution of insulin oligomer appearance at physiologically relevant concentrations. The current study illustrates that CE is a promising technique for monitoring the appearance of oligomeric species during the early events of insulin aggregation and is the first report of the use of UV-CE to monitor insulin oligomer formation at pH 8.0 and physiological salt concentration. UV-CE was employed to demonstrate that a change in salt concentration from 100 mM NaCl to 250 mM NaCl had little effect on the formation of small oligomeric species. A comparison between the

use of UV-CE and ThT binding for monitoring insulin aggregation revealed that CE was able to detect the appearance of aggregated species at significantly earlier times than ThT binding, demonstrating that CE and ThT binding may be used as complementary techniques to identify insulin species present at all times throughout aggregation. The lowest concentration of monomeric insulin that can be detected was determined using both UV and LIF detection modes. Physiologically relevant insulin concentrations in the picomolar range were detectable using LIF detection while concentrations in the micromolar range were required for UV detection. Using UV-CE and LIF-CE to simultaneously monitor the aggregation of a mixture of FITC-labeled insulin and unlabeled insulin, this study was the first to show that FITC-labeled insulin was unable to incorporate into oligomers formed by the unlabeled protein. These results demonstrate that while CE is a promising technique for the detection of physiologically relevant insulin concentrations, caution must be taken when choosing a dye for detection of oligomeric and aggregate insulin species. This necessitates further investigation to identify optimum fluorescent labels for the study of insulin oligomer formation at physiological insulin concentrations.

Acknowledgements

This work was supported by the Arkansas Applied Biosciences Institute, University of Arkansas start-up funds, National Institutes of Health and National Center for Research Resources under Grant No. 1P30RR031154-02, and the National Science Foundation and EPSCoR under Grant No. EPS-0447660. Any opinions, findings, and conclusions or recommendations expressed in this material are those of the authors and do not necessarily reflect the views of the National Science Foundation, National Institutes of Health, or National Center for Research Resources.

References

1. Hales, C.N. The role of insulin in the regulation of glucose metabolism. *Symp. Proc.* **1971**, *30*, 282–288.
2. Blundell, T.; Dodson, G.; Hodgkin, D.; Mercola, D. Insulin: Structure in the crystal and its reflection in chemistry and biology. *Adv. Protein Chem.* **1972**, *26*, 279–402.
3. Grudzielanek, S.; Smirnovas, V. Solvation-assisted pressure tuning of insulin fibrillation: From novel aggregation pathways to biotechnological applications. *J. Mol. Biol.* **2006**, *356*, 497–509.
4. Waugh, D.F.; Wilhelmson, D.F. Studies of the nucleation and growth reactions of selected types of insulin fibrils. *J. Am. Chem. Soc.* **1953**, *75*, 2592–2600.
5. Nielsen, L.; Khurana, R.; Fink, A. Effect of environmental factors on the kinetics of insulin fibril formation: Elucidation of the molecular mechanism. *Biochemistry* **2001**, *40*, 6036–6046.
6. Dobson, C.M. Protein misfolding, evolution and disease. *Trends Biochem. Sci.* **1999**, *24*, 329–332.
7. Sluzky, V.; Tamada, J.; Klivanov, A.; Langer, R. Kinetics of insulin aggregation in aqueous solutions upon agitation in the presence of hydrophobic surfaces. *Proc. Natl. Acad. Sci. USA* **1991**, *88*, 9377–9381.
8. Jeffrey, P.; Milthorpe, B.; Nichol, L. Polymerization pattern of insulin at pH 7.0. *Biochemistry* **1976**, *15*, 4660–4665.
9. Dische, F.E.; Wernstedt, C. Insulin as an amyloid-fibril protein at sites of repeated insulin injections in a diabetic patient. *Diabetologia* **1988**, *31*, 158–161.
10. Brange, J.; Andersen, L. Toward understanding insulin fibrillation. *J. Pharm. Sci.* **1997**, *86*, 517–525.
11. Shikama, Y.; Kitazawa, J.; Yagihashi, N.; Uehara, O.; Murata, Y.; Yajima, N.; Wada, R.; Yagihashi, S. Localized amyloidosis at the site of repeated insulin injection in a diabetic patient. *Intern Med.* **2010**, *49*, 397–401.
12. Mauro, M.; Craparo, E. Kinetics of different processes in human insulin amyloid formation. *J. Mol. Biol.* **2007**, *366*, 258–274.
13. Herman, W.; Ilag, L. A clinical trial of continuous subcutaneous insulin infusion *versus* multiple daily injections in older adults with type 2 diabetes. *Diabetes Care* **2005**, *28*, 1568–1573.

14. Grudzielanek, S.; Velkova, A. Cytotoxicity of insulin within its self-assembly and amyloidogenic pathways. *J. Mol. Biol.* **2007**, *370*, 372–384.
15. Carulla, N.; Zhou, M.; Giralt, E.; Robinson, C.; Dobson, C. Structure and intermolecular dynamics of aggregates populated during amyloid fibril formation studied by hydrogen/deuterium exchange. *Acc. Chem. Res.* **2010**, *43*, 1072–1079.
16. Ahmad, A.; Uversky, V.; Hong, D.; Fink, A. Early events in the fibrillation of monomeric insulin. *J. Biol. Chem.* **2005**, *280*, 42669–42675.
17. Iurascu, M.; Cozma, C.; Tomczyk, N.; Rontree, J.; Desor, M.; Drescher, M.; Przybylski, M. Structural characterization of β -amyloid oligomer-aggregates by ion mobility mass spectrometry and electron spin resonance spectroscopy. *Anal. Bioanal. Chem.* **2009**, *395*, 2509–2519.
18. Maji, S.; Ogorzalek Loo, R.; Inayathullah, M.; Spring, S.; Vollers, S.; Condrón, M.; Bitan, G.; Loo, J.; Teplow, D. Amino acid position-specific contributions to amyloid β -protein oligomerization. *J. Biol. Chem.* **2009**, *284*, 23580–23591.
19. Palmblad, M.; Westlind-Danielsson, A.; Bergquist, J. Oxidation of methionine 35 attenuates formation of amyloid β -peptide 1–40 oligomers. *J. Biol. Chem.* **2002**, *277*, 19506–19510.
20. Bernstein, S.; Wyttenbach, T.; Baumketner, A.; Shea, J.; Bitan, G.; Teplow, D.; Bowers, M. Amyloid β -protein: Monomer structure and early aggregation states of A β 42 and its pro¹⁹ alloform. *J. Am. Chem. Soc.* **2005**, *127*, 2075–2084.
21. Bernstein, S.; Dupuis, N.; Lazo, N.; Wyttenbach, T.; Condrón, M.; Bitan, G.; Teplow, D.; Shea, J.; Ruotolo, B.; Robinson, C.; *et al.* Amyloid- β protein oligomerization and the importance of tetramers and dodecamers in the aetiology of Alzheimer's disease. *Nat. Chem.* **2009**, *1*, 326–331.
22. Bitan, G.; Kirkitadze, M.; Lomakin, A.; Vollers, S.; Benedek, G.; Teplow, D. Amyloid β -protein (A β) assembly: A β 40 and A β 42 oligomerize through distinct pathways. *Proc. Natl. Acad. Sci. USA* **2003**, *100*, 330–335.
23. Murray, M.; Bernstein, S.; Nyugen, V.; Condrón, M.; Teplow, D.; Bowers, M. Amyloid β protein: A β 40 inhibits A β 42 oligomerization. *J. Am. Chem. Soc.* **2009**, *131*, 6316–6317.
24. Kaye, R.; Head, E.; Thompson, J.L.; McIntire, T.M.; Milton, S.C.; Cotman, C.W.; Glabe, C.G. Common structure of soluble amyloid oligomers implies common mechanism of pathogenesis. *Science* **2003**, *300*, 486–489.
25. Kaye, R.; Head, E.; Sarsoza, F.; Saing, T.; Cotman, C.W.; Necula, M.; Margol, L.; Wu, J.; Breydo, L.; Thompson, J.L.; *et al.* Fibril specific, conformation dependent antibodies recognize a generic epitope common to amyloid fibrils and fibrillar oligomers that is absent in prefibrillar oligomers. *Mol. Neurodegener.* **2007**, *2*, doi:10.1186/1750-1326-2-18.

26. Ladiwala, A.; Lin, J.; Bale, S.; Marcelino-Cruz, A.; Bhattacharya, M.; Dordick, J.; Tessier, P. Resveratrol selectively remodels soluble oligomers and fibrils of amyloid A β into off-pathway conformers. *J. Biol. Chem.* **2010**, *285*, 24228–24237.
27. Podlisny, M.; Walsh, D.; Selkoe, D. Oligomerization of endogenous and synthetic amyloid β -protein at nanomolar levels in cell culture and stabilization of monomer by congo red. *Biochemistry* **1998**, *37*, 3602–3611.
28. Ward, R.; Jennings, K.; Howlett, D. Fractionation and characterization of oligomeric, protofibrillar and fibrillar forms of β -amyloid peptide. *Biochem. J.* **2000**, *348*, 137–144.
29. Zhang, Y.; Wang, X.; He, J.-S.; Bao, F.-X.; Sun, W.-M.; Dai, X.-X.; Wang, X.-B.; Li, Y.-Q.; Zhen, X.-X.; Hu, H.-G.; *et al.* Preparation and characterization of a monoclonal antibody with high affinity for soluble A β oligomers. *Hybridoma* **2009**, *28*, 349–354.
30. Satoh, Y.; Hirakura, Y.; Kirino, Y. B-amyloid peptides inhibit acetylcholine release from cholinergic presynaptic nerve endings isolated from an electric ray. *Neurosci. Lett.* **2001**, *302*, 97–100.
31. Lambert, M.P.; Barlow, A.K.; Chromy, B.A.; Edwards, C.; Freed, R.; Liosatos, M.; Morgan, T.E.; Rozovsky, I.; Trommer, B.; Viola, K.L.; *et al.* Diffusible, nonfibrillar ligands derived from A β 1–42 are potent central nervous system neurotoxins. *Proc. Natl. Acad. Sci. USA* **1998**, *95*, 6448–6453.
32. Stine, W.B., Jr.; Dahlgren, K.N.; Krafft, G.A.; LaDu, M.J. *In vitro* characterization of conditions for amyloid- β peptide oligomerization and fibrillogenesis. *J. Biol. Chem.* **2003**, *278*, 11612–11622.
33. Walsh, D.; Tseng, B.; Rydel, R.; Podlisny, M.; Selkoe, D. The oligomerization of amyloid β -protein begins intracellularly in cells derived from human brain. *Biochemistry* **2000**, *39*, 10831–10839.
34. Walsh, D.; Hartley, D.; Condrón, M.; Selkoe, D.; Teplow, D. *In vitro* studies of amyloid β -protein fibril assembly and toxicity provide clues to the aetiology of flemish variant (Ala⁶⁹² \rightarrow Gly) Alzheimer's disease. *Biochem. J.* **2001**, *355*, 869–877.
35. Walsh, D.; Klyubin, I.; Fadeeva, J.; Cullen, W.; Anwyl, R.; Wolfe, M.; Rowan, M.; Selkoe, D. Naturally secreted oligomers of amyloid β protein potently inhibit hippocampal long-term potentiation *in vivo*. *Nature* **2002**, *416*, 535–539.
36. Ryan, D.; Narrow, W.; Federoff, H.; Bowers, W. An improved method for generating consistent soluble amyloid- β oligomer preparations for *in vitro* neurotoxicity studies. *J. Neurosci. Methods* **2010**, *190*, 171–179.

37. Dahlgren, K.N.; Manelli, A.M.; Stine, W.B., Jr.; Baker, L.K.; Krafft, G.A.; LaDu, M.J. Oligomeric and fibrillar species of amyloid- β peptides differentially affect neuronal viability. *J. Biol. Chem.* **2002**, *277*, 32046–32053.
38. Kato, M.; Kinoshita, H.; Toyo'oka, T. Analytical method for β -amyloid fibrils using CE-laser induced fluorescence and its application to screening for inhibitors of β -amyloid protein aggregation. *Anal. Chem.* **2007**, *79*, 4887–4891.
39. Lee, J.; Ryu, J.; Park, C.B. High-throughput analysis of Alzheimer's β -amyloid aggregation using a microfluidic self-assembly of monomers. *Anal. Chem.* **2009**, *81*, 2751–2759.
40. Picou, R.; Kheterpal, I.; Wellman, A.; Minnamreddy, M.; Ku, G.; Gilman, S.D. Analysis of A β (1–40) and A β (1–42) monomer and fibrils by capillary electrophoresis. *J. Chromatogr. B* **2011**, *879*, 627–632.
41. Sabella, S.; Quaglia, M.; Lanni, C.; Racchi, M.; Govoni, S.; Caccialanza, G.; Calligaro, A.; Bellotti, V.; Lorenzi, E. Capillary electrophoresis studies on the aggregation process of β -amyloid 1–42 and 1–40 peptides. *Electrophoresis* **2004**, *25*, 3186–3194.
42. Ortner, K.; Buchberger, W. Capillary electrokinetic chromatography of insulin and related synthetic analogues. *J. Chromatogr. A* **2009**, *1216*, 2953–2957.
43. Brambilla, D.; Verpillot, R.; Taverna, M.; De Kimpe, L.; Le Droumagust, B.; Nicolas, J.; Canovi, M.; Gobbi, M.; Mantegazza, F.; Salmona, M.; *et al.* New method based on capillary electrophoresis with laser-induced fluorescence detection (CE-LIF) to monitor interaction between nanoparticles and the amyloid- β peptide. *Anal. Chem.* **2010**, *82*, 10083–10089.
44. Sureshbabu, N.; Kirubakaran, R.; Jayakumar, R. Surfactant-induced conformational transition of amyloid β -peptide. *Eur. Biophys. J.* **2009**, *38*, 355–367.
45. Yamamoto, S.; Hasegawa, K.; Yamaguchi, I.; Tsutsumi, S.; Kardos, J.; Goto, Y.; Gejyo, F.; Naiki, H. Low concentrations of sodium dodecyl sulfate induce the extension of β_2 -microglobulin-related amyloid fibrils at a neutral pH. *Biochemistry* **2004**, *43*, 11075–11082.
46. Bitan, G.; Fradinger, E.A.; Spring, S.M.; Teplow, D.B. Neurotoxic protein oligomers—What you see is not always what you get. *Amyloid* **2005**, *12*, 88–95.
47. Fukuyama, R.; Mizuno, T.; Mori, S.; Nakajima, K.; Fushiki, S.; Yanagisawa, K. Age-dependent change in the levels of A β 40 and A β 42 in cerebrospinal fluid from control subjects, and a decrease in the ratio of A β 42 to A β 40 level in cerebrospinal fluid from Alzheimer's disease patients. *Eur. Neurol.* **2000**, *43*, 155–160.
48. Lewczuk, P.; Esselmann, H.; Otto, M.; Maler, J.M.; Henkel, A.W.; Henkel, M.K.; Eikenberg, O.; Antz, C.; Krause, W.R.; Reulbach, U.; *et al.* Neurochemical diagnosis of

- Alzheimer's dementia by CSF A β 42, A β 42/A β 40 ratio and total tau. *Neurobiol. Aging* **2004**, *25*, 273–281.
49. Zuberovic, A.; Hanrieder, J.; Wetterhall, M. Proteome profiling of human cerebrospinal fluid: Exploring the potential of capillary electrophoresis with surface modified capillaries for analysis of complex biological samples. *Eur. J. Mass Spectrom.* **2008**, *14*, 249–260.
 50. Pinto, D.; Arriaga, E.; Dovichi, N. Solid-phase fluorescent labeling reaction of picomole amounts of insulin in very dilute solutions and their analysis by capillary electrophoresis. *Electrophoresis* **1995**, *16*, 534–540.
 51. Shihabi, Z.; Friedberg, M. Insulin stacking for capillary electrophoresis. *J. Chromatogr. A* **1998**, *807*, 129–133.
 52. Kunkel, A.; Gunter, S.; Watzig, H. Quantitation of insulin by capillary electrophoresis and high-performance liquid chromatography Method comparison and validation. *J. Chromatogr. A* **1997**, *781*, 445–455.
 53. Yu, C.; Chin, C. *In situ* probing of insulin aggregation in chromatography effluents with spectroturbidimetry. *J. Colloid Interface Sci.* **2006**, *299*, 733–739.
 54. Nayak, A.; Sorci, M.; Krueger, S.; Belfort, G. A universal pathway for amyloid nucleus and precursor formation for insulin. *Proteins* **2008**, *74*, 556–565.
 55. Nettleton, E.; Tito, P. Characterization of the oligomeric states of insulin in self-assembly and amyloid fibril formation by mass spectrometry. *Biophys. J.* **2000**, *79*, 1053–1065.
 56. Vestergaard, B.; Groenning, M.; Roessle, M.; Kastrup, J.S.; van de Weert, M.; Flink, J.M.; Frokjaer, S.; Gajhede, M.; Svergun, D.I. A helical structural nucleus is the primary elongating unit of insulin amyloid fibrils. *PLoS Biol.* **2007**, *5*, 1089–1097.
 57. Fodera, V.; Librizzi, F.; Leone, M. Secondary nucleation and accessible surface in insulin amyloid fibril formation. *J. Phys. Chem.* **2007**, *112*, 3853–3858.
 58. Seyrek, E.; Dubin, P.; Tribet, C.; Gamble, E. Ionic strength dependence of protein-polyelectrolyte interactions. *Biomacromolecules* **2003**, *4*, 273–282.
 59. Giger, K.; Vanam, R.P.; Seyrek, E.; Dubin, P.L. Suppression of insulin aggregation by heparin. *Biomacromolecules* **2008**, *9*, 2338–2344.
 60. LeVine, H. Thioflavine T Interaction with synthetic Alzheimer's disease β -amyloid peptides: Detection of amyloid aggregation in solution. *Protein Sci.* **1993**, *2*, 404–410.
 61. Nielsen, L.; Frokjaer, S. Probing the mechanism of insulin fibril formation with insulin mutants. *Biochemistry* **2001**, *40*, 8397–8409.

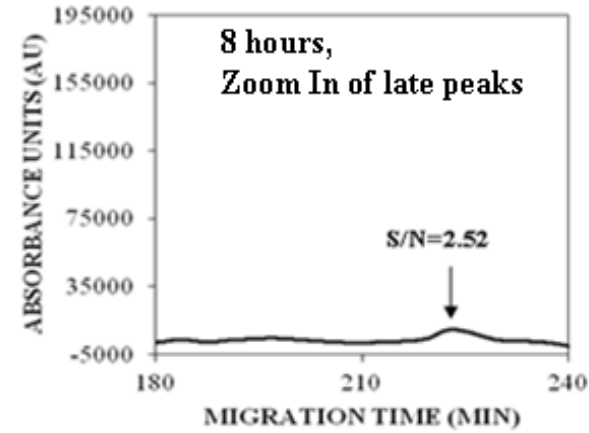
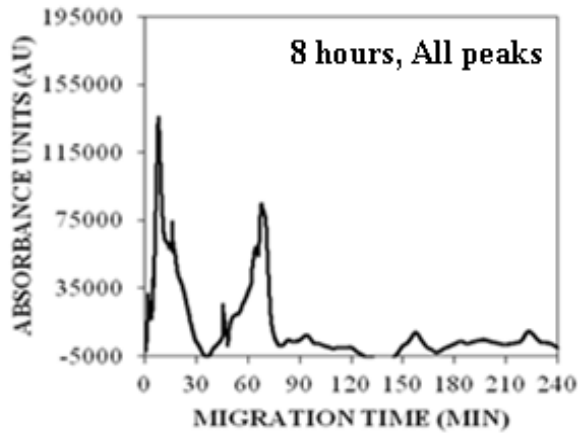
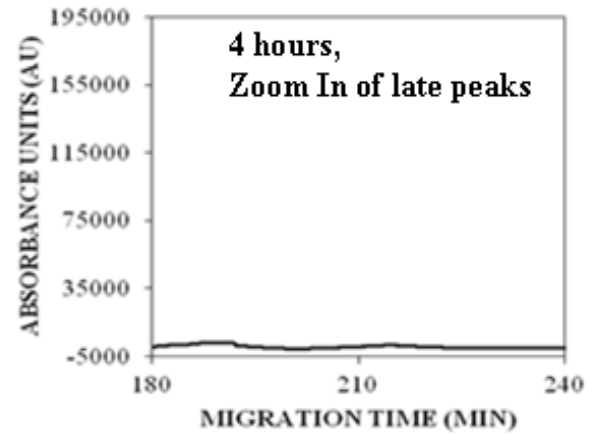
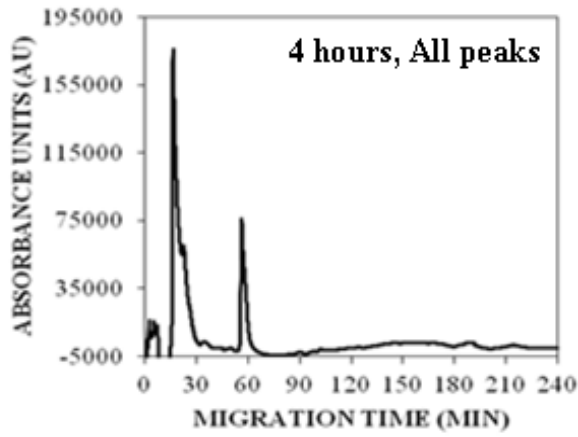
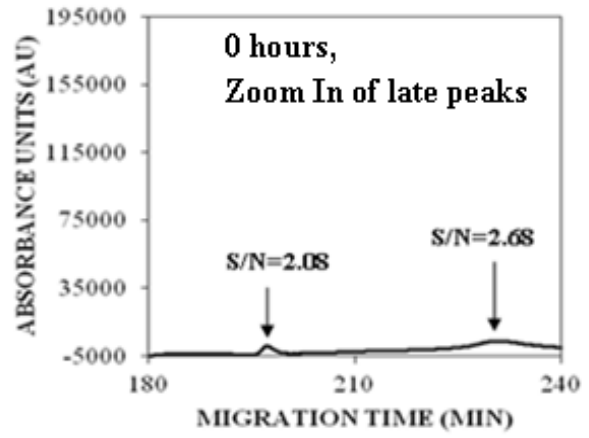
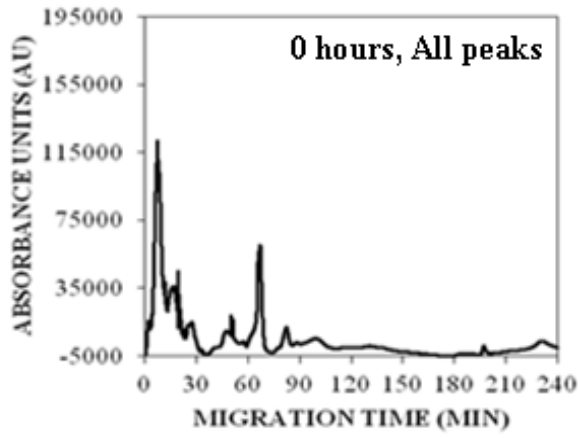
62. Ahmad, A.; Millett, I. Partially folded intermediates in insulin fibrillation. *Biochemistry* **2003**, *42*, 11404–11416.
63. Sasahara, K.; Yagi, H.; Sakai, M.; Naiki, H.; Goto, Y. Amyloid nucleation triggered by agitation of β 2-microglobulin under acidic and neutral pH conditions. *Biochemistry* **2008**, *47*, 2650–2660.
64. Picotti, P.; Franceschi, G.; Frare, E.; Spolaore, B.; Zambonin, M.; Chiti, F.; Polverino de Laureto, P.; Fontana, A. Amyloid fibril formation and disaggregation of fragment 1–29 of apomyoglobin: Insights into the effect of pH on protein fibrillogenesis. *J. Mol. Biol.* **2007**, *367*, 1237–1245.
65. Jain, S.; Udgaonkar, J. Evidence for stepwise formation of amyloid fibrils by the mouse prion protein. *J. Mol. Biol.* **2008**, *382*, 1228–1241.
66. Lin, M.; Chen, L.; Tsai, H.; Wang, S.; Chang, Y.; Higuchi, A.; Chen, W. Investigation of the mechanism of β -amyloid fibril formation by kinetic and thermodynamic analyses. *Langmuir* **2008**, *24*, 5802–5808.
67. Dick, G.; Sturek, M. Effects of a physiological insulin concentration on the endothelin-sensitive Ca^{2+} store in porcine coronary artery smooth muscle. *Diabetes* **1996**, *45*, 876–880.
68. Lee, Y.-H.; Maus, R.G.; Smith, B.W.; Winefordner, J.D. Laser-induced fluorescence detection of a single molecule in a capillary. *Anal. Chem.* **1994**, *66*, 4142–4149.
69. Skeidsvoll, J.; Ueland, P. Analysis of double-stranded DNA by capillary electrophoresis with laser-induced fluorescence detection using the monomeric dye SYBR green I. *Anal. Biochem.* **1995**, *231*, 359–365.
70. Lim, H.B.; Lee, J.J.; Lee, K. Simple and sensitive laser-induced fluorescence detection for capillary electrophoresis and its application to protein separation. *Electrophoresis* **1995**, *16*, 674–678.
71. Ren, J.; Li, B.; Deng, Y.; Cheng, J. Indirect thermo-optical detection for capillary electrophoresis. *Talanta* **1995**, *42*, 1891–1895.
72. Brange, J.; Skelbaek-Pedersen, B. The Physicochemical and Pharmaceutical Aspects of Insulin and Insulin Preparations. In *Galenics of Insulin*; Springer-Verlag: Berlin, Germany, 1987; pp. 369–319, 370–456.
73. Grudzielanek, S.; Jansen, R. Solvational tuning of the unfolding, aggregation and amyloidogenesis of insulin. *J. Mol. Biol.* **2005**, *351*, 879–894.
74. Schultz, N.; Kennedy, R. Rapid immunoassays using capillary electrophoresis with fluorescence detection. *Anal. Chem.* **1993**, *65*, 3161–3165.

75. Tao, L.; Kennedy, R. On-line competitive immunoassay for insulin based on capillary electrophoresis with laser-induced fluorescence detection. *Anal. Chem.* **1996**, *68*, 3899–3906.
76. Nichols, M.; Moss, M.; Rosenberry, T. Growth of β -amyloid(1–40) protofibrils by monomer elongation and lateral association. Characterization of distinct products by light scattering and atomic force microscopy. *Biochemistry* **2002**, *41*, 6115–6127.
77. Gu, X.; Greiner, E.R.; Mishra, R.; Kodali, R.; Osmand, A.; Finkbeiner, S.; Steffan, J.S.; Thompson, L.M.; Wetzel, R.; Yang, X.W. Serines 13 and 16 are critical determinants of full-length human mutant huntingtin induced disease pathogenesis in HD mice. *Neuron* **2009**, *64*, 828–840.
78. Morshedi, D.; Ebrahim-Habibi, A.; Moosavi-Movahedi, A.A.; Nemat-Gorgani, M. Chemical modification of lysine residues in lysozyme may dramatically influence its amyloid fibrillation. *Biochim. Biophys. Acta (BBA)* **2010**, *1804*, 714–722.
79. Choi, S.; Connelly, S.; Reixach, N.; Wilson, I.A.; Kelly, J.W. Chemoselective small molecules that covalently modify one lysine in a non-enzyme protein in plasma. *Nat. Chem. Biol.* **2010**, *6*, 133–139.
80. DeFelippis, M.R.; Bakaysa, D.L.; Bell, M.A.; Heady, M.A.; Li, S.; Pye, S.; Youngman, K.M.; Radziuk, J.; Frank, B.H. Preparation and characterization of a cocryst. Suspension of [LysB28,ProB29]-human insulin analog. *J. Pharm. Sci.* **1998**, *87*, 170–176.
81. Kotzke, G.; Schuett, M.; Missler, U.; Moller, D.E.; Fehm, H.L.; Klein, H.H. Binding of human, porcine and bovine insulin to insulin receptors from human brain, muscle and adipocytes and to expressed recombinant alternatively spliced insulin receptor isoforms. *Diabetologia* **1995**, *38*, 757–763.
82. Moses, S. *Bovine Porcine and Human Insulin. A Present Day Comparative Appraisal and Policy Discussions*, 1st ed.; IDDT (Insulin Dependent Diabetes Trust): Chennai, India, 2002.
83. Albarghouthi, M.; Stein, T.; Barron, A. Poly-*N*-hydroxyethylacrylamide as a novel, adsorbed coating for protein separation by capillary electrophoresis. *Electrophoresis* **2003**, *24*, 1166–1175.
84. Davis, T.J.; Soto-Ortega, D.D.; Kotarek, J.A.; Gonzalez-Velasquez, F.J.; Sivakumar, K.; Wu, L.; Wang, Q.; Moss, M.A. Comparative study of inhibition at multiple stages of amyloid- β self assembly provides mechanistic insight. *Mol. Pharmacol.* **2009**, *76*, 405–413.

© 2011 by the authors; licensee MDPI, Basel, Switzerland. This article is an open access article distributed under the terms and conditions of the Creative Commons Attribution license (<http://creativecommons.org/licenses/by/3.0/>).

Appendix

Electropherograms for insulin oligomer time course with longer run times



I (Christa Hestekin) give permission to Elizabeth Pryor to reproduce the following copyrighted publications in her dissertation:

Publication 1) Pryor, E.; Moss, M. A.; Hestekin, C. N. Int. J. Mol. Sci. Unraveling the Early Events of A β Aggregation: Techniques for the Determination of A β Aggregate Size 2012, 13, 3038-3072

Publication 2) Pryor, E.; Kotarek, J. A.; Moss, M. A.; Hestekin, C. N. Int. J. Mol. Sci. Monitoring Insulin Oligomer Formation Via Capillary Electrophoresis, 2011, 12, 9369-9388

As one of the copyright holders for both of these publications, I verify that more than 50% of the work was conducted by Elizabeth Pryor and thus grant her permission to reproduce these two publications in her dissertation.

I, Melissa A Moss, give permission to Elizabeth Pryor to reproduce the following copyrighted publications in her dissertation:

Publication 1) Pryor, E.; Moss, M. A.; Hestekin, C. N. Int. J. Mol. Sci. Unraveling the Early Events of A β Aggregation: Techniques for the Determination of A β Aggregate Size 2012, 13, 3038-3072
Publication 2) Pryor, E.; Kotarek, J. A.; Moss, M. A.; Hestekin, C. N. Int. J. Mol. Sci. Monitoring Insulin Oligomer Formation Via Capillary Electrophoresis, 2011, 12, 9369-9388

As one of the copyright holders for both of these publications, I verify that more than 50% of the work was conducted by Elizabeth Pryor and thus grant her permission to reproduce these two publications in her dissertation.

I, Joseph Kotarek, give permission to Elizabeth Pryor to reproduce the following copyrighted publication in her dissertation:

Pryor, E.; Kotarek, J. A.; Moss, M. A.; Hestekin, C. N. *Int. J. Mol. Sci.* Monitoring Insulin Oligomer Formation Via Capillary Electrophoresis, 2011, *12*, 9369-9388

As one of the copyright holders for this publication, I confirm that more than 50% of the work was conducted by Elizabeth Pryor and grant her permission to reproduce this publication in her dissertation. If there are any other questions I can address, please let me know.

CHAPTER 4: MONITORING AB AGGREGATION VIA CAPILLARY

ELECTROPHORESIS

1. Introduction

Alzheimer's Disease (AD) is a devastating neurodegenerative disorder which currently affects 5.4 million Americans and is the 6th leading cause of death [1]. The amyloid β protein ($A\beta$) is a partially folded protein that contributes to the neurodegenerative effects of AD. In its monomer form, this protein is harmless [2]. This monomer can self-assemble into $A\beta$ oligomers and eventually fibrillar aggregates which deposit as amyloid plaques in the brain [3]. Controversy currently exists over the direct effect $A\beta$ has on neurodegeneration, but it appears likely that soluble aggregates of $A\beta$ (protofibrils or oligomers), rather than monomers or insoluble fibrils, may be responsible for the toxic effects of AD [4-7]. This hypothesis is supported by experimental observations *in vitro* which showed that soluble aggregates formed by synthetic $A\beta_{1-40}$ and $A\beta_{1-42}$ induced toxicity in cultured cells [8,9] and *in vivo* where soluble $A\beta$ aggregates generated in cell cultures drastically inhibited hippocampal long-term potentiation in rats [10]. Furthermore, the direct neuron-to-neuron transfer and corresponding toxicity of soluble oligomers formed by synthetic $A\beta_{1-42}$ has been demonstrated [11].

The detection of soluble $A\beta$ oligomeric species, specifically $A\beta_{1-40}$, is challenging due to the fact that these intermediate sized species are difficult to isolate because they are transient [12,13], and present at low concentrations [14]. Many different techniques have been examined for their ability to detect the smaller oligomeric $A\beta$ species. These include SDS-PAGE and/or Western blotting [8,15-27], mass spectrometry [20,28-33], and size exclusion chromatography (SEC) [15]. SDS-PAGE with Western blotting is one of the most common electrophoretic techniques used for studies of $A\beta$ aggregation. It has been shown that the resolution of low

molecular weight A β ₁₋₄₀ oligomers ranging from 8-24 kDa is difficult due to gel smearing [15]. This study also compared SDS-PAGE to SEC and found that A β ₁₋₄₀ was aggregating into higher molecular weight species (>24 kDa) which were not detectable using SDS-PAGE. SEC is further complicated by the dissociation of reversible aggregates that occurs upon sample dilution [34]. Western blotting also has been shown to be a promising technique for the detection of oligomeric A β species, but it requires the use of expensive antibodies and gel smearing often limits the ability to distinguish molecular weights. Mass spectrometry has also been used alone and in combination with SDS-PAGE to evaluate the sizes formed during the early stages of A β aggregation [20,28-31,33]. Studies by Iurascu *et al.* and Maji *et al.* have utilized MS in combination with SDS-PAGE to detect A β ₁₋₄₀ species ranging from monomer to hexamer [28,29]. Since aggregated species have highly similar mass-to-charge ratios, ion-mobility coupled with MS (IM-MS) has been the most effective method for the separation of small oligomers of A β by both size and charge. An aggregation mechanism for A β ₁₋₄₀ has been proposed which involves the formation of dimers and tetramers followed by the slow formation of fibrils containing a β -sheet structure [20,31]. IM-MS is expensive and the addition of a step such as ion-mobility also increases the time needed for analysis and therefore decrease the chances of detecting transient species. In addition, these techniques are not capable of detecting the A β oligomerization process under physiological concentrations.

Capillary electrophoresis (CE) as a technique for the detection of A β species formed throughout aggregation is still in its early stages. Therefore, studies on the use of CE for the detection of A β aggregates, especially, A β ₁₋₄₀, are limited. The detection of proteins via CE can be conducted using either ultraviolet (UV) absorbance or laser induced fluorescence (LIF) detection modes. UV can detect proteins without any additional labeling, but typically has a

lower sensitivity than LIF. LIF usually requires labeling of the molecules, but is highly sensitive, with previous reports of LIF-CE detection of synthetic A β down to 35 nM [35]. The process of fluorescence occurs when a photon is emitted by an electronically excited molecule as it relaxes to its ground electronic state [36]. For LIF-CE, the fluorescence excitation source is typically a He-Cd, Ar-ion, or He-Ne laser [36]. In general, the fluorescent compound used to label proteins for analysis via LIF-CE can be 1) covalently bound to the protein or 2) specific for a certain protein conformation. Furthermore, these fluorescent probes are typically bulky, aromatic compounds.

The ability of UV-CE to detect A β aggregates has been demonstrated in the literature. A study by Sabella *et al.* utilized UV-CE to detect small A β_{1-40} species ranging from 3 - 30 kDa and A β_{1-42} species ranging from 3 - 50 kDa and > 50 kDa [37]. However, this study looked at a small size range (3 – 50 kDa) and did not use a sieving matrix within the capillary to enhance resolution. The separation of larger fibrillar species from monomer has been achieved for both A β_{1-40} and A β_{1-42} using UV-CE [38]. The detection of intermediate sizes larger than monomer which are formed prior to fibrils was not accomplished. These studies demonstrate the ability of UV-CE to detect sizes from monomers to fibrils but highlight the need for more studies on the use of UV-CE to monitor the A β aggregation process over time.

The ability of LIF-CE to detect A β aggregates using dyes which are specific for the β -sheet conformation has been demonstrated in the literature [3,38,39]. These dyes bind structures containing β -sheets and therefore cannot be used for the detection of small oligomers which precede β -sheet formation. Carboxy-fluorescein (FAM) and fluorescein isothiocyanate (FITC) are covalently bound fluorescent dyes which have been used for the detection of monomeric

insulin and A β via LIF-CE [35,40]. Less attention has been paid to the use of LIF-CE to detect oligomeric and aggregated species formed by FAM or FITC-labeled insulin and A β .

These previous studies highlight the potential for CE using a buffer solution to analyze early stages of the A β ₁₋₄₀ oligomerization process. In this chapter, we report the first study on the use of UV-CE with a polymer separation matrix to detect smaller oligomeric native A β ₁₋₄₀ species (10 – 30 kDa) and larger oligomeric and aggregate species (100– 300 kDa and > 300 kDa). To our knowledge this is the first study to investigate the use of a polymer matrix to increase the effect of hydrodynamic radius of the oligomer species on CE separation to study the early oligomerization process of A β ₁₋₄₀. In addition, we have compared the oligomeric species sizes detected utilizing a traditional A β ₁₋₄₀ oligomer sample preparation with initial dilution into NaOH compared to a sample thought to contain SEC-purified A β ₁₋₄₀ monomer as the initial species present in solution. Dot blots were utilized to verify the presence of A β oligomeric species detected via UV-CE. Furthermore, we have probed the ability of CE to detect physiological concentrations of A β ₁₋₄₀. The potential for LIF-CE to monitor the aggregation of FAM-labeled A β ₁₋₄₂ is explored and the limitations of LIF-CE as a tool to monitor amyloid aggregation will be given. We believe that these are the first CE studies to use a polymer matrix to enhance the separation of native A β ₁₋₄₀ oligomers and to determine and compare UV versus LIF detection limits.

2. Materials and Methods

2.1. A β preparation

A β ₁₋₄₀ and FAM-A β ₁₋₄₀ were stored desiccated at -20°C. 4.33 mg/mL A β ₁₋₄₀ and 0.47 mg/mL FAM-A β ₁₋₄₀ peptide stocks were prepared in hexafluoroisopropanol (HFIP) in order to break down larger aggregates. These stock solutions were split into vials containing 0.0625 mg for

A β_{1-40} and 0.01563 mg for FAM-A β_{1-40} and the HFIP was allowed to evaporate overnight. Vials were stored at -80°C.

SEC-purified A β_{1-40} monomer samples were prepared in the laboratory of Dr. Melissa Moss as described previously [41]. Briefly, A β_{1-40} peptide was reconstituted to a final concentration of 2 mg/mL in 50 mM NaOH. Preexisting aggregates were removed by size exclusion chromatography (SEC) on a Superdex 75 HR10/30 column (GE Healthcare, Piscataway, NJ, USA). Purified A β_{1-40} monomer was flash frozen and shipped overnight on dry ice to the laboratory of Dr. Christa Hestekin. The purified A β_{1-40} monomer was used fresh or stored at -80°C.

A β_{1-42} and FAM-A β_{1-42} were stored desiccated at -20°C. 4.51 mg/mL A β_{1-42} and 0.49 mg/mL FAM-A β_{1-42} peptide stocks were prepared in hexafluoroisopropanol (HFIP) in order to ensure the samples were monomeric. These stock solutions were split into vials containing 0.0271 mg for A β_{1-42} and 0.006775 mg for FAM-A β_{1-42} and the HFIP was allowed to evaporate overnight. Vials were stored at -80°C. 5 mM stock solutions of FAM-labeled A β_{1-42} and unlabeled A β_{1-42} were prepared separately in 100% DMSO and diluted to 0.14 mg/mL in 40 mM Tris (pH 8.0) containing 10 mM NaCl. These samples were then combined to yield a total final concentration of 0.14 mg/mL containing 50 – 80% unlabeled A β_{1-42} and 20 – 50% FAM-labeled A β_{1-42} .

2.2. *Poly(ethylene oxide) coating and separation matrix synthesis*

The utility of poly(ethylene oxide) as a capillary coating and separation matrix was investigated due to the commercial availability of this polymer. All UV-CE studies were conducted using PEO as a coating and separation matrix in the capillary. One sample of long-chained EO polymer ($M_w = 2,000,000$ g/mol) and one sample of short-chained EO polymers

($M_w = 100,000$ g/mol) were obtained from Sigma-Adrich (St. Louis, MO). The EO polymer with $M_w = 2,000,000$ g/mol was diluted to 0.5% w/v in de-ionized water and used for the capillary coating and the EO polymer with $M_w = 100,000$ g/mol was diluted to 0.5% w/v in 100 mM Tris-HCl and used as the protein separation matrix.

2.3. Poly-N-hydroxyethyl acrylamide coating and separation matrix synthesis and characterization

All LIF-CE studies were conducted using PHEA as a coating and separation matrix in the capillary. Two samples of long-chained HEA polymers ($M_w = 6,230,000$ g/mol and 5,100,000 g/mol) were synthesized as described previously [42] with the following changes: 4% w/w initial monomer concentration and polymerization for 5 hours. One sample of short-chained HEA polymer ($M_w = 2,700,000$ g/mol) was synthesized as described previously [43] with the following changes: 3.5 mL isopropanol added to 200 mL of 4% w/w initial monomer solution. Solution deoxygenated by bubbling nitrogen through mixture at 47°C for 2 h followed by polymerization for 4 hours. Once the polymerization was complete, the polymer was dialyzed, lyophilized, and characterized to confirm its molecular weight by multi-angle laser light scattering (Wyatt Technology, Santa Barbara, CA). The HEA polymer with $M_w = 6,230,000$ g/mol was diluted to 0.1% w/v in de-ionized water and used for the capillary coating and the HEA polymers with $M_w = 5,100,000$ and 2,700,000 g/mol were diluted to 1% (UV and LIF insulin studies) and 0.5% (LIF A β studies), respectively, in 40 mM Tris (pH 8.0) and used as protein separation matrices.

2.4. Electrophoresis conditions for UV and LIF studies

A β_{1-40} oligomer formation studies with analysis via UV-CE were carried out in 0.5% w/v PEO coated capillaries with a 0.5% PEO separation matrix and a capillary temperature of 25°C.

A β limit of detection and oligomer formation studies with analysis via LIF-CE were carried out in 0.1% w/v PHEA coated capillaries with a 0.1–1% PHEA separation matrix and a capillary temperature of 25 °C. Capillary dimensions for UV-CE studies were $L_t = 31$ cm, $L_d = 10$ cm and for LIF-CE studies were $L_t = 36$ cm, $L_d = 10$ cm. CE separations using UV detection were carried out using a P/ACE MDQ Glycoprotein System from Beckman Coulter, Inc. (Fullerton, CA) (214 nm filter) interfaced with an IBM computer utilizing 32 Karat software (V. 5.0, Beckman Coulter, Inc.) for data collection. Samples were pressure injected at 0.5 psi for 8 s and separated at 7 kV. Between each run, the capillary was rinsed with deionized water for 10 minutes to ensure that the A β_{1-40} was not retained on the capillary wall. CE separations using LIF detection were carried out using an Applied Biosystems (Foster City, CA) 3130 Genetic Analyzer (excitation = 494 nm, emission = 522 nm) interfaced with a Dell computer utilizing Foundation Data Collection V 3.0 software from Applied Biosystems (Foster City, CA). For limit of detection studies, A β_{1-40} and A β_{1-42} samples were electrokinetically injected at 12 kV for 12 s and separated at 15 kV. For oligomer formation studies, A β_{1-42} samples were electrokinetically injected at 7 kV for 7 s and separated at 7 kV.

2.5. A β oligomer formation assay

To observe the time course for A β_{1-40} oligomer formation, A β_{1-40} was dissolved in 5 mM NaOH and diluted into 40 mM Tris-HCl (pH 8.0) supplemented with 5 mM NaCl to a final concentration of 0.22 mg/mL and incubated at 25°C under continuous agitation (800 rpm). Both prior to the onset of aggregation and at times between 5 and 48 hours following the onset of aggregation, a 15 μ L sample was removed and analyzed by UV-CE to determine the elution time and intensity of all peaks. Separate experiments were conducted using the same sample preparation and CE conditions in order to determine the size range of A β_{1-40} oligomers observed.

At 0 and 28 hours, a 50 μ L sample was taken and ultrafiltrated (20 minutes, 14,100 x g) through Amicon filters with cut-off values of 10, 30, 50, and 300 kDa. The filtrate and retentate were removed and analyzed via UV-CE to determine the relative size of oligomers.

To observe the effect of model inhibitory compounds on the formation of $A\beta_{1-40}$ oligomeric species, $A\beta_{1-40}$ was dissolved in 5 mM NaOH and diluted into 40 mM Tris-HCl (pH 8.0) supplemented with 5 mM NaCl to a final concentration of 0.22 mg/mL. Congo Red and Orange G were dissolved in DMSO and added to $A\beta_{1-40}$ to obtain a mixture containing 2% DMSO, 0.15 mg/mL Orange G or 0.23 mg/mL Congo Red and incubated at 25°C under continuous agitation (800 rpm). Both prior to the onset of aggregation and at times of 24 and 28 hours following the onset of aggregation, a 15 μ L sample was removed and analyzed by UV-CE to determine the elution time and intensity of all peaks.

To compare the effect of sample preparation on the $A\beta_{1-40}$ sizes formed, SEC-purified $A\beta_{1-40}$ was diluted into 40 mM Tris-HCl (pH 8.0) supplemented with 5 mM NaCl to a final concentration of 0.22 mg/mL and incubated at 25°C under continuous agitation (800 rpm). Identical time points and aliquot volumes as those given in the previous paragraph were taken and analyzed via UV-CE. Separate experiments were conducted using the same sample preparation and CE conditions in order to determine the size range of $A\beta_{1-40}$ oligomers observed. At 0 and 5 hours, a 50 μ L sample was taken and ultrafiltrated (20 minutes, 14,100 x g) through Amicon filters with cut-off values of 10 and 30 kDa (0 hours) and 30, 50, and 300 kDa (5 hours). The filtrate and retentate were removed and analyzed via UV-CE to determine the relative size of oligomers.

The co-incorporation of unlabeled $A\beta_{1-42}$ and FAM-labeled $A\beta_{1-42}$ into oligomers was examined using LIF-CE. 5 mM stock solutions of FAM-labeled $A\beta_{1-42}$ and unlabeled $A\beta_{1-42}$ were

prepared separately in 100% DMSO and diluted to 0.14 mg/mL in 40 mM Tris (pH 8.0) containing 10 mM NaCl. These samples were then combined to yield a total final concentration of 0.14 mg/mL containing 50 – 80% unlabeled A β ₁₋₄₂ and 20 – 50% FAM-labeled A β ₁₋₄₂. This oligomer preparation was then incubated at 25°C and both prior to the onset of oligomer formation and at times between 3 and 24 hours following the onset of oligomer formation, a 27 μ L sample was removed and combined with 3 μ L of 1% tween to obtain a final volume containing 0.1% tween for analysis by LIF-CE. Tween was added in order to stop oligomer formation.

2.6. Dot blot analyses of A β aggregation

To validate A β ₁₋₄₀ oligomer detection via CE with a more commonly used technique for oligomer detection, A β ₁₋₄₀ aggregates were analyzed via dot blotting. A β ₁₋₄₀ aggregation reactions were prepared and incubated as described above for CE measurements on A β ₁₋₄₀ oligomer formation. Both prior to the onset of aggregation and at times between 5 and 48 hours following the onset of aggregation, 3 μ L aliquots were spotted on nitrocellulose membranes (VWR) and allowed to dry for at least 1 hour. Membranes were blocked in 5% skim milk in tris buffered saline containing 0.01% Tween 20 (TBS-T) for 1 hour. After washing 3 times with TBS-T, membranes were incubated with either A β ₁₋₁₆ specific 6E10 antibody (1:2000 dilution), A β oligomer specific A11 antibody (1:2000 dilution), or A β fibril specific OC antibody (1:4000 dilution) for 1 hour at 4°C with gentle shaking. Membranes were again washed with TBS-T and bound 6E10, A11, and OC antibodies were detected by incubation for 1 hour at 4°C with alkaline phosphatase-conjugated anti-mouse IgG (1:2000 dilution) or alkaline phosphatase-conjugated anti-rabbit IgG (1:3000 dilution). All antibodies were diluted in 5% skim milk in TBS-T. After washing with TBS-T/MgCl₂, a substrate solution containing 15 mL TBS-T/MgCl₂

+ 50 μ L of 50 mg/mL 5-bromo-4-chloro-3-indolyl phosphate (BCIP) + 50 μ L of 50 mg/mL nitroblue tetrazolium chloride (NBT) was used to develop the membranes.

2.7. *Limit of detection studies*

A 0.22 mg/mL unlabeled A β ₁₋₄₀ stock solution was prepared in 5 mM NaOH and 40 mM Tris-HCl (pH 8.0) supplemented with 5 mM NaCl and diluted to concentrations of 0.0087 - 0.043 mg/mL in 40 mM Tris-HCl (pH 8.0). A 0.47 mg/mL stock solution of FAM-A β ₁₋₄₀ and FAM-A β ₁₋₄₂ were prepared separately and diluted in 40 mM Tris-HCl (pH 8.0) to concentrations of 0.0047 - 4140 ng/mL for FAM-A β ₁₋₄₀ and 0.0049 - 4870 ng/mL for FAM-A β ₁₋₄₂. Immediately following preparation, 25 and 10 μ L samples were analyzed by UV and LIF-CE, respectively, to determine the intensity of the first peak. Between runs for determining the limit of detection, the capillary was rinsed with deionized water for 10 minutes, and elution of deionized water was analyzed to ensure that A β ₁₋₄₀, FAM-A β ₁₋₄₀ and FAM-A β ₁₋₄₂ were not retained on the capillary wall.

2.8. *Statistical analysis*

The elution time and intensity of peaks were analyzed using Chromagna (VO 9.8) software (provided by Mark Miller, NIH) and Origin (V. 8.0) software from OriginLab Corporation (Northampton, MA). Chromagna software was used to convert the fsa file format of the ABI 3130 Genetic Analyzer to excel files, which are compatible with Origin software. For UV-CE studies, a Gaussian fit was used to calculate the peak area and migration time in Origin. The peak height for the peaks detected in the UV and LIF limit of detection studies was determined and the signal-to-noise ratio was calculated. Peaks with a signal-to-noise ratio > 3 were considered significant. Unpaired *t*-tests were performed using GraphPad QuickCalcs (GraphPad Software Inc., San Diego, CA) to compare peak areas. For LIF-CE studies, the

migration times of peaks observed in the $A\beta_{1-42}$ oligomer time course studies were normalized in order to draw qualitative conclusions about the sizes of $A\beta_{1-42}$ species present at various times throughout aggregation. Peak migration times were determined by normalizing the migration time for the last peak observed relative to the migration time of the first peak observed prior to the onset of aggregation. Unpaired *t*-tests were performed using GraphPad QuickCalcs (GraphPad Software Inc., San Diego, CA) to compare CE normalized migration times.

3. Results and Discussion

3.1. Detection of $A\beta_{1-40}$ oligomers using CE with UV detection

Although insoluble $A\beta$ fibrils are a post mortem signature, recent studies suggest that soluble $A\beta$ oligomers impair cognitive function and in addition to synapse loss, correlate most accurately with the stage of neurological impairment [44-46]. Therefore, it is important to have a technique which is capable of detecting these soluble oligomeric $A\beta$ species. To explore the utility of CE for the detection of $A\beta_{1-40}$ oligomers that appear during early stages of $A\beta_{1-40}$ aggregation, $A\beta_{1-40}$ was solubilized in 5 mM NaOH, diluted into 40 mM Tris (pH 8.0), subjected to 5 mM NaCl, and agitated at 800 rpm to promote amyloid assembly. The reaction was analyzed using UV-CE at early and late time points to assess the appearance of oligomers and progression into larger aggregate species. At 0 hours, UV-CE demonstrated the presence of an early, sharp peak at ~9 min (**Figure 1B**) in addition to a broader peak migrating at 220 minutes (**Figure 1A**). The size of these species was estimated using a filtration analysis similar to that performed by Sabella *et al.* who used molecular weight cutoff membranes to size early amyloid- β aggregation species detected via UV-CE [37]. For our experiments, we used membranes with molecular weight cutoffs of 10, 30, 50, 100, and 300 kDa to analyze the filtrate obtained after 0 and 28 hours of aggregation (**Appendix**). The peak obtained at ~9 min was estimated to have a

molecular weight between 10 – 30 kDa, or oligomers of 2 - 6 monomer units. Furthermore, a broad peak at 220 min was obtained and indicates the presence of larger species. A similar monomer peak pattern was obtained after 5, 10, and 24 hours (**Figure 1B**) while the later peak became more broad and exhibited a progressively shorter migration time (**Figure 1A**). This later broad peak was estimated to have a molecular weight of 100 – 300 kDa. At 28 hours, a set of sharp peaks with migration times between 8 – 8.5 minutes appeared (**Figure 1B**). The size of these species was estimated by filtration analysis to be > 300 kDa, or larger than 70 monomer units. Furthermore, we have confirmed that this sharp peak corresponds to an oligomeric structure, and not a fibril structure by looking at the affect of model inhibitory compounds (**Figure 2**). These compounds include Orange G, which is known to inhibit the formation of A β fibrils and Congo Red, which is known to inhibit the formation of A β oligomers [47]. By 36 and 48 hours, the intensity for the sharp peak at ~8.5 minutes increased and appeared to resolve into a single species.

In order to better understand the growth process, the peak area for the initially present species (10 – 30 kDa peak at ~9 minutes) was compared to the peak area for the > 300 kDa oligomer peak at ~8.5 minutes, which appeared after 28 hours of aggregation (**Figure 3**). As shown in **Figure 3**, the peak area for the 10 – 30 kDa peak initially increases over an

Figure 1. Detection of smaller, intermediate, and larger molecular weight $A\beta_{1-40}$ aggregation states using UV-CE. $A\beta_{1-40}$ was aggregated under agitation (800 rpm) at 0.22 mg/mL in 40 mM Tris (pH 8.0) containing 5 mM NaCl and at 25 °C. At 0 – 48 hours, CE was performed in conjunction with UV detection with a 0.5 psi pressure injection for 8 s with separation at 7 kV using 0.5% PEO separation matrix in a PEO coated capillary. Panel **A)** shows all peaks while panel **B)** is zoomed in on the smaller peaks. Results are representative of three independent experiments.

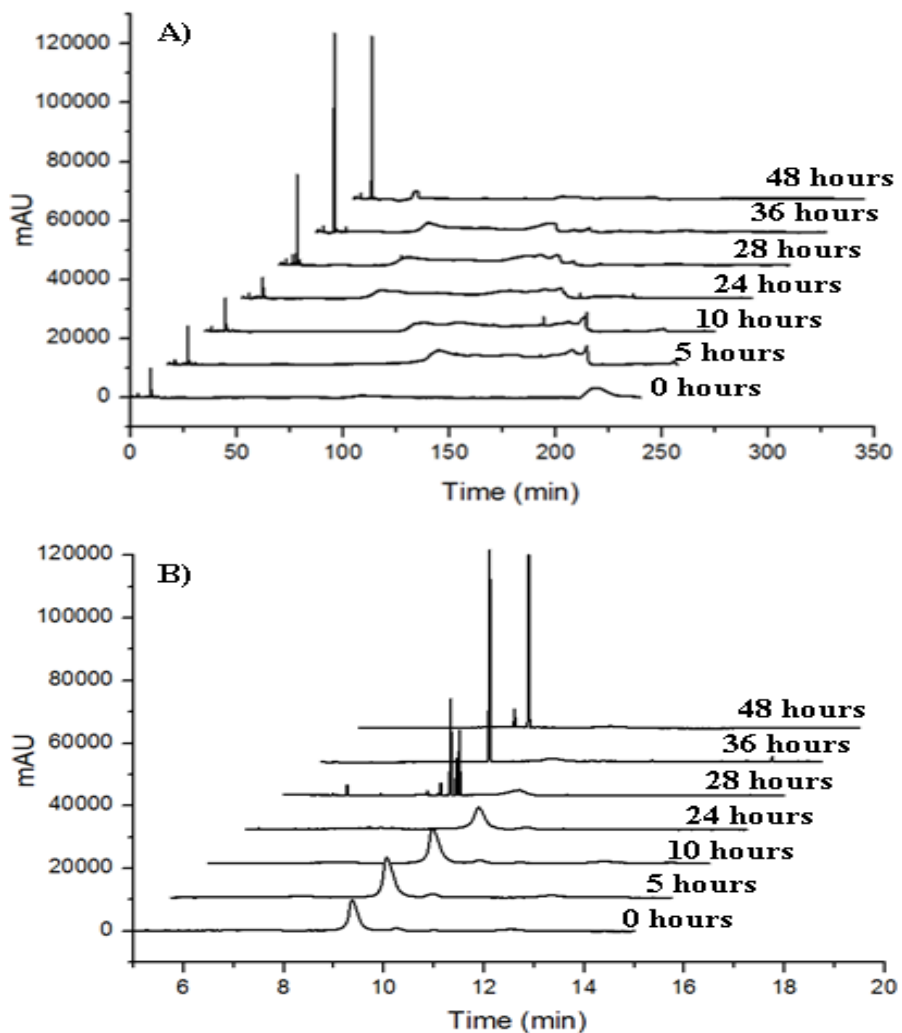


Figure 2. Comparison of A β ₁₋₄₀ peak pattern obtained with and without the presence of inhibitory compounds. A β ₁₋₄₀ was aggregated under agitation (800 rpm, 25 °C) at 0.22 mg/mL in 40 mM Tris (pH 8.0) containing 5 mM NaCl in the absence of inhibitor, or in the presence of 0.23 mg/mL Congo Red or 0.15 mg/mL Orange G. At 0 – 28 hours, CE was performed in conjunction with UV detection with a 0.5 psi pressure injection for 8 s with separation at 7 kV using 0.5% PEO separation matrix in a PEO coated capillary.

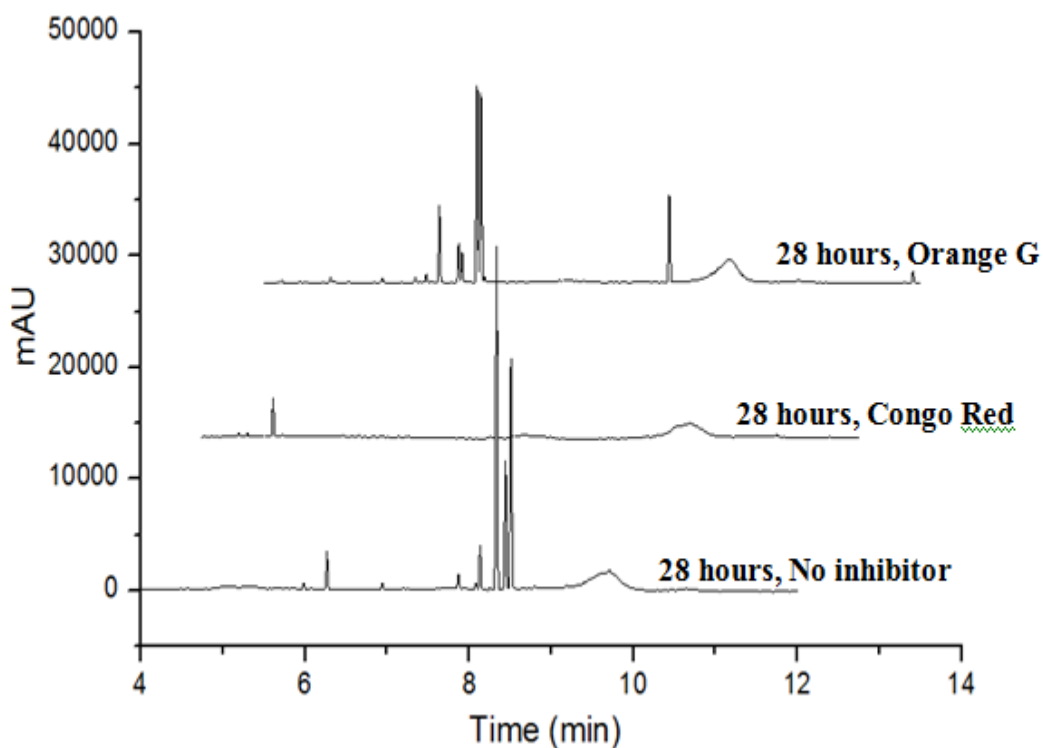
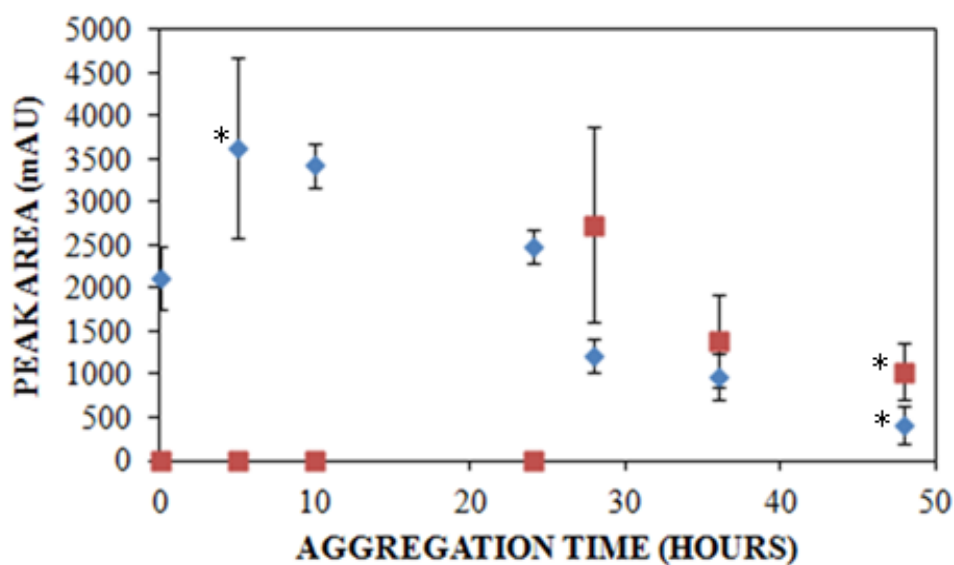


Figure 3. Effect of aggregation time on the peak areas obtained for 10 – 30 kDa (◆, $n = 3$) and > 300 kDa (■, $n = 3$) $A\beta_{1-40}$ species. $A\beta_{1-40}$ was aggregated under agitation (800 rpm) at 0.22 mg/mL in 40 mM Tris (pH 8.0) containing 5 mM NaCl and at 25 °C. At 0 – 48 hours, CE was performed in conjunction with UV detection with a 0.5 psi pressure injection for 8 s with separation at 7 kV using 0.5% PEO separation matrix in a PEO coated capillary. A * represents the first time point in which peak areas are statistically different with $p < 0.05$.



aggregation time of 24 hours. This initial increase in peak area could be due to the breakdown of the larger species present at 0 hours into 10 – 30 kDa species. After 28 hours, the 10 – 30 kDa peak area decreases and a new peak (> 300 kDa) with a faster migration time than the 10 – 30 kDa peak appears. Finally, between 28 – 48 hours of aggregation, both the 10 – 30 kDa and > 300 kDa peak areas further decrease. We hypothesize that sharp peak (> 300 kDa) with a faster migration time which appears after 28 hours of aggregation represents a species with an increased negative surface charge due to conformational changes which occur during oligomer formation. An increase in negative surface charge of A β ₁₋₄₂ fibrils has been observed by Wang *et al* [48]. This study utilized surface plasmon resonance to monitor the absorption of A β ₁₋₄₂ at various times throughout aggregation to four model self-assembled monolayers: hydrophobic CH₃-terminated SAM, hydrophilic OH-terminated SAM, negatively charged COOH-terminated SAMs, and positively charged NH₂-terminated SAM. They found that as A β grew into larger aggregates, the amount absorbed onto positively charged NH₂-SAM increased while the amount absorbed onto negatively charged COOH-SAM decreased. This increase in electrostatic interactions with the positively charged NH₂-SAM suggests an increase in negative surface charge of A β ₁₋₄₂ aggregates. Furthermore, a structural model for A β ₁₋₄₀ fibrils has been suggested by Petkova *et al.* in which the negatively charged N-terminus residues are exposed to solution on the outside of the fibril [49].

A previous study by Sabella *et al.* utilized UV-CE with an SDS rinse for the detection of A β ₁₋₄₀ oligomers formed in PBS (pH 7.4) at room temperature [37]. A decrease in the intensity of the 10 to 30 kDa peak was observed over an incubation period of 24 hours with the disappearance of all peaks after 48 hours. In contrast to our results, no new peaks were observed over an aggregation period of 48 hours. Furthermore, Western blot analyses of SDS-PAGE

separations have been utilized to characterize SDS-stable A β ₁₋₄₀ assemblies [22,24,27,32]. A smear for A β ₁₋₄₀ species ranging from ~60 - 80 kDa was obtained after incubation at 4°C for 6 weeks of an A β ₁₋₄₀ oligomer preparation employing DMSO and F12 culture media at pH 7.4, 150 mM NaCl [24,27]. This smear obtained with Western blotting could represent the broad peaks with longer migration times seen in our UV-CE studies (**Figure 1A**). Our studies are the first to utilize UV-CE to detect the formation of native A β ₁₋₄₀ species ranging from 100 – 300 kDa and > 300 kDa at near physiological pH.

3.2. Effect of sample preparation on A β ₁₋₄₀ aggregate sizes formed

The type of solvent used to dissolve lyophilized A β ₁₋₄₀ has been shown to have an effect on the initial conformation and subsequent aggregation kinetics of this peptide [50]. However, this study employed organic solvents, which have been known to accelerate A β aggregation and misrepresent the true “native” aggregation of the protein [51]. Furthermore, larger aggregates which are initially present in solution can serve as “seeds” that promote the formation oligomeric species [52,53]. Therefore, since a range of A β ₁₋₄₀ sizes were detected at the onset of aggregation (**Figure 1A**) using a sample preparation thought to produce smaller A β sizes, we explored the aggregation of a sample containing SEC-purified A β ₁₋₄₀ as the starting material. Furthermore, we utilized a non-organic solvent, sodium hydroxide, for initial dissolution of A β ₁₋₄₀ peptide. Preexisting A β ₁₋₄₀ aggregates were removed by SEC and samples thought to contain purified A β ₁₋₄₀ monomer were diluted into 40 mM Tris (pH 8.0), subjected to 5 mM NaCl, and agitated at 800 rpm to promote amyloid assembly. The reaction was analyzed using UV-CE at various points throughout the aggregation process to assess the appearance of oligomers and progression into larger aggregate species. Similar to the filtration analyses conducted with non-purified A β ₁₋₄₀, we used membranes with molecular weight cutoffs of 10, 30, 50, and 300 kDa to analyze the

filtrate obtained after 0 and 5 hours of aggregation (**Appendix**). At 0 hours, a peak migrating at ~9.5 min was observed, which was estimated to range in size from 10 – 30 kDa (**Figure 4A**). After 5 hours of aggregation, a new peak with a faster migration time of ~8 min appeared. The size of these species was estimated by filtration analysis to be > 300 kDa, or larger than 70 monomer units. A similar peak pattern for the 10 – 30 kDa species and faster eluting oligomer species was obtained after 10 – 48 hours (**Figure 4B**) while a later peak appeared which became more broad and exhibited a progressively shorter migration time (**Figure 4A**). The size of this peak was estimated by filtration analyses to be 100 - 300 kDa.

In order to better visualize the differences between SEC-purified A β_{1-40} and non-purified A β_{1-40} samples, the peak pattern obtained at 0 hours for SEC-purified samples and non-purified samples is compared (**Figure 5A and B**). Compared to the non-SEC purified A β_{1-40} sample, no peak was observed at 220 min for the SEC-purified A β_{1-40} sample, indicating the presence of predominantly 10 – 30 kDa A β_{1-40} at 0 hours (**Figure 5**). Furthermore, the area for the 10 – 30 kDa peak at ~9 minutes is compared to the peak area for the > 300 kDa oligomer peak at ~8.5 minutes. **Figure 6A** shows peak areas for the non-purified A β_{1-40} sample while **Figure 6B** shows the peak areas for the SEC-purified A β_{1-40} sample. Compared to the non-purified A β_{1-40} sample, the SEC-purified A β_{1-40} sample showed a decrease in the 10 – 30 kDa peak area and appearance of > 300 kDa oligomer peak after 5 hours, which is ~23 hours earlier than non-purified A β_{1-40} sample. **Figure 7** shows changes in the 10 – 30 kDa peak area for the SEC-purified A β_{1-40} sample compared to the non-purified A β_{1-40} sample. Initially, an increase in the 10 – 30 kDa peak area is observed for the non-purified A β_{1-40} sample. Furthermore, the 10 – 30 kDa peak for the non-purified A β_{1-40} sample decreased after 28 hours while the 10 – 30 kDa peak for the SEC-purified A β_{1-40} sample decreases after just 5 hours. The decrease in the 10 – 30 kDa

Figure 4. Detection of smaller, intermediate, and larger SEC-purified A β_{1-40} molecular weight aggregation states using UV-CE. SEC-purified A β_{1-40} was aggregated under agitation (800 rpm) at 0.22 mg/mL in 40 mM Tris (pH 8.0) containing 5 mM NaCl and at 25 °C. At 0 – 48 hours, CE was performed in conjunction with UV detection with a 0.5 psi pressure injection for 8 s with separation at 7 kV using 0.5% PEO separation matrix in a PEO coated capillary. Panel **A)** shows all peaks while panel **B)** is zoomed in on the smaller peaks. Results are representative of three independent experiments.

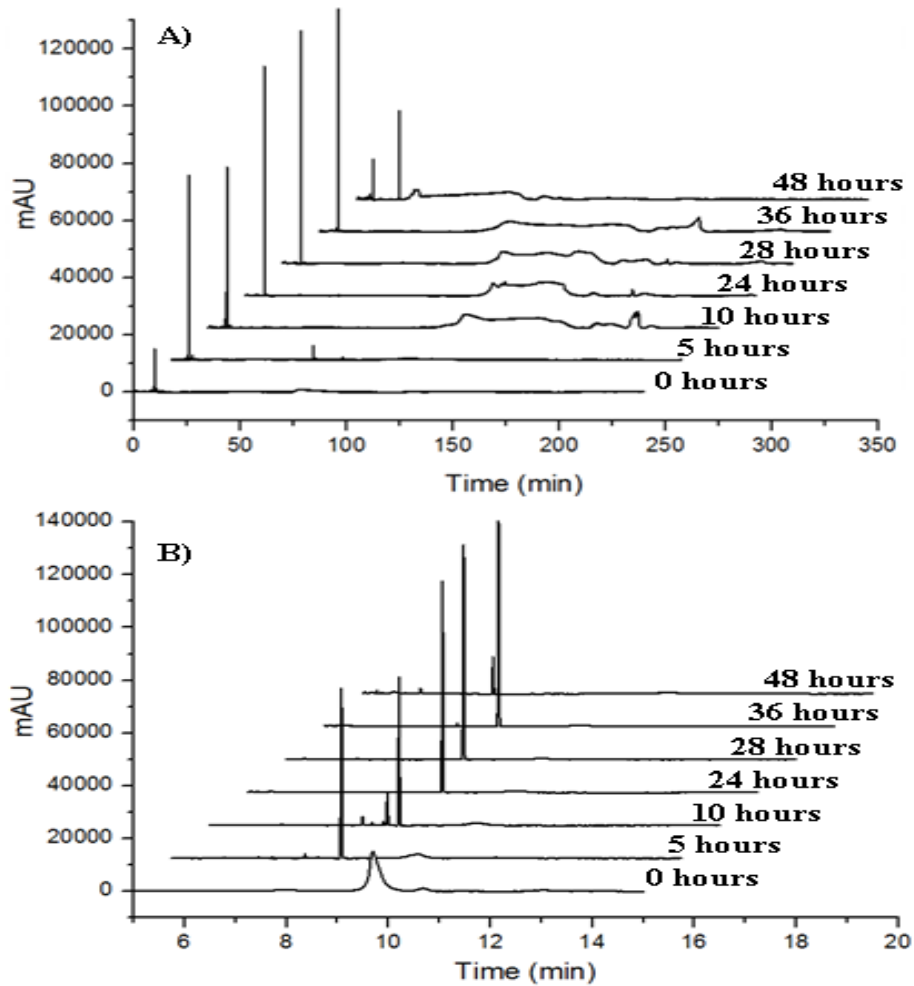


Figure 5. Comparison of peak pattern obtained at the onset of aggregation for SEC-purified A β ₁₋₄₀ and non-purified A β ₁₋₄₀ using UV-CE. SEC-purified A β ₁₋₄₀ and non-purified A β ₁₋₄₀ were aggregated under agitation (800 rpm) at 0.22 mg/mL in 40 mM Tris (pH 8.0) containing 5 mM NaCl and at 25 °C. At 0 hours, CE was performed in conjunction with UV detection with a 0.5 psi pressure injection for 8 s with separation at 7 kV using 0.5% PEO separation matrix in a PEO coated capillary. Panel **A)** shows all peaks while panel **B)** is zoomed in on the smaller peaks.

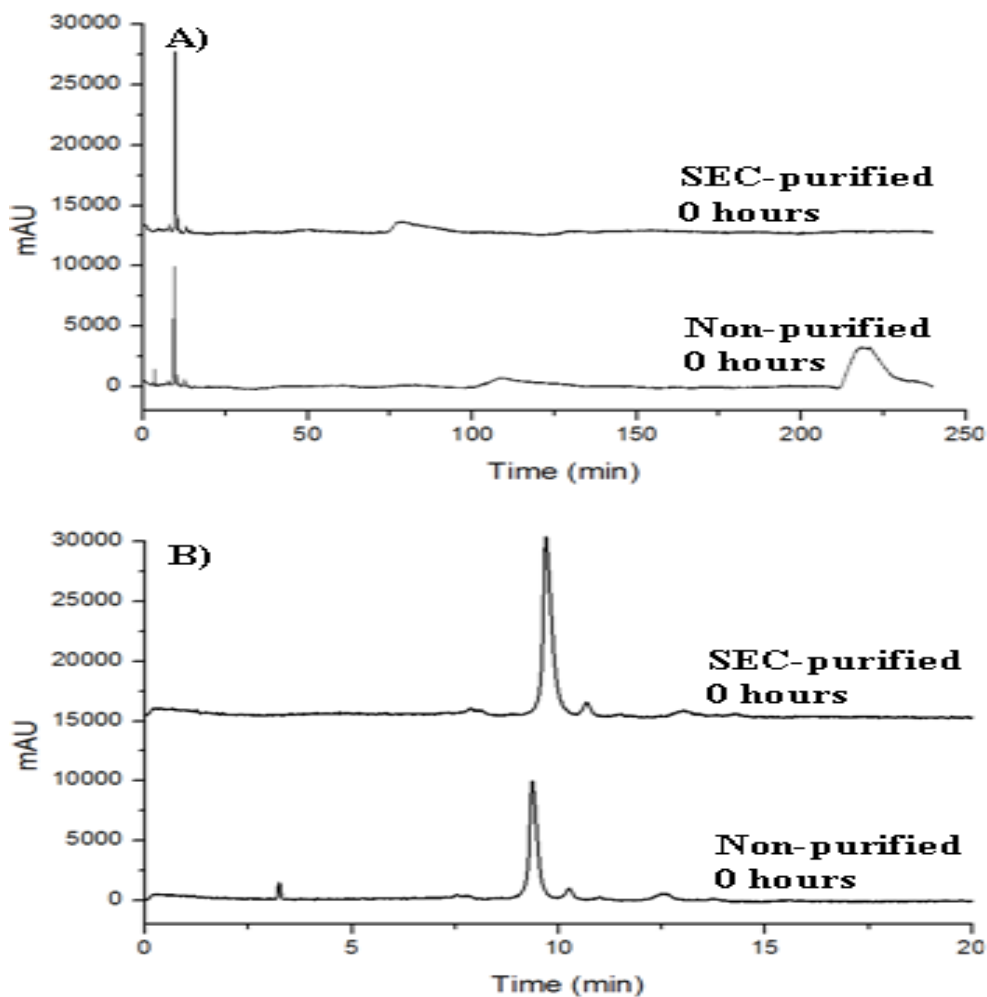


Figure 6. Effect of aggregation time on the peak areas obtained for **A)** 10 – 30 kDa (◆, *n* = 3) and > 300 kDa (■, *n* = 3) non-purified A β ₁₋₄₀ species and **B)** 10 – 30 kDa (●, *n* = 3) and > 300 kDa (▲, *n* = 3) SEC-purified A β ₁₋₄₀ species. SEC-purified and non-purified A β ₁₋₄₀ were aggregated under agitation (800 rpm) at 0.22 mg/mL in 40 mM Tris (pH 8.0) containing 5 mM NaCl and at 25 °C. At 0 – 48 hours, CE was performed in conjunction with UV detection with a 0.5 psi pressure injection for 8 s with separation at 7 kV using 0.5% PEO separation matrix in a PEO coated capillary. A * represents the first time point in which peak areas are statistically different with *p* < 0.05 for non-purified A β ₁₋₄₀ samples and *p* < 0.02 for SEC-purified A β ₁₋₄₀ samples.

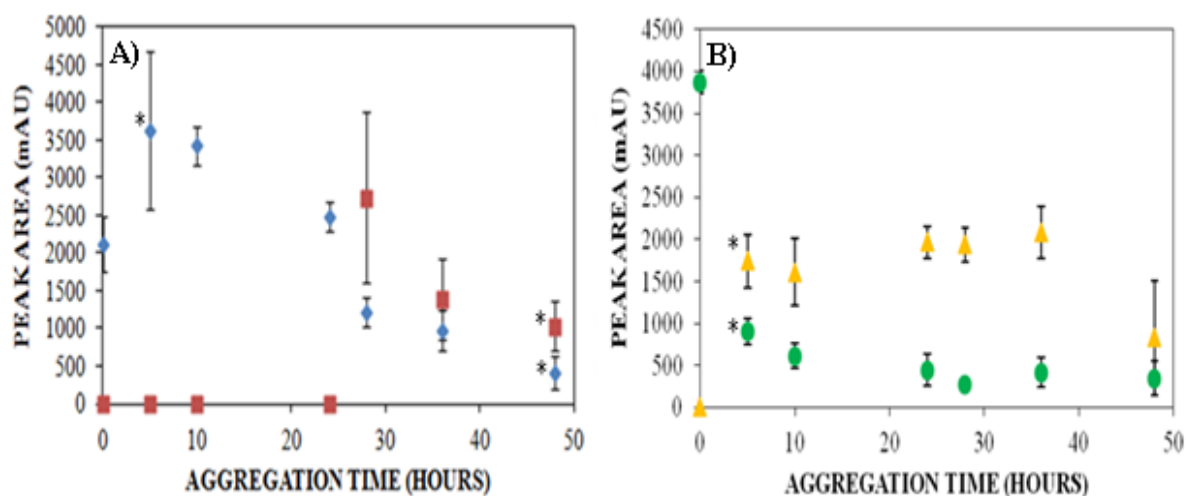
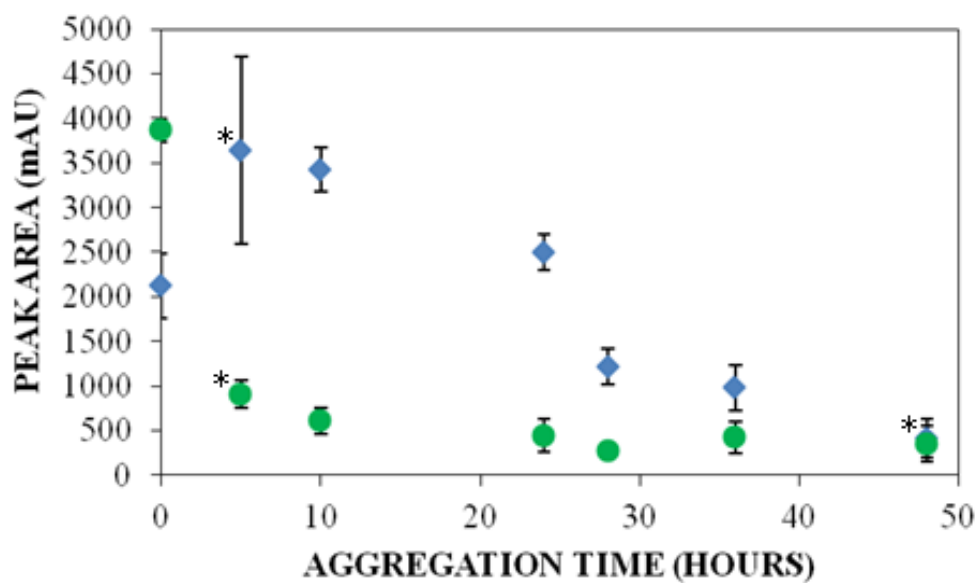


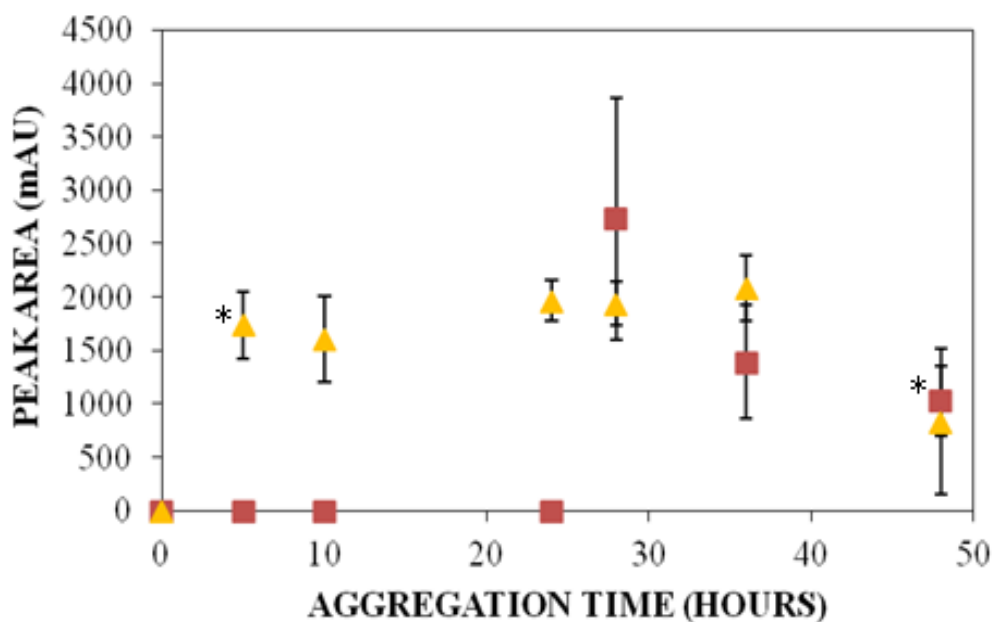
Figure 7. Effect of aggregation time on the 10 – 30 kDa peak areas obtained for non-purified (◆, $n = 3$) and SEC-purified (●, $n = 3$) $A\beta_{1-40}$ species. SEC-purified and non-purified $A\beta_{1-40}$ were aggregated under agitation (800 rpm) at 0.22 mg/mL in 40 mM Tris (pH 8.0) containing 5 mM NaCl and at 25 °C. At 0 – 48 hours, CE was performed in conjunction with UV detection with a 0.5 psi pressure injection for 8 s with separation at 7 kV using 0.5% PEO separation matrix in a PEO coated capillary. A * represents the first time point in which peak areas are statistically different with $p < 0.05$ for non-purified $A\beta_{1-40}$ samples and $p < 0.0002$ for SEC-purified $A\beta_{1-40}$ samples.



peak area is accompanied by the appearance of a > 300 kDa oligomer peak for both non-purified and SEC-purified A β ₁₋₄₀ samples. **Figure 8** compares the area for the > 300 kDa peak for non-purified and SEC-purified A β ₁₋₄₀ samples. This peak appears ~23 hours earlier compared to non-purified A β ₁₋₄₀ samples.

Our findings that a very short lag time to aggregate formation exists when SEC-purified monomer is the predominant A β ₁₋₄₀ species at the onset of aggregation are similar to those observed by Taylor *et al* [54]. This study prepared a solution of A β ₁₋₄₀ which consisted of predominantly monomer, as confirmed by HPLC, and monitored aggregate formation by dilution to 50 μ M in PBS and agitation at 800 rpm. Turbidity measurements showed that aggregate formation occurred after 60 min. They propose a three-step kinetic model for A β ₁₋₄₀ in which; 1) an unactivated monomer is slowly converted to an activated monomer, 2) an oligomeric nucleus is formed by the cooperative interaction between four activated monomers that serves as the growing site for the fibril, 3) fibril growth proceeds by the successive addition of unactivated monomer to elongate the aggregates. As shown in Figure 3.7, SEC-purified A β ₁₋₄₀ has a much larger initial population of 10 – 30 kDa species compared to the non-purified A β ₁₋₄₀. In addition, the population of 10 – 30 kDa species for the non-purified A β ₁₋₄₀ increases initially and then begins to decrease before forming larger oligomeric species > 300 kDa. This suggests that a critical concentration of 10 – 30 kDa species is necessary in order to progress to the next aggregation state. Furthermore, as shown in Figure 3.8, the > 300 kDa species formed by non-purified A β ₁₋₄₀ samples increases after 28 hours and begins to decrease after 36 hours while the peak area for the > 300 kDa species formed by SEC-purified A β ₁₋₄₀ increases after 5 hours but does not begin to decrease until 48 hours. We hypothesize that a key size is needed, which is formed at later points during aggregation, for the seeding effect to encourage the larger

Figure 8. Effect of aggregation time on the > 300 kDa peak area obtained for non-purified (■, $n = 3$) and SEC-purified (▲, $n = 3$) $A\beta_{1-40}$ species. SEC-purified and non-purified $A\beta_{1-40}$ were aggregated under agitation (800 rpm) at 0.22 mg/mL in 40 mM Tris (pH 8.0) containing 5 mM NaCl and at 25 °C. At 0 – 48 hours, CE was performed in conjunction with UV detection with a 0.5 psi pressure injection for 8 s with separation at 7 kV using 0.5% PEO separation matrix in a PEO coated capillary. A * represents the first time point in which peak areas are statistically different with $p < 0.04$ for non-purified $A\beta_{1-40}$ samples and $p < 0.02$ for SEC-purified $A\beta_{1-40}$ samples.



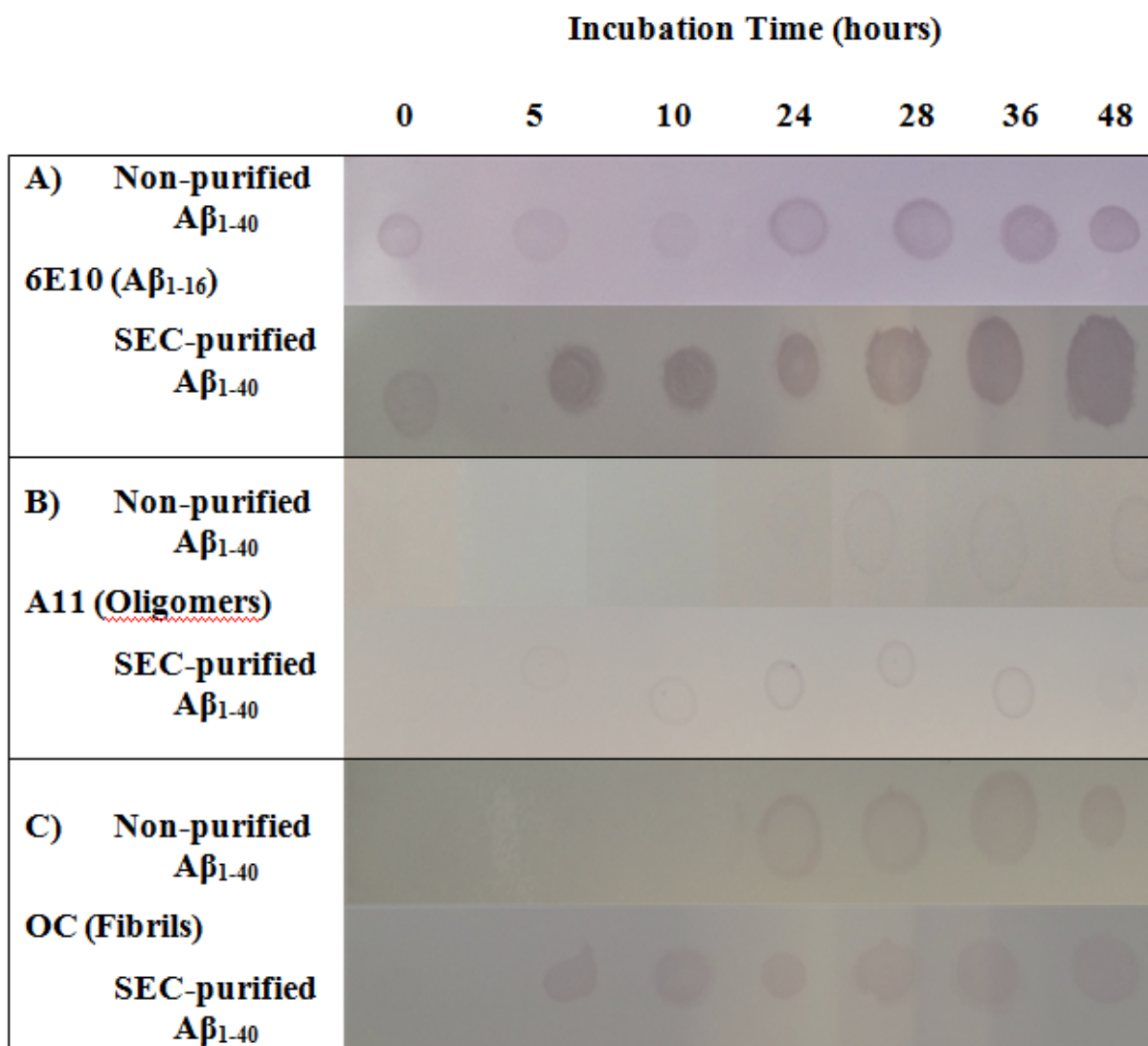
aggregation growth. Whatever the cause, the differences between lag times in addition to peak areas for samples containing larger aggregates at the onset of aggregation and samples containing predominantly smaller species at the onset of aggregation highlights the importance of sample preparation on $A\beta_{1-40}$ aggregation.

3.3 Validation of CE detection with traditional measures of $A\beta$ aggregation states

The recent development of antibodies specific for $A\beta$ oligomers has led to an increase in the application of dot blotting to study $A\beta$ aggregation [55-57]. Furthermore, antibodies which are specific for a certain part of the $A\beta$ sequence or a particular conformation can be used to detect $A\beta_{1-16}$ and $A\beta$ fibrillar species, respectively. In these studies, we utilized the conformation specific antibodies A11 and OC, which are known to recognize $A\beta$ prefibrillar oligomers [55,56] and $A\beta$ fibrils [55], respectively, and the sequence specific antibody 6E10, which is known to recognize $A\beta_{1-16}$ [55,56]. Non-purified and SEC-purified $A\beta_{1-40}$ samples were agitated using the same sample and aggregation conditions as were used in the UV-CE studies. **Figure 9** shows the dot blot analysis of $A\beta_{1-40}$ monomer (**Panel A, 6E10 antibody**), oligomer (**Panel B, A11 antibody**), and fibril (**Panel C, OC antibody**). The top row in each panel is for non-purified $A\beta_{1-40}$ samples while the bottom row is for SEC-purified $A\beta_{1-40}$ samples. At all times during aggregation, both non-purified and SEC-purified $A\beta_{1-40}$ samples contain 6E10 positive stains (**Figure 9A**). This is expected as both $A\beta$ oligomer and fibril samples have been shown to react with 6E10 in the literature [55]. A11 and OC positive dots are detected in non-purified $A\beta_{1-40}$ samples after 24 hours and in SEC-purified $A\beta_{1-40}$ samples after 5 hours (**Figure 9B, C**). This indicates that for non-purified $A\beta_{1-40}$ samples, oligomeric and fibrillar $A\beta_{1-40}$ species begin to

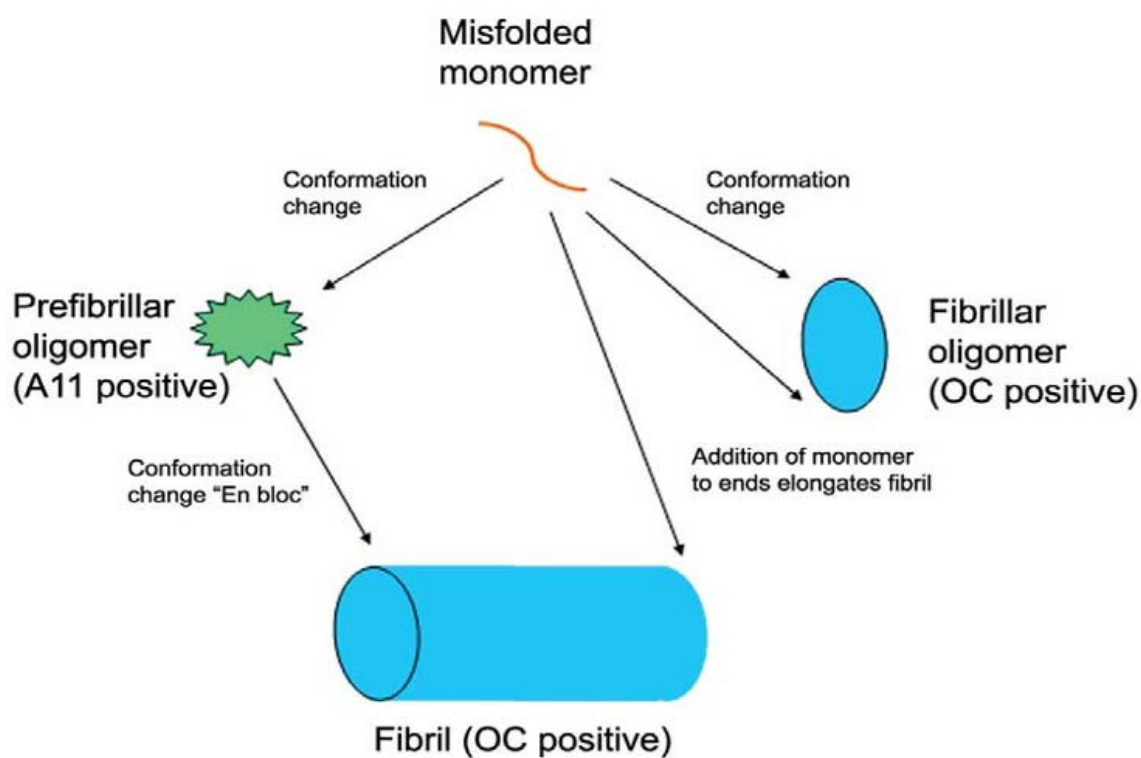
form after 24 hours of aggregation while for SEC-purified A β_{1-40} samples oligomeric and fibrillar A β_{1-40} species begin to form after 5 hours of aggregation.

Figure 9. Monitoring $A\beta_{1-40}$ aggregation by dot blotting. Non-purified $A\beta_{1-40}$ and SEC-purified $A\beta_{1-40}$ samples were aggregated under agitation (800 rpm) at 0.22 mg/mL in 40 mM Tris (pH 8.0) containing 5 mM NaCl and at 25 °C. At 0 – 48 hours, samples were taken and spotted onto a nitrocellulose membrane. Membranes were stained with $A\beta_{1-16}$ specific antibody 6E10 (Panel A), oligomer specific antibody A11 (Panel B) and fibril specific antibody OC (Panel C).



These results are in agreement with previous studies which utilized dot blots to monitor A β_{1-40} aggregation. A study by Wong *et al.* utilized dot blotting to monitor the aggregation of a 50 μ M A β_{1-40} sample containing 10 mM NaH₂PO₄ and 150 mM NaCl at pH 7.4 incubated at 37°C [56]. They observed positive stains for the 6E10 antibody at times ranging from 0 – 3 days with the highest signal intensity at 1 and 2 days followed by a decrease in intensity at 3 days. A similar trend to the 6E10 antibody was observed for the A11 antibody but with a much lower signal intensity at day 0. This study did not look at the binding of OC to A β_{1-40} . A comparison between the binding of A11 and OC to A β_{1-42} has been investigated by Kaye *et al* [55]. This study incubated A β_{1-42} under two sets of conditions, one known to promote the formation of fibrillar oligomers and fibrils while the other set of conditions is known to promote the formation of prefibrillar oligomers. A mechanism for aggregation was suggested (**Figure 10**) whereby; 1) misfolded monomer aggregates to form prefibrillar oligomers (recognized by A11), 2) prefibrillar oligomers align to form protofibrils followed by a conformational change to form fibrils (recognized by OC). An alternative mechanism of aggregation was also suggested where; 1) misfolded monomer aggregates to form fibrillar oligomers (recognized by OC), 2) fibrillar oligomers elongate by the addition of monomer onto the ends of fibrillar oligomers, thus resulting in fibril formation. A comparison of our dot blot results with the results obtained from UV-CE suggests that both of these mechanisms of aggregation may be occurring under our incubation conditions. This is supported by examination of the non-purified A β_{1-40} time course. After 24 hours of aggregation, dot blots reveal positive stains for A11 and OC (**Figure 9B and C**) while the UV-CE peak pattern for the 10 – 30 kDa peak at ~9 min (**Figure 1B**) remains virtually the same as earlier time points. After 28 hours, UV-CE shows that the area for the 10 – 30 kDa peak

Figure 10. Representation of distinct types of $A\beta_{1-42}$ oligomers and their relationship to $A\beta_{1-42}$ fibrils. Monomeric $A\beta_{1-42}$ misfolds and aggregates to form two different conformations. One conformation formed is a prefibrillar oligomer, recognized by A11 (left pathway), which aligns to form protofibrils and undergoes another conformational change “en bloc” to form fibrils. Alternatively, a fibrillar oligomeric conformation can be formed which is recognized by OC (right pathway). The fibrillar oligomers may represent the fibril nuclei which are capable of elongating by recruiting additional monomers. Addition of monomers to the ends of fibrillar oligomers and fibrils results in fibril growth. Reprinted from [55] with permission from Charles Glabe, cglabe@uci.edu, corresponding author for this publication. Copyright 2007 by the authors; licensee BioMed Central, an open access journal.



decreases while a new peak with a faster migration time of ~8 – 8.5 min (> 300 kDa) appears. Therefore, this fast peak could correspond to the conformational change that the prefibrillar oligomer undergoes.

3.4 Determination of $A\beta_{1-40}$ limit of detection

The physiological concentration of $A\beta$ in CSF is 100 – 2000 pM [58]. Therefore, the ability of a technique to detect $A\beta$ at these low concentrations is necessary to analyze patient samples. In Chapter 2, we determined the limit of detection for insulin protein to be 1.72 μ M and 48.4 pM using UV- and LIF-CE, respectively. To determine the $A\beta_{1-40}$ limit of detection using UV-CE, $A\beta_{1-40}$ was prepared at concentrations ranging from 0.0087 mg/mL to 0.043 mg/mL and analyzed. The S/N ratio of the $A\beta_{1-40}$ peak was > 3 at concentrations of 0.02 mg/mL and higher, defining 0.02 mg/mL (5 μ M) as the limit of detection for $A\beta_{1-40}$ using UV-CE. The definition of the detection limit as the analyte concentration with a S/N ratio > 3 has been used previously in studies utilizing CE detection [59,60]. The $A\beta$ detection limit obtained is in agreement with the detection limit obtained in our previous studies on insulin protein of 1.72 μ M [61]. A study by Verpillot *et al.* obtained a lower detection limit for $A\beta$ using UV-CE of 0.002 mg/mL (0.5 μ M) [62]. This study utilized a 20 s injection time at 0.5 psi where our studies were conducted using a 8 s injection at 0.5 psi. Therefore, the amount of $A\beta$ injected into the capillary was most likely higher in the Verpillot *et al.* study, which would lead to a lower detection limit. Furthermore, the $A\beta$ detection limit achieved by Verpillot *et al.* is higher than the physiological $A\beta$ concentration in CSF of 100 – 2000 pM [58].

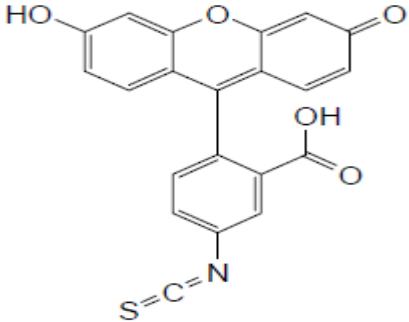
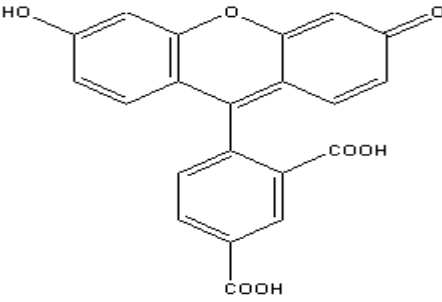
A parallel limit of detection study was performed for carboxy-fluorescein (FAM)-labeled $A\beta_{1-40}$ and $A\beta_{1-42}$ using LIF-CE. The optimized injection conditions used previously for the detection of FITC-insulin were utilized in these studies. To determine the $A\beta_{1-40}$ and $A\beta_{1-42}$

detection limits using LIF-CE, FAM-labeled A β ₁₋₄₀ and A β ₁₋₄₂ were prepared at concentrations ranging from 0.0047 - 4140 ng/mL for FAM-A β ₁₋₄₀ and 0.0049 – 4870 ng/mL for FAM-A β ₁₋₄₂. The S/N ratio of the FAM-A β ₁₋₄₀ peak was > 3 at concentrations of 0.09 ng/mL and higher, thus establishing 0.09 ng/mL (20 pM) as the limit of detection for FAM-A β ₁₋₄₀ using LIF-CE. Furthermore, the S/N ratio of the FAM-A β ₁₋₄₂ peak was > 3 at concentrations of 0.0049 ng/mL and higher, thus establishing 0.0049 ng/mL (1 pM) as the limit of detection for FAM-A β ₁₋₄₂ using LIF-CE and illustrating the superior limit of FAM-A β ₁₋₄₂ detection for LIF-CE compared with FAM-A β ₁₋₄₀. In fact, the LIF detection limits of 1 and 20 pM are lower than the physiological A β concentration in CSF of 100 – 2000 pM [58] and to the authors' knowledge, is the lowest LIF detection limit of A β for an electrophoresis based method. A study by Verpillot *et al.* obtained a LIF-CE detection limit for FAM-A β of 35 nM [35], thus exhibiting the superior LIF-CE detection limit for A β (1 – 20 pM) obtained in our studies. Thus, LIF-CE is a promising technique for the detection of physiologically relevant A β concentrations.

3.5 Analysis of FAM tracer incorporation into unlabeled A β

Similar to FITC, FAM is a fluorescein derivative which contains a carboxylic acid reactive group where FITC contains an isothiocyanate reactive group (**Table 1**). These reactive groups react with primary amines present on internal lysine residues and N-terminal residues via an S_N2 reaction. Insulin contains two N-terminal residues and one lysine residue whereas A β contains one N-terminal residue and two lysine residues. Therefore, the number of possible attachment sites between the two proteins is similar. Since A β ₁₋₄₂ is highly prone to aggregation, the FAM label may be more likely to incorporate into aggregates formed by A β ₁₋₄₂.

Table 1: Structure and spectral properties of FAM and FITC.

Fluorophore	Structure	Excitation/Emission Wavelength
Fluorescein isothiocyanate		494/518 [63]
5-Carboxy-fluorescein		492/518 [64]

The potential for LIF-CE to monitor the ability of FAM-labeled $A\beta_{1-42}$ to incorporate into unlabeled $A\beta_{1-42}$ was investigated using a sample preparation method which has been previously shown to promote $A\beta_{1-42}$ oligomer formation [65]. **Figure 11** shows the LIF-CE peak pattern obtained where **Panel A** is a zoom in of the data shown in **Panel B**. At 0 hours, LIF-CE demonstrated the presence of three peaks with migration times < 30 min (**Figure 11A**) in addition to larger, more broad peaks with migration times ranging from 50 – 70 min (**Figure 11B**). After 3 hours, a similar peak pattern was obtained with the appearance of two more peaks with migration times of ~ 31 and 36 min, respectively (**Figure 11A**). In addition, a peak with a faster migration time of ~ 6 min appeared. The area for the peak with a faster migration time of ~ 6 min increased over an aggregation time of 9 hours then decreased after 24 hours (**Figure 12A**, yellow squares). The area for the larger peak at 70 min decreased over a time period of 24 hours (**Figure 12A**, green triangles). **Figure 12B** shows changes in the normalized migration time for the last peaks in **Figure 11A** (~ 36 min) and **Figure 11 B** (~ 70 min) relative to the first peak at ~ 15 min, thus representing growth for faster and slower migrating species, respectively. The normalized migration time for later peaks did not change over time while the normalized migration time for earlier peaks increased. These results suggest that FAM-labeled $A\beta_{1-42}$ was incorporating into smaller unlabeled $A\beta_{1-42}$ species but was interfering with the formation of larger $A\beta_{1-42}$ species. Based on the peak pattern obtained in Chapter 3 for $A\beta_{1-40}$ after 28 hours of aggregation with analysis via UV-CE, we estimate that the peak formed after 3 hours of aggregation at ~ 6 min corresponds to a larger species. Furthermore, the peaks with migration times > 40 min were estimated to be due to larger aggregates. Filtration or dot blot analyses were not conducted since the studies in Chapter 4 were performed prior to the studies in Chapter 3.

Figure 11. Coaggregation of FAM-labeled $A\beta_{1-42}$ and unlabeled $A\beta_{1-42}$. $A\beta_{1-42}$ solutions consisting of 30% FAM-labeled $A\beta_{1-42}$ and 70% unlabeled $A\beta_{1-42}$ with LIF detection ($n = 2$) were prepared at a concentration of 0.14 mg/mL in 40 mM Tris (pH 8.0) containing 10 mM NaCl. Solutions were allowed to sit at room temperature and the formation of aggregates was monitored. Panel **A** is zoomed in on the early peaks while panel **B** shows all peaks. LIF-CE was performed with a sample injection at 7 kV for 7 s with 7 kV separation using 0.5% PHEA separation matrix in PHEA coated capillary.

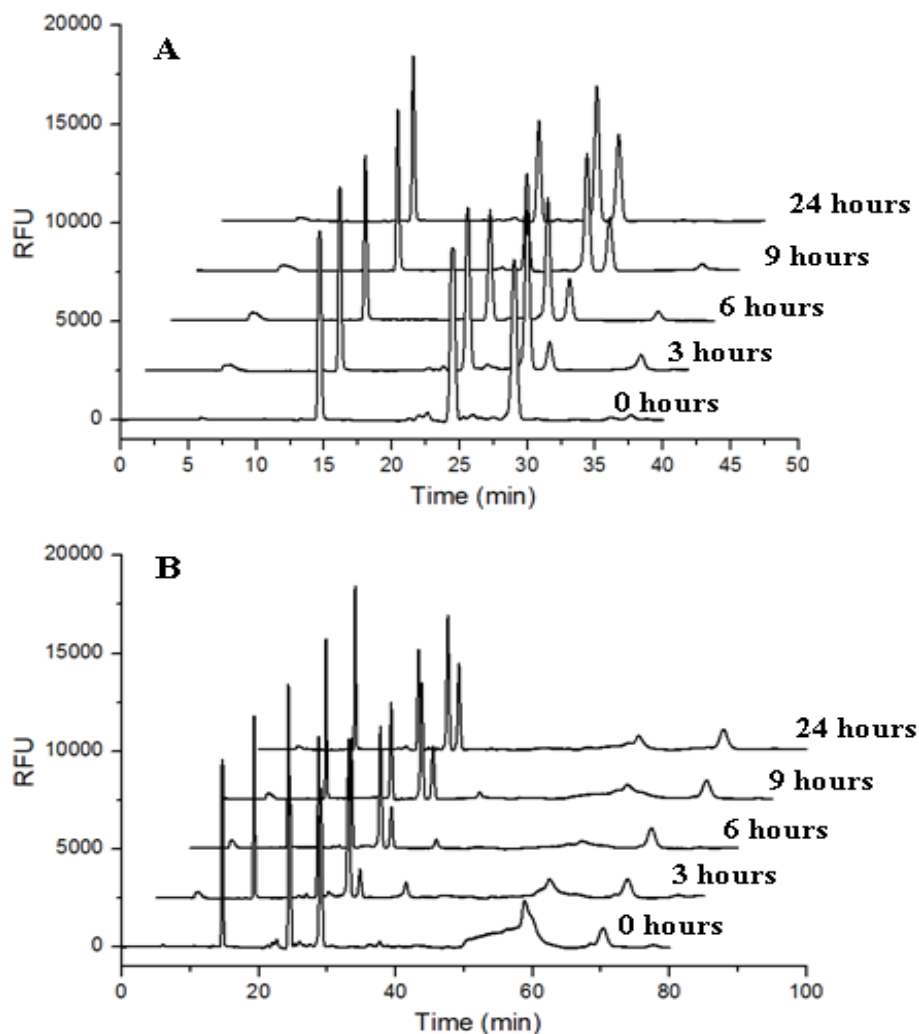
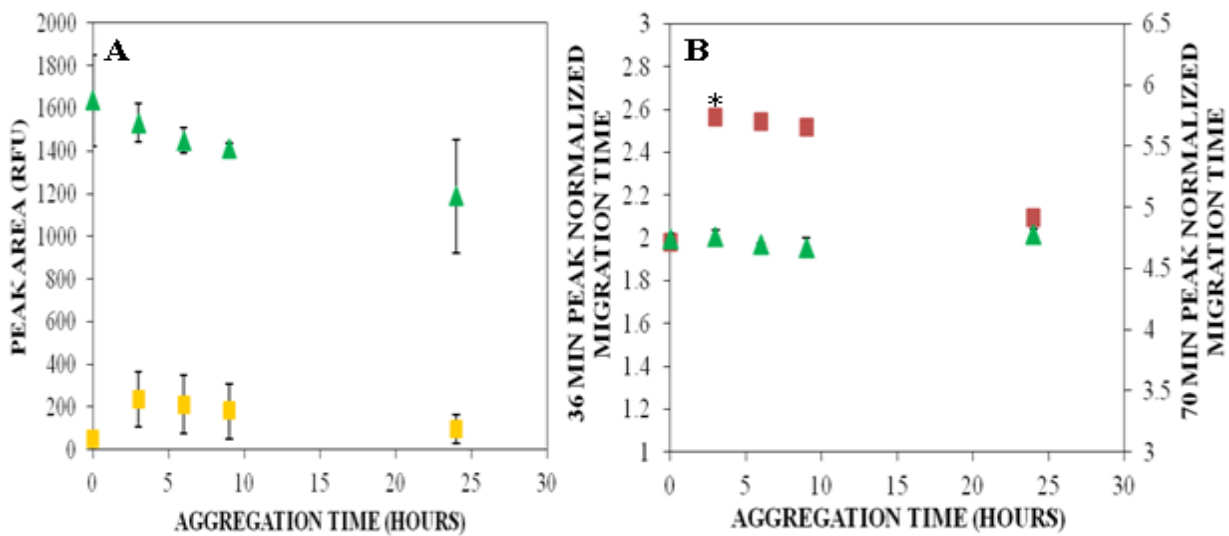


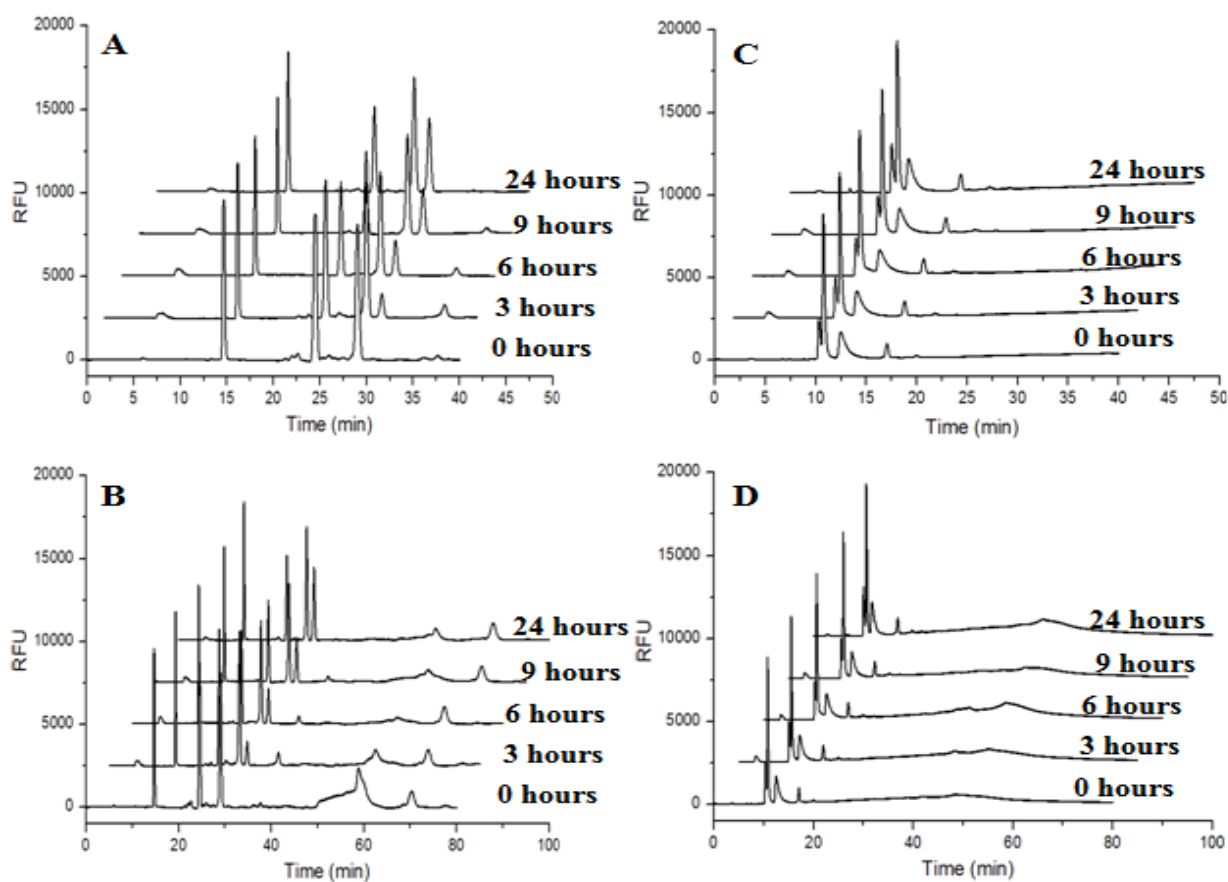
Figure 12. Change in peak areas and normalized migration times for the coaggregation of FAM-labeled $A\beta_{1-42}$ and unlabeled $A\beta_{1-42}$. $A\beta_{1-42}$ solutions consisting of 30% FAM-labeled $A\beta_{1-42}$ and 70% unlabeled $A\beta_{1-42}$ with LIF detection were prepared at a concentration of 0.14 mg/mL in 40 mM Tris (pH 8.0) containing 10 mM NaCl. Solutions were allowed to sit at room temperature and the formation of small and large species was monitored. **Panel A** shows the change in peak area for peaks at ~6 min (■, $n = 2$), and 70 min (▲, $n = 2$). **Panel B** shows the changes in normalized migration time for the peak at 36 min (■, $n = 2$) and 70 min (▲, $n = 2$). LIF-CE was performed with a sample injection at 7 kV for 7 s with 7 kV separation using 0.5% PHEA separation matrix in PHEA coated capillary. Peak migration times were determined by normalizing the migration time for the last peak observed relative to the migration time of the first peak observed for each incubation time point. A * represents the first time point in which peak normalized migration times are statistically different with $p < 0.004$.



Other researchers have examined the effect of the FAM label on aggregation. Similar results were obtained by Jungbauer *et al.* using SDS-PAGE with Western blotting to analyze a 100 μ M FAM-labeled A β_{1-42} sample incubated in phenol-red free Hams F12 media, pH 7.4 at 4°C for 24 hours [66]. This study observed bands for monomer, dimer, trimer, and tetramer (~4.5 – 13.5 kDa) with a smear for larger molecular weight species ranging from 35 – 60 kDa for FAM-A β_{1-42} . Compared to oligomers formed by labeled A β_{1-42} , the unlabeled A β_{1-42} trimer and tetramer bands were less intense and the high molecular weight smear ranged from 40 – 100 kDa. These results suggest that the FAM label could be interfering with the formation of high molecular weight species ranging from 60 – 100 kDa. Alternatively, the FAM label could be affecting the kinetics for the formation of A β_{1-40} aggregates as a study by Edwin *et al.* found that in some cases it took longer than 3 weeks to observe FAM-A β_{1-40} aggregates using fluorescence photobleaching recovery [67].

Although it appears that FAM-labeled A β_{1-42} was capable of incorporating into smaller A β_{1-42} species, we found this behavior to be highly dependent upon the lot obtained from the manufacturer. Aggregation studies were conducted using identical sample and LIF-CE conditions as those used to obtain the data shown in **Figures 11** and **12** but using different FAM-labeled A β_{1-42} and unlabeled A β_{1-42} lots. Furthermore, these lots were obtained from the same manufacturer (Anaspec). **Figures 13A** and **B** show the peak pattern obtained for the old lot while **Figures 13C** and **D** show the peak pattern obtained for the new lot. **Panels A** and **C** are a zoom in of the early peaks in **Panels B** and **D**. Peaks at ~31 and 36 min appear after 3 hours of aggregation with the old lot (**Figure 13A**) but not with the new lot (**Figure 13C**). In both lots, the peak with a faster migration time of ~5 min appears after 3 hours of

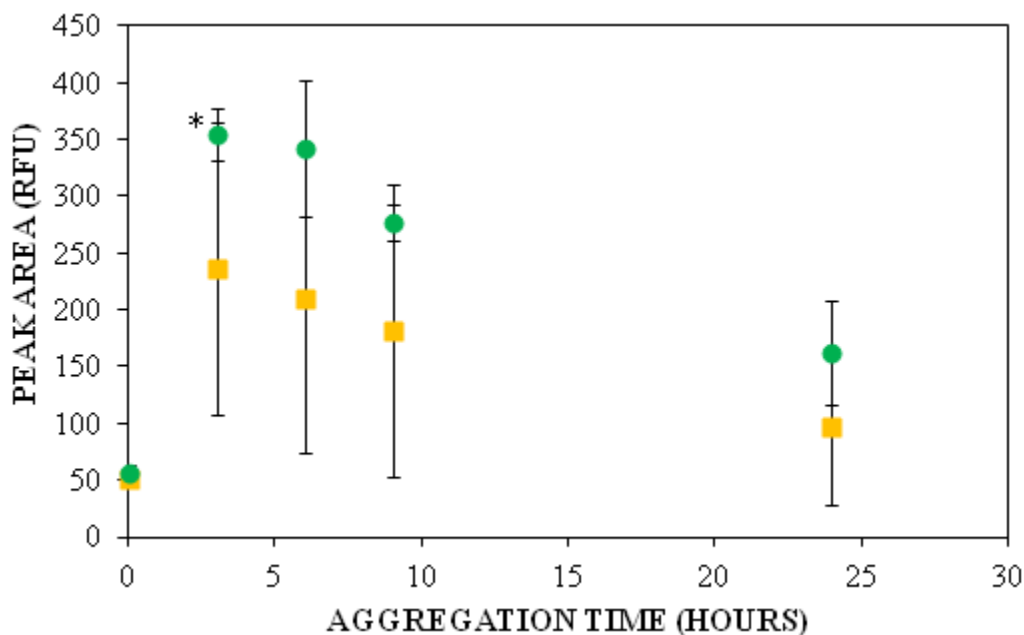
Figure 13. Effect of peptide lot on the coaggregation of FAM-labeled $A\beta_{1-42}$ and unlabeled $A\beta_{1-42}$. $A\beta_{1-42}$ solutions consisting of 30% FAM-labeled $A\beta_{1-42}$ and 70% unlabeled $A\beta_{1-42}$ with LIF detection ($n = 2$) were prepared at a concentration of 0.14 mg/mL in 40 mM Tris (pH 8.0) containing 10 mM NaCl. Solutions were allowed to sit at room temperature and the formation of aggregates was monitored. **Panels A** and **B** show the peak pattern obtained for the old lot. **Panels C** and **D** show the peak pattern obtained for the new lot. **Panels A** and **C** are zoomed in on the early peaks shown in **Panels B** and **D**. LIF-CE was performed with a sample injection at 7 kV for 7 s with 7 kV separation using 0.5% PHEA separation matrix in PHEA coated capillary.



aggregation (**Figures 13A and C**). **Figure 14** compares the change in area for the peak with a faster migration time obtained with the old lot (yellow squares) and the new lot (green circles). The overlap in error bars between the two sets of data makes it difficult to draw conclusions about differences in peak area for the two lots. A similar trend of an increase in peak area after 3 hours followed by a decrease in area after 24 hours is exhibited with both lots.

Lot-to-lot variability in synthetic preparations of A β peptides has been observed in the literature [68,69]. A study by Wogulis *et al.* observed varying amounts of fibrillar A β_{1-40} for three lots upon solubilization in water and dilution to 30 μ M in tissue culture medium [68]. Furthermore, they found that neuronal cell death required the presence of both soluble and fibrillar forms of A β . Similar to Wogulis *et al.*, we have observed significant lot-to-lot variations that have the potential to impact the aggregation process. This indicates the complexity of the A β aggregation process and further highlights the need for a screening technique which more accurately represents the aggregation process.

Figure 14. Change in early peak area for the coaggregation of FAM-labeled A β_{1-42} and unlabeled A β_{1-42} using two different lots. A β_{1-42} solutions consisting of 30% FAM-labeled A β_{1-42} and 70% unlabeled A β_{1-42} with LIF detection were prepared at a concentration of 0.14 mg/mL in 40 mM Tris (pH 8.0) containing 10 mM NaCl. Solutions were allowed to sit at room temperature and the formation of oligomers and aggregates was monitored. The change in area for the peak with a faster migration time of ~6 min is shown for the old lot (■, $n = 2$) and the new lot (●, $n = 2$). LIF-CE was performed with a sample injection at 7 kV for 7 s with 7 kV separation using 0.5% PHEA separation matrix in PHEA coated capillary. A * represents the first time point in which peak areas are statistically different with $p < 0.0008$.



4. Conclusions

Although the exact nature of Alzheimer's Disease is not well understood, there are significant indications that it involves the aggregation of the A β protein, in particular the ~40 residue hydrophobic proteins A β_{1-40} and A β_{1-42} [70]. This highlights the importance of the development of a technique which is capable of detecting A β sizes produced throughout aggregation, in particular during the earliest stages of aggregation. Although there are certain advantages to using techniques such as SDS-PAGE, Western blotting, mass spectrometry, and SEC for A β detection, there are disadvantages as well. These limitations highlight the importance of employing a complementary technique to explore the evolution of A β oligomer appearance. Therefore, in these studies, we explored the potential of UV-CE to monitor the A β_{1-40} aggregation process. In particular, we utilized a PEO separation matrix to enhance the resolution of A β_{1-40} oligomers and aggregates. Strikingly, we found that the lag time to oligomer formation for SEC-purified A β_{1-40} samples was ~23 hours shorter compared to non-purified A β_{1-40} samples. This indicates that the initial sample sizes present have a drastic effect on the lag time to oligomer formation. The size of smaller, intermediate, and larger species was estimated using membrane filtration units. It should be noted that a spherical shape is assumed in order to generate the molecular weight cutoff for these membranes, thus providing a range of sizes. Therefore, we confirmed that these species were oligomeric in nature by utilizing dot blots and two compounds known to inhibit fibrils and oligomers, respectively. Furthermore, we utilized the sequence specific antibody 6E10 and conformation specific antibodies A11 and OC to confirm the presence of A β_{1-16} , A β prefibrillar oligomers, and A β fibrils, respectively. The presence of 6E10 positive spots was observed at all times throughout aggregation for both non-purified A β_{1-40} samples and SEC-purified A β_{1-40} samples. Positive spots for A11 and OC were

obtained after 24 hours of aggregation for non-purified A β_{1-40} samples and after 5 hours of aggregation for SEC-purified A β_{1-40} samples. A comparison of the dot blot and UV-CE results suggests that non-purified A β_{1-40} samples begin to form both prefibrillar oligomers (A11 positive) and fibrillar oligomers or fibrils (OC positive) after 24 hours of aggregation. These prefibrillar oligomers could then undergo a conformational change after 28 hours, which is represented by a sharp UV-CE peak with a faster mobility that corresponds to A β_{1-40} species > 300 kDa. Similar results were obtained for SEC-purified A β_{1-40} samples but with much faster lag times (~5 hours). Furthermore, we have determined the lowest concentration of A β that can be detected using both UV and LIF detection modes. Physiologically relevant A β concentrations in the picomolar range were detectable using LIF detection while concentrations in the micromolar range were required for UV detection.

Using UV-CE and LIF-CE to simultaneously monitor the aggregation of a mixture of FAM-labeled A β_{1-42} and unlabeled A β_{1-42} , this study was the first to show that FAM-labeled A β_{1-42} was capable of incorporating into smaller species formed by unlabeled A β_{1-42} but this ability was highly dependent on the lot employed. This further illustrates the complexity of the A β_{1-42} aggregation process and necessitates further investigation to identify optimum fluorescent labels for the study of insulin and A β oligomer formation at physiological concentrations. In particular, less bulky fluorescent probes, such as BODIPY, or attachment of dyes exclusively at the *N*- or *C*-terminus would be less likely to impact aggregate formation. Furthermore, since dyes often change the net protein charge, alternative dyes such as CE503 which do not alter the net charge may be explored. A more detailed discussion of alternative dyes will be given in the future work section of this thesis (Chapter 6).

The studies in Chapter 4 were conducted in order to explore the ability of UV-CE to monitor the aggregation of $A\beta_{1-40}$ in a native state and highlight certain advantages and disadvantages of UV-CE compared to other traditional $A\beta$ detection techniques. In theory, CE is a fast and highly efficient technique for the detection of charged molecules. Due to the small charge and/or large size of certain $A\beta$ species present throughout aggregation, the UV-CE analysis time exceeds 4 hours. Furthermore, there are no commercially available size standards for the detection of native protein states with CE, thereby making the estimation of $A\beta$ size difficult. In addition, we found that larger $A\beta$ species can exhibit a shorter migration time, which is contrary to the general theory of CE which predicts an increase in migration time with size. Our studies are the first to utilize a polymer separation matrix to enhance the resolution of $A\beta$ species. CE is also a powerful tool to monitor the disappearance of 10 – 30 kDa $A\beta$ species and appearance of new peaks throughout aggregation, thereby providing a complementary technique in which to validate the general trends observed for $A\beta$ aggregation.

In addition, the studies in Chapter 4 were conducted in order to determine the ability of LIF-CE to monitor FAM-labeled $A\beta_{1-42}$ aggregation. The limitations of LIF-CE for amyloid aggregate detection are; 1) the requirement of a fluorescent probe which can interfere with aggregation and thereby misrepresent the “true” native aggregation of the protein and 2) the dependence of LIF-CE to monitor aggregation on the particular protein lot employed. The focus of this thesis is on the detection of amyloid aggregates formed under conditions which mimic native protein aggregation rather than the detection of physiologically relevant concentrations. Since it was shown that FITC and FAM could misrepresent native aggregation states, alternative techniques for the detection of native $A\beta$ were proposed such as dot blots. Therefore, dot blots were employed in conjunction with UV-CE to better analyze the native aggregation of $A\beta$.

References

1. Alzheimer's Association. 2012 Alzheimer's Disease Facts and Figures. *Alzheimer's and Dementia* 2012, 8, 1-72.
2. Moss, M.; Varvel, N.; Nichols, M.; Reed, D.; Rosenberry, T. Nordihydroguaiaretic Acid does Not Disaggregate β -Amyloid(1-40) Protofibrils but does Inhibit Growth Arising from Direct Protofibril Association. *Mol. Pharmacol.* 2004, 66, 592-600.
3. Kato, M.; Kinoshita, H.; Toyooka, T. Analytical Method for β -Amyloid Fibrils using CE-Laser Induced Fluorescence and its Application to Screening for Inhibitors of β -Amyloid Protein Aggregation. *Anal. Chem.* 2007, 79, 4887-4891.
4. Nichols, M.; Moss, M.; Rosenberry, T. Amyloid-Aggregates Formed at Polar-Nonpolar Interfaces Differ from Amyloid-Protofibrils Produced in Aqueous Buffers. *Microscopy Research and Technique* 2005, 67, 164-174.
5. Caughey, B.; Lansbury, P.T. Protofibrils, Pores, Fibrils, and Neurodegeneration: Separating the Responsible Protein Aggregates from the Innocent Bystanders. *Annu. Rev. Neurosci.* 2003, 26, 267-298.
6. Glabe, C.G. Common Mechanisms of Amyloid Oligomer Pathogenesis in Degenerative Disease. *Neurobiol. Aging* 2006, 27, 570-575.
7. Roychaudhuri, R.; Yang, M.; Hoshi, M.M.; Teplow, D.B. Amyloid β -Protein Assembly and Alzheimer's Disease. *J. Biol. Chem.* 2009, 284, 4749-4753.
8. Lambert, M.P.; Barlow, A.K.; Chromy, B.A.; Edwards, C.; Freed, R.; Liosatos, M.; Morgan, T.E.; Rozovsky, I.; Trommer, B.; Viola, K.L. *et al.* Diffusible, Nonfibrillar Ligands Derived from A β 1-42 are Potent Central Nervous System Neurotoxins. *Proc. Natl. Acad. Sci. USA* 1998, 95, 6448-6453.
9. Hartley, D.M.; Walsh, D.M.; Ye, C.P.; Diehl, T.; Vasquez, S.; Vassilev, P.M.; Teplow, D.B.; Selkoe, D.J. Protofibrillar Intermediates of Amyloid β -Protein Induce Acute Electrophysiological Changes and Progressive Neurotoxicity in Cortical Neurons. *J. Neurosci.* 1999, 19, 8876-8884.
10. Walsh, D.M.; Klyubin, I.; Fadeeva, J.V.; Rowan, M.J.; Selkoe, D.J. Amyloid-B Oligomers: Their Production, Toxicity and Therapeutic Inhibition. *Biochem. Soc. Trans.* 2002, 30, 552-557.
11. Nath, S.; Agholme, L.; Kurudenkandy, F.R.; Granseth, B.; Marcusson, J.; Hallbeck, M. Spreading of Neurodegenerative Pathology Via Neuron-to-Neuron Transmission of β -Amyloid. *J. Neurosci.* 2012, 32, 8767-8777.

12. Wei, G.; Jewett, A.I.; Shea, J. Structural Diversity of Dimers of the Alzheimer Amyloid- β (25-35) Peptide and Polymorphism of the Resulting Fibrils. *Phys. Chem. Chem. Phys.* 2010, *12*, 3622-3629.
13. Kittner, M.; Knecht, V. Disordered Versus Fibril-Like Amyloid β (25-35) Dimers in Water: Structure and Thermodynamics. *J Phys Chem B* 2010, *114*, 15288-15295.
14. Hashimoto, T.; Adams, K.W.; Fan, Z.; McLean, P.J.; Hyman, B.T. Characterization of Oligomer Formation of Amyloid- β Peptide using a Split-Luciferase Complementation Assay. *J. Biol. Chem.* 2011, *286*, 27081-27091.
15. Podlisny, M.; Walsh, D.; Selkoe, D. Oligomerization of Endogeneous and Synthetic Amyloid β -Protein at Nanomolar Levels in Cell Culture and Stabilization of Monomer by Congo Red. *Biochemistry* 1998, *37*, 3602-3611.
16. Ward, R.; Jennings, K.; Howlett, D. Fractionation and Characterization of Oligomeric, Protofibrillar and Fibrillar Forms of β -Amyloid Peptide. *Biochem. J.* 2000, *348*, 137-144.
17. Satoh, Y.; Hirakura, Y.; Kirino, Y. B-Amyloid Peptides Inhibit Acetylcholine Release from Cholinergic Presynaptic Nerve Endings Isolated from an Electric Ray. *Neuroscience Letters* 2001, *302*, 97-100.
18. Walsh, D.; Lomakin, A.; Benedek, G.; Condron, M.; Teplow, D. Amyloid β -Protein Fibrillogenesis: Detection of a Protofibrillar Intermediate. *The Journal of Biological Chemistry* 1997, *272*, 22364-22372.
19. Moore, B.; Rangachari, V.; Tay, W.; Milkovic, N.; Rosenberry, T. Biophysical Analyses of Synthetic Amyloid- β (1-42) Aggregates before and After Covalent Cross-Linking. Implications for Deducing the Structure of Endogenous Amyloid- β Oligomers. *Biochemistry* 2009, *48*, 11796-11806.
20. Bernstein, S.; Dupuis, N.; Lazo, N.; Wytttenbach, T.; Condron, M.; Bitan, G.; Teplow, D.; Shea, J.; Ruotolo, B.; Robinson, C. *et al.* Amyloid- β Protein Oligomerization and the Importance of Tetramers and Dodecamers in the Aetiology of Alzheimer's Disease. *Nature Chemistry* 2009, *1*, 326-331.
21. Walsh, D.; Tseng, B.; Rydel, R.; Podlisny, M.; Selkoe, D. The Oligomerization of Amyloid β -Protein Begins Intracellularly in Cells Derived from Human Brain. *Biochemistry* 2000, *39*, 10831-10839.
22. Walsh, D.; Hartley, D.; Condron, M.; Selkoe, D.; Teplow, D. *in Vitro* studies of Amyloid β -Protein Fibril Assembly and Toxicity Provide Clues to the Aetiology of Flemish Variant (Ala⁶⁹² \rightarrow Gly) Alzheimer's Disease. *Biochem. J.* 2001, *355*, 869-877.

23. Walsh, D.; Klyubin, I.; Fadeeva, J.; Cullen, W.; Anwyl, R.; Wolfe, M.; Rowan, M.; Selkoe, D. Naturally Secreted Oligomers of Amyloid β Protein Potently Inhibit Hippocampal Long-Term Potentiation *in Vivo*. *Nature* 2002, *416*, 535-539.
24. Dahlgren, K.N.; Manelli, A.M.; Stine, W.B., Jr.; Baker, L.K.; Krafft, G.A.; LaDu, M.J. Oligomeric and Fibrillar Species of Amyloid- β Peptides Differentially Affect Neuronal Viability. *J. Biol. Chem.* 2002, *277*, 32046-32053.
25. Ying, Z.; Xin, W.; Jin-Sheng, H.; Fu-Xiang, B.; Wei-Min, S.; Xin-Xian, D.; Xiao-Bo, W.; Yi-Qin, L.; Xian-Xian, Z.; Hong-Gang, H. *et al.* Preparation and Characterization of a Monoclonal Antibody with High Affinity for Soluble A β Oligomers. *Hybridoma* 2009, *28*, 349-354.
26. Ryan, D.; Narrow, W.; Federoff, H.; Bowers, W. An Improved Method for Generating Consistent Soluble Amyloid- β Oligomer Preparations for *in Vitro* Neurotoxicity Studies. *Journal of Neuroscience Methods* 2010, *190*, 171-179.
27. Stine, W.B., Jr.; Dahlgren, K.N.; Krafft, G.A.; LaDu, M.J. In Vitro Characterization of Conditions for Amyloid- β Peptide Oligomerization and Fibrillogenesis. *J. Biol. Chem.* 2003, *278*, 11612-11622.
28. Iurascu, M.; Cozma, C.; Tomczyk, N.; Rontree, J.; Desor, M.; Drescher, M.; Przybylski, M. Structural Characterization of β -Amyloid Oligomer-Aggregates by Ion Mobility Mass Spectrometry and Electron Spin Resonance Spectroscopy. *Anal Bioanal Chem* 2009, *395*, 2509-2519.
29. Maji, S.; Ogorzalek Loo, R.; Inayathullah, M.; Spring, S.; Vollers, S.; Condrón, M.; Bitan, G.; Loo, J.; Teplow, D. Amino Acid Position-Specific Contributions to Amyloid β -Protein Oligomerization. *J. Biol. Chem.* 2009, *284*, 23580-23591.
30. Bernstein, S.; Wytténbach, T.; Baumketner, A.; Shea, J.; Bitan, G.; Teplow, D.; Bowers, M. Amyloid β -Protein: Monomer Structure and Early Aggregation States of A β 42 and its Pro19 Alloform. *J. Am. Chem. Soc.* 2005, *127*, 2075-2084.
31. Murray, M.; Bernstein, S.; Nyugen, V.; Condrón, M.; Teplow, D.; Bowers, M. Amyloid β Protein: A β 40 Inhibits A β 42 Oligomerization. *JACS* 2009, *131*, 6316-6317.
32. Bitan, G.; Kirkitadze, M.; Lomakin, A.; Vollers, S.; Benedek, G.; Teplow, D. Amyloid β -Protein (A β) Assembly: A β 40 and A β 42 Oligomerize through Distinct Pathways. *PNAS* 2003, *100*, 330-335.
33. Palmblad, M.; Westlind-Danielsson, A.; Bergquist, J. Oxidation of Methionine 35 Attenuates Formation of Amyloid β -Peptide 1-40 Oligomers. *J. Biol. Chem.* 2002, *277*, 19506-19510.

34. Yu, C.; Chin, C. In Situ Probing of Insulin Aggregation in Chromatography Effluents with Spectroturbidimetry. *Journal of Colloid and Interface Science* 2006, *299*, 733-739.
35. Verpillot, R.; Essellmann, H.; Mohamadi, M.R.; Klafki, H.; Poirier, F.; Lehnert, S.; Otto, M.; Wiltfang, J.; Jean, L.; Viovy; Taverna, M. Analysis of Amyloid- β Peptides in Cerebrospinal Fluid Samples by Capillary Electrophoresis Coupled with LIF Detection. *Anal. Chem.* (Washington, DC, U. S.) 2011, *83*, 1696-1703.
36. Landers, J.P. *Handbook of Capillary and Microchip Electrophoresis and Associated Microtechniques*, 3rd ed.; CRC Press: Boca Raton, FL, 2008; pp. 1567.
37. Sabella, S.; Quaglia, M.; Lanni, C.; Racchi, M.; Govoni, S.; Caccialanza, G.; Calligaro, A.; Bellotti, V.; Lorenzi, E. Capillary Electrophoresis Studies on the Aggregation Process of β -Amyloid 1-42 and 1-40 Peptides. *Electrophoresis* 2004, *25*, 3186-3194.
38. Picou, R.; Kheterpal, I.; Wellman, A.; Minnamreddy, M.; Ku, G.; Gilman, S.D. Analysis of A β (1-40) and A β (1-42) Monomer and Fibrils by Capillary Electrophoresis. *J. Chromatogr. B* 2011, *879*, 627-632.
39. Picou, R.A.; Schrum, D.P.; Ku, G.; Cerqua, R.A.; Kheterpal, I.; Gilman, S.D. Separation and Detection of Individual A β Aggregates by Capillary Electrophoresis with Laser-Induced Fluorescence Detection. *Anal. Biochem.* 2012, *425*, 104-112.
40. Schultz, N.M.; Huang, L.; Kennedy, R.T. Capillary Electrophoresis-Based Immunoassay to Determine Insulin Content and Insulin Secretion from Single Islets of Langerhans. *Anal. Chem.* 1995, *67*, 924-929.
41. Kotarek, J.A.; Johnson, K.C.; Moss, M.A. Quartz Crystal Microbalance Analysis of Growth Kinetics for Aggregation Intermediates of the Amyloid- β Protein. *Anal. Biochem.* 2008, *378*, 15-24.
42. Albarghouthi, M.; Stein, T.; Barron, A. Poly-N-Hydroxyethylacrylamide as a Novel, Adsorbed Coating for Protein Separation by Capillary Electrophoresis. *Electrophoresis* 2003, *24*, 1166-1175.
43. Hert, D.G.; Fredlake, C.P.; Barron, A.E. DNA Sequencing by Microchip Electrophoresis using Mixtures of High-and Low-Molar Mass Poly(N,N-Dimethylacrylamide) Matrices. *Electrophoresis* 2008, *29*, 4663-4668.
44. Westerman, M.; Cooper-Blacketer, D.; Mariash, A.; Kotilinek, L.; Kawarabayashi, T.; Younkin, L.; Carlson, G.; Younkin, S.; Ashe, K. The Relationship between A β and Memory in the Tg2576 Mouse Model of Alzheimer's Disease. *J. Neurosci.* 2002, *22*, 1858-1867.

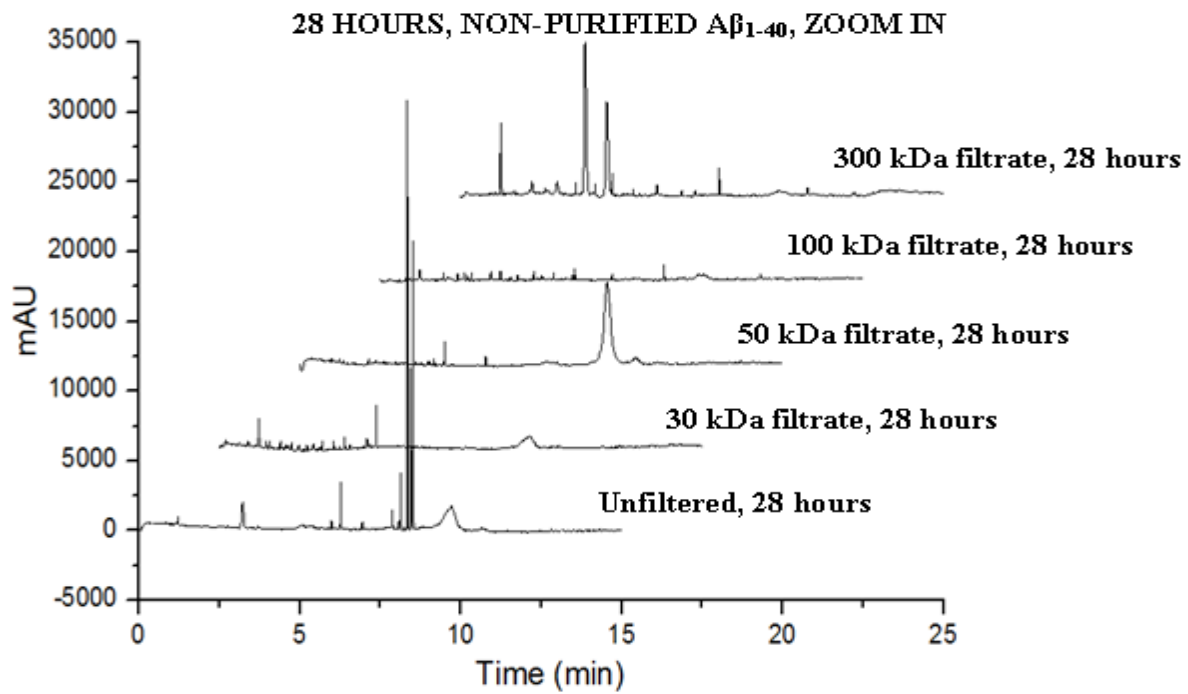
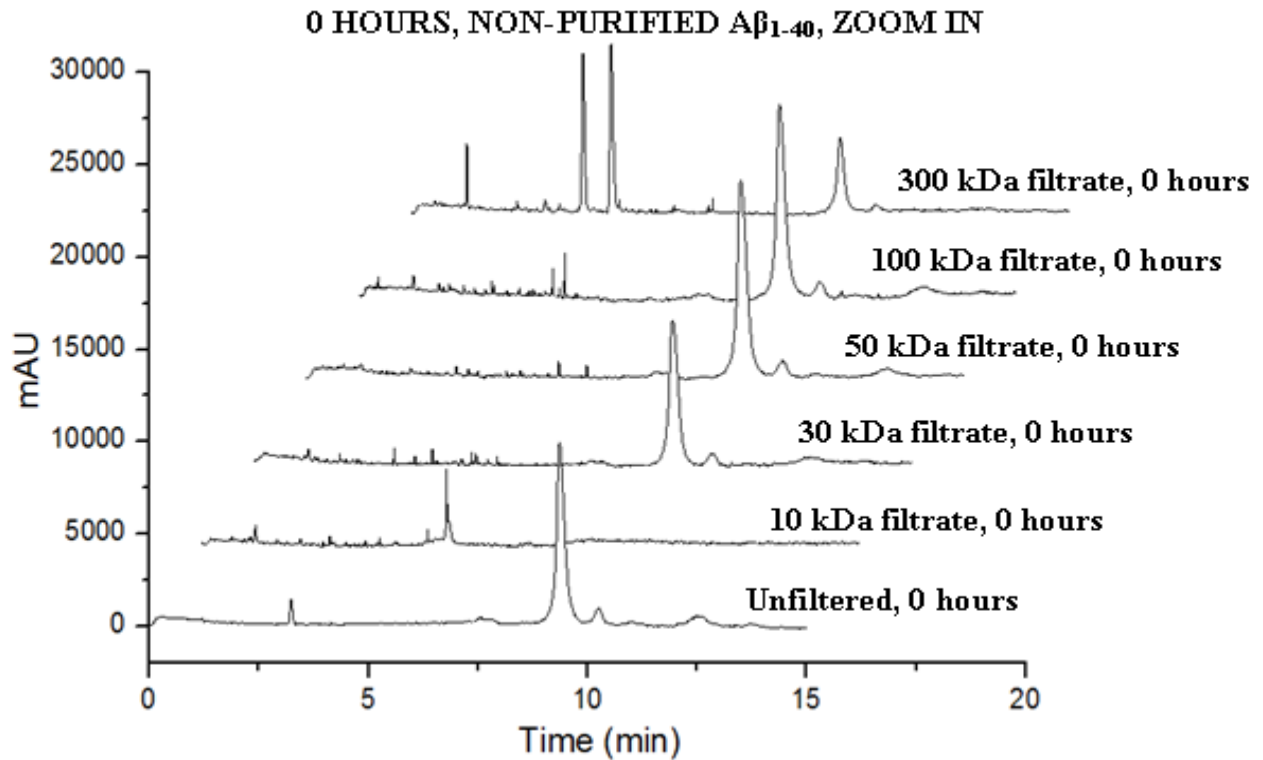
45. Lue, L.F.; Kuo, Y.M.; Roher, A.E.; Brachova, L.; Shen, Y.; Sue, L.; Beach, T.; Kurth, J.H.; Rydel, R.E.; Rogers, J. Soluble Amyloid β Peptide Concentration as a Predictor of Synaptic Change in Alzheimer's Disease. *Am. J. Pathol.* 1999, *155*, 853-862.
46. Scheff, S.; Price, D.; Schmitt, F.; Mufson, E. Hippocampal Synaptic Loss in Early Alzheimer's Disease and Mild Cognitive Impairment. *Neurobiology of Aging* 2006, *27*, 1372-1384.
47. Necula, M.; Kaye, R.; Milton, S.; Glabe, C.G. Small Molecule Inhibitors of Aggregation Indicate that Amyloid β Oligomerization and Fibrillization Pathways are Independent and Distinct. *J. Biol. Chem.* 2007, *282*, 10311-10324.
48. Wang, Q.; Shah, N.; Zhao, J.; Wang, C.; Zhao, C.; Liu, L.; Li, L.; Zhou, F.; Zheng, J. Structural, Morphological, and Kinetic Studies of β -Amyloid Peptide Aggregation on Self-Assembled Monolayers. *Phys. Chem. Chem. Phys.* 2011, *13*, 15200-15210.
49. Petkova, A.T.; Ishii, Y.; Balbach, J.J.; Antzutkin, O.N.; Leapman, R.D.; Delaglio, F.; Tycko, R. A Structural Model for Alzheimer's β -Amyloid Fibrils Based on Experimental Constraints from Solid State NMR. *Proc. Natl. Acad. Sci. U. S. A.* 2002, *99*, 16742-16747.
50. Wang, S.S.-.; Chen, Y.; Chen, P.; Liu, K. A Kinetic Study on the Aggregation Behavior of β -Amyloid Peptides in Different Initial Solvent Environments. *Biochem. Eng. J.* 2006, *29*, 129-138.
51. Sureshbabu, N.; Kirubakaran, R.; Jayakumar, R. Surfactant-Induced Conformational Transition of Amyloid Beta-Peptide. *EBJ* 2009, *38*, 355-367.
52. Kirkitadze, M.; Condron, M.; Teplow, D. Identification and Characterization of Key Kinetic Intermediates in Amyloid β -Protein Fibrillogenesis. *J. Mol. Biol.* 2001, *312*, 1103-1119.
53. Terzi, E.; Hoelzemann, G.; Seelig, J. Interaction of Alzheimer β -Amyloid Peptide(1-40) with Lipid Membranes. *Biochemistry* 1997, *36*, 14845-14852.
54. Taylor, B.M.; Sarver, R.W.; Fici, G.; Poorman, R.A.; Lutzke, B.S.; Molinari, A.; Kawabe, T.; Kappenman, K.; Buhl, A.E.; Epps, D.E. Spontaneous Aggregation and Cytotoxicity of the β -Amyloid A β 1-40: A Kinetic Model. *J. Protein Chem.* 2003, *22*, 31-40.
55. Kaye, R.; Head, E.; Sarsoza, F.; Saing, T.; Cotman, C.W.; Necula, M.; Margol, L.; Wu, J.; Breydo, L.; Thompson, J.L. *et al.* Fibril Specific, Conformation Dependent Antibodies Recognize a Generic Epitope Common to Amyloid Fibrils and Fibrillar Oligomers that is Absent in Prefibrillar Oligomers. *Mol Neurodegener* 2007, *2*, 18.

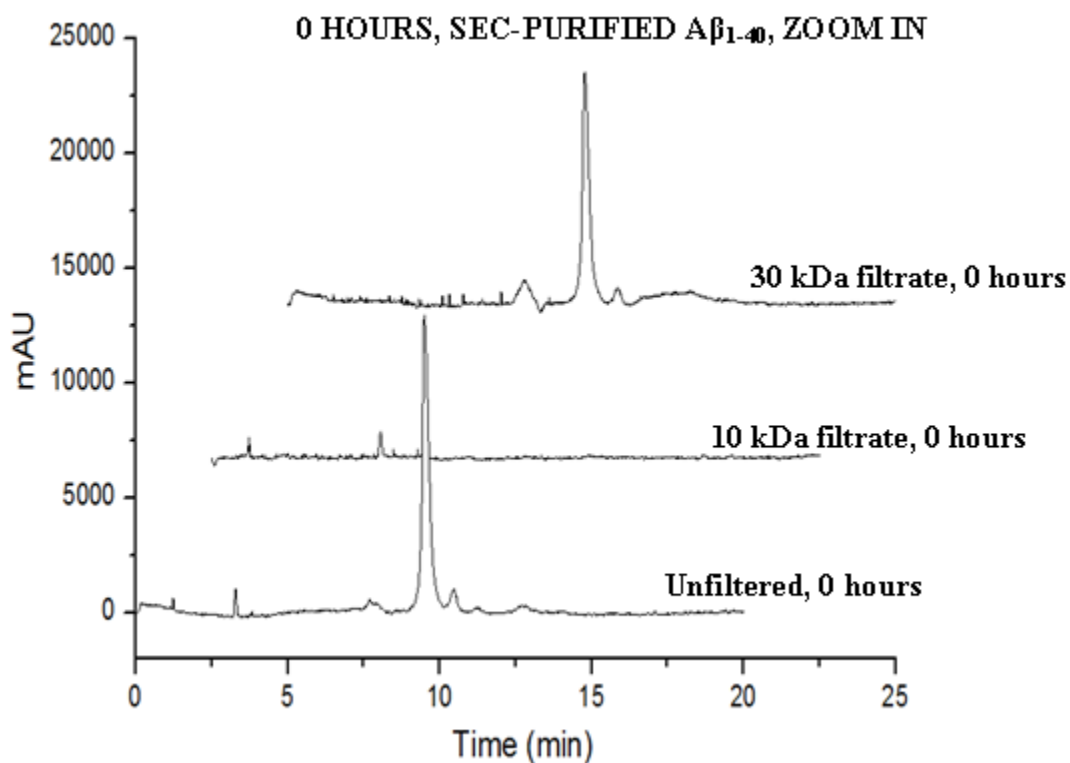
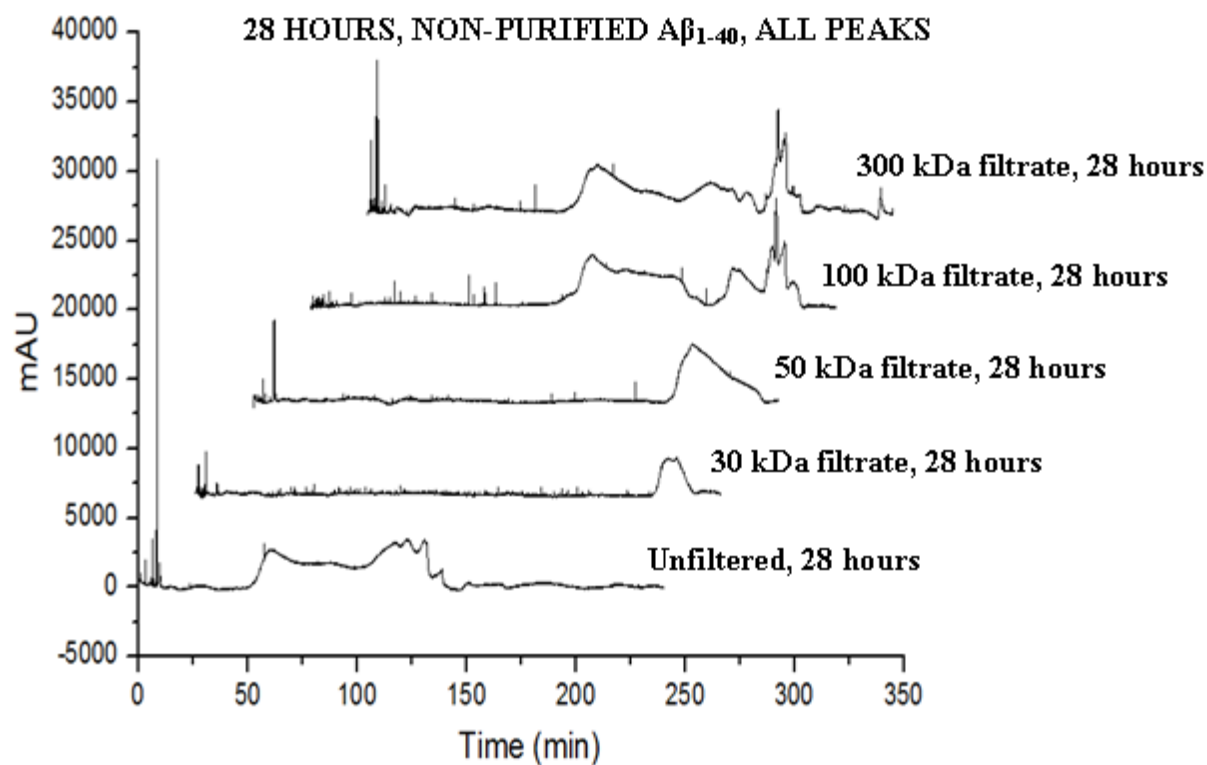
56. Wong, H.E.; Qi, W.; Choi, H.; Fernandez, E.J.; Kwon, I. A Safe, Blood-Brain Barrier Permeable Triphenylmethane Dye Inhibits Amyloid- β Neurotoxicity by Generating Nontoxic Aggregates. *ACS Chem. Neurosci.* 2011, *2*, 645-657.
57. Ladiwala, A.R.; Litt, J.; Kane, R.S.; Aucoin, D.S.; Smith, S.O.; Ranjan, S.; Davis, J.; Vannstrand, W.E.; Tessier, P.M. Conformational Differences between Two Amyloid β Oligomers of Similar Size and Dissimilar Toxicity. *J. Biol. Chem.* 2012, *287*, 24765-24773.
58. Fukuyama, R.; Mizuno, T.; Mori, S.; Nakajima, K.; Fushiki, S.; Yanagisawa, K. Age-Dependent Change in the Levels of A β 40 and A β 42 in Cerebrospinal Fluid from Control Subjects, and a Decrease in the Ratio of A β 42 to A β 40 Level in Cerebrospinal Fluid from Alzheimer's Disease Patients. *Eur. Neurol.* 2000, *43*, 155-160.
59. Lim, H.B.; Lee, J.J.; Lee, K. Simple and Sensitive Laser-Induced Fluorescence Detection for Capillary Electrophoresis and its Application to Protein Separation. *Electrophoresis* 1995, *16*, 674-678.
60. Ren, J.; Li, B.; Deng, Y.; Cheng, J. Indirect Thermo-Optical Detection for Capillary Electrophoresis. *Talanta* 1995, *42*, 1891-1895.
61. Pryor, E.; Kotarek, J.A.; Moss, M.A.; Hestekin, C.N. Monitoring Insulin Oligomer Formation Via Capillary Electrophoresis. *Int. J. Mol. Sci.* 2011, *12*, 9369-9388.
62. Verpillot, R.; Otto, M.; Taverna, M. Simultaneous Analysis by Capillary Electrophoresis of Five Amyloid Peptides as Potential Biomarkers of Alzheimer's Disease. *Journal of Chromatography A* 2008, *1214*, 157-164.
63. Thermo Scientific. FITC and Fluorescein Dyes and Labeling Kits. 2012, 2012.
64. Anaspec. 5-FAM. 2011, 2012.
65. Levine, H. Alzheimer's β -Peptide Oligomer Formation at Physiologic Concentrations. *Anal. Biochem.* 2004, *335*, 81-90.
66. Jungbauer, L.M.; Yu, C.; Laxton, K.J.; La, D.,M.J. Preparation of Fluorescently-Labeled Amyloid-Beta Peptide Assemblies: The Effect of Fluorophore Conjugation on Structure and Function. *J. Mol. Recognit.* 2009, *22*, 403-413.
67. Edwin, N.J.; Hammer, R.P.; McCarley, R.L.; Russo, P.S. Reversibility of β -Amyloid Self-Assembly: Effects of pH and Added Salts Assessed by Fluorescence Photobleaching Recovery. *Biomacromolecules.* 2010, *11*, 341-347.
68. Wogulis, M.; Wright, S.; Cunningham, D.; Chilcote, T.; Powell, K.; Rydel, R.E. Nucleation-Dependent Polymerization is an Essential Component of Amyloid-Mediated Neuronal Cell Death. *J. Neurosci.* 2005, *25*, 1071-1080.

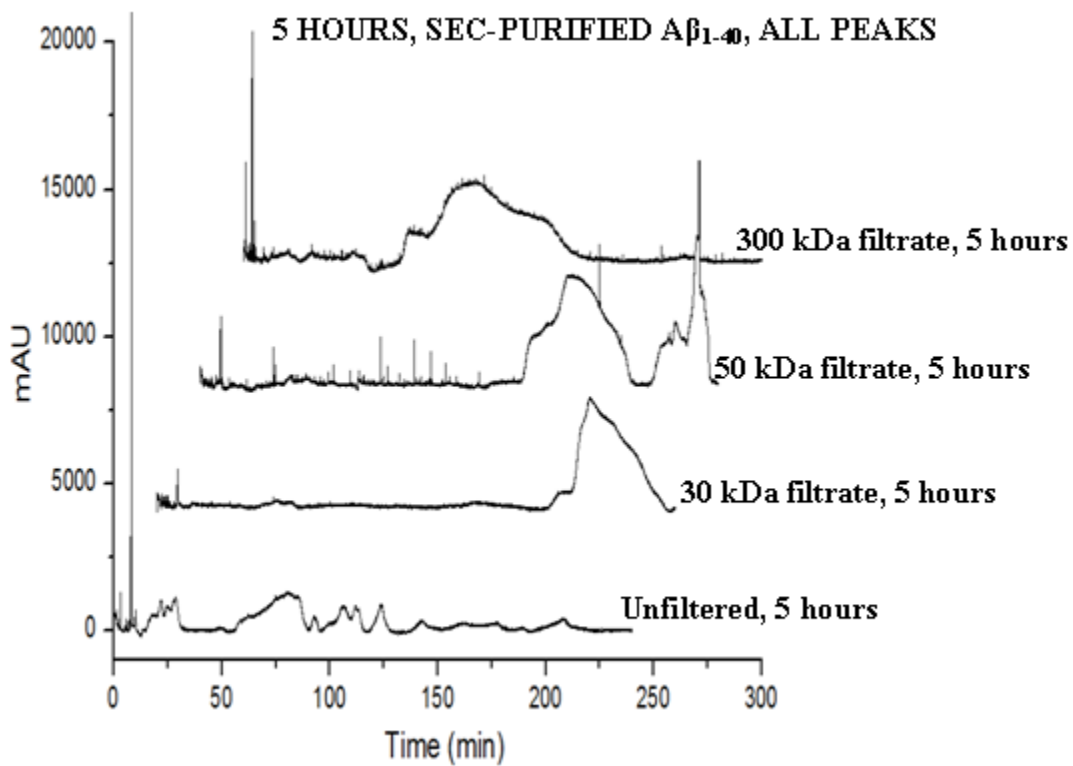
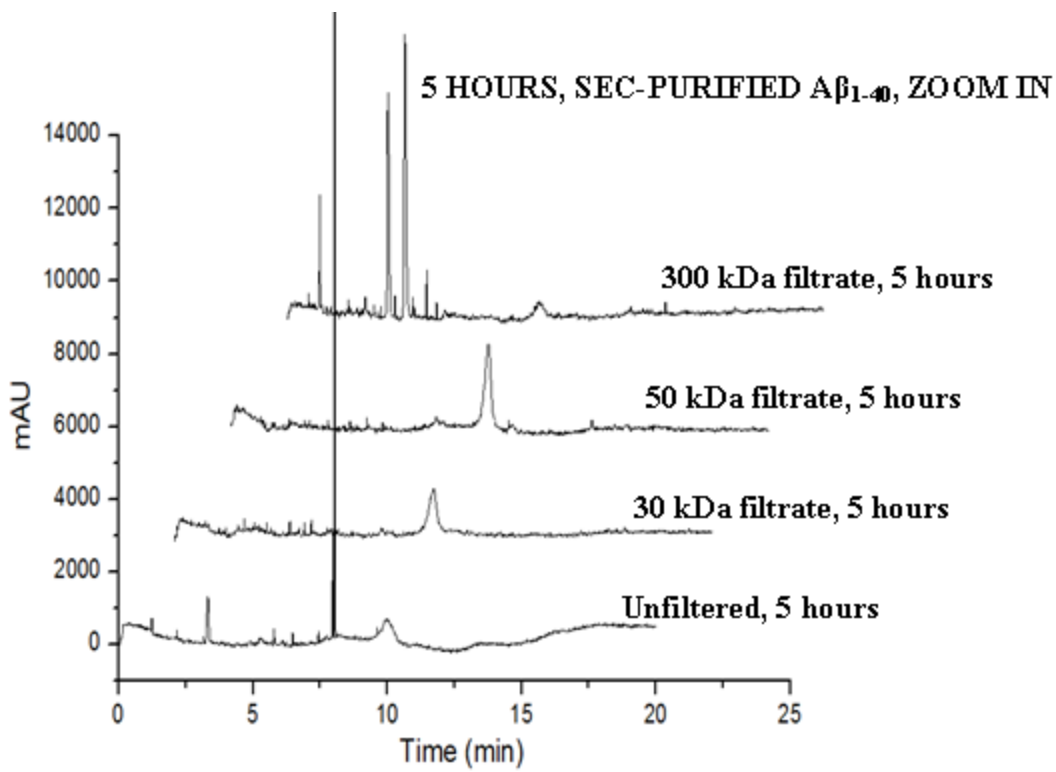
69. May, P.C.; Gitter, B.D.; Waters, D.C.; Simmons, L.K.; Becker, G.W.; Small, J.S.; Robison, P.M. β -Amyloid Peptide in Vitro Toxicity: Lot-to-Lot Variability. *Neurobiol. Aging* 1992, *13*, 605-607.
70. Klein, W.L.; Krafft, G.A.; Finch, C.E. Targeting Small AB Oligomers: The Solution to an Alzheimer's Disease Conundrum. *Trends Neurosci.* 2001, *24*, 219-223.

Appendix

Filtration analyses for A β ₁₋₄₀







CHAPTER 5: MICROCHIP ELECTROPHORESIS FOR DETECTION OF B-SHEET FORMATION BY AB AGGREGATES

1. Introduction

Electrophoresis in flat planar microchips, or microchip electrophoresis (ME), was implemented by Harrison, Manz and Widmer in 1992 [1,2]. This miniaturization allowed electrophoretic processes to be performed in seconds as opposed to minutes with capillary instrumentation. ME possesses other advantages over conventional electrophoretic methods including low sample consumption and a strong potential for automation and integration [3,4]. As a result, the application of ME for the analysis and separation of proteins has advanced enormously in recent years [5].

When considering the translation of protein separations from a capillary format to a microchip format, several parameters must be taken into account. One of the major challenges for the application of ME to peptide and protein analyses is the adsorption of protein onto the silanoate groups present in glass microchannel walls [6,7]. This can lead to peak “tailing” and decrease the analytical efficiency. Therefore, two main strategies have been devised to suppress electroosmotic flow (EOF) in glass capillaries and microchannels; 1) covalent modification of the microchannel surface and 2) dynamic coating of the microchannel surface. Previous studies in our lab have demonstrated the ability of the dynamic coatings poly(ethylene oxide) (PEO) and poly-N-hydroxyethyl acrylamide (PHEA) to effectively suppress EOF and enhance the separation of insulin and A β proteins in capillaries [8,9]. In addition, the microchannel separation length is much shorter than the capillary separation length (8 cm versus 33 cm). Since the peak resolution increases as the square root of the separation length, the analytical selectivity of ME is lower than CE. A polymer matrix can be utilized as a separation medium in the microchannel to

increase the effect of protein hydrodynamic radius on ME separation, thereby leading to enhanced resolution. However, higher polymer concentrations or molecular weights must be utilized with ME compared to CE separations.

Although ME has been applied for analyses of monomeric proteins, less attention has been paid to the use of ME for the detection of A β oligomers and aggregates in the literature. A study by Mohamadi *et al.* used a microchannel coating consisting of poly(dimethylacrylamide-co-allyl glycidyl ether) and with methylcellulose-Tween 20 in the electrophoresis buffer to achieve the separation of five synthetic Fluoroprobe-488 labeled A β peptides (A β ₁₋₃₇, A β ₁₋₃₈, A β ₁₋₃₉, A β ₁₋₄₀, and A β ₁₋₄₂) [6]. The detection of A β species larger than monomer was not achieved. One particularly interesting aspect of A β aggregation is the formation of a β -sheet containing fibrillar structure. Traditionally, the detection of β -sheet aggregates is conducted by monitoring the emission of Thioflavin T (ThT) using a fluorometer. ThT is an intercalating fluorescent dye that binds to the β -sheet structure within amyloid fibrils, giving rise to a shifted excitation maximum at 450 nm and a shifted and enhanced emission at 482 nm [10,11]. A study by Lee *et al.* utilized a microfluidic platform and ThT to detect A β ₁₋₄₂ aggregates [12]. A β ₁₋₄₂ monomers were immobilized on the microchannel surface via N-hydroxysuccinimide ester activation of the internal surfaces. A fresh solution of A β ₁₋₄₂ was continuously fed into the microchannels and A β ₁₋₄₂ aggregation was monitored using ThT fluorescence microscopy, but electrophoresis was not used to separate A β aggregates in this study. In addition to ThT, other β -sheet binding dyes such as BTA-1 exist for the detection of A β aggregates. BTA-1 is an uncharged benzothiazole ThT analogue which has been shown to bind A β aggregates with a higher affinity (11.5 nM – 20 nM [13,14] versus 240 – 890 nM [14-16] for ThT) and is 3000 times more fluorescent than ThT [14]. Studies have indicated the ability of BTA-1 to stain both

plaques and neurofibrillary tangles in post-mortem AD brains, with a preference for plaque staining [16,17]. Furthermore, the ability of BTA-1 to cross the blood-brain barrier makes it an attractive candidate for *in vivo* detection of A β fibrils [13]. Unlike ThT, there is no shift in the excitation and emission maxima of BTA-1 upon binding to β -sheet containing aggregates. Therefore, the aggregates must be separated prior to analysis with a fluorometer, thus highlighting the need for a technique which is capable of both separating and detecting β -sheet containing aggregates.

ME offers the potential to monitor the binding of BTA-1 to A β aggregates. Previous studies in our lab have demonstrated that covalently bound dyes can interfere with the formation of insulin and A β aggregates and thereby misrepresent the “true” native aggregation of the protein [8]. The use of dyes which bind to the β -sheet structure offer a way to monitor the native aggregation of A β . However, the analysis time for the detection of native unlabeled A β aggregates via UV-CE is very long (~4 hours). ME provides a way to overcome these problems by; 1) offering the capability to detect the excitation and emission wavelengths of β -sheet binding dyes and 2) achieving the separation of A β aggregates in a much shorter time (minutes versus hours). Therefore, in these studies, we have explored the utility of ME to detect both monomeric FAM-labeled A β_{1-42} and the binding of BTA-1 to β -sheet containing A β_{1-40} aggregates. The ME results obtained with BTA-1 are compared to results obtained using a fluorometer to detect ThT fluorescence.

2. Materials and Methods

2.1. A β preparation

A β_{1-40} and FAM-A β_{1-42} were stored dessicated at -20°C. 4.33 mg/mL A β_{1-40} and 0.49 mg/mL FAM-A β_{1-42} peptide stocks stock were prepared in hexafluoroisopropanol (HFIP) in order to

ensure the samples were monomeric. These stock solutions were split into vials containing 0.0625 mg $A\beta_{1-40}$ and 0.006775 mg FAM- $A\beta_{1-42}$ and the HFIP was allowed to evaporate overnight. Vials were stored at -80°C . For studies on the detection of FAM- $A\beta_{1-42}$ via LIF-ME, FAM- $A\beta_{1-42}$ was dissolved in 5 mM NaOH and diluted into 40 mM Tris-HCl (pH 8.0) to a final concentration of 0.15 mg/mL.

2.2. Poly-N-hydroxyethyl acrylamide coating and separation matrix synthesis and characterization

One sample of long-chained HEA polymer ($M_w = 12,500,000$ g/mol) was synthesized as described previously [18] with the following changes: 4% w/w initial monomer concentration and polymerization for 5 hours. One sample of short-chained HEA polymer ($M_w = 1,380,000$ g/mol) was synthesized as described previously [19] with the following changes: 3.5 mL isopropanol added to 200 mL of 4% w/w initial monomer solution. Solution deoxygenated by bubbling nitrogen through mixture at 47°C for 2 h followed by polymerization for 4 hours. Once the polymerization was complete, the polymer was dialyzed, lyophilized, and characterized to confirm its molecular weight by multi-angle laser light scattering (Wyatt Technology, Santa Barbara, CA). The HEA polymer with $M_w = 12,500,000$ g/mol was diluted to 0.1% w/v in deionized water and used for the capillary coating and the HEA polymer with $M_w = 1,380,000$ g/mol was diluted to 1% in 40 mM Tris (pH 8.0) for FAM- $A\beta_{1-42}$ studies and 1.5% in 40 mM Tris (pH 8.0) for $A\beta_{1-40}$ oligomer studies with BTA-1 and used as protein separation matrices.

2.3. $A\beta_{1-40}$ aggregation assay with BTA-1 and ThT

To observe the time course for $A\beta_{1-40}$ aggregate formation, $A\beta_{1-40}$ was dissolved in 5 mM NaOH and diluted into 40 mM Tris-HCl (pH 8.0) supplemented with 5 mM NaCl to a final concentration of 0.22 mg/mL (50 μM) and incubated at 25°C under continuous agitation (800

rpm). A 1 mg/mL BTA-1 stock solution was prepared in 100% DMSO and diluted to 0.0064 mg/mL (4160 μ M) in 40 mM Tris-HCl (pH 8.0). Both prior to the onset of aggregation and at times between 8 and 28 hours following the onset of aggregation, an aliquot of A β ₁₋₄₀ was removed and combined with BTA-1 for final A β ₁₋₄₀ and BTA-1 concentrations of 0.021 mg/mL (4.8 μ M) and 0.0058 mg/mL (24.2 μ M), respectively. A final BTA-1 concentration in solution (24.2 μ M) was chosen, which was 5 times the final A β ₁₋₄₀ concentration (4.84 μ M). This sample was analyzed by LIF-ME to determine the elution time and intensity of all peaks.

In parallel experiments, aggregation was monitored using ThT binding as described previously [20,21] with the following changes: dilution of A β ₁₋₄₀ into ThT for final A β ₁₋₄₀ and ThT concentrations of 0.021 mg/mL (4.8 μ M) and 0.0077 mg/mL (24.2 μ M), respectively. Fluorescence was monitored at the onset of aggregation and at times between 5 and 28 hours following the onset of aggregation using a Shimadzu RF-Mini-150 fluorometer (Columbia, MD) (excitation = 460 nm, emission = 480–500 nm).

2.4. Microfluidic chips and polymer matrix loading into microfluidic chips

Glass borosilicate microfluidic chips (Micralyne, Edmonton, Alberta, Canada) with the following properties were used in the experiments: double T injector with an offset of 100 μ m, channel width of 50 μ m, channel depth of 20 μ m, and separation length of 79 mm. Prior to being used for ME runs, the uncoated glass microchips were conditioned and dynamically coated by rinsing them via vacuum with the following: water for 15 min, HCl (aq., 1M) for 15 min, poly-*N*-hydroxyethylacrylamide (coating reagent, aq., 0.1%,) for 15 min, followed by a water rinse. The chip was filled with the separation matrix polymer (1 – 1.5% PHEA) via vacuum prior to each experiment.

2.5. Microchip Electrophoresis

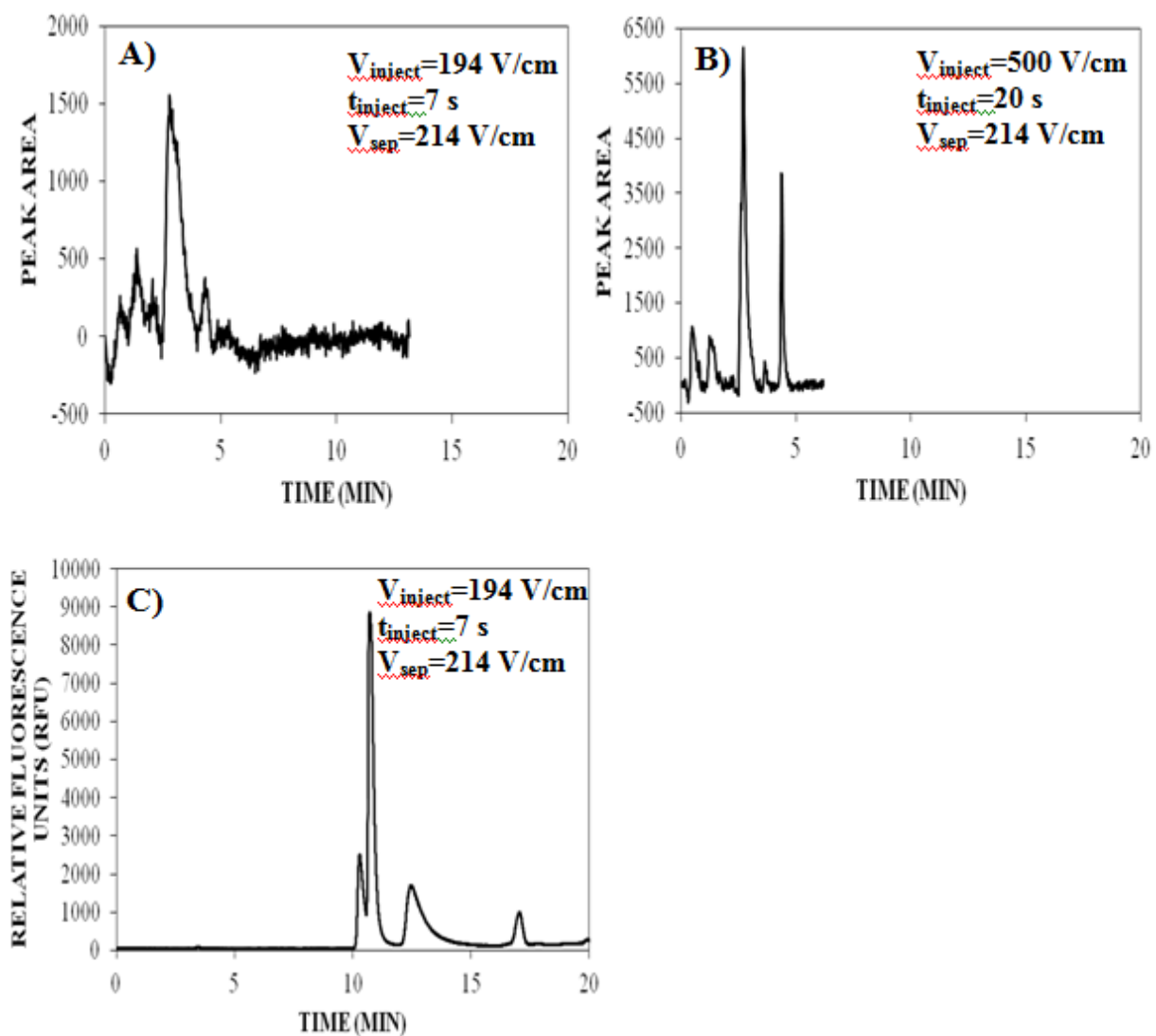
FAM-A β_{1-42} samples were injected at 194-500 V/cm for 20 s and electrophoresed at 214-380 V/cm with 24 V/cm pullback at ambient temperature (17-20 °C). A β_{1-40} samples with BTA-1 were injected at 200-600 V/cm for 10-20 s and electrophoresed at 380 V/cm with 12-24 V/cm pullback at ambient temperature (17-20 °C). The microchip electrophoresis system was custom-built in the laboratory of Dr. Christa Hestekin. The system consisted of a high voltage power supply (LabSmith Inc., Livermore, CA) with the ability to independently control 4 electrodes, a 488 nm argon ion laser (JDS Uniphase, San Jose, CA) and a 355 nm semi-conductor laser (Coherent Inc., Santa Clara, CA), and a high-quantum-efficiency, 1024 x 128 pixel charge-coupled device (CCD) cooled to -50 °C (Andor, South Windsor, CT).

3. Results and Discussion

3.1. Detection of FAM-A β_{1-40} using LIF-ME

The utility of LIF-ME for the detection of FAM-labeled A β_{1-42} was explored. In order to compare the peak pattern obtained using LIF-ME with that obtained previously with LIF-CE, the LIF-CE sample injection voltage and time (194 V/cm for 7 s) as well as separation voltage (214 V/cm) were used. **Figure 1A** shows the LIF-ME peak pattern obtained under these conditions. In order to enhance the signal intensity, the LIF-ME injection voltage and time were increased to 500 V/cm for 20 s (**Figure 1B**). The FAM-labeled A β_{1-42} peak pattern obtained utilizing LIF-ME (**Figure 1B**) is similar to that obtained using LIF-CE (**Figure 1C**). In addition, the run time for LIF-ME is ~3.5 times faster than LIF-CE. In order to further decrease the LIF-ME

Figure 1 Detection of FAM-labeled $A\beta_{1-42}$ using LIF-ME and LIF-CE. FAM-labeled $A\beta_{1-42}$ was prepared at 0.15 mg/mL in 40 mM Tris-HCl (pH 8.0) and analyzed via **A)** LIF-ME with 194 V/cm injection for 7 s with 214 V/cm separation with 24 V/cm pullback, **B)** LIF-ME with 500 V/cm injection for 20 s with 214 V/cm separation and **C)** LIF-CE with 194 V/cm injection for 7 s with 214 V/cm separation. All runs were performed in 0.1% PHEA coated chip or capillary with 1% PHEA separation matrix.



analysis time, the separation voltage was increased to 380 V/cm (**Figure 2**). This led to a separation ~5 times faster compared to LIF-CE.

A previous study by Mohamadi *et al.* utilized LIF-ME to separate five synthetic Fluoroprobe-488 labeled A β peptides (A β ₁₋₃₇, A β ₁₋₃₈, A β ₁₋₃₉, A β ₁₋₄₀, and A β ₁₋₄₂) dissolved in borate buffer (pH 10.5) [6]. The migration time obtained for A β ₁₋₄₂ was ~1.5 min, which is similar to the migration time obtained in our studies for FAM-A β ₁₋₄₂ (**Figure 2**). The separation channel length used in our studies was about twice as long as what was utilized in the Mohamadi *et al.* study (7.9 cm versus 3.5 cm). This suggests that a faster FAM-A β ₁₋₄₂ migration time could be obtained in our studies if a shorter separation channel distance is used. Furthermore, the Mohamadi *et al.* study observed extraneous peaks before and after the peak for A β ₁₋₄₂, which they suggest are due to unbound dye and peptide containing variations in the label number, respectively. Our study demonstrates the ability of the LIF-ME system built in our laboratory to detect FAM-A β ₁₋₄₂ with a similar peak pattern to LIF-CE, but with a greatly reduced analysis time.

3.2. Detection of β -sheet formation by A β ₁₋₄₀ using LIF-ME and comparison to ThT binding

Insoluble A β fibrils containing a β -sheet structure are important for the clinical determination of Alzheimer's Disease [22,23]. Various fluorescent dyes exist which are capable of binding to the β -sheet structure present in A β aggregates such as ThT and BTA-1. BTA-1 is an uncharged benzothiazole ThT analogue which has been shown to bind A β aggregates with a higher affinity than ThT (11.5 nM [13] versus 240 – 890 nM [15,16] for ThT) and is 3000 times more fluorescent than ThT [14]. The structures of ThT and BTA-1 are shown in **Table 1**.

Figure 2 Effect of increased LIF-ME separation voltage on the detection of FAM-labeled $A\beta_{1-42}$. FAM-labeled $A\beta_{1-42}$ was prepared at 0.15 mg/mL in 40 mM Tris-HCl (pH 8.0) and analyzed via LIF-ME with 500 V/cm injection for 20 s and 214 V/cm or 380 V/cm separation with 24 V/cm pullback. All runs were performed in 0.1% PHEA coated chip with 1% PHEA separation matrix.

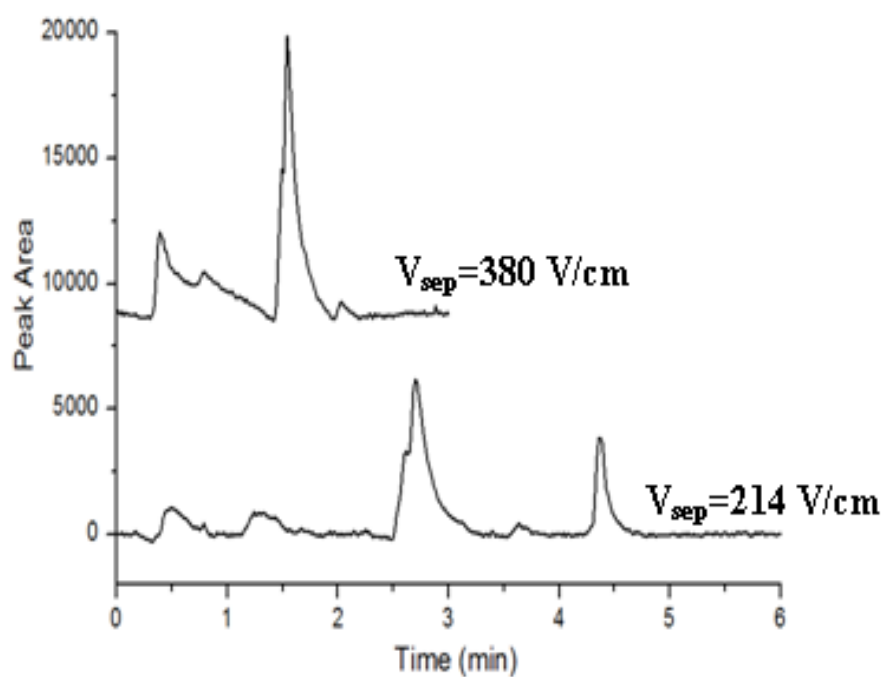
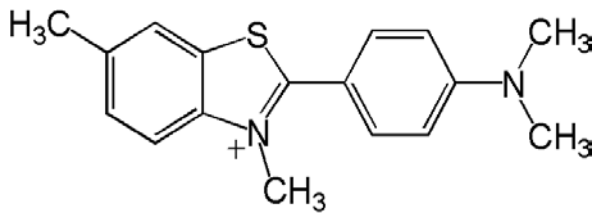
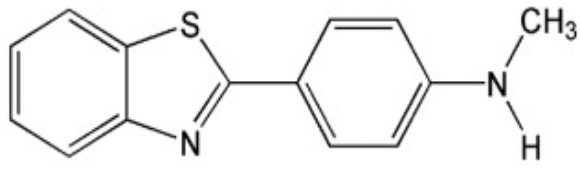


Table 1 Structure and spectral properties of ThT and BTA-1.

Fluorophore	Structure	Excitation/Emission Wavelength
Thioflavin T		Unbound 385/445 [11] Bound 450/482 [11]
BTA-1		360/460 [14]

The purpose of our studies is twofold; 1) investigate the ability of LIF-ME to detect the binding of BTA-1 to A β ₁₋₄₀ aggregates and 2) validate β -sheet formation using a fluorometer to detect ThT binding. In Chapter 3, we have previously demonstrated the detection of A β ₁₋₄₀ oligomers > 300 kDa via UV-CE after ~28 hours of agitation at 800 rpm. To explore the utility of ME for the detection of β -sheet containing A β ₁₋₄₀ aggregates, the same sample preparation utilized in Chapter 3 was used to promote amyloid assembly. The reaction was analyzed using ME at early and late time points to assess the appearance of β -sheet containing A β ₁₋₄₀ aggregates. At 0 hours, no peaks with S/N > 3 were observed using ME (**Figure 3**). After 8 and 24 hours of aggregation, two small peaks were detected with migration times of ~3 and 6 min. A similar peak pattern was obtained after 28 hours with the appearance of two sharper, more intense peaks at ~4.5 min with S/N > 3. Furthermore, the S/N ratio for the peak at ~3 min was > 3.

A study by Levine *et al.* explored the binding of BTA-1 to A β ₁₋₄₀ fibrils using fluorometry [14]. Since there is no change in BTA-1 fluorescence upon binding to A β ₁₋₄₀ fibrils [14], centrifugation was necessary in order to determine the amount of bound BTA-1 in the resuspended fibril pellet. This pre-separation step is unnecessary for ME analyses due to the ability of ME to separate and detect aggregates in one step.

In order to validate the results obtained via ME to a more traditional method of detecting amyloid aggregates containing a β -sheet structure, ThT with analysis via fluorometry was used to follow A β aggregation. A β ₁₋₄₀ aggregate detection using ThT with fluorometry was conducted simultaneously on the same sample as the studies utilizing BTA-1 with ME. A β ₁₋₄₀ was aggregated at pH 8.0 (40 mM Tris) and 25 °C with agitation (800 rpm) in the presence of 5 mM

NaCl. The general trend for the growth of aggregates analyzed via ThT fluorescence (**Figure 4**) was similar to that observed using ME, thus validating the formation of β -sheet aggregates.

Figure 3 Detection of BTA-1 binding to A β_{1-40} using LIF-ME. A β_{1-40} was aggregated under agitation (800 rpm) at 0.22 mg/mL in 40 mM Tris (pH 8.0) containing 5 mM NaCl and at 25 °C. At 0 – 28 hours, A β_{1-40} was diluted into BTA-1 for final A β_{1-40} and BTA-1 concentrations of 0.021 mg/mL (4.8 μ M) and 0.0058 mg/mL (24.2 μ M), respectively. Fluorescence was monitored via ME with LIF detection with a 200-600 V/cm injection for 10-20 s with a 380 V/cm separation with 12-24 V/cm pullback. All runs were performed in 0.1% PHEA coated chip with 1.5% PHEA separation matrix.

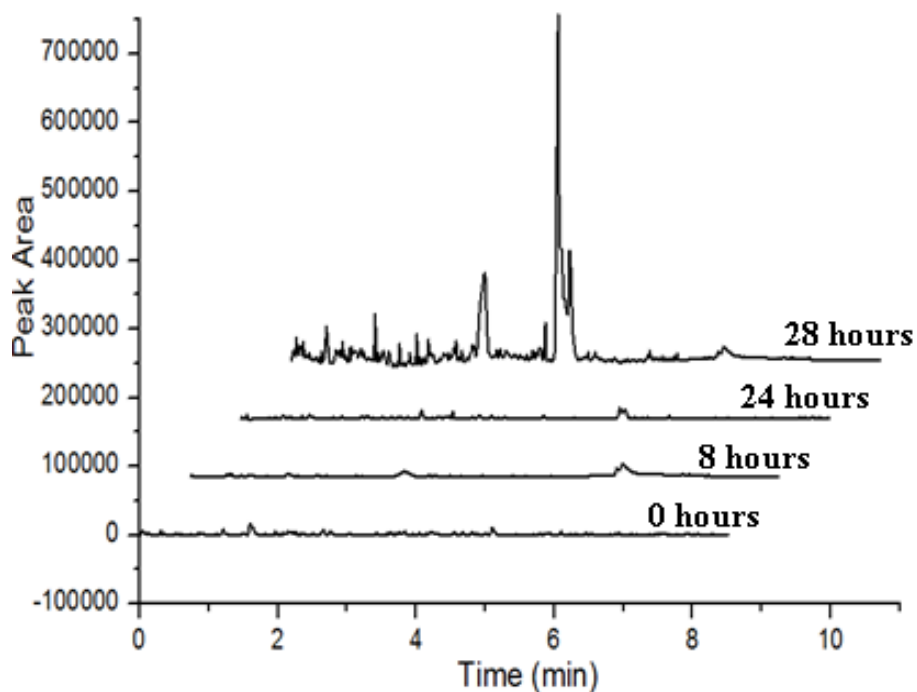
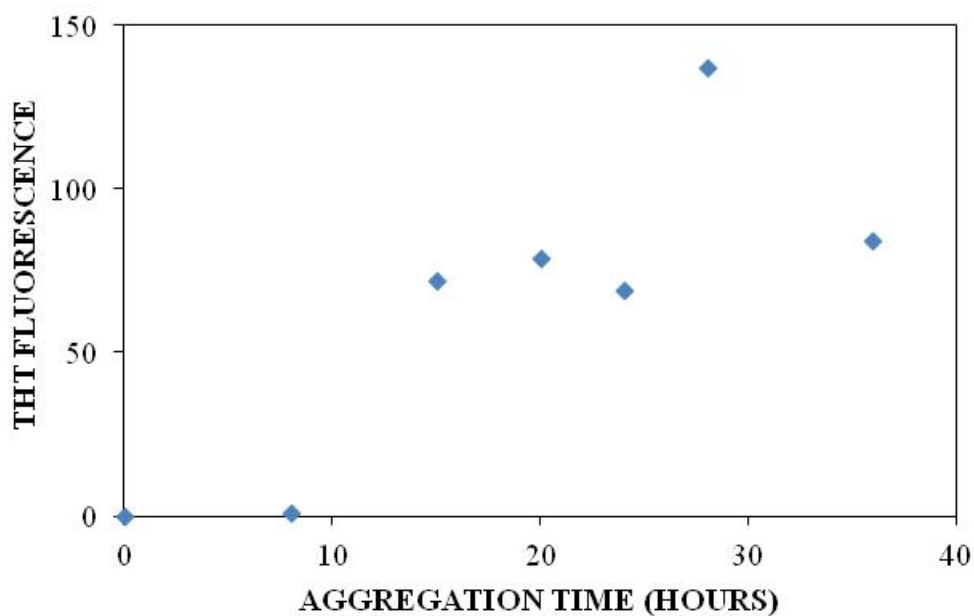


Figure 4 Detection of ThT binding to $A\beta_{1-40}$ using fluorometry. $A\beta_{1-40}$ was aggregated under agitation (800 rpm) at 0.22 mg/mL in 40 mM Tris (pH 8.0) containing 5 mM NaCl and at 25 °C. At 0 – 36 hours, $A\beta_{1-40}$ was diluted into ThT for final $A\beta_{1-40}$ and ThT concentrations of 0.021 mg/mL (4.8 μ M) and 0.0077 mg/mL (24.2 μ M), respectively. Fluorescence was monitored via fluorometry (excitation = 460 nm, emission = 480–500 nm).



4. Conclusions

In these studies, we have demonstrated the capability of ME to detect both monomeric FAM-A β_{1-42} and A β_{1-40} aggregates. The detection of FAM-A β_{1-42} was achieved in ~1.5 minutes, which is ~5 times faster than analyses via LIF-CE. Furthermore, ME was utilized to detect β -sheet formation using the conformationally specific dye BTA-1. A fluorometer was also employed in order to validate β -sheet formation using ThT binding. We found that similar trends were observed for BTA-1 binding detection via ME compared to ThT binding detection via fluorometry. Although BTA-1 is an attractive alternative to ThT for the detection of A β_{1-40} aggregates, A β_{1-40} aggregates must be separated in order for the use of BTA-1 to be effective and this separation is typically achieved via centrifugation for ~15 min. We have demonstrated the utility of ME to both separate and detect A β_{1-40} aggregates using BTA-1 in < 7 min, which is 2 – 3 times faster than traditional measures of BTA-1 fluorescence (ie. centrifugation with fluorometry). Further studies must be conducted which optimize the BTA-1 and A β_{1-40} concentrations for analysis via ME. In particular, a saturation binding curve must be generated for BTA-1 by varying the BTA-1 concentration with a constant concentration of A β_{1-40} and analyzing the peak pattern obtained via ME. This will give the maximum BTA-1 fluorescence which can be obtained at a given A β_{1-40} concentration. In order to explore the utility of ME to detect physiologically relevant concentrations of β -sheet aggregates formed by A β_{1-40} , the saturation binding curve will be repeated for different A β_{1-40} concentrations down to physiologically relevant concentrations (ie. varying the BTA-1 concentration with 5 μ M A β_{1-40} , varying the BTA-1 concentration with 0.5 μ M A β_{1-40} , etc). This will give the optimal BTA-1 concentration necessary for a range of A β_{1-40} concentrations and further indicate whether ME is capable of detecting physiologically relevant concentrations. In addition, the ME injection

voltage and time as well as the separation polymer concentration and chip separation length must be optimized in order to achieve the best detection of A β ₁₋₄₀.

References

1. Harrison, D.; Manz, A.; Fan, Z.; Ludi, H.; Widmer, H. Capillary Electrophoresis and Sample Injection Systems Integrated on a Planar Glass Chip. *Anal. Chem.* **1992**, *64*, 1926-1932.
2. Harrison, D.J.; Fluri, K.; Seiler, K.; Fan, Z.; Effenhauser, C.S.; Manz, A. Micromachining a Miniaturized Capillary Electrophoresis-Based Chemical Analysis System on a Chip. *Science (Washington, D. C. , 1883-)* **1993**, *261*, 895-897.
3. Jakeway, S.C.; de Mello, A.J.; Russell, E.L.; Fresenius, J. Miniaturized Total Analysis Systems for Biological Analysis. *Anal. Chem.* **2000**, *366*, 525-539.
4. Chovan, T.; Guttman, A. Microfabricated Devices in Biotechnology and Biochemical Processing. *Trends Biotechnol.* **2002**, *20*, 116-122.
5. Tran, N.T.; Ayed, I.; Pallandre, A.; Taverna, M. Recent Innovations in Protein Separation on Microchips by Electrophoretic Methods: An Update. *Electrophoresis* **2010**, *31*, 147-173.
6. Mohamadi, M.R.; Svobodova, Z.; Verpillot, R.; Esselmann, H.; Wiltfang, J.; Otto, M.; Taverna, M.; Bilkova, Z.; Viovy, J. Microchip Electrophoresis Profiling of A β Peptides in the Cerebrospinal Fluid of Patients with Alzheimer's Disease. *Anal. Chem.* **2010**, *82*, 7611-7617.
7. Zhao, Z.; Malik, A. Solute Adsorption on Polymer-Coated Fused-Silica Capillary Electrophoresis Columns using Selected Protein and Peptide Standards. *Anal. Chem.* **1993**, *65*, 2747-2752.
8. Pryor, E.; Kotarek, J.A.; Moss, M.A.; Hestekin, C.N. Monitoring Insulin Oligomer Formation Via Capillary Electrophoresis. *Int. J. Mol. Sci.* **2011**, *12*, 9369-9388.
9. Pryor, E.; Moss, M.A.; Hestekin, C.N. Use of Capillary Electrophoresis to Monitor A β Aggregation: Effect of Sample Preparation. *Anal. Biochem.* **in preparation**.
10. Nielsen, L.; Khurana, R.; Fink, A. Effect of Environmental Factors on the Kinetics of Insulin Fibril Formation: Elucidation of the Molecular Mechanism. *Biochemistry* **2001**, *40*, 627-632.
11. LeVine, H. Thioflavine T Interaction with Synthetic Alzheimer's Disease β -Amyloid Peptides: Detection of Amyloid Aggregation in Solution. *Protein Sci.* **1993**, *2*, 404-410.

12. Lee, J.; Ryu, J.; Park, C.B. High-Throughput Analysis of Alzheimer's β -Amyloid Aggregation using a Microfluidic Self-Assembly of Monomers. *Anal. Chem.* **2009**, *81*, 2751-2759.
13. Wang, Y.; Mathis, C. Effects of Lipophilicity on the Affinity and Nonspecific Binding of Iodinated Benzothiazole Derivatives. *Journal of Molecular Neuroscience* **2003**, *20*, 255-260.
14. LeVine, H.,3rd. Multiple Ligand Binding Sites on A β (1-40) Fibrils. *Amyloid* **2005**, *12*, 5-14.
15. Yona, R.; Mazeret, S. Thioflavin Derivatives as Markers for Amyloid- β Fibrils: Insights into Structural Features Important for High-Affinity Binding. *Chem Med Chem* **2008**, *3*, 63-66.
16. Klunk, W.; Wang, Y. Uncharged Thioflavin-T Derivatives Bind to Amyloid-Beta Protein with High Affinity and Readily Enter the Brain. *Life Sci.* **2001**, *69*, 1471-1484.
17. Mathis, C.A.; Bacskai, B.J.; Kajdasz, S.T.; McLellan, M.E.; Frosch, M.P.; Hyman, B.T.; Holt, D.P.; Wang, Y.; Huang, G.; Debnath, M.L. *et al.* A Lipophilic Thioflavin-T Derivative for Positron Emission Tomography (PET) Imaging of Amyloid in Brain. *Bioorg. Med. Chem. Lett.* **2002**, *12*, 295-298.
18. Albarghouthi, M.; Stein, T.; Barron, A. Poly-N-Hydroxyethylacrylamide as a Novel, Adsorbed Coating for Protein Separation by Capillary Electrophoresis. *Electrophoresis* **2003**, *24*, 1166-1175.
19. Hert, D.G.; Fredlake, C.P.; Barron, A.E. DNA Sequencing by Microchip Electrophoresis using Mixtures of High-and Low-Molar Mass Poly(N,N-Dimethylacrylamide) Matrices. *Electrophoresis* **2008**, *29*, 4663-4668.
20. Gonzalez-Velasquez, F.J.; Kotarek, J.A.; Moss, M.A. Soluble Aggregates of the Amyloid- β Protein Selectively Stimulate Permeability in Human Brain Microvascular Endothelial Monolayers. *J. Neurochem.* **2008**, *107*, 466-477.
21. Gonzalez-Velasquez, F.J.; Moss, M.A. Soluble Aggregates of the Amyloid- β Protein Activate Endothelial Monolayers for Adhesion and Subsequent Transmigration of Monocyte Cells. *J. Neurochem.* **2008**, *104*, 500-513.
22. Montine, T.J.; Phelps, C.H.; Beach, T.G.; Bigio, E.H.; Cairns, N.J.; Dickson, D.W.; Duyckaerts, C.; Frosch, M.P.; Masliah, E.; Mirra, S.S. *et al.* National Institute on Aging-Alzheimer's Association Guidelines for the Neuropathologic Assessment of Alzheimer's Disease: A Practical Approach. *Acta Neuropathol.* **2012**, *123*, 1-11.

23. Robinson, J.L.; Geser, F.; Corrada, M.M.; Berlau, D.J.; Arnold, S.E.; Lee, V.M.; Kawas, C.H.; Trojanowski, J.Q. Neocortical and Hippocampal Amyloid- β and Tau Measures Associate with Dementia in the Oldest-Old. *Brain* **2011**, *134*, 3708-3715.

CHAPTER 6: CONCLUSIONS AND FUTURE DIRECTIONS

1. Impact of the presented work

The detection of oligomers and aggregates formed by two amyloid proteins, insulin and A β , is of particular importance due to the role which these species play in Diabetes and Alzheimer's disease, respectively. However, existing techniques are limited in the ability to detect insulin and A β oligomers due to the fact that these early aggregates are transient, present at low concentrations, and difficult to isolate. Improvements must be made to existing techniques or alternative techniques must be explored in order to identify and quantify the size of these oligomeric and aggregate species without disrupting their structure and develop treatments that target these pivotal aggregation events.

In Chapters 1 and 2, the advantages and disadvantages of traditional methods for the detection of insulin and A β oligomers and aggregates were outlined. We also introduced the potential of microchannel electrophoresis (CE and ME) as a complimentary technique for the existing analyses. This thesis focuses on addressing previously unexplored areas for the development of CE and ME as early amyloid aggregation detection techniques.

In Chapter 3, we reported the first studies on the use of UV-CE with a polymer separation matrix to detect native insulin aggregates ranging in size from 30 – 100 kDa. In particular, we looked at the ability of UV-CE to detect insulin aggregates formed using a relatively low sample concentration (0.2 mg/mL), near neutral pH (8.0), and physiological salt concentration (150 mM). Thioflavin T binding was utilized to compare the lag times observed with UV-CE and and it was found that UV-CE displayed a lag time ~3 times faster than ThT binding. This suggests that UV-CE is detecting oligomers which are present prior to β -sheet aggregates. In addition, the effect of salt on the formation of insulin aggregates was determined

and it was found that the time to insulin oligomer appearance was unaffected by salt concentrations ranging from 100 – 250 mM. In order to draw conclusions on the ability of CE to detect physiologically relevant insulin and A β concentrations, the detection limit for UV-CE was compared to LIF-CE and it is shown that LIF-CE can detect physiologically relevant FITC-insulin concentrations. Furthermore, the detection sensitivity of LIF-CE was ~35,000 fold higher than UV-CE for the detection of FITC-insulin. In addition, we explored the potential for LIF-CE to monitor the formation of oligomers and aggregates of FITC-labeled insulin. It is shown that FITC-labeled insulin is unable to incorporate into unlabeled insulin oligomers. This demonstrates that LIF-CE is a promising technique for the detection of low concentrations of monomeric FITC-insulin but caution must be taken when choosing a fluorescent dye for the detection of FITC-insulin oligomers and aggregates.

In Chapter 4, we demonstrated ability of UV-CE with a polymer separation matrix to detect native small oligomeric A β ₁₋₄₀ species (10 – 30 kDa) and larger oligomeric species (100–300 kDa and > 300 kDa). Specifically, we looked at the ability of UV-CE to detect A β ₁₋₄₀ aggregates formed using a relatively low sample concentration (0.2 mg/mL), near neutral pH (8.0), and low salt concentration (5 mM). In addition, the effect of sample preparation on the formation of A β aggregates was determined. Dot blots were utilized to verify the presence of A β oligomeric and fibril species detected via UV-CE and compare lag times. It was found that the lag times for oligomers and aggregates obtained using UV-CE were nearly identical to those obtained via dot blotting. Furthermore, we found that the lag time to oligomer formation for SEC-isolated A β ₁₋₄₀ samples was ~23 hours shorter compared to non-purified A β ₁₋₄₀ samples. This indicates that the initial sample sizes present have a drastic effect on the lag time to oligomer formation. In order to draw conclusions on the ability of CE to detect physiologically

relevant A β concentrations, the detection limit for UV-CE was compared to LIF-CE and it was shown that LIF-CE can detect physiologically relevant FAM-A β_{1-40} and FAM-A β_{1-42} concentrations. Furthermore, the detection sensitivity of LIF-CE was 250,000 – 5,000,000 fold higher than UV-CE for the detection of FAM-A β . This demonstrates that LIF-CE is a promising technique for the detection of low concentrations of monomeric FAM-A β . We also explored the potential for LIF-CE to monitor the formation of oligomers and aggregates of FAM-A β_{1-42} and found that FAM-labeled A β_{1-42} is capable of incorporating into unlabeled A β_{1-42} oligomers but not aggregates. Furthermore, the ability to detect FAM- A β_{1-42} is highly dependent on the protein lot utilized. These results demonstrate that while LIF-CE is a promising technique for the detection of physiologically relevant FAM-A β concentrations, caution must be taken when choosing a dye for detection of oligomeric and aggregate species. In particular, dye properties including size, effect of dye on the net protein charge, or dye attachment site may interfere with the native aggregation of insulin and A β and thereby misrepresent the species detected via LIF-CE.

Since the studies in Chapters 3 and 4 demonstrated that covalently bound dyes can interfere with the formation of insulin and A β aggregates and thereby misrepresent the “true” native aggregation of the protein [1], we investigated the use of dyes which bind to the β -sheet structure and offer a way to monitor the native aggregation of A β in Chapter 5. Due to the fact that the UV- and LIF-CE instruments in our lab are not capable of detecting the excitation and emission wavelengths associated with β -sheet binding amyloid dyes (ie. BTA-1), we explored the utility of ME to detect β -sheet formation. In particular, we determined that ME could detect monomeric FAM-labeled A β_{1-42} in ~1.5 min and the binding of BTA-1 to β -sheet containing A β_{1-40} aggregates in < 7 min. Furthermore, the ME results obtained with BTA-1 were compared

to results obtained using a fluorometer to detect ThT fluorescence. We found that BTA-1 was capable of detecting low levels of A β ₁₋₄₀ aggregates ~7 hours earlier compared to ThT binding. Further studies must be conducted which optimize the BTA-1 and A β ₁₋₄₀ concentrations for analysis via ME.

In this work, we have demonstrated that UV-CE is capable of detecting insulin and A β oligomers in a native state. The drawbacks of current techniques include the requirement of conditions that induce non-native behavior (SDS-PAGE) or destabilize oligomers (SEC), limited resolution of individual sizes of oligomers and aggregates (Native-PAGE, DLS, FCS, and TEM), limited ability to detect a wide range of populations (oligomers - fibrils) within a sample (MALS), inability to provide size information about oligomers or fibrils (dot blotting, ELISA), and reliance on assumptions in the model to predict size (centrifugation, FCS). The main advantages of UV-CE over alternative techniques are the ability to detect the native formation of oligomers and aggregates and the ability to detect a wide range of sizes (oligomers - fibrils) within a sample. The advantages of LIF-CE and ME compared to UV-CE are the capability to detect physiologically relevant concentrations and enhanced resolution. Further improvements must be made in order to model and determine limitations on the ability of CE and ME to resolve different species. A major disadvantage of LIF-CE is the interference of fluorescent dyes necessary for detection with native protein aggregation. Compared to fluorometry, ME is capable of monitoring the binding of conformationally dependent dyes which do not exhibit a shift in fluorescence upon binding without the use of another separation method. Further improvements to LIF-CE and ME must be made in order to overcome the disadvantages associated with these techniques. These include the exploration of alternative dyes which do not interfere with aggregation (LIF-CE) and the optimization of dye and protein concentrations (ME) to determine

whether physiologically relevant concentrations of β -sheet aggregates can be detected via ME. The specifics for these improvements are given in the next section.

2. Future directions

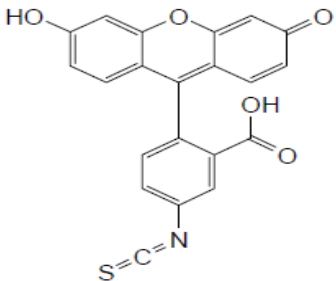
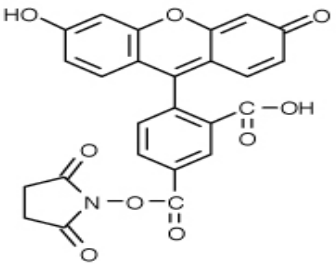
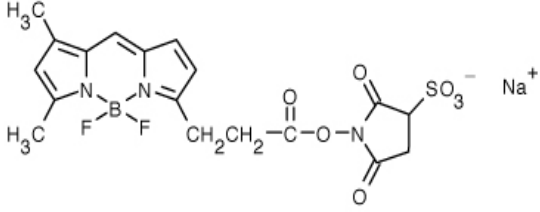
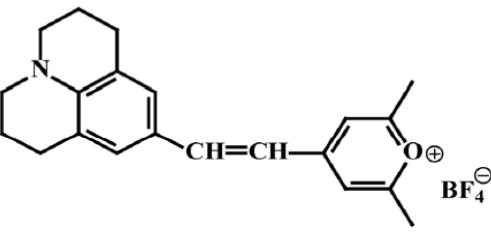
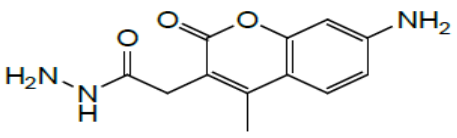
2.1. Testing of alternative dyes with LIF-CE

The use of a fluorescent dye which is covalently bound to amyloid proteins is necessary in order to achieve detection via LIF-CE of smaller oligomeric species formed prior to species containing a β -sheet structure. In Chapter 3, we demonstrated the ability to detect physiologically relevant concentrations of monomeric FITC-insulin and FAM-A β using LIF-CE. In order to determine whether physiologically relevant concentrations of oligomeric insulin and A β could be detected via LIF-CE, we explored the ability of FITC-insulin and FAM-A β to incorporate into oligomers formed by unlabeled insulin and A β in Chapter 4. We found that FITC-labeled insulin was unable to incorporate into oligomers formed by the unlabeled protein while FAM-labeled A β_{1-42} was capable of incorporating into oligomers formed by unlabeled A β_{1-42} but not aggregate species. However, the ability of FAM-labeled A β_{1-42} to incorporate into oligomers formed by unlabeled A β_{1-42} was highly dependent on the lot employed. These findings necessitate the exploration of alternative covalently bound fluorescent dyes. Since some small compounds have been previously reported as inhibitors of β -sheet formation, it is possible that the FITC and FAM labels are acting as inhibitors to aggregation. Another possibility is that the FITC and FAM attachment sites are critical for proper β -sheet folding. A similar extension of the lag time to aggregation has been observed following the methylation of amino groups within the A β protein [2] and the introduction of a mutant that mimics phosphorylation of serine residues within the Huntington protein [3]. In addition, the quantity of amyloid aggregates formed is reduced following the citraconylation of lysine residues within lysozyme [4] or stilbine modification of ϵ -

amino groups within transthyretin [5]. Therefore, dyes with alternative properties or attachment sites may need to be explored. In particular, dyes with a wider linker region, such as BODIPY, dyes which do not alter the net protein charge, or attachment of dyes exclusively at the *N*- or *C*-terminus would be less likely to impact aggregate formation. **Table 1** gives the structures for FITC and FAM as well as three alternative dyes which we are interested in exploring. Since FITC and FAM are bulky dyes, alter the net protein charge upon attachment, and are attached to the *N*-terminus and Lysine residues, we have chosen the alternative dyes BODIPY, CE503, and AMCA-Hydrazide in order to explore the three properties given above, respectively.

Preliminary studies in our lab have indicated the potential for BODIPY to be used to monitor the formation of oligomers and larger aggregates formed by unlabeled A β_{1-40} . Since we already had data for the behavior of 100% unlabeled A β_{1-40} (Chapter 3), we used this data as a control to determine the effect of the wider linker region of BODIPY on the aggregation of unlabeled A β_{1-40} . Therefore, we used identical A β_{1-40} sample and aggregation conditions to determine whether BODIPY-A β_{1-40} interfered with the formation of oligomers and aggregates. A β_{1-40} was labeled with BODIPY according to the manufacturers' protocol. Separate stock solutions of unlabeled A β_{1-40} and BODIPY-labeled A β_{1-40} were prepared in 5 mM NaOH and diluted into 40 mM Tris (pH 8.0) containing 5 mM NaCl. These solutions were combined to yield a sample consisting of 80% unlabeled A β_{1-40} and 20% BODIPY-A β_{1-40} with a total A β_{1-40} concentration of 0.22 mg/mL (50 μ M) and incubated at 25°C under continuous agitation (800 rpm). Both prior to the onset of aggregation and at times between 5 and 72 hours following the onset of aggregation, a 20 μ L sample was removed and analyzed by LIF-CE to determine the elution time and intensity of all peaks. **Figure 1** shows the peak pattern obtained at all time

Table 1 Structure and spectral properties of FITC, FAM, BODIPY, CE503, and AMCA-Hydrazide

Fluorophore	Structure	Excitation/Emission Wavelength
Fluorescein, isothiocyanate (FITC)		494/518 [6]
Fluorescein, succinimidyl ester (FAM)		492/518 [7]
BODIPY, sulfosuccinimidyl ester		504/513 [8]
CE503		Unconjugated 612/665 [9] Conjugated 503/600 [9]
AMCA-Hydrazide		350/450 [10]

points where **Panel A** shows all peaks and **Panel B** is zoomed in on the early peaks with migration times < 40 min. At 0 hours, a sharp peak at ~20 min (**Peak 3, Figure 1A and B**) was observed in addition to several smaller intensity peaks with migration times ranging from 10 – 40 min (**Peaks 1, 2, and 4 – 8, Figure 1A and B**). A possible explanation for the observance of several smaller intensity peaks is that these peaks are due to variations in the BODIPY label number since BODIPY labels the *N*-terminus and Lysine residues, thus creating 7 different possible variations of label number per A β ₁₋₄₀ peptide. A similar peak pattern was observed after 5 and 10 hours with an initial increase in the intensity of peaks 1 – 8 followed by a decrease after 10 hours. After 24 hours, two new peaks with an S/N > 3 were observed; a sharp peak with a faster migration time at ~8 min (**Peak 9, Figure 1A and B**) and a small peak with a longer migration time at ~53 min (**Peak 10, Figure 1A**). Furthermore, the intensity of peaks 1 - 8 was drastically reduced. The same peak pattern as was obtained after 24 hours was obtained after 28 – 72 hours with an increase in intensity of peak 9 at ~8 min and peak 10 at ~53 min. In addition, dot blots showed a positive A11 (oligomer) stain at 28 hours (data not shown).

In order to better understand the growth process, the area for peaks 1 – 8 with migration times ranging from 10 – 40 min was compared to the area for peak 9 with a migration time of ~8 min which appeared after 24 hours of aggregation. As shown in **Figure 2**, the area for peaks 1 – 8 initially increases and then starts to decrease after 10 hours (blue diamonds). This initial increase in peak area is similar to the results obtained in Chapter 3 using UV-CE to detect oligomers formed by 0.22 mg/mL unlabeled A β ₁₋₄₀. After 24 hours, the area for peaks 1 - 8 decreases further (blue diamonds) while peak 9 with a faster migration time of ~8 min appears (red squares). The sharp peak observed at 24 hours using LIF-CE is similar to the sharp peak

Figure 1 Coaggregation of BODIPY-labeled $A\beta_{1-40}$ and unlabeled $A\beta_{1-40}$ with analysis via LIF-CE. $A\beta_{1-40}$ solutions consisting of 20% BODIPY-labeled $A\beta_{1-40}$ and 80% unlabeled $A\beta_{1-40}$ were prepared at a concentration of 0.22 mg/mL in 40 mM Tris (pH 8.0) containing 5 mM NaCl and aggregated under agitation (800 rpm, 25°C). At 0 – 72 hours, CE was performed in conjunction with LIF detection ($n = 1 - 2$) with a 7 kV injection for 7 s with separation at 7 kV using 1.5% PHEA separation matrix in a PHEA coated capillary. Panel **A** shows all peaks while panel **B** is zoomed in on the early peaks.

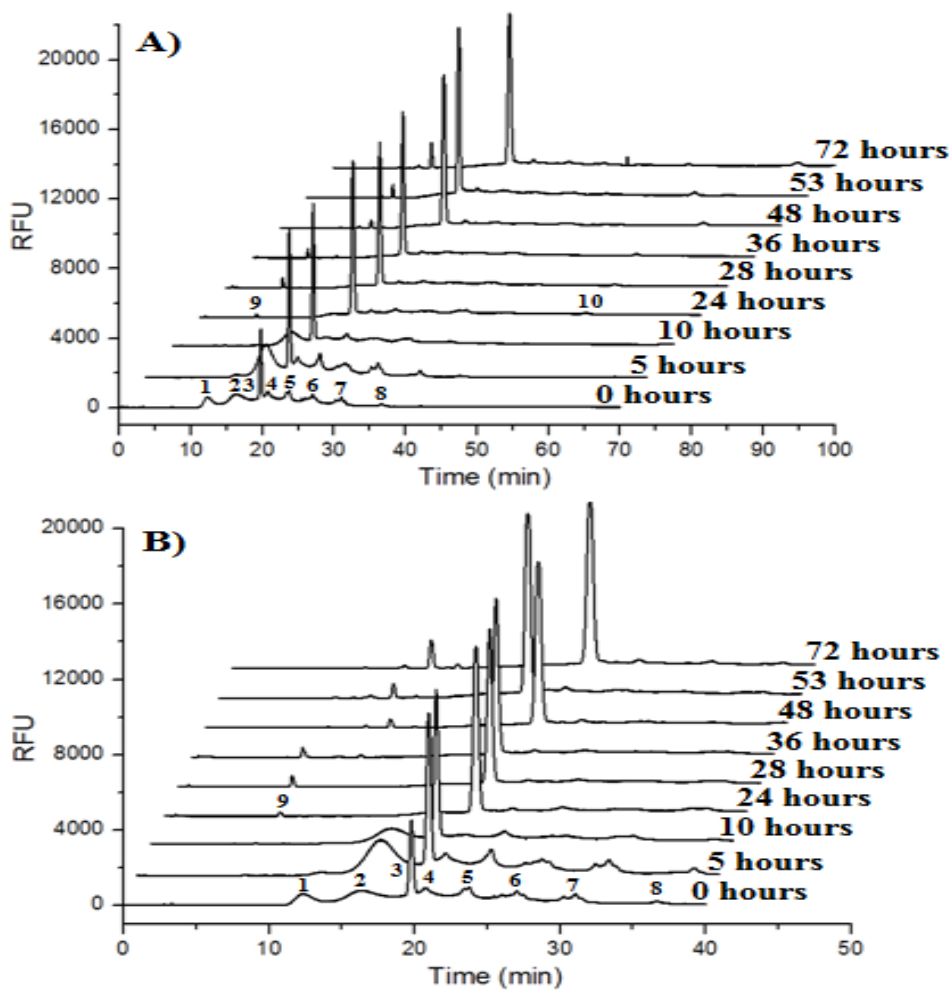
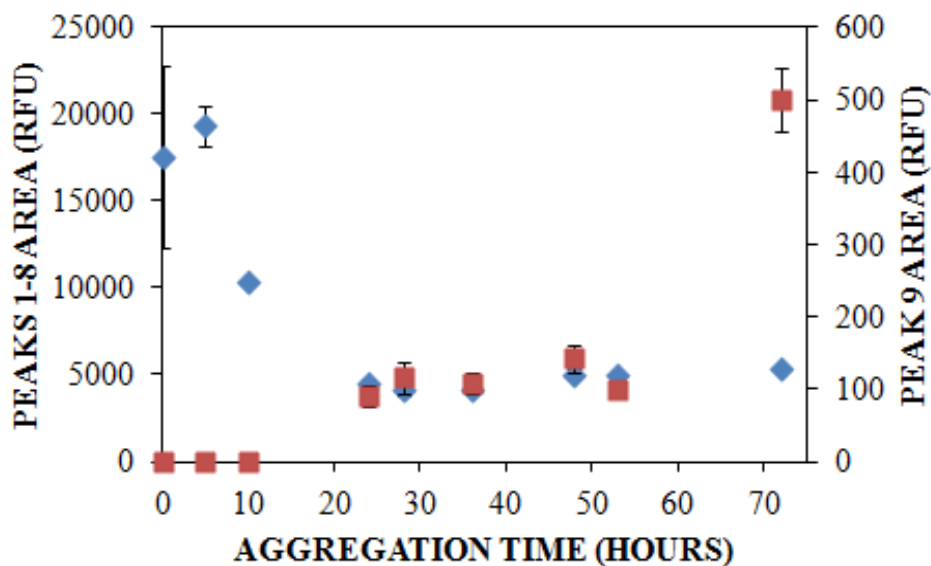


Figure 2 Effect of aggregation time on the area for peaks 1 - 8 (\blacklozenge , $n = 1 - 2$) and peak 9 (\blacksquare , $n = 1 - 2$) obtained for BODIPY- $A\beta_{1-40}$. $A\beta_{1-40}$ was aggregated under agitation (800 rpm) at 0.22 mg/mL in 40 mM Tris (pH 8.0) containing 5 mM NaCl and at 25 °C. At 0 – 72 hours, CE was performed in conjunction with LIF detection with a 7 kV injection for 7 s with separation at 7 kV using 1.5% PHEA separation matrix in a PHEA coated capillary.



observed after 28 hours using UV-CE to detect oligomers formed by 0.22 mg/mL unlabeled $A\beta_{1-40}$ in Chapter 3. Furthermore, the overall trend for the changes in peak areas are similar for aggregates formed by 100% unlabeled $A\beta_{1-40}$ with analysis via UV-CE (**Figure 3A**) and aggregates formed by a mixture of 80% unlabeled $A\beta_{1-40}$ and 20% BODIPY- $A\beta_{1-40}$ with analysis via LIF-CE (**Figure 3B**). Since a similar peak pattern is obtained for UV-CE and LIF-CE after 28 hours, this suggests that BODIPY- $A\beta_{1-40}$ has the potential to be used to detect oligomers formed by unlabeled $A\beta_{1-40}$. In addition, since 20% of BODIPY- $A\beta_{1-40}$ is mixed with unlabeled $A\beta_{1-40}$, only 20% of oligomers formed will be labeled with BODIPY- $A\beta_{1-40}$ and detected via LIF-CE. **Figure 4** shows the UV-CE data obtained for 100% unlabeled $A\beta_{1-40}$ multiplied by 20% and the LIF-CE data obtained for a mixture of 80% unlabeled $A\beta_{1-40}$ and 20% BODIPY- $A\beta_{1-40}$. Overall, the peak areas obtained after 0, 5, 10, 24, 36, and 48 hours are similar while the peak areas obtained after 28 hours are somewhat different. This further demonstrates that BODIPY- $A\beta_{1-40}$ has the potential to be used to detect oligomers formed by unlabeled $A\beta_{1-40}$.

The appearance of a peak with a faster migration time was obtained using both BODIPY and FAM (Chapter 4) for the analysis of $A\beta_{1-40}$ and $A\beta_{1-42}$, respectively. In contrast, BODIPY was able to detect the appearance of peaks with migration times > 40 min. This indicates that dye size may play a role in the ability of LIF-CE to detect $A\beta_{1-40}$ oligomers and aggregates. In addition, we have successfully labeled $A\beta_{1-40}$ with CE503 and AMCA-Hydrazide in our lab. CE503 is a dye which does not alter the net protein charge upon attachment while AMCA-Hydrazide is attached exclusively to the C-terminus. Future studies will be conducted to explore the effects of net protein charge (CE503) and attachment site (AMCA-Hydrazide) on the ability of LIF-CE to

Figure 3 Effect of aggregation time on the peak areas obtained for **A)** 10 – 30 kDa (\blacklozenge , $n = 3$) and > 300 kDa (\blacksquare , $n = 3$) $A\beta_{1-40}$ species analyzed via UV-CE and **B)** peak 1 - 8 (\blacklozenge , $n = 1 - 2$) and peak 9 (\blacksquare , $n = 1 - 2$) BODIPY- $A\beta_{1-40}$ species analyzed via LIF-CE. Samples containing 100% $A\beta_{1-40}$ and samples containing 20% BODIPY-labeled $A\beta_{1-40}$ and 80% unlabeled $A\beta_{1-40}$ were aggregated under agitation (800 rpm) at 0.22 mg/mL in 40 mM Tris (pH 8.0) containing 5 mM NaCl and at 25 °C. At 0 – 48 hours, CE was performed in conjunction with **A)** UV detection with a 0.5 psi pressure injection for 8 s with separation at 7 kV using 0.5% PEO separation matrix in a PEO coated capillary or **B)** LIF detection with a 7 kV injection for 7 s with separation at 7 kV using 1.5% PHEA separation matrix in PHEA coated capillary.

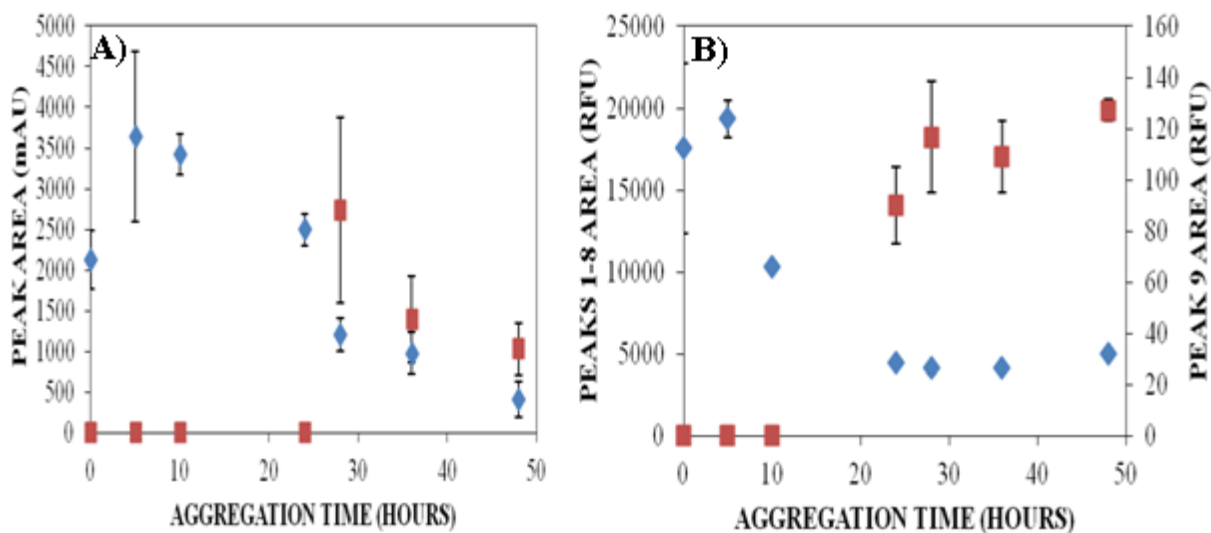
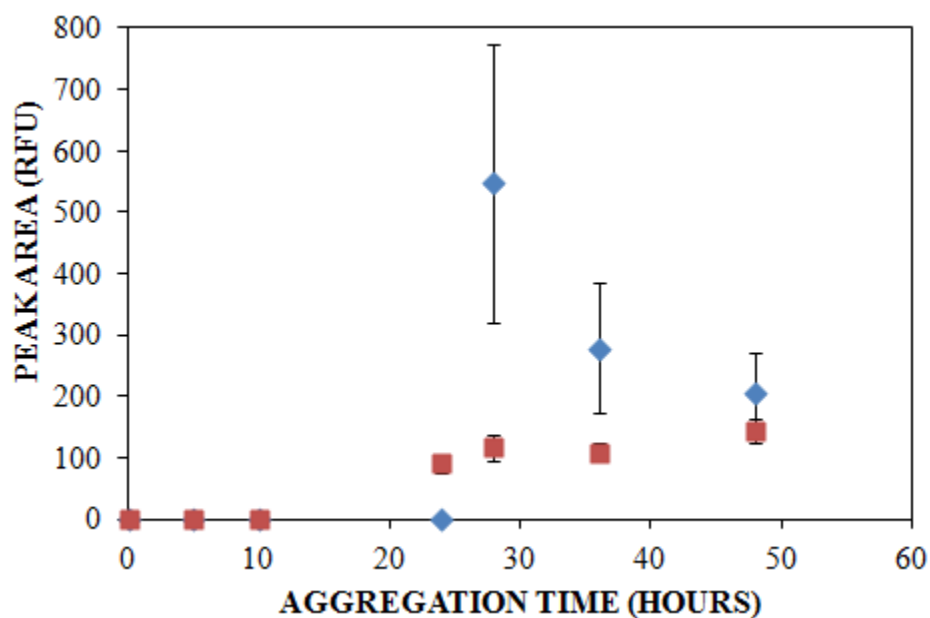


Figure 4 Effect of aggregation time on the peak areas obtained for > 300 kDa (\blacklozenge , $n = 3$) $A\beta_{1-40}$ species detected via UV-CE and peak 9 (\blacksquare , $n = 1 - 2$) BODIPY- $A\beta_{1-40}$ species detected via LIF-CE. The peak areas for the UV-CE data were multiplied by 20% in order to facilitate comparisons between UV-CE and LIF-CE. Samples containing 100% $A\beta_{1-40}$ and samples containing 20% BODIPY-labeled $A\beta_{1-40}$ and 80% unlabeled $A\beta_{1-40}$ were aggregated under agitation (800 rpm) at 0.22 mg/mL in 40 mM Tris (pH 8.0) containing 5 mM NaCl and at 25 °C. At 0 – 48 hours, CE was performed in conjunction with UV detection with a 0.5 psi pressure injection for 8 s with separation at 7 kV using 0.5% PEO separation matrix in a PEO coated capillary or LIF detection with a 7 kV injection for 7 s with separation at 7 kV using 1.5% PHEA separation matrix in PHEA coated capillary.



detect oligomers and aggregates formed by unlabeled A β ₁₋₄₀. Future work will need to be done to determine if these dyes can be used to label the aggregation process in a way that does not affect the natural aggregation. Once the optimal dye is identified, the potential for LIF-CE to detect physiologically relevant concentrations of A β ₁₋₄₀ oligomers and aggregates can be determined.

3. Conclusions

The detection of oligomers and aggregates formed by two amyloid proteins, insulin and A β , is of particular importance due to the role which these species play in Diabetes and Alzheimer's disease, respectively. However, existing techniques are limited in the ability to detect insulin and A β oligomers due to the fact that these early aggregates are transient, present at low concentrations, and difficult to isolate. The present work has demonstrated the potential for CE and ME to detect the native aggregation of insulin and A β proteins, in particular the formation of oligomers and aggregates. Specifically, we have demonstrated that UV-CE is capable of monitoring native aggregation and provides a size range for the oligomeric and aggregate species produced. LIF-CE is capable of detecting physiologically relevant concentrations of FITC-insulin and FAM-A β but the fluorescent dye necessary for these analyses interferes with native aggregation and thus could give inexact information about the amount of oligomers and aggregates formed. ME is capable of detecting physiological concentrations of FAM-A β but detection of the binding of BTA-1 to physiological concentrations of unlabeled A β was not demonstrated. Therefore, significant work lies ahead to investigate alternative fluorescent dyes and optimization of dye concentration in order to achieve the detection of physiologically relevant concentrations of insulin and A β . This work has laid the foundation for future studies by establishing UV-CE, LIF-CE, and LIF-ME protocols for the detection of amyloid aggregates. We feel that this work has demonstrated the potential for LIF-CE and LIF-

ME to detect physiological concentrations although a significant amount of work is needed in the future in order for these techniques to be applied in a clinical setting.

References

1. Pryor, E.; Kotarek, J.A.; Moss, M.A.; Hestekin, C.N. Monitoring Insulin Oligomer Formation Via Capillary Electrophoresis. *Int. J. Mol. Sci.* **2011**, *12*, 9369-9388.
2. Nichols, M.; Moss, M.; Rosenberry, T. Growth of β -Amyloid(1-40) Protofibrils by Monomer Elongation and Lateral Association. Characterization of Distinct Products by Light Scattering and Atomic Force Microscopy. *Biochemistry* **2002**, *41*, 6115-6127.
3. Gu, X.; Greiner, E.R.; Mishra, R.; Kodali, R.; Osmand, A.; Finkbeiner, S.; Steffan, J.S.; Thompson, L.M.; Wetzel, R.; Yang, X.W. Serines 13 and 16 are Critical Determinants of Full-Length Human Mutant Huntingtin Induced Disease Pathogenesis in HD Mice. *Neuron* **2009**, *64*, 828-840.
4. Morshedi, D.; Ebrahim-Habibi, A.; Moosavi-Movahedi, A.A.; Nemat-Gorgani, M. Chemical Modification of Lysine Residues in Lysozyme may Dramatically Influence its Amyloid Fibrillation. *Biochimica et Biophysica Acta (BBA) - Proteins & Proteomics* **2010**, *1804*, 714-722.
5. Choi, S.; Connelly, S.; Reixach, N.; Wilson, I.A.; Kelly, J.W. Chemoselective Small Molecules that Covalently Modify One Lysine in a Non-Enzyme Protein in Plasma. *Nat Chem Biol* **2010**, *6*, 133-139.
6. Thermo Scientific. FITC and Fluorescein Dyes and Labeling Kits. **2012**, 2012.
7. Anaspec. 5-FAM. **2011**, 2012.
8. Life Technologies Corporation. BODIPY® FL, SSE, 4,4-Difluoro-5,7-Dimethyl-4-Bora-3a,4a-Diaza-s-Indacene-3-Propionic Acid, Sulfosuccinimidyl Ester, Sodium Salt. 2012, August 7, 2012, 1.
9. Active Motif. Fluorescent Chromeo Py-Dyes. **2011**, August 7, 2012, 1.
10. Thermo Scientific. AMCA Fluorescent Dyes. **2012**, August 7, 2012, 1.
11. Paparcone, R.; Buehler, M.J. Failure of Alzheimer's A β (1-40) Amyloid Nanofibrils Under Compressive Loading. *JOM* **2010**, *62*, 64-68.
12. Xu, Z.; Paparcone, R.; Buehler, M.J. Alzheimer's A β (1-40) Amyloid Fibrils Feature Size-Dependent Mechanical Properties. *Biophys. J.* **2010**, *98*, 2053-2062.

13. Smith, M.I.; Fodera, V.; Sharp, J.S.; Roberts, C.J.; Donald, A.M. Factors Affecting the Formation of Insulin Amyloid Spherulites. *Colloids Surf. , B* **2012**, *89*, 216-222.
14. Sabella, S.; Quaglia, M.; Lanni, C.; Racchi, M.; Govoni, S.; Caccialanza, G.; Calligaro, A.; Bellotti, V.; Lorenzi, E. Capillary Electrophoresis Studies on the Aggregation Process of β -Amyloid 1-42 and 1-40 Peptides. *Electrophoresis* **2004**, *25*, 3186-3194.
15. Landers, J.P. *Handbook of Capillary and Microchip Electrophoresis and Associated Microtechniques*, 3rd ed.; CRC Press: Boca Raton, FL, 2008; pp. 1567.
16. Jing, P.; Kaneta, T.; Imasaka, T. Band Broadening Caused by the Multiple Labeling of Proteins in Micellar Electrokinetic Chromatography with Diode Laser-Induced Fluorescence Detection. *J. Chromatogr. , A* **2002**, *959*, 281-287.
17. Engelhardt, H.; Cunat-Walter, M.A. Use of Plate Numbers Achieved in Capillary Electrophoretic Protein Separations for Characterization of Capillary Coatings. *J. Chromatogr. , A* **1995**, *717*, 15-23.

Appendix

Doctoral committee comments addressed

Shear and temperature sensitivity of the various constructs

The effect of shear stress on $A\beta_{1-40}$ fibrils has been previously investigated [11,12]. The Young's Moduli for $A\beta_{1-40}$ fibrils ranges from 12 – 30 GPa where longer fibrils are generally more stable [11,12]. For $A\beta_{1-40}$ fibrils < 50 nm in length, Xu *et al.* found that shear effects dominate lateral deformation.[12] However, the amount of total stress necessary to break apart hydrogen bonds in $A\beta_{1-40}$ fibrils is ~0.14 GPa (20,300 psi) [11]. Since our studies are conducted at atmospheric pressure (14.7 psi), it is unlikely that shear effects would produce a significant change in the structure of the $A\beta$ constructs produced in our experiments. Furthermore, the radius of the pores within the polymer network of the capillary is in the μm range which results in a relatively open network for the $A\beta$ constructs to travel through.

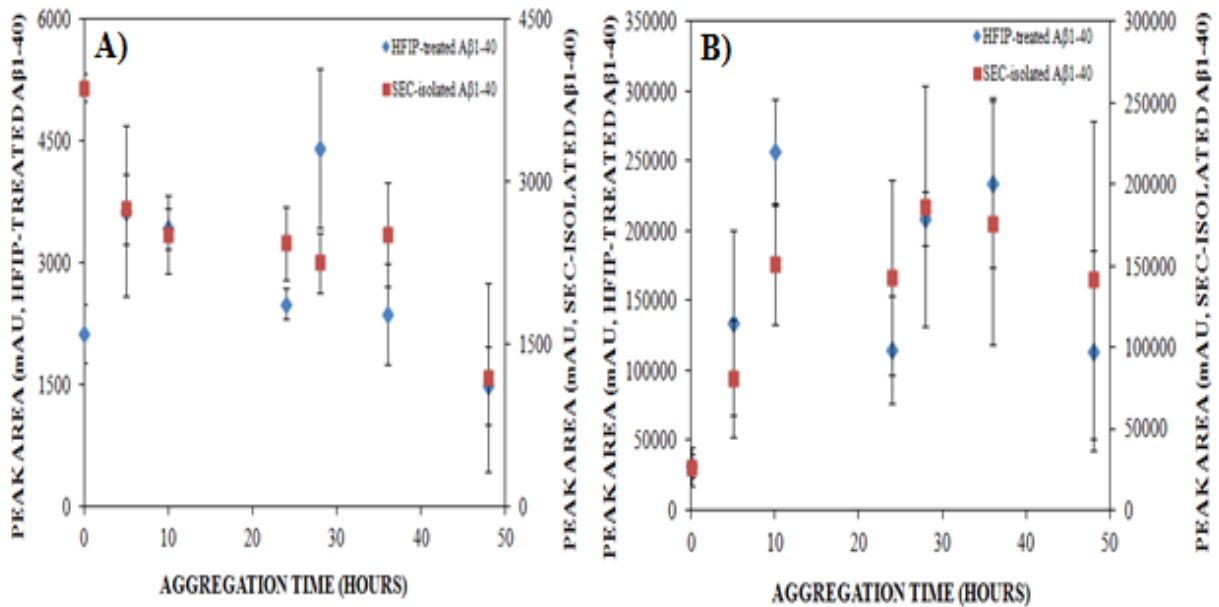
It is widely accepted that an increase in temperature leads to an increase in the rate of fibrillation for amyloid proteins [13]. Thus, larger aggregate sizes will be obtained at elevated temperatures. During CE experiments, an increase in capillary temperature may occur as a result of Joule heating. In order to determine what run voltages will produce a significant amount of Joule heating, an Ohm's law plot was generated for the $A\beta_{1-40}$ conditions utilized in these studies. It was found that above a separation voltage of 9 kV, Joule heating began to occur. Therefore, all $A\beta_{1-40}$ experiments were carried out at a separation voltage of 7 kV in order to minimize the production of heat. Furthermore, the capillary is surrounded by coolant which pulls heat away and maintains a constant capillary temperature during the experiments. A study by Sabella *et al.* found that increasing the CE separation voltage from 1 – 16 kV had no effect on

the peak pattern obtained for A β_{1-40} [14]. It is unlikely that the change in temperature occurring during these CE experiments has an affect on the stability of the amyloid constructs.

Mass balances in electropherograms

In order to determine whether a mass balance could be performed using the CE electropherograms, the peak areas obtained for experiments in Chapter 3 were summed. The values obtained were not constant over time. When the 10 – 30 kDa and > 300 kDa peak areas were summed, the total peak area decreased over an aggregation time of 48 hours for both HFIP-treated and SEC-isolated A β_{1-40} samples (Figure A). Since we did not account for the peaks with longer migration times in these calculations, this decrease in area could be due to the incorporation of the 10 – 30 kDa peak into larger aggregate sizes which would elute at longer migration times. When all peaks with S/N > 3 were summed, the total peak area increased over an aggregation time of 48 hours for both HFIP-treated and SEC-isolated A β_{1-40} samples (Figure B). Since the β -sheet structure absorbs light at around 214 nm, this increase in area over time could be due to the presence of this structure. Alternatively, A β could be retained on the capillary wall between runs which would lead to an increase in area over time. These observations highlight the difficulty of performing a mass balance analysis of this data.

Figure: Effect of aggregation time on the peak areas obtained for **A)** 10 – 30 kDa + > 300 kDa (HFIP-treated, \blacklozenge , $n = 3$ and SEC-isolated, \blacksquare , $n = 3$) $A\beta_{1-40}$ species and **B)** All Peaks (HFIP-treated, \blacklozenge , $n = 3$ and SEC-isolated, \blacksquare , $n = 3$) $A\beta_{1-40}$ species. $A\beta_{1-40}$ was aggregated under agitation (800 rpm) at 0.22 mg/mL in 40 mM Tris (pH 8.0) containing 5 mM NaCl and at 25 °C. At 0 – 48 hours, CE was performed in conjunction with UV detection with a 0.5 psi pressure injection for 8 s with separation at 7 kV using 0.5% PEO separation matrix in a PEO coated capillary.



Results of reinjection of capillary effluent

The volume injected into the capillary using a pressure injection can be calculated according to the following equation:

$$Volume = \pi r^2 \times \frac{\Delta P r^2 t_{inj}}{8\eta L_t} \times 0.00069$$

Where volume = volume introduced (nL), ΔP = pressure difference (psi), r = inner radius of capillary (μm), t_{int} = introduction time (s), η = viscosity of sample (mPa*s), L_t = total length of capillary (cm). For the experimental conditions used in Chapter 3, the volume introduced is ~14 nL. The recovery of such a small volume of sample makes the reinjection of the capillary effluent quite difficult, since the sample would be highly diluted in buffer solution at the outlet.

Number of theoretical plates calculations

The number of theoretical plates (N) was calculated for the 10 – 30 kDa and > 300 kDa peaks obtained in Chapter 3 experiments. The equations used to calculate N are as follows[15]:

$$N = \frac{L_t}{HETP}$$

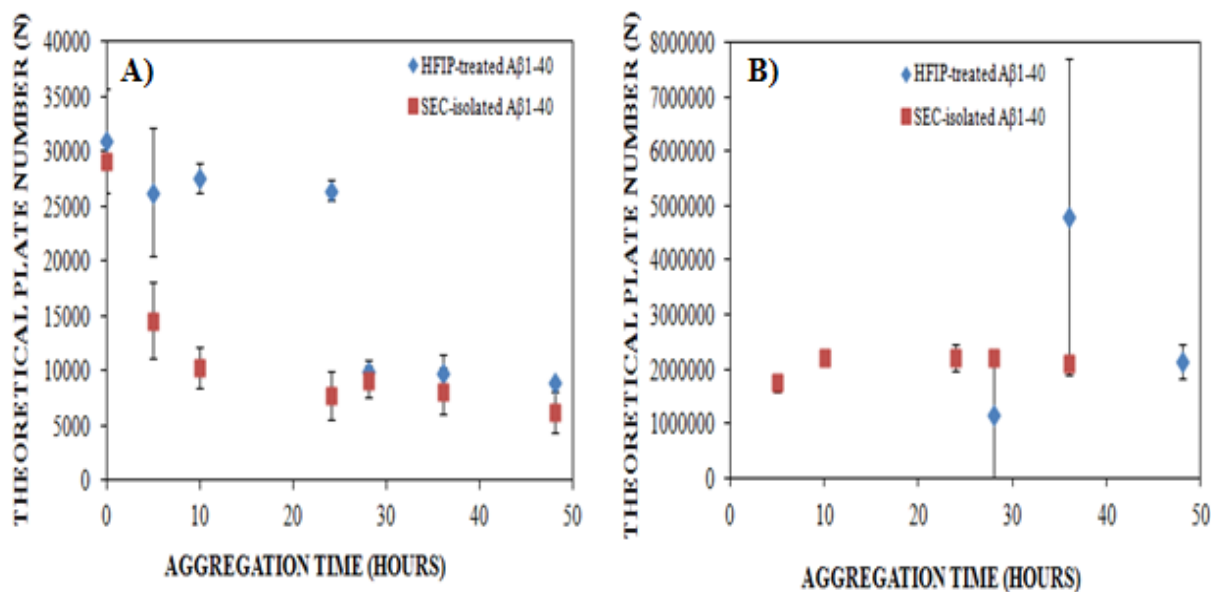
Where N = number of theoretical plates, L_t = total capillary length (cm), and HETP = height equivalent of a theoretical plate (cm). HETP is calculated as follows[16]:

$$HETP = \frac{L_d}{5.54} \times \left(\frac{W_{1/2}}{t_m} \right)^2$$

Where L_d = effective capillary length to detector (cm), $W_{1/2}$ = peak width at half maximum (min), and t_m = migration time (min). The number of theoretical plates obtained for the 10 – 30 kDa peak at various points throughout aggregation is shown in Figure A. For both HFIP-treated $A\beta_{1-40}$ and SEC-isolated $A\beta_{1-40}$, N for the 10 – 30 kDa peak decreases over an aggregation time of 48 hours. The number of theoretical plates obtained for the > 300 kDa peak at various points throughout aggregation is shown in Figure B. The values of N obtained for this peak are

significantly larger (~70 times greater) compared to the values obtained for the 10 – 30 kDa peak. Similar values as those obtained for the number of theoretical plates for the > 300 kDa peak have been obtained in the literature for cytochrome C [17]. The HETP for capillary electrophoresis can be thought of as the fraction of the capillary occupied by the analyte. Since higher values of N are obtained for the > 300 kDa peak versus the 10 – 30 kDa peak, this indicates that the > 300 kDa is occupying less space in the capillary.

Figure: Effect of aggregation time on the theoretical plate number obtained for **A)** 10 – 30 kDa (HFIP-treated, \blacklozenge , $n = 3$ and SEC-isolated, \blacksquare , $n = 3$) $A\beta_{1-40}$ species and **B)** > 300 kDa (HFIP-treated, \blacklozenge , $n = 3$ and SEC-isolated, \blacksquare , $n = 3$) $A\beta_{1-40}$ species. $A\beta_{1-40}$ was aggregated under agitation (800 rpm) at 0.22 mg/mL in 40 mM Tris (pH 8.0) containing 5 mM NaCl and at 25 °C. At 0 – 48 hours, CE was performed in conjunction with UV detection with a 0.5 psi pressure injection for 8 s with separation at 7 kV using 0.5% PEO separation matrix in a PEO coated capillary.



Experimental Protocols

Long Chain Poly-N-Hydroxyethyl Acrylamide Polymerization Protocol (Coating Polymer)

NOTE: Wear gloves and a lab coat at all times as HEA monomer is very toxic.

4% Initial Monomer Solution:

Add 16.5 mL of N-hydroxyethyl acrylamide to 383.5 mL of dH₂O

Note: The N-hydroxyethylacrylamide solution is 97% w/w aqueous solution so calculate amounts by

$$M_1V_1 = M_2V_2$$

$$(97)*(x) = (4)*(400)$$

x = 16.5 mL N-hydroxyethyl acrylamide (PHEA) so 400-16.5 = 383.5 mL of dH₂O

-Run 400 mL PHEA solution through MEHQ inhibitor remover column at speed 6 (~1.8 mL/min). The solution will take ~ 4 hours to run through the column.

Solution de-oxygenation:

-Deoxygenate solution in 47°C water bath by bubbling nitrogen through the mixture for 2 hours.

0.02% V-50 Solution:

0.04 mL (40 µL) of V-50 for every 200 mL of polymer solution.

-Add 40 µL of V-50 to 200 mL PHEA solution and then blow nitrogen over the solution for 4-5 hours.

-Transfer final solution to dialysis tubing bags (MWCO = 100,000 Da).

-Place dialysis tubes with polymer in them in the fish bowls (4 tubes per fish bowl) and fill fish bowls with 18 MΩ de-ionized water so the water covers tubing.

Water changes:

-Change the de-ionized water in the fish bowls 10 times total. Each water change should be *at least* 4 hours apart.

Freezing and lyophilizing polymer:

-After 10 water changes have been completed, transfer the polymer to 45 mL falcon tubes (~35 mL polymer solution in each tube).

-Place falcon tubes in freezer box and store in -80°C freezer for 2 days.

-After polymer has been stored in -80°C freezer for 2 days, lyophilize polymer for 2 days, making sure polymer does not melt during lyophilization.

Short Chain Poly-N-Hydroxyethyl Acrylamide Polymerization Protocol (Separation Polymer)

NOTE: Wear gloves and a lab coat at all times as HEA monomer is very toxic.

4% Initial Monomer Solution:

Add 16.5 mL of N-hydroxyethyl acrylamide to 383.5 mL of dH₂O

Note: The N-hydroxyethylacrylamide solution is 97% w/w aqueous solution so calculate amounts by

$$M_1 V_1 = M_2 V_2$$

$$(97)*(x) = (4)*(400)$$

x = 16.5 mL N-hydroxyethyl acrylamide (PHEA) so 400-16.5 = 383.5 mL of dH₂O

-Run 400 mL PHEA solution through MEHQ inhibitor remover column at speed 6 (~1.8 mL/min). The solution will take ~ 4 hours to run through the column.

Isopropanol (chain transfer agent):

-For ~770 kDa polymer, 2 mL isopropanol (IPA) added to 100 mL of 5% initial monomer solution (Hert *et al.*) Therefore, add 3.2 mL IPA to 200 mL of 4% initial monomer solution. Swirl IPA into solution.

$$2 \text{ mL IPA}/100 \text{ mL of 5\% initial monomer} = x \text{ mL}/200 \text{ mL of 4\% initial monomer}$$

$$2 \text{ mL IPA}/5 \text{ mL initial monomer} = x \text{ mL}/8 \text{ mL initial monomer}$$

$$x = 3.2 \text{ mL IPA}$$

-Deoxygenate solution in 47°C water bath by bubbling nitrogen through the mixture for 2 hours.

0.02% V-50 Solution:

0.04 mL (40 µL) of V-50 for every 200 mL of polymer solution.

-Add 40 µL of V-50 to 200 mL PHEA solution and then blow nitrogen over the solution for 4-5 hours.

-Transfer final solution to dialysis tubing bags (MWCO = 100,000 Da).

-Place dialysis tubes with polymer in them in the fish bowls (4 tubes per fish bowl) and fill fish bowls with 18 M Ω de-ionized water so the water covers tubing.

Water changes:

-Change the de-ionized water in the fish bowls 10 times total. Each water change should be *at least* 4 hours apart.

Freezing and lyophilizing polymer:

-After 10 water changes have been completed, transfer the polymer to 45 mL falcon tubes (~35 mL polymer solution in each tube).

-Place falcon tubes in freezer box and store in -80°C freezer for 2 days.

-After polymer has been stored in -80°C freezer for 2 days, lyophilize polymer for 2 days, making sure polymer does not melt during lyophilization.

Polymer Molecular Weight determination using Multi-Angle Light Scattering (MALS)

NOTE: Wear gloves and safety glasses when handling polymer solutions!

Sample preparation:

-Prepare 6 mL of a 5 mg/mL stock solution of your polymer in **de-ionized water**. For example, if analyzing PDMA polymer, dissolve 30 mg of dry PDMA in 6 mL of de-ionized water. If sample limited, adjust calculations accordingly.

-Prepare 10 mL of the following concentrations by diluting 5 mg/mL stock PDMA solution:

1 mg/mL

0.75 mg/mL

0.5 mg/mL

0.25 mg/mL

0.1 mg/mL

For example, to prepare 1 mg/mL dilution:

$$M_1V_1 = M_2V_2$$

$$(5 \text{ mg/mL}) \cdot (V_1) = (1 \text{ mg/mL}) \cdot (10 \text{ mL})$$

$$V_1 = 2 \text{ mL of } 5 \text{ mg/mL stock PDMA solution}$$

So add 2 mL of 5 mg/mL stock PDMA solution to 8 mL of **de-ionized** water

Fill five 10 mL **plastic** syringes (without rubber tips) with PDMA dilutions.

Fill one 10 mL plastic syringe with de-ionized water.

Use 0.02 μm syringe filters for water/solvent solutions and 0.2 μm syringe filters for PDMA samples.

Computer:

Double click the Astra 5.3.4.14 icon.

Click the green circle to start experiment.

Once experiment has started, use the syringe pump to flush water through system until ~5 minutes of a stable baseline is obtained.

Using syringe pump, flush 1 mg/mL polymer solution through system until ~3 minutes of a stable line is obtained.

Using syringe pump, flush 0.75 mg/mL polymer solution through system until ~3 minutes of a stable line is obtained.

Using syringe pump, flush 0.5 mg/mL polymer solution through system until ~3 minutes of a stable line is obtained.

Using syringe pump, flush 0.25 mg/mL polymer solution through system until ~3 minutes of a stable line is obtained.

Using syringe pump, flush 0.1 mg/mL polymer solution through system until ~3 minutes of a stable line is obtained.

Using syringe pump, flush water through system until ~5 minutes of a stable baseline is obtained.

NOTE: Water must be flushed through the system before and after sample data collection in order to obtain a proper baseline for data analysis.

Once water and all 5 sample dilutions have been flushed through system, press the red stop button at the top of the page.

The software will ask you to draw your baseline and define peaks. You must do this before the software will generate a Zimm Plot!

Under the Procedures tab, click “Peaks” and enter in the concentrations for each peak you have defined and a dn/dc value of 0.175 for each peak. You must enter in these values to generate the Zimm Plot!

View the Zimm Plot by clicking “A2, Mass & Radius from LS”. The mass and rms radius are given under the Zimm Plot.

Cleaning MALS Flowcell with 0.1 M Nitric Acid

NOTE: Nitric Acid (HNO_3) is extremely toxic. Work with in hood and do not inhale fumes.

0.1 M HNO_3 is in fume hood in BEC 2238.

- 1) Flow ~6 mL of 0.1 M HNO_3 through the MALS instrument.
- 2) Let solution sit in MALS instrument for 3 hours.
- 3) After 3 hours, rinse with filtered de-ionized water for 15 min (or flow ~5 mL through)
- 4) Rinse with 100% ethanol for 15 min (or flow ~5 mL through)
- 5) Rinse with 100% toluene for 15 min (or flow ~5 mL through)
- 6) Rinse with 100% ethanol for 15 min (or flow ~5 mL through)
- 7) Rinse with filter de-ionized water for 15 min (or flow ~5 mL through)

Compare the light scattering voltages for the toluene to the voltages given in the certificate of performance. If similar, the flow cell should be clean.

Polymer Solution Preparation for use on CE

NOTE: All solution percents are calculated as weight/volume (w/v).

Preparation of coating polymer:

Coating polymers should have a higher molecular weight (ie. > 1,500,000 g/mol)

To prepare a 1% PHEA solution, use the following calculation:

$$\begin{aligned} & \text{Amount of water needed (mL)} \\ = & \frac{(\text{polymer weight (mg)}) - \left(\frac{1\%}{100} \times \text{polymer weight (mg)}\right)}{\left(\frac{1\%}{100}\right)} \end{aligned}$$

Always add water to coating polymer solutions!

Preparation of separation matrix polymer:

Separation matrix polymers should have a lower molecular weight (ie. < 1,500,000 g/mol)

Same protocol as above except dissolve separation polymer solutions in CE separation buffer (ie.

40 mM Tris-HCl, pH 8.0 for LIF-CE and ME or 100 mM Tris-HCl, pH 8.0 for UV-CE)

0.1% Polyhydroxyethyl acrylamide (PHEA) Capillary Coating Protocol

-Capillary should be 31 cm total length, 10 cm effective length, and 50 μ m ID.

-All steps done using reverse rinses (outlet to inlet)

15 minute de-ionized water rinse at 20 psi

15 minute 1 M HCl rinse at 20 psi

20 minute 0.1% w/v PHEA polymer solution rinse at 20 psi

15 minute de-ionized water rinse at 20 psi

-Ensure 4 outlet vials contain liquid at end of procedure to ensure proper coating.

0.5% Polyethylene oxide (PEO) Capillary Coating Protocol

- Capillary should be 31 cm total length, 10 cm effective length, and 50 μm ID.
- Protocol adapted from Fung *et al.* 1995-“High-Speed DNA Sequencing by Using Mixed Poly(ethylene oxide) Solutions in Uncoated Capillary Columns”
- All steps done using reverse rinses (outlet to inlet)
 - 10 min rinse with water at 20 psi
 - 15 min rinse with 0.1 M HCl at 20 psi
 - 30 min rinse with 0.5% PEO at 50 psi
(PEO from Sigma Cat # 372803, $M_v \sim 2,000,000$ prepared in de-ionized water)
 - 15 min rinse with water at 20 psi
- Ensure 4 outlet vials contain liquid at end of procedure to ensure proper coating.

Microchip Coating Procedure

15 min de-ionized water

15 min 1 M HCl

20 min 0.1% PHEA (dissolved in de-ionized water)

15 min de-ionized water

- Pull solution through channels with the vacuum pump.
- Let each solution sit in chip for given amount of time. Watch for evaporation. If evaporation occurs, pull more solution through channel.
- After given amount of time, pull solution out of channels.
- Repeat procedure for each solution.
- Store chip dry with no buffer.

40 mM Tris-HCl Protocol

Buffer recipe, generated by Buffer Calculator (c) Rob Beynon 1996-2006

<http://www.liv.ac.uk/buffers>

BUFFER:

To make 1000 ml of 0.04 M Tris ($pK_a = 8.06$) Buffer, $pH = 8$,

Ionic strength = 0.022 M,

(Ionic strength due to the buffer = 0.022M)

Thermodynamic $pK_a = 8.06$, Apparent $pK_a' = 8.12$

Temperature coefficient = -0.028 per $^{\circ}C$

Prepared at $25^{\circ}C$, used at $25^{\circ}C$

RECIPE:

Weigh out 3.594 g Tris-HCl crystals (0.0228 mol of acid component)

Weigh out 2.071 g Tris base crystals (0.0171 mol of basic component)

(No added neutral salts, I due to buffer alone.)

Make up to 1000 ml with pure water

Check to make sure $pH = 8.0$. If pH does not equal 8, add 0.04 g more Tris-HCl crystals and 0.04 g more Tris base crystals.

NOTE: Can also make 100 mM Tris-HCl ($pH 8.0$) with this calculator.

Monomerization by HFIP and storage of A β ₁₋₄₀ peptide

Objective: A β ₁₋₄₀ storage

Stock Solutions:

A. Assay Buffer:

HFIP (1,1,1,3,3,3-hexafluoro-2-propanol)

B. A β ₁₋₄₀: 1mg/vial Anaspec

Procedure:

1. Solid A β ₁₋₄₀ is stored as a solid at -80C. Remove and place on ice when ready to prepare stock peptide films.
2. Place 1,1,1,3,3,3-hexafluoro-2-propanol (HFIP) on ice in the hood and allow to cool. HFIP is highly corrosive and very volatile. Add enough HFIP to A β ₁₋₄₀ such that the final peptide concentration is 1mM (e.g. 231 ul cold HFIP to 1 mg A β ₁₋₄₀). Rinse vial thoroughly.
3. Incubate at room temperature for 60 min, keeping vial closed. Solution should be clear and colorless. Any traces of yellow color or cloudy suspension indicate poor peptide quality and should not be used.
4. Place peptide—HFIP solution back on ice for 5–10 min.
5. Separate the HFIP into vials with 0.0625 mg/vial. That means each vial has 14.4 μ L stock.
6. Aliquot solution into non-siliconized microcentrifuge tubes. Do not close tubes.
7. Allow HFIP to evaporate overnight in the hood at room temperature.
8. All traces of HFIP must be removed. The resulting peptide should be a thin clear film at the bottom of the tubes. The peptide should not be white or chunky.
9. Store dried peptide films over desiccant at -80C. These stocks should be stable for several months.

Monomerization by HFIP and storage of FAM-A β ₁₋₄₀ peptide

Objective: FAM-A β ₁₋₄₀ storage

Stock Solutions:

A. Assay Buffer:

HFIP (1,1,1,3,3,3-hexafluoro-2-propanol)

B. FAM-A β ₁₋₄₀: 0.1mg/vial Anaspec

Procedure:

1. Solid FAM-A β ₁₋₄₀ is stored as a solid at -80C. Remove and place on ice when ready to prepare stock peptide films.
2. Place 1,1,1,3,3,3-hexafluoro-2-propanol (HFIP) on ice in the hood and allow to cool. HFIP is highly corrosive and very volatile. Add enough HFIP to FAM-A β ₁₋₄₀ such that the final peptide concentration is 0.1 mM (e.g. 213.3 μ L cold HFIP to 0.1 mg FAM-A β ₁₋₄₀). Rinse vial thoroughly.
3. Incubate at room temperature for 60 min, keeping vial closed. Solution should be clear and colorless. A cloudy suspension indicates poor peptide quality and should not be used.
4. Place peptide—HFIP solution back on ice for 5–10 min.
5. Separate the HFIP into vials with 0.01563 mg/vial. That means each vial has 33.3 μ L stock.
6. Aliquot solution into non-siliconized microcentrifuge tubes. Do not close tubes.
7. Allow HFIP to evaporate overnight in the hood at room temperature. Cover with foil!
8. All traces of HFIP must be removed. The resulting peptide should be a thin clear film at the bottom of the tubes. The peptide should not be white or chunky.
9. Store dried peptide films over desiccant at -80C. These stocks should be stable for several months.

Monomerization by HFIP and storage of A β ₁₋₄₂ peptide

Objective: A β ₁₋₄₂ storage

Stock Solutions:

A. Assay Buffer:

HFIP (1,1,1,3,3,3-hexafluoro-2-propanol)

B. A β ₁₋₄₂: 1mg/vial Anaspec

Procedure:

1. Solid A β ₁₋₄₂ is stored as a solid at -80C. Remove and place on ice when ready to prepare stock peptide films.
2. Place 1,1,1,3,3,3-hexafluoro-2-propanol (HFIP) on ice in the hood and allow to cool. HFIP is highly corrosive and very volatile. Add enough HFIP to A β ₁₋₄₂ such that the final peptide concentration is 1mM (e.g. 222 μ L cold HFIP to 1 mg A β ₁₋₄₂). Rinse vial thoroughly.
3. Incubate at room temperature for 60 min, keeping vial closed. Solution should be clear and colorless. Any traces of yellow color or cloudy suspension indicate poor peptide quality and should not be used.
4. Place peptide—HFIP solution back on ice for 5–10 min.
5. Separate the HFIP into vials with 0.0271 mg/vial. That means each vial has 6.02 μ L stock.
6. Aliquot solution into non-siliconized microcentrifuge tubes. Do not close tubes.
7. Allow HFIP to evaporate overnight in the hood at room temperature.
8. All traces of HFIP must be removed. The resulting peptide should be a thin clear film at the bottom of the tubes. The peptide should not be white or chunky.
9. Store dried peptide films over desiccant at -80C. These stocks should be stable for several months.

Monomerization by HFIP and storage of FAM-A β ₁₋₄₂ peptide

Objective: FAM-A β ₁₋₄₂ storage

Stock Solutions:

A. Assay Buffer:

HFIP (1,1,1,3,3,3-hexafluoro-2-propanol)

B. FAM-A β ₁₋₄₂: 0.1mg/vial Anaspec

Procedure:

1. Solid FAM-A β ₁₋₄₂ is stored as a solid at -80C. Remove and place on ice when ready to prepare stock peptide films.
2. Place 1,1,1,3,3,3-hexafluoro-2-propanol (HFIP) on ice in the hood and allow to cool. HFIP is highly corrosive and very volatile. Add enough HFIP to FAM-A β ₁₋₄₂ such that the final peptide concentration is 0.1mM (e.g. 205.2 μ l cold HFIP to 0.1 mg FAM-A β ₁₋₄₂). Rinse vial thoroughly.
3. Incubate at room temperature for 60 min, keeping vial closed. Solution should be clear and colorless. A cloudy suspension indicates poor peptide quality and should not be used.
4. Place peptide—HFIP solution back on ice for 5–10 min.
5. Separate the HFIP into vials with 0.006775 mg/vial. That means each vial has 13.9 μ L stock.
6. Aliquot solution into non-siliconized microcentrifuge tubes. Do not close tubes.
7. Allow HFIP to evaporate overnight in the hood at room temperature. Cover tubes with foil!
8. All traces of HFIP must be removed. The resulting peptide should be a thin clear film at the bottom of the tubes. The peptide should not be white or chunky.
9. Store dried peptide films over desiccant at -80C. These stocks should be stable for several months.

Insulin Oligomer Time Course Protocol for Analysis Via UV-CE

1 mg/mL insulin stock sample preparation:

1) Weigh out ~1 mg insulin and add 5 mM NaOH such that the ratio of NaOH:40 mM Tris-HCl is 500:10000, assuming a 1 mg/mL final concentration. For example, if 1 mg insulin weighed out, amount of NaOH added is as follows:

$$\left(\frac{500}{10000} \times 1000 \mu\text{L}\right) = 50 \mu\text{L } 5 \text{ mM NaOH}$$

2) Let insulin solution sit in 5 mM NaOH for 30 min.

3) Bring up to 1 mg/mL with 40 mM Tris-HCl (pH = 8.0)

4) Dilute the 1 mg/mL solution to 0.2 mg/mL in 40 mM Tris-HCl supplemented with 0 - 250 mM NaCl by adding the appropriate amount of 4.4 M NaCl to the tube. The final total volume should be 800 μL . For example, the amount of 40 mM Tris-HCl and 4.4 M NaCl to add for a sample supplemented with 150 mM NaCl is as follows:

$$M_1V_1 = M_2V_2$$

$$(4,400 \text{ mM NaCl}) \times (x) = (150 \text{ mM NaCl}) \times (800 \mu\text{L})$$

$$x = 27.3 \mu\text{L } 4,400 \text{ mM NaCl}$$

$$\left(1 \frac{\text{mg}}{\text{mL}} \text{ insulin}\right) \times (x) = \left(0.2 \frac{\text{mg}}{\text{mL}} \text{ insulin}\right) \times (800 \mu\text{L})$$

$$x = 160 \mu\text{L } 1 \frac{\text{mg}}{\text{mL}} \text{ insulin}$$

So, for a total volume of 800 μL , add 160 μL 1 $\frac{\text{mg}}{\text{mL}}$ insulin + 27.3 μL 4,400 mM NaCl

$$+ (800 \mu\text{L} - 27.3 \mu\text{L} - 160 \mu\text{L}) = 612.7 \mu\text{L } 40 \text{ mM Tris} - \text{HCl (pH 8.0)}$$

5) Agitate sample at 25°C and 185 rpm. At various time points, take 50 μL sample and analyze via UV-CE.

CE conditions:

NOTE: For studies in this thesis, 0.1% poly-N-hydroxyethyl acrylamide (PHEA) was used to coat the capillary and 0.5% PHEA was used for separation. However, PHEA interferes with the detection of insulin at 214 nm so 0.5% poly-ethylene oxide (PEO) coated capillaries should be utilized with 0.5% PEO separation matrix. A new capillary should be coated before each time course.

Capillary dimensions: $L_t = 31$ cm, $L_d = 10$ cm

Before each time point run, perform the following steps on the Beckman P/ACE instrument:

Reverse rinse (ie. outlet = inlet) with de-ionized water for 10 min at 50 psi

Reverse rinse with 0.5% PEO for 10 min at 50 psi

0.5 psi injection for 8 s

7 kV normal polarity separation using 100 mM Tris-HCl for 60 - 240 min.

A β ₁₋₄₀ Oligomer Time Course Protocol for Analysis Via UV-CE

50 μ M (0.22 mg/mL) A β ₁₋₄₀ Sample Concentration:

- 1) Take vial containing 0.0625 mg A β ₁₋₄₀ out of -80°C freezer. Add 5 mM NaOH such that the ratio of NaOH:40 mM Tris-HCl is 500:10000, assuming a 0.22 mg/mL final concentration (ie. add 14.2 μ L 5 mM NaOH).
- 2) Let A β ₁₋₄₀ solution sit in 5 mM NaOH for 5 min.
- 3) Bring up to 0.22 mg/mL in 40 mM Tris-HCl supplemented with 5 mM NaCl by adding the appropriate amount of 4.4 M NaCl to the tube. The final total volume should be 284 μ L. For example, the amount of 40 mM Tris-HCl and 4.4 M NaCl to add for a sample supplemented with 5 mM NaCl is as follows:

$$M_1V_1 = M_2V_2$$

$$(4,400 \text{ mM NaCl}) \times (x) = (5 \text{ mM NaCl}) \times (284 \text{ } \mu\text{L})$$

$$x = 0.33 \text{ } \mu\text{L 4,400 mM NaCl}$$

So, for a total volume of 284 μ L, add (284 μ L – 0.33 μ L – 14.2 μ L)

$$= 269.5 \text{ } \mu\text{L 40 mM Tris – HCl (pH 8.0)}$$

- 5) Agitate sample at 25°C and 800 rpm. At various time points, take 20 μ L sample and analyze via UV-CE.

CE conditions:

NOTE: 0.5% poly-ethylene oxide (PEO) coated capillaries should be utilized with 0.5% PEO separation matrix. A new capillary should be coated before each time course.

Capillary dimensions: L_t = 31 cm, L_d = 10 cm

Before each time point run, perform the following steps on the Beckman P/ACE instrument:

Reverse rinse (ie. outlet = inlet) with de-ionized water for 10 min at 50 psi

Reverse rinse with 0.5% PEO for 10 min at 50 psi

0.5 psi injection for 8 s

7 kV normal polarity separation using 100 mM Tris-HCl for 60 - 240 min.

Size Estimation Analysis Via Centrifugal Filter Units

- 1) Perform protocols for either “Insulin Oligomer Time Course” or “A β ₁₋₄₀ Oligomer Time Course”.
- 2) When taking time points throughout aggregation, take a 50 μ L sample and centrifuge at 14,000 x g for 20 minutes.
- 3) Analyze filtrate and retained solutions via UV-CE.

Protocol for Aggregation of A β ₁₋₄₀ in Presence of Congo Red

Congo Red stock solution:

1) Prepare a 16.7 μ M (0.23 mg/mL) stock solution of congo red in DMSO by adding ~18.9 mg congo red + 1.6 mL 100% DMSO.

NOTE: Amounts may be adjusted according to how much congo red is weighed out.

A β ₁₋₄₀ Aggregation Assay with Congo Red:

1) Take vial containing 0.0625 mg A β ₁₋₄₀ out of -80°C freezer. Add 5 mM NaOH such that the ratio of NaOH:40 mM Tris-HCl is 500:10000, assuming a 0.221 mg/mL (51.02 μ M) final concentration (ie. add 14.15 μ L 5 mM NaOH).

2) Let A β ₁₋₄₀ solution sit in 5 mM NaOH for 5 min.

3) Bring up to 0.221 mg/mL in 40 mM Tris-HCl supplemented with 5 mM NaCl by adding the appropriate amount of 4.4 M NaCl to the tube. The final total volume should be 282.93 μ L. For example, the amount of 40 mM Tris-HCl and 4.4 M NaCl to add for a sample supplemented with 5 mM NaCl is 268.5 μ L 40 mM Tris-HCl (pH 8.0) and 0.32 μ L 4.4 M NaCl.

4) Add 5.77 μ L of 16.7 μ M congo red stock solution to sample in Step 3. The final percent DMSO in solution should be 2% and the final A β ₁₋₄₀ concentration should be 50 μ M.

5) Agitate sample at 25°C and 800 rpm. At various time points, take 20 μ L sample and analyze via UV-CE.

CE conditions:

NOTE: 0.5% poly-ethylene oxide (PEO) coated capillaries should be utilized with 0.5% PEO separation matrix. A new capillary should be coated before each time course.

Capillary dimensions: L_t = 31 cm, L_d = 10 cm

Before each time point run, perform the following steps on the Beckman P/ACE instrument:

Reverse rinse (ie. outlet = inlet) with de-ionized water for 10 min at 50 psi

Reverse rinse with 0.5% PEO for 10 min at 50 psi

0.5 psi injection for 8 s

7 kV normal polarity separation using 100 mM Tris-HCl for 60 - 240 min.

Protocol for Aggregation of A β ₁₋₄₀ in Presence of Orange G

Orange G stock solution:

1) Prepare a 16.7 μ M (0.23 mg/mL) stock solution of orange G in DMSO by adding ~12.1 mg congo red + 1.6 mL 100% DMSO.

NOTE: Amounts may be adjusted according to how much orange G is weighed out.

A β ₁₋₄₀ Aggregation Assay with Orange G:

1) Take vial containing 0.0625 mg A β ₁₋₄₀ out of -80°C freezer. Add 5 mM NaOH such that the ratio of NaOH:40 mM Tris-HCl is 500:10000, assuming a 0.221 mg/mL (51.02 μ M) final concentration (ie. add 14.15 μ L 5 mM NaOH).

2) Let A β ₁₋₄₀ solution sit in 5 mM NaOH for 5 min.

3) Bring up to 0.221 mg/mL in 40 mM Tris-HCl supplemented with 5 mM NaCl by adding the appropriate amount of 4.4 M NaCl to the tube. The final total volume should be 282.93 μ L. For example, the amount of 40 mM Tris-HCl and 4.4 M NaCl to add for a sample supplemented with 5 mM NaCl is 268.5 μ L 40 mM Tris-HCl (pH 8.0) and 0.32 μ L 4.4 M NaCl.

4) Add 5.77 μ L of 16.7 μ M orange G stock solution to sample in Step 3. The final percent DMSO in solution should be 2% and the final A β ₁₋₄₀ concentration should be 50 μ M.

5) Agitate sample at 25°C and 800 rpm. At various time points, take 20 μ L sample and analyze via UV-CE.

CE conditions:

NOTE: 0.5% poly-ethylene oxide (PEO) coated capillaries should be utilized with 0.5% PEO separation matrix. A new capillary should be coated before each time course.

Capillary dimensions: L_t = 31 cm, L_d = 10 cm

Before each time point run, perform the following steps on the Beckman P/ACE instrument:

Reverse rinse (ie. outlet = inlet) with de-ionized water for 10 min at 50 psi

Reverse rinse with 0.5% PEO for 10 min at 50 psi

0.5 psi injection for 8 s

7 kV normal polarity separation using 100 mM Tris-HCl for 60 - 240 min.

A β ₁₋₄₀ Dot Blot Protocol

NOTE: Wear gloves and safety glasses when dealing with antibodies.

Chemicals Needed:

5% milk/TBS-T

Dissolve 2 g dry milk in 40 mL 1X TBST

A11 primary antibody (anti-A β oligomer, 1 mg/mL)

Anti-rabbit secondary antibody (use with A11 and OC primary, 2 mg/mL)

6E10 primary antibody (anti-A β monomer, 1 mg/mL)

Anti-mouse secondary antibody (use with 6E10 primary, 0.6 mg/mL)

OC primary antibody (anti-A β fibril)

Procedure:

1) Cut single nitrocellulose membrane into 0.5" wide pieces. At each aggregation time point, spot 3 μ L of sample onto each membrane.

2) After all spots have been applied to membrane, allow last applied spot to dry for 1 hour.

3) Block membranes in 5% milk/TBS-T solution at 4°C for 1 hour with gentle shaking.

4) Wash membranes 3 times in 1X TBS-T.

5) Cover each membrane with the following amounts of primary antibody:

Membrane 1: 5 mL 5% milk/TBS-T + 2.5 μ L A11 primary antibody (1:2000 dilution)

Membrane 2: 5 mL 5% milk/TBS-T + 2.5 μ L 6E10 primary antibody (1:2000 dilution)

Membrane 3: 5 mL 5% milk/TBS-T + 1.25 μ L OC primary antibody (1:4000 dilution)

6) Incubate with gentle shaking at 4°C for 1 hour.

7) Wash membranes 3 times in 1X TBS-T.

8) Cover each membrane with the following amounts of secondary antibody:

Membrane 1: 5 mL 5% milk/TBS-T + 0.83 μ L anti-rabbit secondary antibody (1:3000 dilution)

Membrane 2: 5 mL 5% milk/TBS-T + 4.17 μ L anti-mouse secondary antibody (1:2000 dilution)

Membrane 3: 5 mL 5% milk/TBS-T + 0.83 μ L anti-rabbit secondary antibody (1:3000 dilution)

9) Incubate with gentle shaking at 4°C for 1 hour.

7) Wash membranes 3 times in **TBS-T/MgCl₂**. NOTE the use of **TBS-T/MgCl₂** for this step.

8) Develop membranes by adding the following amounts of developing solution to each membrane:

Membrane 1: 15 mL TBS-T/MgCl₂ + 50 μ L BCIP (50 mg/mL) + 100 μ L NBT (50 mg/mL)

Membrane 2: 15 mL TBS-T/MgCl₂ + 50 μ L BCIP (50 mg/mL) + 100 μ L NBT (50 mg/mL)

Membrane 3: 15 mL TBS-T/MgCl₂ + 50 μ L BCIP (50 mg/mL) + 100 μ L NBT (50 mg/mL)

NOTE: Stock BCIP (50 mg/mL) prepared in 100% DMF and stock NBT (50 mg/mL) prepared in 70% DMSO.

9) Allow membranes to develop and when begin to see spots, rinse membrane with 10% acetic acid to stop reaction. It typically takes 5-10 minutes for membranes to develop.

25% FITC-labeled Insulin/75% Unlabeled Insulin Oligomer Time Course Protocol for Analysis

Via LIF-CE

-Prepare unlabeled insulin and FITC-labeled insulin separately:

Unlabeled Insulin (0.3 mg/mL) supplemented with 150 mM NaCl:

0.3 mg unlabeled insulin + 966 μ L of 40 mM Tris-HCl + 34.1 μ L of 4.4 M NaCl

Note: If exact amounts are not weighed out, adjust volumes using excel spreadsheet but do not weigh out more than 0.3 mg unlabeled insulin!

FITC-labeled Insulin (0.2 mg/mL) supplemented with 150 mM NaCl:

0.1 mg FITC-labeled insulin + 483 μ L of 40 mM Tris-HCl + 17 μ L of 4.4 M NaCl

Note: If exact amounts are not weighed out, adjust volumes using excel spreadsheet but do not weight out more than 0.1 mg FITC-labeled insulin!

-Combine unlabeled insulin with FITC-labeled insulin so that final unlabeled insulin concentration is 0.2 mg/mL and final FITC-labeled insulin concentration is 0.067 mg/mL and place on shaking incubator at 185 rpm.

-After 0, 4, 8, 10, 24, and 36 hours, take 20 μ L of sample and dilute to 0.013 mg/mL in 40 mM Tris-HCl (pH 8.0). Run sample on LIF-CE.

CE conditions:

Rinse capillary with de-ionized water in between each run using syringe pump.

12 kV injection for 12 s

15 kV separation

A β ₁₋₄₂/FAM-A β ₁₋₄₂ Oligomer Formation Assay with DMSO and Tween for Analysis Via LIF-CE

- 1) When ready to start experiment, take vial containing 0.0271 mg A β ₁₋₄₂ and 0.006775 mg FAM-A β ₁₋₄₂ out of the -80°C freezer. Make a 5 mM A β ₁₋₄₂ stock and a 1.16 mM FAM-A β ₁₋₄₂ stock in 100% DMSO. Pipette thoroughly, washing down the sides of the tube to ensure complete re-suspension of peptide film.
- 2) Dilute A β ₁₋₄₂ and FAM-A β ₁₋₄₂ peptide stocks to 30 μ M (0.14 mg/mL) with 40 mM Tris-HCl (pH 8.0) supplemented with 10 mM NaCl.
- 3) Combine A β ₁₋₄₂ and FAM-A β ₁₋₄₂ samples to yield a total final concentration of 30 μ M (0.14 mg/mL) containing 50 – 80% unlabeled A β ₁₋₄₂ and 20 – 50% FAM-labeled A β ₁₋₄₂.

NOTE: Look at excel spreadsheet for exact volume amounts.

- 4) Allow oligomer prep to sit in microcentrifuge tube at room temperature (25°C) with cap on.
- 5) At 0, 3, 6, 9, and 24 hours, add tween to obtain a final volume containing 0.1% tween. (ie. Prepare 1% tween stock solution by adding 10 μ L pure tween to 990 μ L de-ionized water. Take 27 μ L aliquot and add 3 μ L of 1% tween.
- 6) Analyze sample via LIF-CE.

CE conditions:

Rinse capillary with de-ionized water in between each run using syringe pump.

7 kV injection for 7 s

7 kV separation

A β ₁₋₄₀ Oligomer Formation Assay With BTA-1 for Analysis Via LIF-ME

BTA-1 stock solution:

- 1) Prepare a 1 mg/mL stock solution of BTA-1 by adding ~1 mg BTA-1 to ~1 mL 100% DMSO.
- 2) Dilute stock solution to 0.0064 mg/mL (4160 μ M) in 40 mM Tris-HCl (pH 8.0).

50 μ M (0.22 mg/mL) A β ₁₋₄₀ Sample Concentration:

- 1) Take vial containing 0.0625 mg A β ₁₋₄₀ out of -80°C freezer. Add 5 mM NaOH such that the ratio of NaOH:40 mM Tris-HCl is 500:10000, assuming a 0.22 mg/mL final concentration (ie. add 14.2 μ L 5 mM NaOH).
- 2) Let A β ₁₋₄₀ solution sit in 5 mM NaOH for 5 min.
- 3) Bring up to 0.22 mg/mL in 40 mM Tris-HCl supplemented with 5 mM NaCl by adding the appropriate amount of 4.4 M NaCl to the tube. The final total volume should be 284 μ L (ie. add 269.5 μ L 40 mM Tris-HCl and 0.33 μ L 4.4 M NaCl).
- 4) Agitate sample at 25°C and 800 rpm. At various time points, take aliquot and combine with BTA-1 for final A β ₁₋₄₀ and BTA-1 concentrations of 0.021 mg/mL (4.8 μ M) and 0.0058 mg/mL (24.2 μ M), respectively. The final BTA-1 concentration in solution (24.2 μ M) should be 5 times the final A β ₁₋₄₀ concentration (4.84 μ M). Analyze sample via LIF-ME.

ME conditions:

- 1% PHEA dissolved in 40 mM Tris-HCl used for separation matrix
- 40 mM Tris-HCl used for buffer
- 200-600 V/cm injection for 10-20 s
- 380 V/cm separation with 12-24 V/cm pullback

A β ₁₋₄₀ Oligomer Formation Assay With Thioflavin T for Analysis Via Fluorometer

Thioflavin T (ThT) stock solution:

- 1) Prepare a 2.32 mM ThT stock in de-ionized water.
- 2) Solution is stable in 20°C freezer for 2-6 months.
- 3) On day of experiment, dilute ThT stock to 26.8 μ M in 40 mM Tris-HCl (pH 8.0).

50 μ M (0.22 mg/mL) A β ₁₋₄₀ Sample Concentration:

- 1) Take vial containing 0.0625 mg A β ₁₋₄₀ out of -80°C freezer. Add 5 mM NaOH such that the ratio of NaOH:40 mM Tris-HCl is 500:10000, assuming a 0.22 mg/mL final concentration (ie. add 14.2 μ L 5 mM NaOH).
- 2) Let A β ₁₋₄₀ solution sit in 5 mM NaOH for 5 min.
- 3) Bring up to 0.22 mg/mL in 40 mM Tris-HCl supplemented with 5 mM NaCl by adding the appropriate amount of 4.4 M NaCl to the tube. The final total volume should be 284 μ L (ie. add 269.5 μ L 40 mM Tris-HCl and 0.33 μ L 4.4 M NaCl).
- 4) Agitate sample at 25°C and 800 rpm. At various time points, take aliquot and combine with ThT for final A β ₁₋₄₀ and ThT concentrations of 0.021 mg/mL (4.8 μ M) and 0.0077 mg/mL (24.2 μ M), respectively (ie. add 19.4 μ L A β ₁₋₄₀ to 180.6 μ L 26.8 μ M ThT). Use 1.5 mL quartz cuvette for analyses.
- 5) Monitor fluorescence at the onset of aggregation and at times between 5 and 28 hours following the onset of aggregation using a Shimadzu RF-Mini-150 fluorometer (Columbia, MD) (excitation = 460 nm, emission = 480–500 nm). Blank with 26.8 μ M ThT solution.

Protocol for Labeling A β ₁₋₄₀ with BODIPY

Step 1: Prepare 100 μ l of 0.5 mg/ml A β pre-treated with HFIP in 0.1 M sodium bicarbonate, pH 8.3 on ice.

Step 2: Add 7.5 μ l dye –BODIPY-FL (Invitrogen D6140 MW = 491.20 g/mol)

BODIPY was dissolved in sequencing grade DMF at 10 mg/mL from dried aliquots in -20°C freezer

Step 3: Incubate on ice for 1.5 hours

Step 4: Stop the reaction by adding 10 μ L of freshly prepared 1.5 M hydroxylamine, pH 8.5,

(To prepare hydroxylamine soln. carefully, add only ½ volume of sodium bicarbonate soln. then pH)

Step 5: Incubate on ice an additional 30 minutes

Step 6: Rinse Centricon 3kDa with 40 mM Tris, pH 8.0, Add Reaction soln. dilute to 500 μ l

Spin at 14 krpm in microcentrifuge in refrigerator for 20 min; repeat 5 more times to change buffer to Tris and separate unreacted dye - should be approx. 100 μ l volume at end

Step 7: Store at -80°C until need

To figure concentration of dye BODIPY-FL:

Use Beer's Law $A = \epsilon \times \text{path length} \times \text{concentration}$

A = Absorbance maxima 502 nm shifts to 504 nm after conjugation

$$\epsilon = 75,000 \text{ cm}^{-1} \text{ M}^{-1}$$

Path length is typically 1 cm (on nanodrop path length can change so use protein:dye program)

Solve for dye concentration in M (moles/L) $c = \epsilon \times \text{path length} / A$

To figure concentration of protein (This requires additional steps)

Use Beer's Law $A = \epsilon \times \text{path length} \times \text{concentration}$

$\epsilon = 1490 \text{ cm}^{-1} \text{ M}^{-1}$ at 280 nm

Some of the absorbance at 280 nm will be due to the BODIPY dye

$$\text{Therefore } A_{280\text{nm}} \times 0.0573 = A_{\text{dye}}$$

To Solve for concentration of A β in M (moles/L) $c = \epsilon \times \text{path length} / (A_{280\text{nm}} - A_{\text{dye}})$

(Caution on attributing 280nm to A β concentration the extinction coefficient will change depending on the oligomeric/monomer state- therefore this method has been somewhat inconsistent)

We do know that approx. 30% of total protein we started with is lost during our labeling procedures.

Double-check your numbers for A β

Determination of degree of labeling

Concentration of dye (M) / Concentration of protein (M) will give you a ratio of dye:protein per mole

A β ₁₋₄₀/BODIPY-A β ₁₋₄₀ Oligomer Time Course Protocol for Analysis Via LIF-CE

50 μ M (0.22 mg/mL) A β ₁₋₄₀ Sample Concentration:

- 1) Take vial containing 0.0625 mg A β ₁₋₄₀ out of -80°C freezer. Add 5 mM NaOH such that the ratio of NaOH:40 mM Tris-HCl is 500:10000, assuming a 0.22 mg/mL final concentration (ie. add 14.2 μ L 5 mM NaOH).
- 2) Let A β ₁₋₄₀ solution sit in 5 mM NaOH for 5 min.
- 3) Bring up to 0.22 mg/mL in 40 mM Tris-HCl supplemented with 5 mM NaCl by adding the appropriate amount of 4.4 M NaCl to the tube. The final total volume should be ~284 μ L (ie. add 269.5 μ L 40 mM Tris-HCl and 0.33 μ L 4.4 M NaCl).
- 4) Add BODIPY-A β ₁₋₄₀ to unlabeled A β ₁₋₄₀ such that final total concentration is ~50 μ M A β .

NOTE: See excel spreadsheet for exact volumes.

- 5) Agitate sample at 25°C and 800 rpm. At various time points, take 7 μ L sample and analyze via LIF-CE.

CE conditions:

Rinse capillary with de-ionized water in between each run using syringe pump.

1.5% PHEA separation matrix in 0.1% PHEA coated capillary

7 kV injection for 7 s

7 kV separation

Chip System 488 nm Laser Alignment and Operation

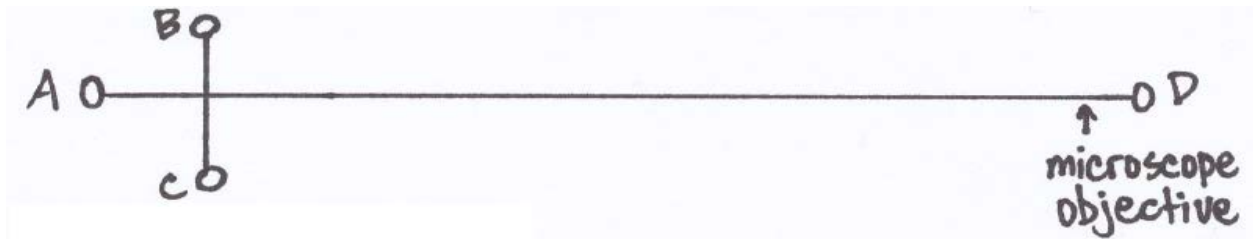
NOTE: Always wear safety glasses which are resistant to laser wavelength (orange lenses in container on the wall). Always close the curtain around the chip system when conducting experiments. Light put out by the laser can damage skin and eyes! Never shine the laser towards yourself or your eyes!

488 nm Laser Operation:

- Align laser so it is shining into the back of the microscope.
- Ensure the 488 nm filter cube is in the correct position.
- Ensure both filter wheels are in the “O” position.
- Ensure the microscope is on the “Eye” port.
- Ensure the key switch for the laser is in the “off” position (vertical up and down).
- The “interlock” light should be green.
- Plug in the laser fan.
- Turn the key switch to the “on” position (horizontal side to side).
- The laser will warm up and you will hear a click when it turns on.
- Use the remote interface to turn the discharge switch to “On” and the run switch to “On”.
- Turn off the laser by switching the remote interface discharge switch to “off”, run switch to “idle”, and the key switch on the power supply box to the “off” position.

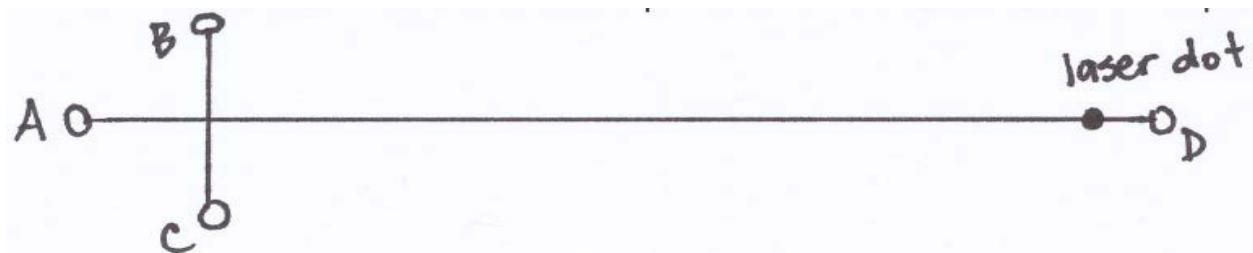
488 nm Laser Alignment:

NOTE: Before turning the laser on, ensure that the microscope objective is near well “D” of the microchip. Also, ensure the microscope is on the “Eye” port.



-Turn on the 488 nm laser.

-You should see a dot for the laser in the microchip well. You will need a source of light (flashlight) in order to see the laser dot on the microchip. Adjust the stage of the microscope so that the dot for the laser is in the middle of the microchip well and as close to well “D” as possible.



-Record the position of the gauges on each side of the microscope stage.

-Record the position of the actual laser on the table.

-These readings will be used each time the laser is utilized.

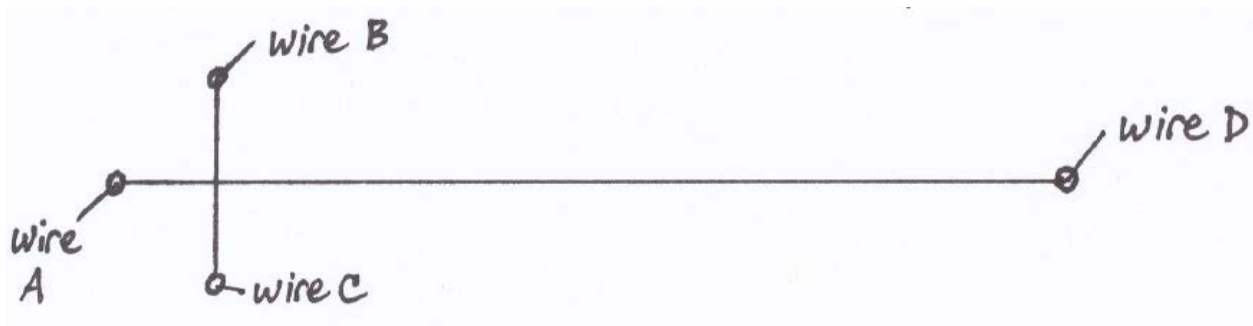
Chip System High Voltage Power Supply Operation

NOTE: Always be cautious when operating the high voltage power supply. NEVER touch the stage or microchip when the high voltage power supply is enabled. This will result in electrocution!

High Voltage Power Supply (HVPS) Operation:

-See directions from George on using the metal chip holder and plastic cover. Never try to pull your chip out of the metal holder. This will break the chip! Instead, remove entire metal holder from stage to remove chip from stage.

-Place the electrodes for each HVPS wire into the microchip wells as follows:




-Ensure the electrodes are submerged in buffer within each well. In proper placement will result in loss of current.

-Turn on the HVPS by pushing the button on the front of the HVPS box.

-Click the “Sequence” icon on the desktop.

-You can create your own program by going to “tools, simple sequence wizard”.


-Press the  icon to toggle between offline and online status.

-The  icon should be highlighted. This means the high voltage is not enabled.

-Press the  icon to enable high voltage. Do NOT touch any part of the stage or microchip!

-Run your sequence by clicking the “Sequencer” tab and pressing the “A” button.

-You can monitor the output of voltage and current for each well. The voltage values should equal what you set the program for and the current values should remain relatively steady.

-When the run is finished, press the  and turn off the HVPS.

Chip System Microscope Parts

Microscope ports:

There are 3 ports located on the microscope base:

- 1) **Eye**-Put on this when want to look through eyepiece at microchip
- 2) **R**-Right side port-Put on this when want to operate CCD camera (Hamamatsu)
- 3) **L**-Left side port-Put on this when want to operate CCD camera (Andor)
- 4) **Aux**-We will not use this port

Microscope should be set on “Eye” by default.

NOTE: *Never* turn the knob to **R** or **L** with the CCD camera *ON* and the overhead lights *ON*.

This will burnout the CCD camera!

Filter cube wheel positions:

There are 2 positions on the filter cube wheel:

- C) Closed
- O) Open

Filter wheels should be set to “C” by default.

There are 6 filter cube positions within the filter wheel.

The 488 nm laser filter cube is in **position 6** on the lower filter wheel.

NOTE: Excitation filter = 470 nm and emission filter = 500 nm long pass

The 355 nm laser filter cube is in **position 5** on the lower filter wheel.

NOTE: Excitation filter = 355 nm and emission filter is interchangeable with either 430
or 525 nm

Chip System UV Laser Alignment and Operation

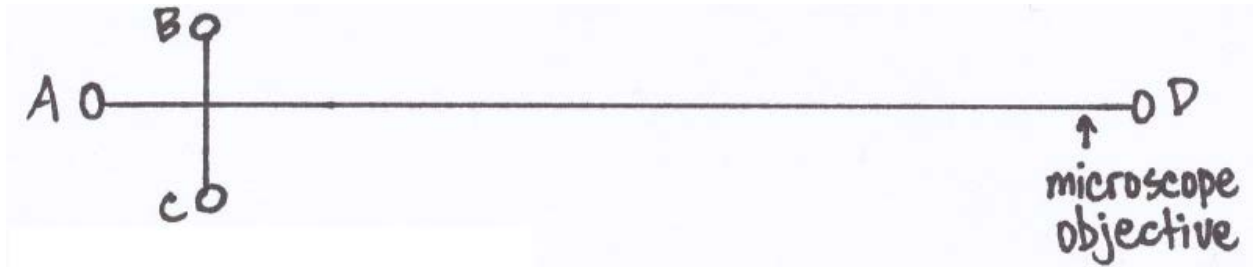
NOTE: Always wear safety glasses which are UV resistant (orange lenses in container on the wall). Always close the curtain around the chip system when conducting experiments with the UV laser. Light put out by the UV laser can damage skin and eyes! Never shine the laser towards yourself or your eyes!

UV Laser Operation:

- Align laser so it is shining into the back of the microscope.
- Ensure the 355 nm filter cube is in the correct position.
- Ensure both filter wheels are in the “O” position.
- Ensure the microscope is on the “Eye” port.
- Ensure the key switch is in the “off” position (vertical up and down).
- Turn on the power button on the back of the power supply box (Coherent) for the UV laser.
- Click the “OPSL” icon on the desktop. This is the user interface to operate the UV laser from the computer.
- Wait until the “system fault” light is not red and the “interlock OK” light is yellow. The laser is now warmed up.
- Turn the key switch to the “on” position (horizontal side to side).
- The “laser on” light should be green indicating that the laser is on.
- You can adjust the laser power using the “control” tab. Click “local” and set the power in the white box in the top part of the user interface.
- Turn off the laser by switching the key switch to the “off” position and turning the power button off.

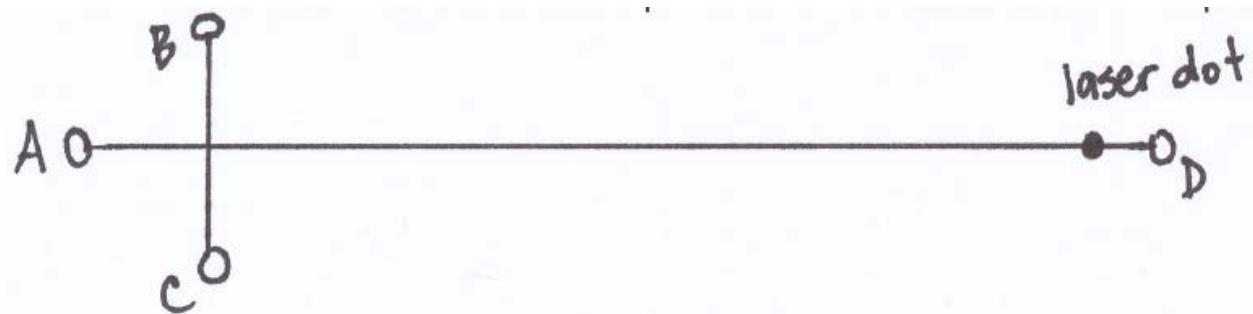
UV Laser Alignment:

NOTE: Before turning the UV laser on, ensure that the microscope objective is near well “D” of the microchip. Also, ensure the microscope is on the “Eye” port.



-Turn on the UV laser and adjust power to ~10?

-You should see a dot for the laser in the microchip well. You will need a source of light (flashlight) in order to see the laser dot on the microchip. Adjust the stage of the microscope so that the dot for the laser is in the middle of the microchip well and as close to well “D” as possible.



-Record the position of the gauges on each side of the microscope stage.

-Record the position of the actual UV laser on the table.

-These readings will be used each time the UV laser is utilized.

CONCLUSION

Existing techniques are limited in the ability to detect insulin and A β oligomers due to the fact that these early aggregates are transient, present at low concentrations, and difficult to isolate. A literature review was conducted by the author in the Fall of 2009 and later published in the *International Journal of Molecular Sciences*. This publication gave a broad overview of the techniques suitable for the determination of A β oligomer size and was thus reproduced in the literature review portion (Chapter 1) of this dissertation. The author contributed to more than 50% of the work necessary to write this published review paper.

The present work has demonstrated the potential for CE and ME to detect the native aggregation of insulin and A β proteins, in particular the formation of oligomers and aggregates. Specifically, we have demonstrated that UV-CE is capable of monitoring native aggregation and provides a size range for the oligomeric and aggregate species produced. LIF-CE is capable of detecting physiologically relevant concentrations of FITC-insulin and FAM-A β but the fluorescent dye necessary for these analyses interferes with native aggregation and thus could give inexact information about the amount of oligomers and aggregates formed. Chapter 3 outlines studies conducted using CE to detect insulin oligomers and aggregates. This information was published in Fall 2011 in the *International Journal of Molecular Sciences*. Again, since this author contributed to writing over 50% of this publication, this publication was reproduced in Chapter 3 as a part of this dissertation.